

**Study of the mechanisms responsible for anemia
and thrombocytopenia in an experimental mouse
model of visceral leishmaniasis**

Olivier Yvon Giuseppe Preham

PhD

2016

Abstract

Visceral leishmaniasis (VL) is a neglected tropical disease caused by protozoan parasites of the *Leishmania* genus causing between 20 000 and 50 000 deaths *per annum*. The parasites have developed a range of mechanisms to avoid the host's immunity and establish chronic infection of the spleen, liver and bone marrow as intracellular parasites of macrophages. The non-exhaustive list of syndromes associated with VL include hepatomegaly, splenomegaly, fever and pancytopenia. The causes for the reduction of red blood cells, platelets or leukocytes are still unclear. Many studies have focused on the immunological aspects of VL, both in humans and experimental models, but the mechanisms causing haematological disorders remain unclear. In this study, it is shown that mice chronically infected with *Leishmania donovani* (*L. donovani*) develop haematological abnormalities, namely anaemia and thrombocytopenia. Erythropoiesis was quantified in the bone marrow, the main site of haematopoiesis in adult mammals. The number of late erythroid precursors was severely reduced in infected animals. Reduction of medullar erythropoiesis was associated with a reduction of stromal support in the bone marrow shown by a reduction of stromal macrophages expressing high levels of CD169 and a loss of CXCL12-producing stromal fibroblasts. The granulocyte-colony stimulating factor (G-CSF) known to deplete stromal macrophages and inhibit CXCL12 expression was systematically up-regulated in infected mice. Splenomegaly correlated with compensatory extramedullary erythropoiesis confined to the red pulp. Infection of splenectomised mice demonstrated that anaemia was independent of the spleen since medullar erythropoiesis was still impaired in these mice. Infection caused an increase in CD4 and CD8 T cells in the bone marrow and infected B6 RAG2^{-/-} mice lacking mature T and B cells were not anaemic and had no repression of medullar erythropoiesis nor splenomegaly. Alterations of bone marrow stromal cells or up-regulation of G-CSF did not occur in these mice. Splenomegaly was relevant because it was shown to be responsible for thrombocytopenia. Megakaryopoiesis was unaltered by chronic infection and infected splenectomised mice had higher platelet counts than their sham-operated counterparts. Platelet production could be stimulated by injections of recombinant thrombopoietin (TPO) in chronically infected mice. Efficacy of TPO treatment in curing thrombocytopenia correlated negatively with the severity of splenomegaly. The original contribution of this work is the demonstration of a complex immunopathological mechanism causing haematological changes in an experimental model of VL. Better understanding of haematological alterations of VL is a step forward for the improvement of VL therapy, in which these alterations have been associated with the lethality of the disease.

Table of content

Abstract.....	2
Table of content	3
List of figures.....	8
List of tables.....	11
Acknowledgments.....	12
Author's declaration.....	13
Chapter 1 Introduction.....	14
1.1 Leishmaniasis.....	14
1.1.1 Epidemiology	14
1.1.2 Vectors of leishmaniasis	15
1.1.3 Biology of leishmania parasites	16
1.1.4 Host cells of leishmaniasis.....	18
1.1.5 The mechanisms for intracellular survival of <i>Leishmania spp.</i>	19
1.1.6 Adaptive immunity to leishmaniasis.....	20
1.1.7 Current treatments against visceral leishmaniasis	20
1.1.8 Haematological alterations commonly associated with VL.....	21
1.2 Haematopoiesis.....	24
1.2.1 Models of haematopoiesis.....	24
1.2.2 Haematopoietic stem cells	27
1.3 Haematopoiesis in its anatomical context.....	28
1.3.1 Histology of the bone marrow	28
1.3.2 The haematopoietic stem cell niche concept	30
1.3.3 Molecular and cellular constituents of the HSC niche.....	30
1.4 Erythropoiesis	32
1.4.1 Erythropoietic progenitors and precursors.....	32
1.4.2 The niches of erythropoiesis	33
1.4.3 Erythropoiesis and iron homeostasis	35

1.5	Platelets and haemostasis	36
1.5.1	Anatomical description of platelets and their origin.....	36
1.5.2	The coagulation cascade	38
1.5.3	Homeostasis of platelets	38
1.6	Infectious diseases and haematological disorders.....	41
1.7	Summary and aims.....	43
Chapter 2	Material and methods.....	44
2.1	Mice	44
2.2	Experimental Visceral leishmaniasis	44
2.3	Estimation of parasitemia	45
2.4	Administration of granulocyte-colony stimulating factor-neutralising antibody	45
2.5	Administration of thrombopoietin	45
2.5.1	Randomisation of mice	45
2.5.2	Injection of recombinant human thrombopoietin	46
2.6	Blood collection and analysis	46
2.7	Plasma collection	48
2.8	Isolation of bone marrow cells.....	48
2.9	Isolation of splenocytes.....	48
2.10	Fluorescence microscopy.....	48
2.10.1	Preparation of femurs for immunohistochemistry	48
2.10.2	Preparation of spleens for immunohistochemistry	49
2.10.3	Immunohistochemistry	49
2.10.4	Confocal imaging.....	49
2.10.5	Epifluorescence imaging.....	50
2.10.6	Whole-mount microscopy.....	50
2.11	Haematoxylin-eosin staining	50
2.12	Flow cytometry	51
2.12.1	Sample preparation	51

2.12.2	Flow cytometry data analysis.....	51
2.13	Fibroblastic colony-forming unit assay (CFU-F)	52
2.13.1	Sample preparation for CFU-F	52
2.13.2	CFU-F assay	52
2.13.3	Staining and enumeration of CFU-F.....	52
2.14	Quantification of G-CSF and TPO in plasma.....	54
2.14.1	Enzyme-linked immunosorbent assay (ELISA)	54
2.14.2	Analysis of ELISA.....	54
2.15	Neutrophil elastase activity assay	55
2.16	Measurement of mRNA accumulation by RT-qPCR	57
2.16.1	RNA extraction	57
2.16.2	cDNA synthesis	57
2.16.3	Quantitative polymerase-chain reaction	57
2.16.4	Primer design and melt curve	58
2.16.5	Analysis of RT-qPCR data.....	58
2.17	Statistical analyses	59
2.17.1	Comparison between groups.....	59
2.17.2	Determination of reference interval.....	59
Chapter 3	Visceral leishmaniasis and erythropoiesis	64
3.1	Introduction.....	64
3.1.1	Aims.....	66
3.3	Results.....	67
3.3.1	Haematological profile of mice chronically infection with <i>L. donovani</i>	67
3.3.2	Medullary erythropoiesis is repressed during EVL	70
3.3.3	Identification of erythroid precursors	70
3.3.4	<i>L. donovani</i> parasites reside in bone marrow macrophages	76
3.3.5	EVL induces alterations of bone marrow macrophages populations.....	77
3.3.6	EVL correlates with repression of the bone marrow stromal support	81

3.3.7	G-CSF is up-regulated during EVL	86
3.3.8	Splenic erythropoiesis is increased during EVL	90
3.3.9	Splenomegaly correlates with changes of the splenic architecture	90
3.3.10	Extramedullary erythropoiesis occurs in the splenic red pulp	91
3.3.11	Reduction of medullar erythropoiesis is independent of splenomegaly	91
3.3.12	The onset of medullar erythropoiesis reduction correlates with local accumulation of T cells in the bone marrow	101
3.3.13	Visualisation of T cells in the bone marrow	101
3.3.14	Both CD4 ⁺ and CD8 ⁺ T cells accumulate in the bone marrow of infected mice	102
3.3.15	Absence of overt pathogenesis in chronically infected immunocompromised B6 RAG2 ^{-/-} mice	107
3.3.16	Erythropoiesis is not altered in B6 RAG2 ^{-/-} mice	107
3.3.17	Lymphocytes are required for the alteration of the medullar erythropoiesis in infected B6 RAG2 ^{-/-} mice	108
3.4	Discussion	113
Chapter 4	Regulation of platelets during EVL	121
4.1	Introduction	121
4.2	Aims	122
4.3	Results	123
4.3.1	Chronic <i>L. donovani</i> infection induces thrombocytopenia	123
4.3.2	Megakaryopoiesis is unaltered during experimental visceral leishmaniasis	123
4.3.3	Platelet production is stimulated by TPO in infected mice	125
4.3.4	Thrombocytopenia is associated with splenomegaly	125
4.3.5	Splenectomy reduces thrombocytopenia	127
4.4	Discussion	130
Chapter 5	General discussion	134
5.1	Principal findings and relevance	134

5.1.1	Murine visceral leishmaniasis as a model for haematological studies	134
5.2	Erythropoiesis is impaired as a consequence of alterations of the bone marrow microenvironment.....	134
5.2.1	Cells of the adaptive immune system are required for the onset of erythropoiesis repression and alterations of the microenvironment in the bone marrow	135
5.2.2	Alterations of the bone marrow underlie extramedullary erythropoiesis and remodelling the spleen	135
5.2.3	Thrombocytopenia is caused by splenomegaly and can be rescued by recombinant TPO injections	136
5.3	Outstanding questions and future work	137
5.3.1	Confirm the link between G-CSF up-regulation and repression of erythropoiesis.....	137
5.3.2	Functional study of infected macrophages in regards to support of erythropoiesis.....	137
5.3.3	Cells of the adaptive immune system responsible for haematological alterations.....	138
5.3.4	Study the role of the liver in thrombocytopenia	138
	List of abbreviations	141
	Bibliography	144

List of figures

Figure 1-1. Life cycle of <i>Leishmania spp.</i> parasites.....	17
Figure 1-2. The classical model of haematopoiesis.....	26
Figure 1-3. Anatomy of long bones.....	29
Figure 1-4. Markers of erythropoiesis.....	34
Figure 1-5. Mechanism of platelet release from megakaryocytes.....	37
Figure 1-6. The coagulation cascade.....	40
Figure 2-1. Workflow for the randomisation of mice prior to rhTPO administration.	47
Figure 2-2. Identification of CFU-F from the bone marrow.....	53
Figure 2-3. Calculate of neutrophil elastase activity.....	56
Figure 2-4. Assessment of qPCR-specificity by melt curves.....	60
Figure 3-1. Signs associated with reduction in medullary erythropoiesis in <i>L. donovani</i> infected mice.....	72
Figure 3-2 Optimal red blood cell lysis takes away the need to use a DNA label to exclude mature erythrocytes.....	73
Figure 3-3 Gating strategy to identify subsets of erythroid progenitors.....	74
Figure 3-4. Medullar erythropoiesis is repressed in chronically infected C57BL/6 mice.....	75
Figure 3-5. EVL results in focal accumulation of macrophage-like cells in the bone marrow.....	78
Figure 3-6. Markers of bone marrow stromal macrophages co-localise with <i>L. donovani</i> amastigotes in B6 RAG2 ^{-/-} mice.....	79
Figure 3-7. Bone marrow macrophages populations are altered following <i>L. donovani</i> infection.....	80
Figure 3-8. Effect of <i>L. donovani</i> infection on the expression of HSC niche-essential genes in total bone marrow.....	83

Figure 3-9. Visualisation of CXCL12-expressing cells using Cxcl12-DsRed reporter mice strain.	84
Figure 3-10. The bone marrow stromal compartment is impaired during chronic EVL.	85
Figure 3-11. EVL induces down-regulation of CXCL12 expression in the bone marrow in correlation with up-regulation of systemic G-CSF.	88
Figure 3-12. Effect of treatment with a neutralising anti-G-CSF antibody (mG-CSF) on erythropoiesis and circulating G-CSF in mice infected with <i>L. donovani</i>	89
Figure 3-13. Chronic EVL induces splenomegaly.	93
Figure 3-14. Chronic EVL induces extramedullary erythropoiesis in the spleen.	94
Figure 3-15. Histological changes in the spleen associated with chronic EVL.	95
Figure 3-16. Chronic EVL induces induces remodelling of the splenic red pulp.	96
Figure 3-17. EVL-induced extramedullary erythropoiesis is characterised by increase of erythroid progenitors in the splenic red pulp.	97
Figure 3-18. Splenic erythropoiesis is not associated with increased BMP4 staining after 28 day-infection with <i>L. donovani</i>	98
Figure 3-19. EVL-induced anaemia is independent of the spleen.	99
Figure 3-20. Repression of medullar erythropoiesis is independent of the spleen during <i>L. donovani</i> infection.	100
Figure 3-21. The onset of medullar erythropoiesis repression corresponds to local accumulation of T cells in the bone marrow.	103
Figure 3-22. Visualisation of T cells in the bone marrow during EVL.	104
Figure 3-23. Imaging of T cells in relation to <i>L. donovani</i> parasites in the bone marrow of infected mice.	105
Figure 3-24. CD4+ and CD8+ frequencies increase in the bone marrow of mice chronically infected with <i>L. donovani</i>	106

Figure 3-25. Infection of RAG2 ^{-/-} mice with <i>L. donovani</i> does not alter medullar erythropoiesis.....	109
Figure 3-26. Absence of splenomegaly in RAG2 ^{-/-} mice infected with <i>L. donovani</i>	110
Figure 3-27. Absence of G-CSF up-regulation and alteration of the bone marrow microenvironment in infected RAG2 ^{-/-} mice.....	111
Figure 3-28. Adoptive transfer of wild-type splenocytes into chronically infected RAG2 ^{-/-} mice induces repression of medullar erythropoiesis.....	112
Figure 4-1. <i>L. donovani</i> infection induces thrombocytopenia.....	124
Figure 4-2. Treatment of infected mice with recombinant TPO increases circulating platelets.....	126
Figure 4-3. Infection results in higher platelet counts in splenectomised mice.	128
Figure 4-4 Splenectomy results in a reduced hepatomegaly in infected mice.	129
Figure 4-5. Better response of rhTPO in infected splenectomised mice.	129
Figure 5-1. Hypothetical model for the mechanisms of anaemia in experimental visceral leishmaniasis.....	139
Figure 5-2. Hypothetical model for the mechanisms of thrombocytopenia in experimental visceral leishmaniasis.	140

List of tables

Table 2-1. List of antibodies	61
Table 2-2 List of primers for real-time quantitative polymerase chain reaction	63
Table 3-1 Haematological parameters of mice infected with <i>L. donovani</i> .	68
Table 3-2. Reference interval of haematological parameters and distribution of infected mice in relative to the intervals.	69

Acknowledgments

I would like to thank all the people who have helped me and supported me during these years.

I would like to express my sincere gratitude to my supervisor Prof. Paul Kaye for giving me the opportunity to study at York for my PhD and provided guidance all along, for making it possible for me to work on a project I was passionate about.

I would like to thank the members of my training advisory panel, Dr. Paul Genever and Dr. Paul Pryor who have provided the most useful advice.

Many thanks to Dr. Ian Hitchcock for providing guidance on the study of platelets and thrombopoietin.

I have greatly enjoyed these years in the Centre for Immunology and Infection. I would like to particularly thank all the members of the Kaye lab, past and present, with whom I have shared such great moments. Many thanks to Naj, for making my work so much easier than it would have been without her, and for always being so cheerful and to Ana for being so nice and helpful, for sharing these long days in the confinement of the laboratory. I would also like to thank Jane who helped with the redaction of this manuscript, Lynette, John, Mohamed, Jack and Joe.

I am highly indebted to the BSF staff, Hayley, Chris, Karen and Carl, for being incredibly helpful and nice. I am forever grateful to the TF staff as well, Peter, Graeme, Karen Hogg, Karen Hodgkinson and Joe. All this work would not have been possible without them.

This work was made possible by the European Commission through the Framework Programme 7. I would like to thank everyone involved in the Marie Curie initial training network that this project was a part of, for their help and support but most of all for being good friends.

Last but not least I would like to thank Anne, for giving me a helpful hand when needed, for always believing in me and giving me the courage to accomplish this work.

Author's declaration

I declare that this thesis is a presentation of original work and I am the sole author. This work has not previously been presented for an award at this, or any other, University. All sources are acknowledged as References.

Chapter 1 Introduction

Visceral leishmaniasis (VL) is a neglected tropical disease responsible for the death of 20 000 to 50 000 people each year. Visceralising species such as *Leishmania donovani* infect and replicate inside macrophages of the spleen, liver and the bone marrow¹. The disease causes, among other symptoms, a reduction of circulating blood cells. Anaemia, leukopenia, thrombocytopenia – reduction of red blood cells, white blood cells or platelets respectively – or pancytopenia – the reduction of all three lineages – are common occurrence in patients². Yet the mechanisms for haematological alterations are still unclear. Uncovering these mechanisms would allow improved treatment of patients as well as potentially enable better and earlier diagnosis of VL, which is sometimes mistaken for other haematological disorders^{3,4}. The epidemiology and immunobiology of visceral leishmaniasis have been extensively studied previously and will be discussed in this chapter as well as the current knowledge about the haematology of the disease. This study focuses on anaemia and thrombocytopenia so the physiological regulation of red blood cells and platelets will be described. Finally known mechanisms for haematological changes in the context of infectious diseases will be discussed, with a particular focus on parasitic diseases.

1.1 Leishmaniasis

1.1.1 Epidemiology

Leishmaniasis refers to multiple diseases which are caused by protozoan parasites of the *Leishmania* genus¹. Cutaneous leishmaniasis (CL) is the most widespread form of the disease and associated with many parasites throughout the New World and Old World. CL causes nodules (elevated/swollen tissue) on exposed parts of the body. These nodules can sometimes evolve into open lesions (ulcers). The lesions appear typically between 1 week to 3 months after the initial bites. In most cases, infection does not spread further, although satellite lesions can form near the primary lesion and parasites can be found in adjacent draining lymph nodes. In immune-competent individuals, lesions spontaneously regress after 6 to 12 months but leave scars. Species of parasites are able to cause a diffuse cutaneous leishmaniasis (DCL). DCL is most prevalent in the New World although cases have been reported in the Old World as well. A primary lesion similar to that of CL appears, but secondary parasites-containing lesions develop on other parts of the body. The infection however only affects the skin and parasites do not disseminate to internal organs. Secondary lesions are generally non-ulcerative. Mucocutaneous leishmaniasis (MCL) is a mostly New World-disease associated with *Leishmania braziliensis*, *Leishmania*

amazonensis and *Leishmania guyanensis*. MCL is characterised by infection and destruction of mucosal surfaces on the face (nasal cavity, mouth and throat) and can result in severe disfigurement or death from malnutrition or respiratory pneumonia. VL, also known as Kala-azar, is the most severe form of the disease. It is caused by *Leishmania donovani* (*L. donovani*) and *Leishmania infantum* (*L. infantum*) in both the Old World (mostly Sudan, India and Nepal) and in the New World. Compared to all other forms of the disease, VL is characterised by a systemic infection. Parasites are mostly found within the spleen, the liver, the bone marrow, the lymph nodes and other atypical locations. VL causes multiple symptoms among which hepato- and splenomegaly, weight loss, fever and anaemia are the most commonly reported. If left untreated, VL is lethal in close to 100%. For reasons still unclear, VL sometimes evolves into a cutaneous disease termed post kala-azar dermal leishmaniasis (PKDL), causing a rash which usually starts on the face and can spread to other parts of the body. PKDL is mainly reported in Sudan and India and appears within 6 months or 2-3 years after VL treatment, respectively. The epidemiology of PKDL varies between geographical regions. Between 10% to 20% of VL patients will develop PKDL in India whereas as many as 50% to 60% of VL patients will develop PKDL in Sudan⁵.

Altogether, these diseases affect millions of individuals in virtually all continents. According to the latest reports, 1 million new cases of CL occur each year. CL being rarely lethal, the burden is mostly social. As a result of scars or disfigurements, individuals tend to be excluded from society. Most leishmaniasis-related deaths are caused by VL, with 300,000 new cases each year and an estimated 20,000 to 50,000 deaths annually. However, the clinical and epidemiological heterogeneity of leishmaniasis means that the burden of the disease is likely to be underestimated⁶. A certainty is that tropical regions are where most of the leishmaniasis cases occur. Epidemiology of leishmaniasis is closely linked to the biology of its vector.

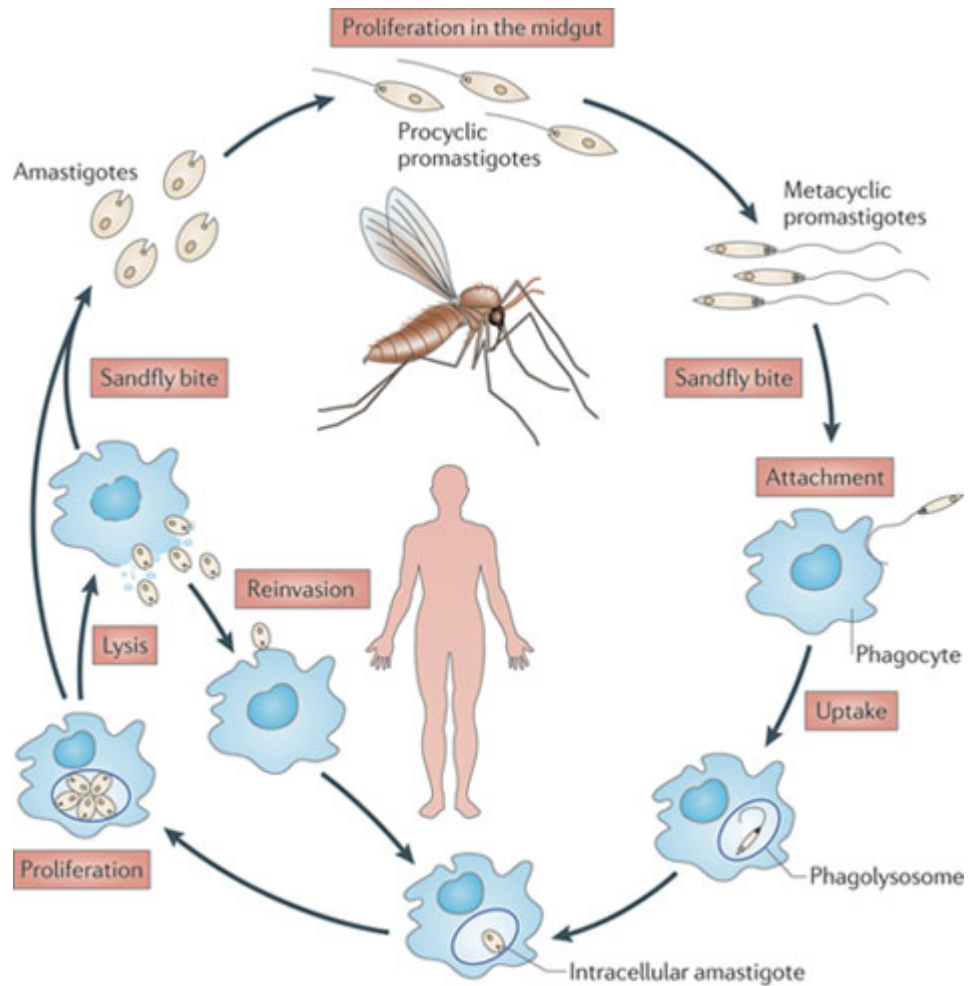
1.1.2 Vectors of leishmaniasis

The main natural vector of leishmaniasis is the female of a small insect of the *Phlebotominae* subfamily, commonly called the “sand fly”. Vectors of leishmaniasis in the Old World belong to the *Phlebotomus* genus whereas in the New World, vectors belong to genus *Lutzomyia*. Leishmaniasis transmission occurs during blood meals. Female sand flies require blood in order to produce eggs⁷. They suck blood from a variety of animals, including mammals, reptiles and birds. Because they are highly sensitive to temperature, sand flies are generally nocturnal in order to avoid dehydration. Blood meals thus usually

happen at dusk or during the night. The requirement of humid environments and high temperature for eggs to develop results in sand fly habitats to be concentrated in the inter-tropical regions, which correlates with the distribution of leishmaniasis. Evidence suggest the distribution of these habitats is currently ongoing changes, notably in Europe⁸. In Australia, where leishmaniasis is virtually absent, a report of autochthonous infection in the red kangaroos was published in 2004⁹. Because the sand fly is not endemic to Australia, studies have showed that female midges were potential vectors^{10,11}. This evidence is still insufficient to confirm that midges are vectors of leishmaniasis since a full infection cycle has not been demonstrated yet in these species^{12,13}.

1.1.3 Biology of leishmania parasites

The *Leishmania* genus belongs to the group of *Trypanosomatidae*, which includes other notable parasites such as *Trypanosoma brucei*, the agent of Chagas disease, and *Trypanosoma cruzi*, the agent of sleeping sickness. They are protozoan parasites, i.e. unicellular eukaryotes. *Leishmania spp.* have a dual life-cycle shared between an insect host, the sand fly, which is also the vector, and a mammalian host. The parasites present two major forms: the promastigote form, an extracellular flagellated form, and the amastigote form, the intracellular form with no external flagella¹. Promastigotes colonise the sand fly's mid-gut where they proliferate (procyclic promastigotes) until they migrate into the proboscis (the tubular mouthpart of the insect used for blood meals) and differentiate into the non-proliferating infective form (metacyclic promastigotes). Upon transmission to a mammal, metacyclic promastigotes are phagocytised by mononuclear phagocytes and differentiate into amastigotes in the phagolysosome of host cells, the latter becoming a parasitophorous vacuole (PV). Amastigotes replicate inside phagolysosome, either in one communal PV (e.g. *L. amazonensis* en *L. Mexicana*) or each in an individual PV (e.g. *L. donovani* and *L. major*)¹⁴. Whereas downward transmission (sand fly to mammal) is relatively well understood, upwards transmission is less clear. Models generally assume that macrophages rupture when the parasite load is too heavy and that intracellular amastigotes are subsequently freed. These free amastigotes are thought to be taken up by sand flies during blood meals, after what they differentiate back to promastigotes, completing the life cycle. This is accepted as the mechanism propagating the infection from one macrophage to others. However, direct evidence for this is still needed. Despite the complexity of *Leishmania spp.* the life cycle, the genome of parasites is constitutively expressed¹⁵, so genetic regulation is at the post-transcriptional level and through changes in ploidy^{16,17}.



Nature Reviews | **Microbiology**

Figure 1-1. Life cycle of *Leishmania spp.* parasites. Metacyclic promastigotes are transmitted to the host by a female sand fly. Promastigotes are then internalised by mononuclear phagocytes in which they transform into amastigotes and proliferate inside parasitophorous vacuoles. Transmission from one host cell to another is thought to occur through lysis of the host cell and subsequent reinvasion. Uptake of amastigotes by a sand fly can occur during a blood meal. Amastigotes differentiate in the sand fly midgut into proliferative procyclic promastigotes then into infective metacyclic promastigote, thus completing the life cycle (reproduced from Kaye and Scott, Nat Rev Microbiol, Jul 2011).

1.1.4 Host cells of leishmaniasis

Leishmania amastigotes are obligate intracellular parasites and most parasites reside within the vacuole of macrophages. However, many studies have shown that the variety of host cells of *Leishmania spp.* is greater than expected.

Mononuclear phagocytes, macrophages and dendritic cells (DCs), are where most parasites can be found. Within each tissue, amastigotes have a preference for resident macrophages. In the spleen they are more readily found within marginal zone macrophages and marginal metallophilic macrophages, which are the macrophages forming the marginal zone around the splenic white pulp. In the liver, Kupffer cells are the main host cells. In the bone marrow, they infect CD169⁺ stromal macrophages^{18,19}. Dermal DCs take up *L. major* parasites within hours of infection²⁰. More host cells are recruited at the site of infection in the form of monocyte-derived DCs (moDCs). Interestingly these moDCs are both host cells and protective cells by stimulating interferon gamma (IFN γ)-producing T cells^{21,22}.

Neutrophils have also been reported as host cells of *Leishmania spp.*¹. Initial intradermal infection by the sand fly or with a needle results in neutrophils swarming towards the site of infection^{23,24}. However, neutrophils are not known to be infected in the long-term. Parasites only reside transiently in neutrophils, which drew researchers to hypothesise that neutrophils are “Trojan horses” for *Leishmania spp.*²⁵. Infected neutrophils become apoptotic and are phagocytised by phagocytic cells, which triggers anti-inflammatory mechanisms by autocrine and paracrine mechanisms involving mediators such as the transforming growth-factor beta (TGF β) and interleukin-10 (IL-10)^{26–28}. According to the Trojan horse hypothesis, engulfment of infected apoptotic neutrophils by macrophages enables the safe passage of parasites to their long-term residence inside mononuclear phagocytes. It has since been demonstrated in *L. major* infected mice. Infected dermal DCs had reduced activation markers when acquiring parasites through neutrophil phagocytosis. Depletion of neutrophils also resulted in higher *L. major*-specific CD4⁺ T-cell responses²⁹. Recently, recruitment of neutrophils by *L. mexicana* has been linked to a decrease in protective moDCs in lymph nodes. Neutropenic mice ultimately healed while lesions were chronic in wild-type mice²².

L. major has been reported to reside in fibroblasts of the skin and draining lymph nodes³⁰. Infected fibroblasts do not express high levels of nitric oxide (NO) that kills intracellular parasites. Most persistent parasites are inside fibroblasts, suggesting stromal cells are a safe haven for intracellular amastigotes. *L. donovani* can infect splenic fibroblasts

expressing the marker ER-TR7³¹. Infected stromal cells produce higher levels of CCL8 and CXCL12. The two cytokines support the development of regulatory DCs which dampen the immune response via IL-10 secretion^{32,33}. These studies all point towards a negative role of stromal cells in regards to leishmaniasis.

1.1.5 The mechanisms for intracellular survival of *Leishmania spp.*

Two mechanisms trigger phagocytosis of pathogens by macrophages. Evolutionary conserved molecules displayed by pathogens, termed pathogen-associated molecular patterns (PAMPs) bind pattern recognition receptors (PRRs). Alternatively, opsonised pathogens are also phagocytised. Opsonisation is a process enhancing phagocytosis which consists in covering pathogens with antibodies, immunoglobulin G being the most potent isotype, or molecules of the complement (C3). Macrophages express antibody receptors, IgG- constant fragment receptor, and Fc γ R, or complement receptors such as CR3. Phagocytosis results in the formation of a pathogen-containing intracellular vesicle called the phagosome. A complex maturation process follows. The phagosome fuses with other vesicles, including highly acidic lysosomes. Matured phagolysosomes have a very low pH, many oxidative species and antimicrobial molecules³⁴. Peptides and molecules issued from the degradation of the parasites can then be displayed on the surface of macrophages in association with the class II major histocompatibility complex (MHCII), inducing adaptive immunity specifically targeted against the parasites.

Despite the hostile environment, phagolysosomes are the subcellular compartments where *Leishmania* parasites proliferate^{35,36}. In order to survive within macrophages, *Leishmania spp.* have developed an arsenal of tools subverting the biology of their host cells. Promastigotes cannot survive the conditions inside phagolysosomes and have therefore acquired the capacity to delay the maturation of phagosomes. This capacity has been attributed to the parasite's surface lipophosphoglycan (LPG) which inhibits several mechanisms of maturation³⁷. The promastigote-derived metalloprotease GP63 cleaves a soluble N-ethylmaleimide attachment protein receptor (SNARE) protein called VAMP8, which mediates the fusion of phagosomes with late endosome^{38,39}. Promastigotes only delay the maturation of phagosomes, which ultimately mature into an acidic phagolysosome. Most likely, promastigotes only delay phagolysosome maturation until they transform into amastigotes, a form adapted to growth in low pH medium⁴⁰. Amastigotes have defence mechanisms involving the reduction of oxidative stress in parasitophorous vacuoles by inhibiting the NADPH oxidase^{41,42}.

1.1.6 Adaptive immunity to leishmaniasis

Despite the mechanisms deployed to avoid antigen presentation, an immune response develops during VL. Efficient adaptive immune response against visceralising *Leishmania spp.* usually has been linked to the expansion of type 1 helper T cells (T_H1). T_H1 cells produce $IFN\gamma$ and promote expansion of CD8 T cells, which also produce $IFN\gamma$ ⁴³. $IFN\gamma$ has a protective role against the infection as it induces NO production and parasites killing by macrophages. IL-12 is a key cytokine for the induction of a T_H1 immune response and has been linked to control of visceral infections^{44,45}. Despite observations that development of VL was associated with a T_H2 type immune response⁴⁶, studies did not report a T_H2 skewing in patients. Together with $IFN\gamma$, active VL is associated with high levels of IL-10^{47,48}, which dampens the immune response and participates in chronic disease^{49,50}. Active disease is usually associated with hypo-responsiveness of peripheral blood-mononucleated cells (PBMCs) stimulated with *Leishmania* antigens⁵⁰. By contrast, PBMCs from cured or asymptomatic patients respond to antigenic stimulation^{51,52}. Another factor contributing to ineffective control of parasites by the adaptive immune response is the exhaustion of effector T cells⁵³. Targeting of the inhibitory receptor expressed by T cells has therefore been investigated as a way to enhance the host's immune response^{54,55}. Recently, in a mouse model of CL, it has been shown that innate immune response against *L. major* induces a detrimental T_H2 adaptive immune response via activation of the Nod-like Receptor P3⁵⁶. B cells are not required for resistance against *L. donovani* in the mouse model, but Immunoglobulins G protect against excessive liver damage⁵⁷.

1.1.7 Current treatments against visceral leishmaniasis

The complexity of VL makes it a hard disease to cure. Because of the variations in *Leishmania spp.* and the epidemiological complexity, finding a single drug efficient in all cases of VL is challenging and seemingly far from reach⁵⁸.

Antimony-based treatments have been in use since the 1940s. Antimony is a heavy metal which has an antiprotozoal effect. Two formulations of antimony are clinically used: sodium stibogluconate (SSG), and meglumine antimoniate. SSG is the most commonly used formulation of the two. Clinically, SSG has a good record of effectively curing the disease in East Africa. However, clinical treatments with SSG have shown a poor efficacy in India. Although the drug is quite cheap, it is absorbed very poorly orally so requires administration via daily intravenous (i.v.) or intramuscular injections. This implies the need for appropriate infrastructures and trained personnel as well as a necessity for patients to move in order to get treated. As VL is prevalent in poor countries, setting the

infrastructure can be challenging and patients might not be able to afford going to the hospital daily. In addition, the toxicity of antimony is an important disadvantage for this drug, especially combined with the relative long treatment needed (20 to 28 days). It causes nausea, vomiting, cardiac and liver dysfunctions. Antimonies are still the first line drugs used against VL in Africa and South America.

From the 1990s, reports from multiple regions of India indicated that the efficacy of SSG was in decline⁵⁸. This drove the research of alternative treatments and most new drugs were targeted to the Indian subcontinent. Amphotericin B is an anti-fungal drug that was shown to be a potent anti-leishmania agent. It is administered i.v. and achieved good cure rates in India, including in SSG-resistant infections. However, the elevated cost of amphotericin B has limited its use and most studies focus on making it more efficient to limit the costs. Lipid formulations of amphotericin B have been shown to be even more potent⁵⁹. Amphotericin B is now the main drug used to treat VL in India.

Paromomycin, a cheap wide-spectrum antibiotic, has been shown to be efficient against VL in India, although clinical trials have so far failed in East Africa. Paromomycin has usually been evaluated in combination with SSG when supplies of SSG were low. Reconditioning of Miltefosine, an alkyl phospholipid previously used for treatment of cancer, occurred after it was shown to have leishmanicidal activity⁶⁰. It is a promising drug which is administered orally and is the first drug used against both VL and CL⁶¹.

Most drugs used against VL aim at killing the parasites directly, although not all mechanisms of action are understood. As this approach is susceptible to resistance, illustrated by the inefficacy of SSG in India, alternative approaches are being investigated. The design of a vaccine capable of enhancing the host's immune response to *Leishmania* parasites is privileged by many researchers. The time and investment required to make anti-leishmaniasis vaccines a reality means conventional therapies will still be used for years to come.

1.1.8 Haematological alterations commonly associated with VL

Alterations of blood cellular components has been reported in human^{3,62-66}, hamster^{67,68}, canine⁶⁹⁻⁷¹ or feline⁷² visceral leishmaniasis. Cytopenia is a common occurrence in human, with anemia being the more frequent, followed by leukopenia and thrombocytopenia^{64,73,74}. Retrospective studies have previously linked haematological disorders with the probability of death. In particular, haemorrhagic tendencies have been associated with less favourable prognosis⁷⁵⁻⁸⁰. Anaemia, while never directly reported as the cause of death in VL patients,

is very likely to participate to general fatigue, while leukopenia in conjunction with immunosuppression potentially increases the risks of secondary opportunistic infections.

Pancytopenia is a general reduction of blood cells and is thus associated with mechanisms that cause reduction of all lineages non-specifically. Mechanisms responsible for the reduction of red blood cells, leukocytes or platelets specifically are described in the next chapter. Much of what is known about pancytopenia comes from clinical data or field data from naturally infected dogs and cats. Immune-mediated elimination of circulating cells has been proposed as a mechanism for pancytopenia. The detection of antibodies against red blood cells, platelets and leukocytes suggests that auto-immunity can develop in chronic infections^{81,82}. However, other studies report that sustained inflammation can also lead to non-specific destruction of blood cells by immune cells. This mechanism is supported by frequent observation of haemophagocytosis^{83,84} (e.g. the presence of erythrocytes inside macrophages). Splenomegaly is also cited as one major cause of pancytopenia. As in other diseases, increase in spleen size causes an increase in splenic capture of circulating cells. While the sequestration and/or destruction of mature circulating cells is a possible cause for pancytopenia, it is also very likely that VL results in an impairment of haematopoiesis in the bone marrow. Studies have reported myelodysplastic features in all three blood cells lineages^{4,85}. Myelodysplasia refers to inefficient production of blood cells. The mouse model of VL has previously been regarded as too different from the human, canine or feline disease to be used in experimental study of haematological disorders. Indeed, chronic infection of mice with *L. donovani* or *L. infantum* is non-fatal and parasite clearance from the liver occurs typically 3 to 4-week post-infection. Nevertheless, Cotterell et al. have demonstrated that *L. donovani* infection of BALB/c mice leads to an increase of haematopoietic activity in the spleen and the bone marrow⁸⁶. More specifically, they showed that an infected bone marrow stromal macrophage cell line enhances myelopoiesis *in vitro* by up-regulation of the production of granulocyte monocyte-colony stimulating factor (GM-CSF) and tumour necrosis factor alpha (TNF α)¹⁹.

Anaemia is the reduction of circulating erythrocytes but can take different forms. In addition to the number of circulating cells, two important parameters for the diagnosis are the size of erythrocytes and their haemoglobin content. Macrocytic anaemia is characterised by enlarged erythrocytes and is associated with multiple conditions such as vitamin B12 deficiency, drugs or alcohol abuse and myelodysplastic syndromes⁸⁷. It is a consequence of abnormal erythropoiesis producing bigger erythrocytes and is associated with enlarged erythroid precursor (megaloblastic anaemia). Microcytic anaemia is

characterised by smaller erythrocytes and occurs most notably in the context of iron or vitamin B6 deficiency anaemia⁸⁸. Reduction in the haemoglobin inside erythrocytes results in hypochromic anaemia which refers to their coloration (since the red coloration of erythrocytes is related to the concentration of haemoglobin). Iron deficiency anaemia is microcytic hypochromic due to ineffective erythropoiesis. A normochromic normocytic anaemia (reduced number but normal size and haemoglobin concentration) is often associated with a reduced but normal erythropoiesis or increased destruction of erythrocytes, such as in chronic inflammation^{89,90}. However, chronic inflammation also disrupts the iron metabolism, resulting then in a microcytic anaemia⁹¹. Anaemia in the context of infection diseases is often multifactorial and complex. Malaria for example causes anaemia through multiple pathological mechanisms such as direct lysis of erythrocytes by parasites, dyserythropoiesis, splenic removal and immune destruction of erythrocytes⁹². Clinical data from patients indicate that typical anaemia of VL is normocytic and normochromic², although macrocytic anaemia has been observed^{73,93}.

A few studies have reported mechanisms specific for anaemia. It has been reported that VL results in increased sequestration of iron inside macrophages. It is believed to be a mechanism favouring the development of intracellular amastigotes since iron is necessary for their growth⁹⁴. Iron is also required for the synthesis of heme during erythropoiesis. It is therefore thought that reduction of available iron participates in the dyserythropoiesis⁹⁵. As an alternative rodent model, the hamster has been favoured because the course of infection is similar to natural infections and reaches a fatal endpoint. Hamsters chronically infected with *L. donovani* display a severe anaemia⁶⁷ associated with a higher apoptosis of erythroid precursors in the bone marrow and induction of stress erythropoiesis in the spleen⁶⁸. The specific mechanisms of thrombocytopenia are unclear as well. Platelets have been shown to be destroyed by immune cells in infected dogs⁹⁶ but not in humans. Because platelet counts return to normal values after splenectomy, hypersplenism is thought to be the main cause of thrombocytopenia^{62,97}. No specific mechanism of leukopenia has been reported².

Overall, there are few mechanistic studies about the haematological changes in VL, especially when compared to the extensive knowledge about the immunological aspect of the disease. As described above, the prognosis of VL is often linked to haematological alterations. Being able to understand the source of these alterations would enable new treatments correcting these alterations and potentially reduce the lethality of the disease. Visceral leishmaniasis is sometimes misdiagnosed as myelodysplasia because little is known about the specifics of haematological alterations³. This emphasises the importance

of a better understanding of the haematological aspects of the disease. The development of diagnostic tools for VL in endemic areas is slow and challenging⁹⁸. Being able to detect signs of VL in patients not yet diagnosed based on their haematological profile would help early detection of VL. To understand how VL affects blood cells, it is first necessary to understand the physiology of blood cells production. In this work, the murine model using C57BL/6 mice chronically infected with *L. donovani* presented both anaemia and thrombocytopenia (Table 3-1). For this reason, the next part focuses on haematopoiesis and the biology of red blood cells and platelets.

1.2 Haematopoiesis

1.2.1 Models of haematopoiesis

The field of stem cell biology, be it induced pluripotent stem cells, haematopoietic stem cells or mesenchymal stem cells, is generating an exploding interest worldwide due to the multitude of potential therapeutic applications, such as for auto-immune diseases, leukaemia and regenerative medicine. Yet, with the expansion of different studies has come the need to define what should be called a stem cell, a progenitor or a precursor⁹⁹. The scientific community has defined a stem cell as a cell that must be capable of unrestricted self-renewal, i.e. symmetrical or asymmetrical division generating at least one identical daughter cell with the same potential so that the stem cell pool is never exhausted, and it must be capable of giving rise to a number of cell types. Totipotent stem cells such as embryonic stem cells, can virtually develop into any cell type found in the body while multipotent stem cells are more restricted. Thus, haematopoietic stem cells (HSCs) are the source of all cells of the haematopoietic lineage. This definition is still ambiguous in the sense that “stem cells” such as embryonic stem cells, or short-term HSCs have a limited self-renewal potential and will be ultimately exhausted.

Greater misunderstanding arises from the terms progenitors and precursors which seem to be used interchangeably in the literature. In this work, the term “progenitor” is used for daughter cells of stem cells whose differentiation potential is more restricted and sometimes have a limited self-renewal ability; i.e. can generate a restricted number of identical daughter cells before exhaustion. One example of a progenitor cell is the common lymphoid progenitor, capable of differentiating into Natural Killer (NK) cells and T or B lymphocytes. The term “precursor” is used for cells that are fully committed into a lineage and do not replicate, giving rise to a single type of mature cell. For this reason, the pro-erythroblasts and erythroblasts are called erythroid precursors here, being only able to differentiate into erythrocytes.

Haematopoiesis refers to the process through which a HSC produces blood cells. HSCs are multipotent stem cells capable of differentiating into any type of blood cell. Although called blood cells, cells issued from haematopoiesis do not necessarily reside in the circulatory system permanently. However, all are released in the blood where they will either stay or transition towards another organ. Haematopoiesis is usually described as a hierarchical differentiation process in which step-wise differentiation of haematopoietic progenitors is associated with progressively restricted differentiation potential (**Figure 1-2**). The classical model of haematopoiesis starts with a HSC which can commit either to the lymphoid lineage or the myeloid lineage, by differentiating into either a common lymphoid progenitor¹⁰⁰ (CLP) or common myeloid progenitor¹⁰¹ (CMP) respectively. According to the classical model, the differentiation potential of CLPs is restricted to T and B lymphocytes as well as NK cells. The differentiation potential of CMPs is restricted to erythrocytes, platelets, granulocytes, monocytes/ macrophages and DCs^{100,101}. Although still in use, this model has been challenged by multiple studies. Initial commitment has been shown to be either myeloerythroid or myelolymphoid, specified by either the expression of transcription factors GATA-1 or PU.1, respectively¹⁰². Maturation of T cells involves precursors leaving the bone marrow (bone marrow) for the thymus, where differentiation involves diversification of the T cell receptor (TCR) and negative selection of auto-reactive cells. However, early thymic precursors of T cells have been shown to be able to differentiate into DCs¹⁰³ and macrophages^{104,105}, while lacking B cell potential. In another study, HSCs were sorted on the basis of the transcription factor Flt3. Flt3⁺ HSCs preserved the granulocytes, macrophages, T and B cells potential but lacked megakaryocyte-erythrocyte potential as opposed to Flt3⁻ HSCs¹⁰⁶. Commitment to the platelet and red blood cell lineages might therefore occur from the HSC stage not from the CMP stage as originally described. This shows that the binary model of lymphoid vs myeloid lineage is limited in regards to its representation of reality. Other models have therefore been proposed to incorporate the complexity of haematopoiesis¹⁰⁷. These models refute that determination between lymphoid and myeloid lineages occurs at the apex of the haematopoietic tree. They illustrate the lack of consensus regarding the map of haematopoietic lineages. As a consequence, the classic model is still used, including in this work, despite its known limitations¹⁰⁷. However, all models agree that haematopoiesis originates from a HSC.

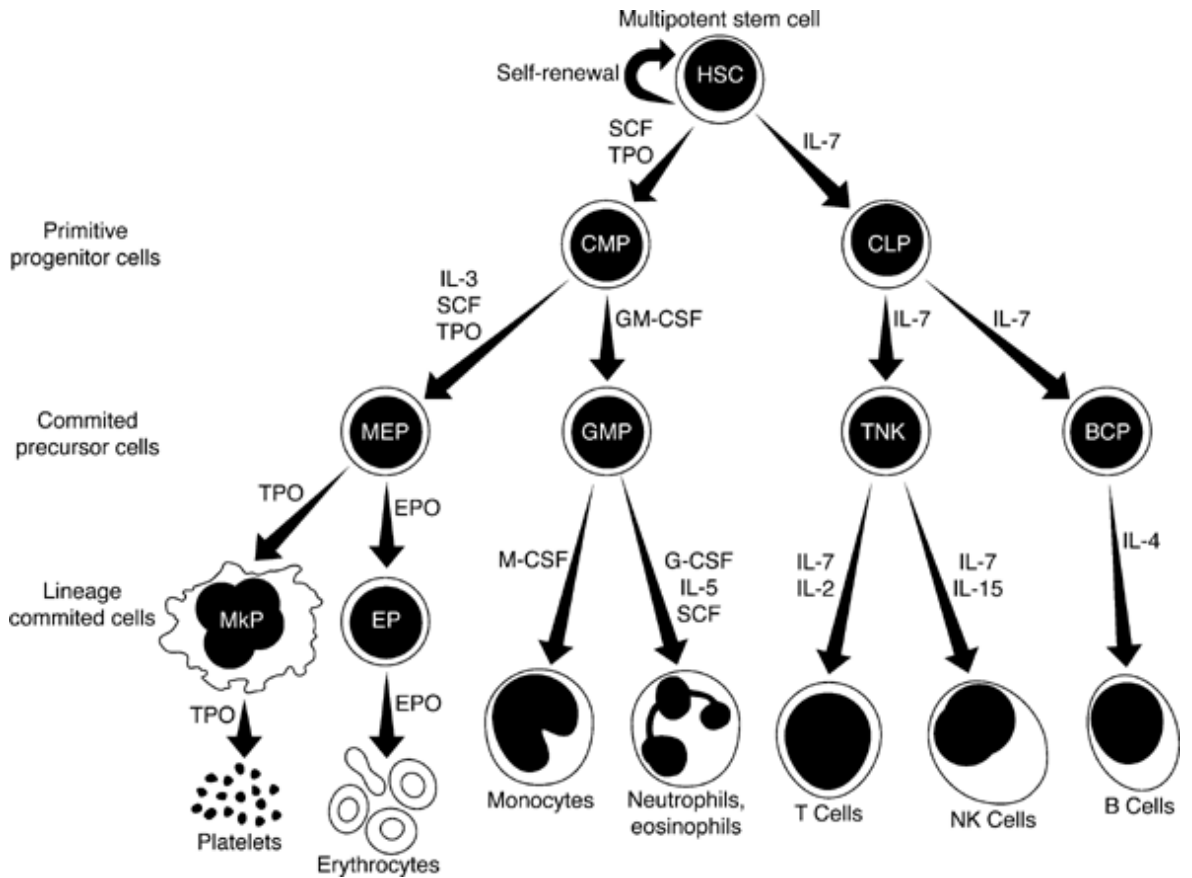


Figure 1-2. The classical model of haematopoiesis. The classical model of haematopoiesis describes a step by step differentiation of HSCs towards mature blood cells. According to the classical model, the first decision is commitment to the myeloid lineage (platelets, RBC, monocytes and granulocytes) or the lymphoid lineage (T and B lymphocytes and NK cells). Each decision is associated with a restriction of the differentiation potential, so that myeloid-committed cells can't differentiate into lymphoid cells and inversely. However, this model has been challenged multiple time as discussed in 1.2.1. Adapted from Robb, *Oncogene*, Oct 2007¹⁰⁸.

1.2.2 Haematopoietic stem cells

Till and McCulloch published the first evidence that the mouse bone marrow contained a population of radio-sensitive cells capable of forming haematopoietic colonies in the spleen (spleen colony forming units, CFU-S) when transferred into an irradiated mice¹⁰⁹. The number of colonies formed inside the spleen in transferred mice correlated with the number of transplanted cells, suggesting that a single colony was the product of a single cell clone. These cells also had the particularity of producing heterogeneous colonies of blood cells. The concept of HSC was born through the marking and tracking of clones and the discovery that all types of mature blood cells could arise from a single clone¹¹⁰⁻¹¹². HSCs are described as cells capable of producing any blood cell type while maintaining a stable pool of HSCs throughout the organism's life. Evidence showed that HSCs are heterogeneous in their capacity to repopulate blood cells in the long term¹¹³. This introduced the concept of long-term HSC (LT-HSC) and short-term HSC (ST-HSC). LT-HSCs are capable of repopulating blood cells of a recipient in the long term, a capacity that is preserved after serial transplantation. ST-HSCs are less persistent and lose their ability to repopulate blood cells over time, and the pool is eventually depleted after serial transplantation¹¹⁴. The term multipotent progenitors (MPP) is used when the self-renewal potential is reduced but the differentiation potential includes all lineages¹¹⁵. Phenotypic markers for the purification of HSCs were established¹¹⁶, including for LT-HSC^{115,117}. However, subsequent studies showed that LT-HSCs also represent a heterogeneous population of cells in regards to their repopulation kinetics and bias towards a particular lineage¹¹⁸⁻¹²⁰. Indeed, Sieburg et al. have determined, in mice, that long-term repopulating cells could be associated to 16 different kinetic profiles of repopulation when transferred to a new host. They state that these 16 profiles encompass all possible variations of repopulation kinetics observed in HSCs¹¹⁸. However, these profiles do not take into account what type of blood cell the HSCs produce. Dykstra et al. have shown that within the LT-HSCs, there were some LT-HSC that were skewed towards myelopoiesis or lymphopoiesis. They have defined 4 groups of LT-HSC according to their lineage-bias¹¹⁹. The LT-HSC population is characterised by a high frequency ($\approx 75\%$) of quiescent cells in G_0 of the cell cycle at a given time, although all cells will have entered the cell cycle in about 57 days¹²¹. Control of the cell cycle is crucial to avoid depletion of the HSC pool^{122,123}. The quiescence/activation regulation of HSCs is flexible, so that haematopoiesis can be adapted to supply more blood cells when a stress occurs¹²⁴.

1.3 Haematopoiesis in its anatomical context

1.3.1 Histology of the bone marrow

The main interest in the study of BM is understanding the relationship between HSCs and their environment. Haematopoiesis starts during embryonic life in the foetal liver and then migrates inside the bone marrow. The bone marrow is the major site of haematopoiesis in adult mammals. The bone marrow is the tissue inside the cavity of long bones (e.g. femur, tibia, humerus and hip bone). Most studies of the bone marrow are done in the femur of mice, being the most accessible and most abundant source of bone marrow in adults (**Figure 1-3**). The epiphysis is the extremity of the femur forming the joint with adjacent bones. The metaphysis sits beneath the epiphysis and is where longitudinal growth of the bone occurs. The diaphysis is the largest part of the bone, it is the middle, tubular shaped part that contains most of the marrow. The outer shell of the femur is called the cortical bone, or compact bone. Projections of the cortical bone inside the cavity form a “spongy” bone called the trabecular bone. The epiphysis and metaphysis are filled with trabecular bone, whereas the diaphysis is almost devoid of it. The bone is a surprisingly dynamic tissue, with cells constantly synthesising new bone and cells degrading it¹²⁵. The endosteum represents the interface between the bone and the bone marrow. It is composed of osteoblasts, cells responsible for the formation of new bone, and osteoclasts, which degrade it. The coupling of this formation and resorption is key to keeping the bone functional. Vasculature is really important in the bone marrow as many cells enter it but more importantly many are released. Haematopoiesis also requires a steady supply of nutrients and oxygen. Along the diaphysis run central arteries. From these thick arteries are derived sinusoids. Sinusoids grow from the centre of the bone marrow towards the endosteum and become gradually smaller. Venous circulation takes the form of a central sinusoid in which sinusoids coalesce^{126,127}.

However, until recently the combination of markers that enabled the identification of HSCs by flow cytometry was too complex for immunostaining. Breakthrough came through the discovery of a small subset of receptors belonging to the signalling lymphocytic activation molecules (SLAM) family that helps identify a small fraction of bone marrow cells containing all serially transplantable HSCs. The expression of CD150, in conjunction with the absence of staining for CD48 and CD41 enabled the *in vivo* analysis of HSCs. This revealed that HSCs were closely associated to the vasculature, as most cells were perivascular. In addition, recent transgenic mice expressing fluorescent protein associated with markers of stromal cells, such as Nestin, CXCL12, or Leptin receptor (Lepr) have provided useful insights into the spatial organisation of the bone marrow¹²⁸⁻¹³⁰.

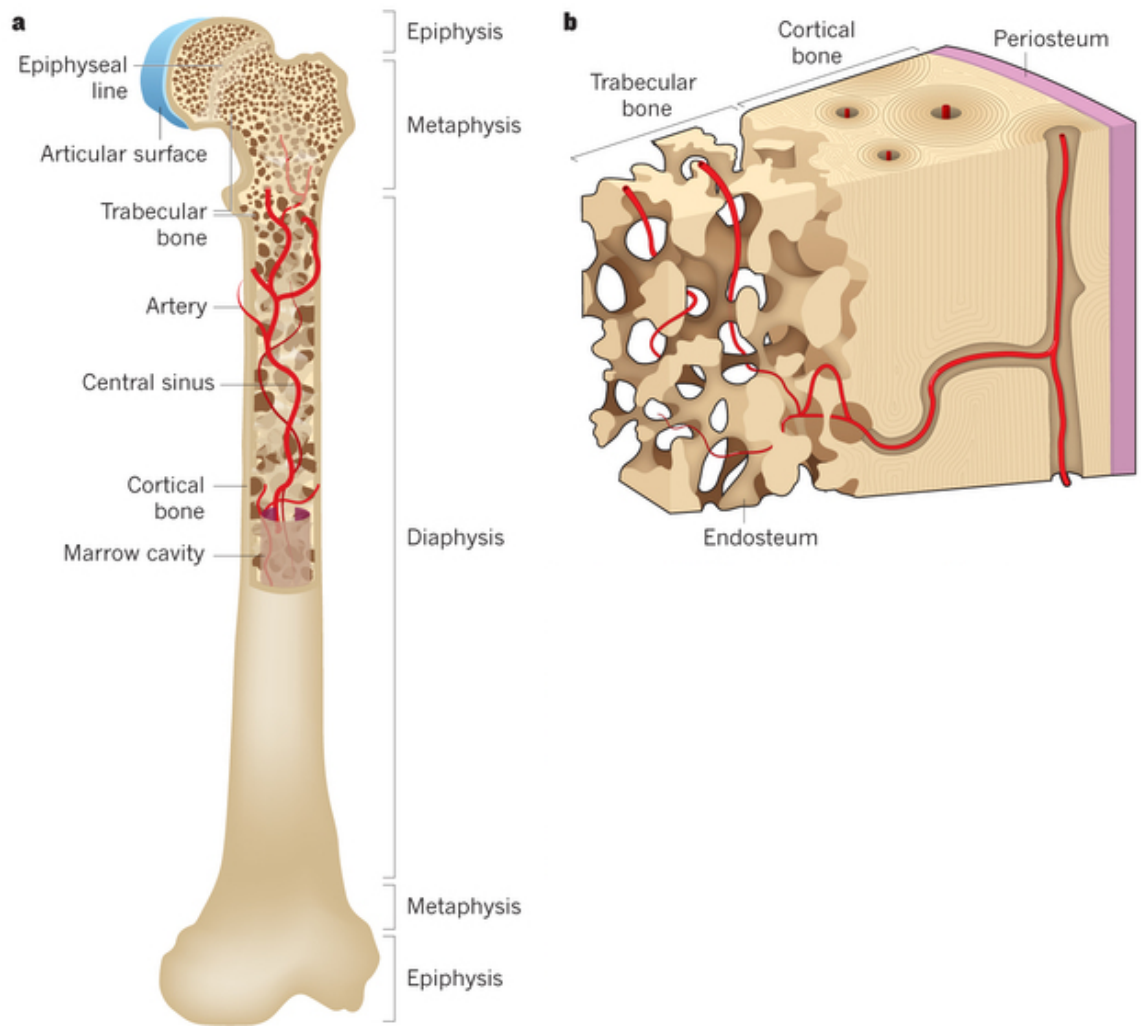


Figure 1-3. Anatomy of long bones. Adapted from Morrison and Scadden, Nature, Jan 2014¹²⁷.

1.3.2 The haematopoietic stem cell niche concept

The concept of niche refers to a specific microenvironment that participates in the development or normal function of cells. Till and McCulloch demonstrated that the bone marrow contained multipotent cells capable of forming haematopoietic colonies in the spleen¹⁰⁹. However, this ability was lost after serial transplantations¹³¹, which conflicts with the hypothesis that HSCs are long-term self-renewing cells capable of producing blood cells throughout the life of an individual. To reconcile the data from Till and McCulloch with this concept, Ray Schofield postulated that “the stem cell is seen in association with other cells which determine its behaviour”¹³². This initiated the concept of HSC niche, a microenvironment in the bone marrow preserving the long-term properties of HSCs. Studies of the differentiation and proliferation potential of HSCs confirmed that some of the properties that were observed following transplantation were lost *in vitro*¹¹⁹. The presence of haematopoiesis-supporting cells in the bone marrow was confirmed by Dexter et al., who successfully established long-term *in vitro* cultures that could maintain haematopoietic cells for several months¹³³. These cultures were derived from the bone marrow of mice and made of a heterogeneous population of cells. Dexter noted that “giant fat” cells were important in the maintenance of haematopoiesis; these non-haematopoietic cells would later be called stromal cells. This initiated the search for bone marrow stromal cells and the dissection of the haematopoietic niche *in vivo*.

The word stroma comes from the Greek word *strōma* meaning “coverlet”, referring to a fabric used to cover a bed. In animal biology, it has originally been used to describe the tissue not directly associated with the function of a given organ, as opposed to the parenchyma. In lymphoid organs, the stroma consists of all non-immune cells, such as fibroblasts or endothelial cells that support and regulate lymphocyte function. In haematopoietic organs, HSCs, haematopoietic progenitors and precursors form the parenchyma while other cells form the stromal compartment.

1.3.3 Molecular and cellular constituents of the HSC niche

The identified cellular constituents of the HSC niche so far include fibroblastic cells, endothelial cells, osteoblasts and macrophages. The niche acts by secreting factors or by cell-cell contacts with HSCs¹²⁷. It is a complex environment subject to several regulatory pathways, including signals from the central nervous system (CNS)¹³⁴.

The secreted stem cell factor (Scf) is one of the first niche-derived cytokines that was discovered. The gene encoding Scf is encoded by the *Sl* locus in mice and binds to its receptor *c-kit*^{135,136}, encoded by the white spotting (*W*) locus¹³⁷. Before any of these two molecules were characterised, evidence showed that mice with a mutation in the *W* or *Sl* loci had a reduced haematopoiesis, measured at the time by the formation of CFU-S^{138,139}. Bone marrow cells from *Sl*-mutant mice were able to form spleen colonies when transferred into irradiated wild-type mice and cure the anaemia of *W*-mutant mice. By contrast, transfer of wild-type bone marrow cells into irradiated *Sl*-mutant mice resulted in very little haematopoietic activity¹³⁹. Scf is produced by radio-resistant stromal cells in the bone marrow, while its receptor *c-kit* is expressed by HSCs. *c-kit* activation on HSCs triggers multiple cell signalling pathways¹⁴⁰. Notably, it activates the signal transducers and activators of transcription 3 and 5A (STAT3 and STAT5A) via recruitment of JAK2, a protein known to be mutated in many myeloproliferative disorders^{141,142}. Ultimately, these pathways enhance the self-renewal of HSCs through control of the cell cycle or of the viability. Another key factor of the HSC niche is the chemokine CXCL12. CXCL12 promotes the retention of HSCs in the bone marrow via signalling through the CXCR4 receptor^{143,144}. Depletion of CXCL12-producing cells in mice reduces the number of HSCs in the bone marrow¹³⁰.

The term mesenchymal stem and progenitor cells (MSPCs) is used for a specific population of stem cells found in the bone marrow capable of self-renewal, proliferation and differentiation into fibroblasts, osteoblasts, chondrocytes (cartilage cells), adipocytes and potentially other cell types¹⁴⁵. They are essential constituents of the HSC niche. Knock-in of GFP within the gene encoding CXCL12 highlighted a cell population called CXCL12-abundant reticular cells (CAR cells). These cells were characterised by long cytoplasmic processes and were physically associated with HSCs¹⁴⁴. Depletion of CAR cells in mice reduces the number of non-haematopoietic multipotent progenitors capable of differentiating into osteoblasts and adipocytes *in vitro*¹³⁰. This suggests that CAR cells are actually MSPCs. Purified Nestin-expressing (Nes⁺) cells in the bone marrow contain all the MSPC activity and express high levels of CXCL12¹²⁹. However, neither CXCL12 nor Scf from Nes⁺ cells are essential for HSC maintenance in the bone marrow^{128,146}. Lepr is another marker of MSPCs in the bone marrow. Lepr⁺ cells and endothelial cells produce both CXCL12 and Scf, the latter being essential since conditional deletion of Scf in Lepr⁺ cells depletes HSCs in the bone marrow¹²⁸. In most studies, MSPCs are described as perivascular cells, which correlates with the localisation of HSCs in the bone marrow¹²⁶.

Evidence has shown that sympathetic nerves in the bone marrow induce the mobilisation of HSCs by inhibiting CXCL12 expression¹³⁴.

CD169⁺ stromal macrophages have been shown to regulate the HSC niche in the bone marrow. Their depletion causes reduction of HSC-niche genes such as Cxcl12 and Scf in Nes⁺ cells and the depletion of HSCs in the bone marrow¹⁴⁷. These macrophages impose the circadian rhythm on CXCL12-expressing cells. Aged neutrophils express little CD62-ligand but up-regulate CXCR4. They are drawn to the bone marrow where they are phagocytised by stromal macrophages which in turn inhibit production of CXCL12 by CAR cells. CD169⁺ macrophages therefore synchronise the rhythm of neutrophil clearance (a circadian rhythm) with the rhythm of HSCs egress from the bone marrow¹⁴⁸.

1.4 Erythropoiesis

1.4.1 Erythropoietic progenitors and precursors

Erythropoiesis is the process through which erythrocytes or red blood cells (RBC) are produced from HSCs. The classical model of haematopoiesis involves a step-wise commitment to the erythroid lineage via differentiation into a CMP, then a megakaryocyte-erythrocyte progenitor (MEP) which can engage into the erythroid lineage or towards the production of platelets¹⁴⁹. However, it has been shown that progenitors with a potential restricted to red blood cell and platelet also derived directly from HSCs^{150,151}. The earliest known erythroid-only progenitors are called the erythropoietic burst-forming unit (BFU-E) and erythropoietic colony-forming unit (CFU-E)^{152,153}. These progenitors are observed in *in vitro* cultures of bone marrow or peripheral blood cells stimulated with erythropoietin (EPO), and can synthesise haemoglobin and mature into enucleated cells. The BFU-E have a higher proliferative potential than the CFU-E and are not as discrete as colonies, i.e. individual cells are less easy to discriminate from one another. The CFU-E derives from the BFU-E. Isolation of murine BFU-E and CFU-E is still challenging, although they can be enriched by negative selection¹⁵⁴⁻¹⁵⁶. In contrast, late erythroid precursors are more easily purified and morphologically identifiable. Using a combination of glycophorin A (Ter119) in conjunction with the transferrin receptor 1 (CD71) or the glycoprotein CD44, Chen et al. have resolved the 5 last stages of erythropoiesis¹⁵⁷ (**Figure 1-4**). The earliest precursor is the proerythroblast, which derives from the CFU-E. Proerythroblasts are characterised by a high expression of CD71 and a low but detectable expression of Ter119. Proerythroblasts then mature into basophilic erythroblasts, polychromatic erythroblasts, orthochromatic erythroblasts, reticulocytes and finally red blood cells. The expression of Ter119 increases from the proerythroblasts and stays high in mature erythrocytes.

Maturation of proerythroblasts is also associated with a progressive decline of CD71 and steady reduction of cell size.

Compared to other lineages, the erythroid lineage has been extensively studied because of its relative simplicity in regards to the molecular interactions involved in erythropoiesis. The earliest factor for the commitment of HSCs towards the megakaryocyte and erythrocyte lineage is the transcription factor GATA-1¹⁰². GATA-1 is necessary for the development of erythroid cells and is antagonised by another transcription factor called PU.1¹⁰². A single hormone is capable of skewing haematopoiesis towards the production of blood cells. This hormone is EPO and is found to be up-regulated during anaemia¹⁵⁸. The mechanism behind how EPO induces erythropoiesis is still unclear. Some studies suggest that EPO acts at the apex of the haematopoietic tree, and induces erythroid differentiation in MPPs¹⁵⁹ while other have shown that the formation of BFU-Es and CFU-Es was independent of EPO¹⁶⁰. EPO is also known to prevent cell death in erythroid progenitors¹⁶¹. At the molecular level, EPO has been shown to induce GATA-1 activation¹⁶². Studies show that PI3 kinase is an important adaptor in EPO signalling and is closely linked to EPO-induced expression of erythroid genes^{159,162}.

1.4.2 The niches of erythropoiesis

Erythropoiesis involves multiple stages of differentiation from the HSC to the mature erythrocytes. As erythropoiesis progresses, the cells have shifting requirements and therefore rely on different niches at different stages. The ligand of c-kit, expressed by stromal cells, is indispensable for erythropoiesis¹⁶³. In mice, mutations in the W of SI loci, respectively coding for c-kit and its receptor, cause anaemia from the embryo stage^{139,163}. The interaction of c-kit with its ligand is known to promote survival and self-renewal of the erythroid progenitors, in collaboration with EPO^{164,165}. However, c-kit is gradually down-regulated in the later stages of erythropoiesis and is not detectable¹⁶⁶. The expression of c-kit inversely correlates with that of Ter119 and is no longer detectable after the basophilic erythroblast stage. Scf has been shown to be expressed by endothelial cells and Lepr+ perivascular cells. As a consequence, earlier stages of erythropoiesis are dependent on the perivascular niche.

More than 50 years ago, the French haematologist Marcel Bessis made an observation that macrophages from the bone marrow were in close contact with erythroblasts¹⁶⁷. He coined the term “erythroblastic island” for a macrophages surrounded by erythroblasts and described it as a functional unit of the bone marrow. Macrophages were shown to associate with erythroid cells from the CFU-E stage^{168,169}. At the CFU-E stage, erythroid

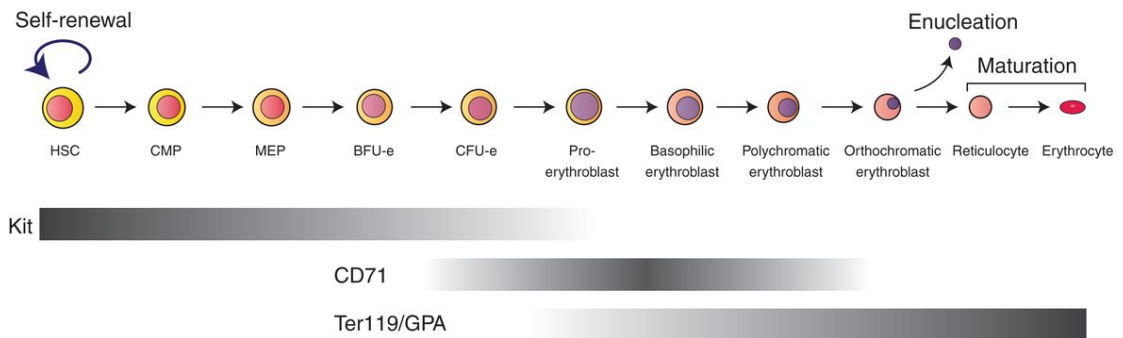


Figure 1-4. Markers of erythropoiesis. The burst-forming unit-erythroid (BFU-E) is the first progenitor restricted to erythropoiesis only. It is followed by the colony-forming unit-erythroid (CFU-E). Both can be identified by colony-formation assay and express the c-Kit receptor. CD71 is expressed early during erythropoiesis and disappears after the pro-erythroblast stage. Ter119 expression starts later on but remains on mature erythrocytes. The transcription factor GATA-1 is expressed during all stages of erythropoiesis. Reproduced from Dzierzak, and Philipsen, Cold Spring Harb Perspect Med, Apr 2013¹⁷⁰.

progenitors still respond to Scf derived from perivascular stromal cells,¹⁶⁶ suggesting that at some stage of erythropoiesis, progenitors are likely to rely on signals from both the HSC niche and the erythroblastic island. Stromal macrophages express several molecules mediating adhesion with erythroblasts, such as the erythroblast macrophage protein (Emp)¹⁷¹, the vascular cell adhesion molecule 1 (VCAM-1) which interacts with the very late activation antigen 4 (VLA-4) expressed by erythroid cells¹⁷² or the alpha V integrin which binds to ICAM-4¹⁷³. The role of erythroblastic island macrophages is unclear. One function appears to be the erythroid precursors' nuclei phagocytosis¹⁷⁴. Genetic inactivation of Emp is lethal in the embryo and associates with an increase in nucleated erythrocytes¹⁷⁵. Crocker et al. have identified a stromal macrophage-restricted marker called sheep erythroid receptor 4 (SER-4) at the time^{176,177}. It was later re-named sialoadhesin or sialic acid-binding immunoglobulin-type lectin 1 (Siglec-1, CD169). The deletion of CD169⁺ cells was shown to dramatically reduce bone marrow erythropoiesis in adult mice¹⁴⁷. In vitro, stromal macrophages promote proliferation of splenic CFU-E in a contact dependent rather than EPO dependent way¹⁷⁸.

1.4.3 Erythropoiesis and iron homeostasis

The role of red blood cells is to distribute dioxygen (O₂) and collect carbon dioxide (CO₂) throughout the body. Gas exchange is centralised in the lungs, hence the need for a distribution/collection system. RBC encapsulate haemoglobin (Hb), a large polypeptide made of 2 α -globin chains and 2 β -globin chains. Each chain is associated non-covalently with a heme, a cofactor made of a porphyrin containing ferrous iron (Fe²⁺). The Fe²⁺ ions are where gases bind, except for CO₂, which binds to amino-terminal residues of Hb. Iron is therefore essential for the function of RBC. Haemoglobin synthesis starts early during erythropoiesis and requires a steady supply of iron. Iron is transported as ferric ions (Fe³⁺) in the blood associated with the protein transferrin¹⁷⁹. A key molecule of erythropoiesis is the transferrin receptor 1 (TfR1 or CD71)¹⁸⁰. It is responsible for the interaction of erythropoietic cells with transferrin¹⁸¹. TfR1 is expressed at the surface of immature erythropoietic progenitors and precursors from the CFU-E stage to the reticulocyte stage. It binds iron-bearing transferrin and is then internalised by endocytosis¹⁸². The resulting endosome is acidified, iron is freed from the transferrin and exit the endosome through the Nramp2 (DMT1) transporter¹⁸³. The cytoplasmic Fe²⁺ will then be used for heme synthesis.

The liver acts as a key regulator of systemic iron availability. Hepatocytes produce a small peptide hormone called hepcidin¹⁸⁴. Hepcidin has been shown to bind to ferroportin¹⁸⁵.

Ferroportin exports iron from the cells and animals deficient in ferroportin accumulate iron inside macrophages, enterocytes, hepatocytes and adipocytes¹⁸⁶. Binding of hepcidin to ferroportin causes internalisation and degradation of the complex¹⁸⁵. Therefore, hepcidin induces iron retention in ferroportin-expressing cells, causing a decrease of available iron¹⁸⁷. Overexpression of hepcidin in mice decreases the stock of available iron¹⁸⁷. Because of the importance of iron in the biogenesis of haemoglobin and production of erythrocytes, as described previously, regulation of hepcidin expression has quickly been linked to anaemia and hypoxia¹⁸⁸. To compensate for anaemia and hypoxia, the body stimulates erythropoiesis, which involves an increase need in available iron. As a consequence, hepcidin expression is down-regulated in response to these two stresses¹⁸⁸.

1.5 Platelets and haemostasis

1.5.1 Anatomical description of platelets and their origin

Platelets are anucleate cells that circulate in the blood and are involved in haemostasis. Haemostasis refers to the mechanisms through which bleeding is stopped. They are smaller than any other blood cell. For example, in this study, the average platelet volume of 10-12 week old C57BL/6 mice was measured at 4.3femtoliter (fl). As a mean of comparison, the volume of RBC was 52fl. Priming towards the production of platelets may occur straight from the HSC stage^{106,150,151}. A recent study has demonstrated that a thrombopoietin (TPO)-dependent population of HSCs primed for megakaryopoiesis was present in the bone marrow of mice¹⁵⁰. Platelets derive from megakaryocytes, giant cells found in the bone marrow and to a certain extent in the lungs. Megakaryopoiesis refers to the production and maturation of megakaryocytes. Thrombopoiesis refers to the production of platelets from megakaryocytes. Little is known about thrombopoiesis *in vivo* but recent data have provided valuable insights¹⁸⁹. The prevalent model of thrombopoiesis is the proplatelet model (**Fig 1-5**). Megakaryocytes in the bone marrow extend pseudopodial processes in the bone marrow vasculature through the endothelium. These cytoplasmic processes are called proplatelets and are released into the circulation. However, freshly released proplatelets were found to be bigger than blood platelets, indicating that proplatelets are further fragmented after release. It is thought that the pulmonary vasculature is where the shedding of proplatelets occurs¹⁹⁰.

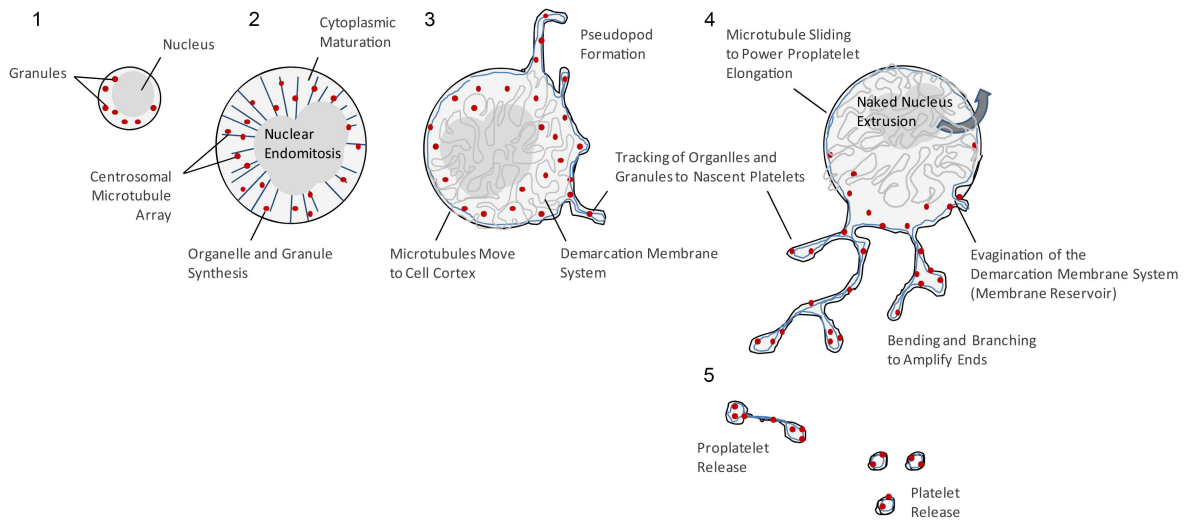


Figure 1-5. Mechanism of platelet release from megakaryocytes. Adapted from Thon et Italiano, *Semin Hematol*, Jul 2010¹⁹⁰.

1.5.2 The coagulation cascade

Coagulation is the process aiming at stopping blood leaving the circulation, a haemorrhage, following a vascular injury (**Fig 1-6**). The process of coagulation can be divided into 3 steps: the initiation, the amplification and the propagation. The initiation phase is triggered by damages to the vasculature and exposition of extravascular cells. Most extravascular cells express tissue factor (TF) on their surface. The coagulation factor VII (FVII) is usually physically separated from TF-expressing cells by the endothelium. Vasculature damage results in formation of the TF:activated FVII (FVIIa) complex which triggers a cascade called the extrinsic pathway, resulting in the activation of the platelet-bound FIXa:FVIIIa complex. The FIXa:FVIIIa complex amplifies the coagulation process by activating another platelet-bound complex called prothrombinase. Prothrombinase can be activated by an alternative pathway triggered by collagen detection by platelets via the glycoprotein VI (GPVI)¹⁹¹. Prothrombinase converts prothrombin into thrombin, an enzyme which catalyses the conversion of fibrinogen into fibrin. Molecules of fibrin coalesce into a gel that participates in the clot formation. Thrombin further activates platelets at the site of injury. During the propagation phase, activated platelets recruit and activate more platelets. Coagulation results in formation of a clot mostly made of platelets embedded in a fibrin matrix. Importantly, haemostasis is complete by repair of vascular damage and lysis of the clot^{192,193}.

1.5.3 Homeostasis of platelets

The number of circulating platelets can vary greatly between individuals. Interestingly, individuals with lower platelet counts have higher mean platelet volumes (MPV). Throughout life, the platelet count of one individual is constant. However, certain conditions can affect the number of circulating platelets. In such events, the body then preserves the platelet mass and not the platelet count. Indeed, it has been shown that in response to thrombocytopenia, the average volume of platelet increases¹⁹⁴.

TPO and its megakaryocyte-specific receptor myeloproliferative leukaemia protein (Mpl) are the main regulators of platelet production¹⁹⁵. TPO induces megakaryopoiesis¹⁹⁶. Regulation of TPO production occurs at multiple levels. TPO is produced in the liver and the kidney in a physiological state. The expression of TPO in the steady state is negligible in the bone marrow, but it is strongly expressed by bone marrow stromal cells following thrombocytopenia¹⁹⁷. Platelets are negative regulators of TPO levels. They express the Mpl receptor and capture circulating TPO, causing its degradation. The amount of circulating TPO is determined by the balance between TPO production and destruction. As a

consequence, a decrease in platelet count causes a reduction of TPO destruction and an increase of circulating TPO. The balance is re-established when the number of platelets returns to normal values. There are exceptions to this model however, in which immune destruction of platelets does not increase TPO levels¹⁹⁸. More recently, a novel pathway of TPO regulation in the liver has been reported. Hepatocytes are known to secrete TPO constitutively¹⁹⁷ but regulators of steady-state TPO production in the liver are unknown. Platelets lifespan is determined by their content in sialylated surface glycoproteins. Sialic acid residues are progressively lost on platelets. Desialylated glycoproteins are recognised by liver macrophages and hepatocytes, which phagocytise and clear old platelets¹⁹⁹. The Ashwell-Morell receptor (AMR) is expressed in the liver and binds desialylated platelets. Activation of the AMR leads to activation of the JAK2-STAT3 signalling pathway and up-regulation of TPO production by hepatocytes²⁰⁰.

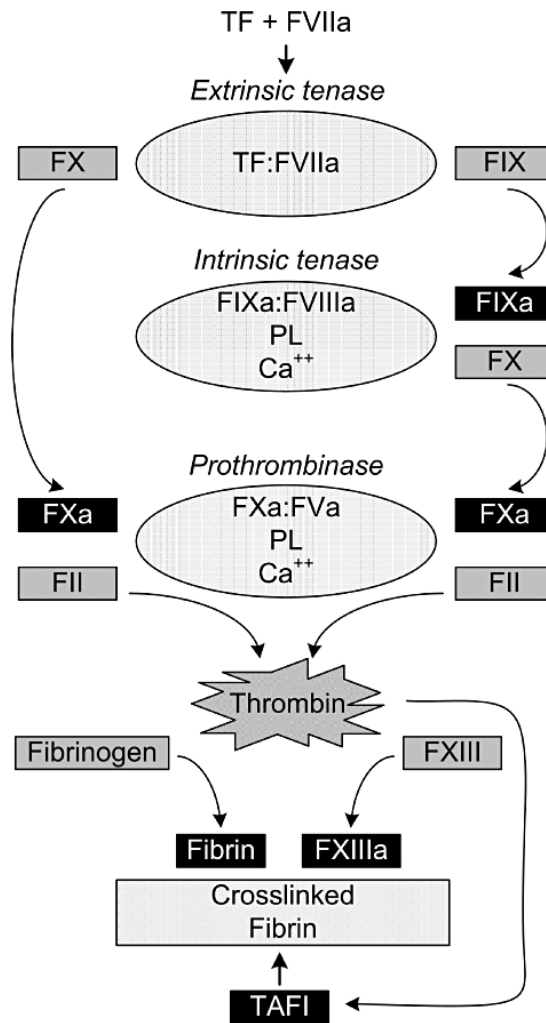


Figure 1-6. The coagulation cascade. The initiation phase starts with the exposure of sub-endothelial cells expressing the Tissue Factor (TF). The Factor VII (FVII) forms an activated complex with TF called the extrinsic tenase. The extrinsic tenase triggers the formation of the FIXa:FVIIIa complex (intrinsic tenase) on the surface of platelets. Both tenase complexes participate in the activation of prothrombinase. Prothrombinase activates Thrombin, which in turns catalyses the formation of Fibrin fibers from Fibrinogen. Thrombine-activable fibrinolysis inhibitor (TAFI) protects the clot from fibrinolysis. The clot result from the crosslinking of fibrin fibers. PL = platelet. Adams and Bird, Nephrology (Carlton), Aug 2009¹⁹².

1.6 Infectious diseases and haematological disorders

Very little is known about the pathology of haematological disorders in the context of VL. For this reason, it is necessary to look at other models to understand pathological perturbations of blood cells and haematopoiesis. In most models, anaemia is the most studied haematological disorder.

Malaria is probably the best known parasitic infection causing anaemia. It is caused by the parasite *Plasmodium falciparum* (*P. falciparum*), which infects RBC. It is the first cause of acquired RBC disorder. Contrary to VL, where macrophages are infected, *P. falciparum* is an intracellular parasite of mature RBC and directly affects their physiology. Notably, the *P. falciparum* modifies the membrane of RBC and is able to translocate proteins from the parasite to the surface of the RBC²⁰¹. The protein P falciparum erythrocyte membrane protein 1 (pfEMP1), when expressed at the surface of erythrocytes, causes them to adhere to the endothelial cells of the blood vasculature and stop circulating²⁰². Parasites replicate inside RBC and cause their direct lysis. Anaemia of malaria is very complex and multifactorial⁹². While parasites cause direct destruction of RBC, erythropoiesis is altered as well. Another product of *P. falciparum*, called P. falciparum Hemozoin (pfHz), has been shown to be phagocytised by monocytes and causes erythropoiesis suppression in the bone marrow^{203,204}. pfHz can induce apoptosis in erythroid precursors²⁰⁵.

Trypanosomiasis is another infectious disease causing anaemia. Here also anaemia is multifactorial. One major cause seems to be the peripheral destruction of RBC by macrophages, notably in the spleen²⁰⁶. *Trypanosoma cruzi*, the causative agent of sleeping sickness, secretes a haemolysin, a molecule capable of lysing erythrocytes by forming pores in the cell membrane²⁰⁷. In addition to direct lysis of erythrocytes, Trypanosomiasis causes auto-immune lysis of RBC and platelets^{208,209}. Incorporation of parasite-derived proteins into the membranes of the host's cells is thought to accentuate destruction of RBC by the immune system²¹⁰. Erythropoiesis in the bone marrow of mice infected with *Trypanosoma brucei* was also suppressed because of local nitric oxide production²¹¹. Anaemia of trypanosomiasis is linked to up-regulation of TNF α and IFN γ while IL-10 has protective effect by countering pro-inflammatory cytokines²¹².

A non-specific cause for anaemia in chronic infectious disease is iron deficiency. Interleukin-6 (IL-6) is a pro-inflammatory cytokine which up-regulate hepcidin expression in the liver²¹³. As described above, hepcidin induces internalisation of ferroportin on macrophages, causing iron to be sequestered inside these cells and no longer available¹⁸⁵. Chronic inflammation and chronic IL-6 production can therefore cause anaemia by

preventing the synthesis of haemoglobin which requires iron. In addition to IL-6, IFN δ and TNF α can cause retention of iron inside monocytic cells by up-regulating the expression of DMT1 on the cell surface and causing iron retention inside these cells²¹⁴. Anaemia of chronic disease is characterised by altered erythropoiesis producing fewer and bigger erythrocytes⁸⁸.

The *Salmonella* Typhimurium murine infection model recently provided further insights into inflammation-induced thrombocytopenia. The authors of the study have shown that innate inflammation triggers the local formation of blood clots in the liver. This process does not depend on the presence of the bacteria but is dependent on IFN δ , which induces the expression of podoplanin on monocytes and Kupffer cells in the liver²¹⁵. Platelets interact with podoplanin via the C-type lectin-like receptor (CLEC-2), which induces coagulation^{216,217}. This process does not require signalling through GPVI. Thrombosis in mice infected with *Salmonella* correlates with the number of circulating platelets²¹⁵. Thrombocytopenia is also commonly associated with liver dysfunction²¹⁸. The liver is the main source of TPO with the kidney¹⁹⁵, and it has been shown to be essential in regulation of platelet turnover, by binding and degrading old platelets and producing more TPO through the AMR²⁰⁰. Hepatitis C virus (HCV) causes fibrosis of the liver which has been associated with thrombocytopenia^{219,220}.

These infectious diseases provide insights into how parasites can cause haematological alterations. Interestingly, anaemia is the most studied haematological aspect in the context of parasitic infections. They also highlight how complex haematological studies are, since most defects are multifactorial.

1.7 Summary and aims

Visceral leishmaniasis is a complex infectious disease associated with intracellular parasitism of mononuclear phagocytes in the spleen, the liver and the bone marrow. The immune response to *Leishmania spp.* is relatively well understood. However, the disease is consistently associated with haematological disorders in patients, in dogs, in cats and in some experimental models. The disease can lead to anaemia, thrombocytopenia, leukopenia or all three deficit combined, pancytopenia. Yet the mechanisms for haematological disorders associated with VL are still unclear. They are often linked to hypersplenism or dysregulation of iron homeostasis, haemophagocytosis and ineffective haematopoiesis. These mechanisms however have not been thoroughly dissected due to the lack of an experimental model. Mice, the most commonly used model in biomedical research, do not develop overt symptoms when compared to the human disease and has hardly been used for haematological studies. Study of other models of infectious diseases which commonly cause haematological disturbances, especially anaemia, can provide useful insights into potential causes for cytopenia in VL.

The main hypothesis of this work is that the experimental mouse model of VL can be used to provide insights into the mechanisms responsible for haematological alterations in the human disease. Despite the absence of clinically relevant symptoms in mice chronically infected with *L. donovani*, we aim at improving the knowledge about haematological aspects of VL using this model. A better understanding of the haematological aspects of VL would help a) improve treatment of patients b) recognising signs of VL from blood analysis. The latter would be useful as sometimes not yet diagnosed patients with VL have haematological disorders and are treated for something else (e.g. myelodysplasia³).

Chapter 2 Material and methods

2.1 Mice

All animal procedures were performed under UK Home Office License (Ref # PPL 60/4377) in accordance with the Animals (Scientific Procedures) Act 1986 (revised under European Directive 2010/63/EU). All regulated procedures received approval from the Animal Procedures and Ethics Committee of the Department of Biology, University of York. Mice were housed in a pathogen-free Category 3 facility with an artificial 12-hour day/night cycle and fed a standard diet for rodent and water *ad libitum*. Unless stated otherwise, experiments were performed using C57BL/6 mice bred in-house. Experiments were performed on 6-8 week old animals.

Cxcl12^{tm2.1Sjm/J²²¹} (CXCL12^{DsRed} reporter) mice were purchased from The Jackson Laboratory as heterozygotes and were crossed with C57BL/6 because homozygotes are non-viable. This is due to the insertion (knock-in) of the DsRed-encoding cassette within the endogenous CXCL12 locus, rendering this copy of the CXCL12 gene non-functional. Litters were genotyped after weaning by a qPCR reaction amplifying the DsRed gene from a digested ear tissue sample.

Fluorescent reporter mice for *in vivo* analysis of T cells were kindly provided by Mark Coles. Expression of the green fluorescent protein (GFP) and DsRed is restricted to T cells and NK cells in the hCD2.GFP and hCD2.DsRed, respectively²²².

Splenectomised C57BL/6 mice were purchased from Charles River. Mice were 6-7 week old at the time of surgery. The wounds were closed with clips and mice were kept in Charles River for two weeks post surgery to allow wound healing and clip removal before shipment. Mice were placed into the Category 3 facility on delivery and were allowed 1 week to adapt to their new surroundings before starting a procedure.

Because haematopoiesis is highly regulated under the circadian rhythm, all animals were killed between 7am and 9am in order to obtain consistent results.

2.2 Experimental Visceral leishmaniasis

All experiments were performed with the Ethiopian strain of *L. donovani* (LV9 and LV9-tdtomato²²³). Amastigotes were maintained by passage in B6 RAG2^{-/-} mice deficient for the recombination-activating gene 2 (RAG2). Passage mice were euthanized by CO₂ asphyxiation before dissection. Freshly isolated spleens were crushed using a sterile glass homogeniser into a single-cell suspension and washed in Roswell Park Memorial Institute

medium (RPMI, Thermo Fisher Scientific, Waltham, MA, USA). The suspension was transferred into a 50ml falcon and dense debris were pelleted by centrifugation at 140g for 5min. The supernatant containing splenocytes was incubated in Saponin (0.125% (w/v) in RPMI) for 5min at room temperature (RT) with regular agitation. This step induces permeabilization of cell membranes and allows parasites to leave the host cells. Parasites were pelleted by centrifugation at 2000g for 10min, the supernatant was discarded and they were washed another three times in RPMI. Parasite number was evaluated using a Thoma counting chamber. Freshly isolated *L. donovani* amastigotes were suspended at a concentration of 1.5×10^8 amastigotes/ml in RPMI. Mice were injected with 200 μ l of parasite preparation (3×10^7 amastigotes) intravenously via the lateral tail vein.

2.3 Estimation of parasitemia

Spleens freshly isolated were cut in half and dried on paper. Imprints were performed on Superfrost slides (Thermo Fisher Scientific). Slides were air-dried, fixed in methanol and stored in dry conditions until further use. For estimation of parasite load, the slides were stained for 30mins in a Giemsa solution, rinsed in tap water and air-dried. For each sample 1000 nuclei were counted on random fields of view. Amastigotes were counted in each field of view based on their morphology. Splenic parasitemia was expressed in Leishman-Donovan units (LDU) where $LDU = \text{number of amastigotes} / 1000 \text{ nuclei} \times \text{spleen weight (in grams)}$.

2.4 Administration of granulocyte-colony stimulating factor-neutralising antibody

Mice were infected with *L. donovani* for 6 weeks. Each mouse received a daily dose of 25 μ g of anti-granulocyte-colony stimulating factor (G-CSF) antibody (cat no. MAB414, R&D Systems, Minneapolis, MN, USA) diluted in phosphate buffered saline (PBS). The antibody was administered by intra-peritoneal injection.

2.5 Administration of thrombopoietin

2.5.1 Randomisation of mice

All experimental mice were tagged with p-Chips (PharmaSeq, Monmouth Junction, NJ, USA) to avoid selection bias. The chips were implanted subcutaneously in the tail prior to the experiment. The chips are identified by the PharmaSeq Wand which activates the chips with a 660nanometer (nm) laser and returns unique 9-digit numbers. The tag number of each animal was recorded in an electronic spreadsheet. Randomisation of treatment was

performed as described in **Figure 2-1**. At the time of treatment, each mouse was picked individually, identified by its tag number and administered the treatment accordingly.

2.5.2 Injection of recombinant human thrombopoietin

Recombinant human thrombopoietin (rhTPO; ZymoGenetics, Seattle, WA, USA) was provided by Dr Ian Hitchcock, University of York. rhTPO was diluted in PBS in concentrations ranging from 5 μ g/ml to 10 μ g/ml, and mice were treated for 5 consecutive days (100 μ l administered by intraperitoneal injection). Naïve or infected mice, treated or not with TPO as above, were killed 5 days after the end of rhTPO administration, and parameters associated with blood and splenic response were measured as described in Chapter 4.

2.6 Blood collection and analysis

Mice were anaesthetised by inhalation with isoflurane prior to blood collection. After induction of anaesthesia in a closed chamber, mice were placed on their back. A mix of isoflurane and oxygen was continuously supplied through a mask attached to the nose of the animal. Deep anaesthesia was confirmed by absence of withdrawal reflex when gently pinching the hind feet. 1ml syringes with 19-gage needles were coated with a Citrate-dextrose solution (ACD, Sigma-Aldrich Company Ltd., Dorset, UK). A negligible amount (<50 μ l) of ACD remained in the dead volume of the syringe. Blood was collected from terminally anaesthetised mice by insertion of the needle into the heart and slowly drawing back blood. When no more blood could be withdrawn, the needle was removed and the syringe depressed slowly to transfer the blood into EDTA-coated Vacutainer (BD, Franklin lakes, NJ, USA). Because the blood was used for platelet counting, caution was taken not to cause too much shear stress, which can activate platelets and make the counts inaccurate. The whole blood was kept in the Vacutainer at RT until analysis since cold temperatures can also alter the platelet counts. The blood analysis was performed with a Hemavet 950FS (Drew Scientific, Miami Lakes, FL, USA). To assure accuracy of the device, a blank (empty) sample and a control of known values were analysed before each experiment.

1. record tag list

Tag	
287024646	
286922498	
287003829	
286987385	
286987911	
286947090	
287069878	
286971063	
286934798	
287070112	

5. associate tag with randomised list

Tag	Treatment
287024646	TPO
286922498	TPO
287003829	PBS
286987385	PBS
286987911	TPO
286947090	TPO
287069878	TPO
286971063	PBS
286934798	PBS
287070112	PBS

2. generate list of experimental conditions

Treatment	Random number
TPO	0.65381832
TPO	0.580023954
TPO	0.513021022
TPO	0.33154258
TPO	0.231128521
PBS	0.984975177
PBS	0.366938162
PBS	0.765135181
PBS	0.338307318
PBS	0.750669031



Treatment	Random number
TPO	0.231128521
TPO	0.33154258
PBS	0.338307318
PBS	0.366938162
TPO	0.513021022
TPO	0.580023954
TPO	0.65381832
PBS	0.750669031
PBS	0.765135181
PBS	0.984975177



3. associate randomly generated number

4. sort list according to numbers (descending/ascending order)

Figure 2-1. Workflow for the randomisation of mice prior to rhTPO administration. Random numbers were generated with the function RAND integrated in the Excel software (Microsoft, Redmon, CA, USA).

2.7 Plasma collection

Blood was collected as described previously. It was decided to use plasma rather than serum since blood samples were used for haematological analysis and should not be clotted. The fraction of whole blood for plasma preparation was kept on ice until use. Plasma was separated from the cellular fraction by centrifugation for 10min at 1500g. The clear supernatant was transferred to a separate tube and kept at -80°C until use.

2.8 Isolation of bone marrow cells

After killing mice, the hind legs were thoroughly washed with 70% ethanol. An incision was made from the ankle upwards and the skin was peeled back. Muscles and ligaments were removed with scissors and the feet cut off. The femurs were gently pulled from their socket at the hip joint. Femur and tibia were separated by cutting the knee joint and opened at both ends to expose the bone cavity. The bone marrow plug was flushed with the wash buffer made of PBS 1% foetal calf serum (FCS) using a 25-gauge needle through a 70µm cell strainer. Cell strainers were thoroughly rinsed with wash buffer. Single cell suspensions were washed by centrifuging 5min at 300g and suspending the pellet in fresh buffer. Red blood cells were lysed with Ammonium-Chloride-Potassium (ACK, Sigma-Aldrich) buffer for 5min at RT, nucleated cells were subsequently counted using a Vi Cell XR Cell Counter (Beckman Coulter, Pasadena, CA, USA).

2.9 Isolation of splenocytes

Spleens were removed and cleaned from any surrounding adipose tissue. They were placed on 70µm cell strainers and crushed through with the plunger of a syringe. The strainers were washed thoroughly with PBS 1% FCS (wash buffer) and the cell washed by centrifuging 5min at 300g and suspending the pellet in fresh buffer. Red blood cells were lysed with ACK buffer for 5min at RT, nucleated cells were subsequently counted using a Vi Cell XR Cell Counter (Beckman Coulter).

2.10 Fluorescence microscopy

2.10.1 Preparation of femurs for immunohistochemistry

Femurs were isolated and cleaned to remove excessive tissue then fixed overnight at 4°C in Periodate-lysine-paraformaldehyde fixative (10mM sodium Periodate dissolved in three parts 0.1M lysine-HCl 0.1M Na₂HPO₄ and one part 20% (w/v) paraformaldehyde) and decalcified for 3 days at 4°C with slow agitation in 10% EDTA, 0.1M Tris, pH6.95. Bones were transferred in 30% sucrose in PBS for a final overnight incubation at 4°C then

embedded in Optimal Cutting Temperature (OCT™) compound (Sakura Finetek Europe, Alphen aan den Rijn, The Netherlands) in Cryomolds® (Sakura Finetek Europe) and snap-frozen on dry ice. Frozen bones were kept at -80°C until required. Femoral 5µm-sections were cut using a CM1900 cryostat (Leica Microsystems, Wetzlar, Germany) onto Polysines® slides (Thermo Fisher Scientific), air-dried for at least 30min at RT and stored at -20°C until further use.

2.10.2 Preparation of spleens for immunohistochemistry

To avoid an anatomical bias between samples, a transversal fragment of the spleen was cut from the middle of the organ. They were placed into Cryomolds® and covered in OCT™. The samples were frozen on dry ice and transferred at -80°C until further use. Transversal 5µm spleen section were cut on a CM1900 cryostat and onto Polysines® slides (Thermo Fisher Scientific), air-dried for at least 30min at RT and stored at -20°C until further use. On the day of the staining, the slides were thawed and covered in ice-cold acetone for 10min to fix the tissues then air-dried.

2.10.3 Immunohistochemistry

Sections were blocked in staining buffer (PBS, 0.05% (w/v) bovine serum albumin (BSA), 5% serum of the same source as the secondary antibody) for 1h at RT. Excess buffer was removed from the slides before adding primary antibodies at the appropriate dilutions in staining buffer for 1h at RT or overnight at 4°C. Slides were washed three times 5min in washing buffer (PBS 0.05% (w/v) BSA) and secondary antibodies or streptavidin conjugates were applied in staining buffer at the appropriate dilutions for 1h at RT. Slides were washed three times 5min in washing buffer, counterstained with 4',6-diamidino-2-phenylindole (DAPI; 1µg/ml in washing buffer) and wash one more time when necessary. Sections were mounted in ProLong® Gold antifade reagent (Thermo Fisher Scientific), cured overnight and sealed before imaging. Antibodies for immunohistochemistry are listed in **Table 2-1**.

2.10.4 Confocal imaging

Confocal images were obtained using LSM780 or LSM710 systems (Leica Microsystems) using the ZEN software. Tissues were scanned sequentially with different lasers (405nm, 488nm, 561nm, 633nm) to avoid any emission overlap between fluorochromes. The pinhole was set to 1 airy unit in the highest-wavelength laser and adjusted for the other lasers in order to capture the same thickness in each channel. The images were taken at optimal resolutions where the size of a pixel corresponds to the smallest object that can be

resolved, as determined by the software. Contrast levels were adjusted post-acquisition to enhance images. The same post-treatment was applied to all images within one experiment.

2.10.5 Epifluorescence imaging

Imaging of whole spleen sections was performed with an automated AxioScan.Z1 slide scanner (Zeiss). The optimal focus was determined based on the DAPI staining. To ensure a sharp image and correct potential inclination of the slide or sample, the optimal focus was re-measured regularly throughout a scan. Tissues were illuminated sequentially with LEDs and reflected fluorescence was recorded by an Orca Flash 4 camera (Hamamatsu, Hamamatsu City, Japan) through a 20x objective.

2.10.6 Whole-mount microscopy

A femur from a mouse infected with the LV9-tdTomato strain was prepared as described previously until the sectioning step. A femur embedded in OCT™ was cut longitudinally using a cryostat until the bone marrow cavity was visible on both sides. The femur was then washed in PBS to remove the excess of OCT™. All following steps were performed at 4°C. The thick section was incubated overnight in blocking buffer (PBS 0.2% Triton 1% BSA, 10% goat serum). The following day, it was transferred in blocking buffer containing a rabbit anti-laminin antibody (Sigma-Aldrich) diluted 1/50 and incubated for 3 days. After primary antibody labelling, the sample was washed overnight in PBS. It was then incubated with the secondary antibody (Alexa Fluor® 488 goat anti-rabbit IgG), at a 1/50 dilution in blocking buffer overnight. It was washed 3 times for 10min in PBS with agitation and transferred to an 80% (v/v in water) glycerol solution for a final overnight incubation. The glycerol solution acts as a clearing agent, allowing light to penetrate deeper into the tissue as well as more light out of the tissue. It was chosen over different clearing agent such as benzyl-alcohol benzyl-benzoate (BABB) because the latter can reportedly cause reduction of emission from fluorescent proteins, although it is more efficient in clearing tissues. The sample was sealed between two glass coverslips in 80% glycerol and imaged on a Zeiss LSM780 confocal microscope. To allow deeper penetration, a multiphoton laser was used with an excitation wavelength of 870nm.

2.11 Haematoxylin-eosin staining

Sections were prepared as described for immunocytochemistry. They were air-dried for several minutes to remove moisture. The slides were immersed in a filtered Harris Haematoxylin solution for 5min at RT and rinsed in cool running H₂O for 5min. They were then placed in

a tray and dipped in 0.5% Eosin (dissolved in 95% ethanol) 12 times. The excess eosin was removed by dipping in distilled H₂O repeatedly until no more eosin could be seen dissolving into the water. The tray containing the slides was dipped into a bath of 50% ethanol 10 times, then 70% ethanol 10 times. Slides were finally left in 95% ethanol for 30sec and pure ethanol for 1min. Slides were left to air-dry then mounted in DPX mounting medium (VWR) under glass coverslips.

2.12 Flow cytometry

2.12.1 Sample preparation

Cells were prepared as described previously. They were then concentrated or diluted to a concentration of 2×10^7 cells/ml in PBS 1% FCS (staining buffer). Unspecific binding of antibodies to Fc receptors was blocked by incubating cells with a purified anti-mouse CD16/32 antibody (Fc Block, eBioscience Ltd., Hatfield, UK) for 10min on ice (1/500 dilution in staining buffer). Cells were washed and plated in a round-bottom 96-well plate. A 2X antibody mix was prepared in staining buffer. The 2X mix was added to the cells at a 1:1 ratio for a final concentration of 1×10^7 cells/ml. The plates were placed in the dark at 4°C for 30min. Cells were then spun for 10min at 300g at 4°C and suspended in 200µl fresh staining buffer. The operation was repeated twice to thoroughly wash the unbound antibodies. In cases where cells fluorescence was not acquired on the same day, cells were fixed with 100µl 2% paraformaldehyde (PFA) in PBS. Plates were incubated for 10min at 4°C and an additional washing step was done. Cells were washed and analysed on a Cyan flow cytometer (Beckman Coulter).

2.12.2 Flow cytometry data analysis

For all experiments, only single events were included. Other events were discriminated on the basis of the pulse width plotted against forward scatter height (FSC). There is a relation between the size of cells and the pulse width, which measures the time it takes to a particle to flow through the laser beam. Doublets tend to be orientated lengthwise and have a larger pulse width with the same height of FSC as individual cells. As such, doublets can be excluded. Dead cells were labelled with Fixable Viability Dye eFluor780 or eFluor450 (eBioscience). Cells positive for the dye were excluded from analysis.

2.13 Fibroblastic colony-forming unit assay (CFU-F)

2.13.1 Sample preparation for CFU-F

Femurs and tibias were isolated as described previously. Femur and tibia were separated and cut at both ends to expose the bone cavity. The bone marrow was flushed with PBS 2% FCS (wash buffer) using a 25-gauge needle through a 70µm cell strainer. Cell strainers were thoroughly rinsed with wash buffer. Cells were washed and suspended in PBS 2% FCS. Only nucleated cells were counted by diluting a small aliquot in 3% Acetic Acid with Methylene Blue and counting the nuclei with a haemocytometer. Cells were left on ice at a final concentration of 10^7 cell/mL until use.

2.13.2 CFU-F assay

Complete MesenCult® medium (STEMCELL technologies, Grenoble, France) was prepared one day prior to the assay. The MSC stimulatory supplements were thawed at RT and added to the MSC basal medium at a 1/5 ratio to make complete MesenCult® medium, according to the manufacturer's instructions. The bone marrow cell suspensions were mixed with the complete medium (1/20 dilution) and 2ml of the dilution was added to each well in 6-well plates (Nalge Nunc, Rochester, NY, USA). A total 1×10^6 cells were plated in each well. Individual samples were plated in duplicate or triplicate. Cells were incubated for 10 days at 37°C in 5% CO₂.

2.13.3 Staining and enumeration of CFU-F

After 10 days in culture, medium was removed from each well by aspiration. Each well was washed twice with 2ml PBS and left to air-dry at RT for 5min. To fix the cells, 2ml of methanol was added to each well. After 5min, the methanol was aspirated and the plates left to air-dry for 5min at RT. 1ml of Giemsa staining solution was added to each well and incubated for 5min. The staining solution was removed and excess stain was washed with ddH₂O until the water was clear. The plates were finally left to air-dry and stored at RT until further use. Colonies were counted microscopically. One CFU-F was defined as a colony comprising more than 10 fibroblast-like cells (spindle shape) as shown in **Fig 2-2**.

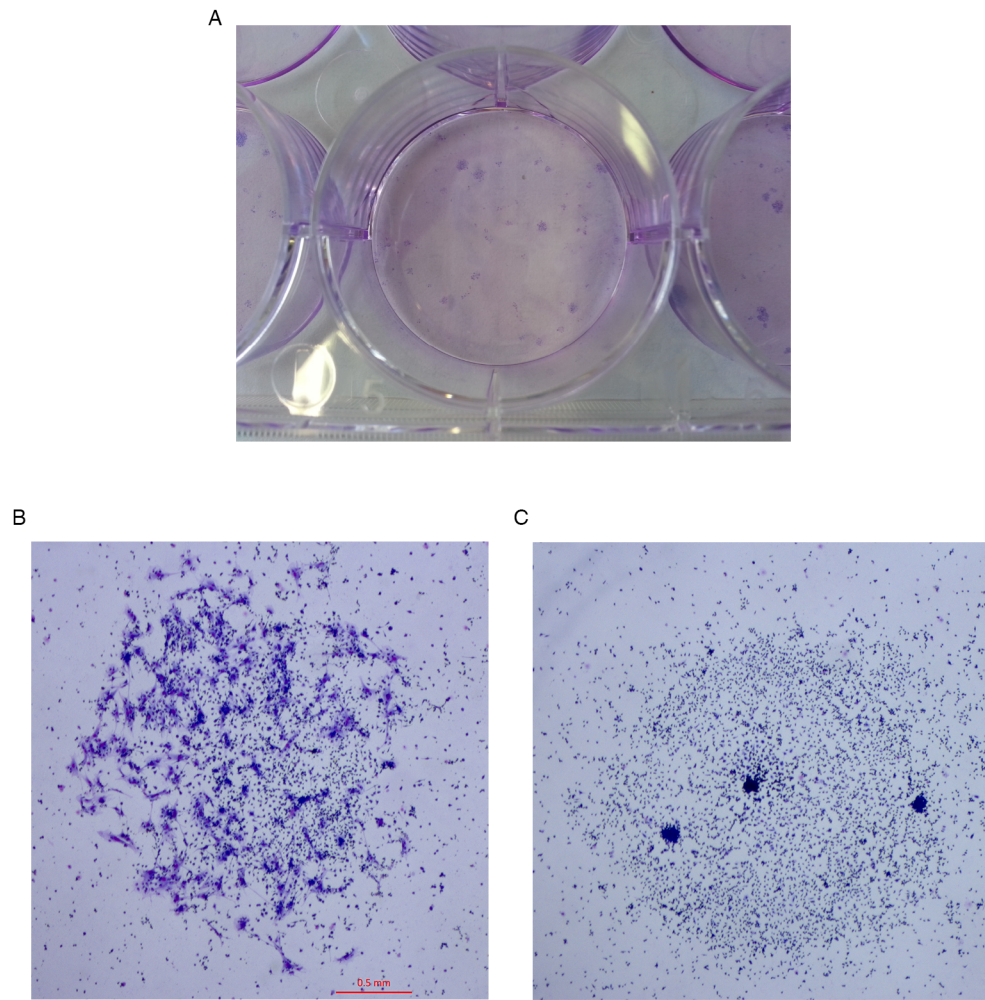


Figure 2-2. Identification of CFU-F from the bone marrow. (A) Macroscopic visualisation of colonies. bone marrow cells were culture for 10 days in MesenCult® medium and stained with Giemsa. (B) Representative example of a CFU-F, visualised under a microscope, characterised by the presence of elongated fibroblast-like cells. (C) Example of a non-fibroblastic colony which looks similar to a CFU-F macroscopically but different when studied under a microscope.

2.14 Quantification of G-CSF and TPO in plasma

2.14.1 Enzyme-linked immunosorbent assay (ELISA)

Plasma was used for the measurements of circulating G-CSF and TPO. Collection and storage of plasma were described previously. Samples were thawed on ice before the assay. Two ELISA kits were used, pre-coated with capture antibodies specific for G-CSF (R&D Systems, MCS00) and TPO (R&D Systems, MTP00). For G-CSF, standards ranging from 900pg/ml to 14.1pg/ml were used. Samples were used pure or diluted to ½ depending on the amount available. For TPO, standards ranging from 4000pg/ml to 62.5pg/ml were used and plasma samples were diluted 5 times in the diluent provided in the kit prior to the assay. Pure or diluted samples and standards were added to the plate in duplicate and incubated for 2h at RT. Each well was then washed with 200µl of wash buffer; the wash buffer was removed by gently inverting and shaking the plate. The operation was repeated an additional three times. The G-CSF or TPO detection antibodies, conjugated to horseradish peroxidase (HRP) were added and left to incubate for 2h at RT. The washing steps were repeated and the colourimetric HRP substrate was added and incubated in the dark for 30min at RT. The reaction was stopped by adding Stop Solution and mixing, according to the manufacturer's instructions.

2.14.2 Analysis of ELISA

Within 30min after stopping the reaction, the optical densities (OD) at 450nm and 570nm were measured in a VersaMax ELISA microplate reader (Molecular Devices, Sunnyvale, CA, USA). The 450nm OD corresponds to the absorbance of the product from the degradation of the substrate from HRP. The OD at 570nm is non-specific and results from optical imperfections of the plate or dust, which absorbs equally at the 450nm and 570nm wavelengths. The 450nm OD was therefore corrected by subtracting the 570nm OD. Duplicates were averaged. The standard curve was plotted and analysed with the SigmaPlot software (Systat Software Inc.). A four parameter logistic curve-fit was generated using the *Standard Curve* function of the software. It is a non-linear regression model resulting in the following equation:

$$Concentration = \frac{\min + (max - \min)}{1 + \frac{OD^{-Hillslope}}{EC50}}$$

Unknown values were computed from the averages of duplicates using this model. A control of known concentration provided by the manufacturer was used to assess the reliability of the assay.

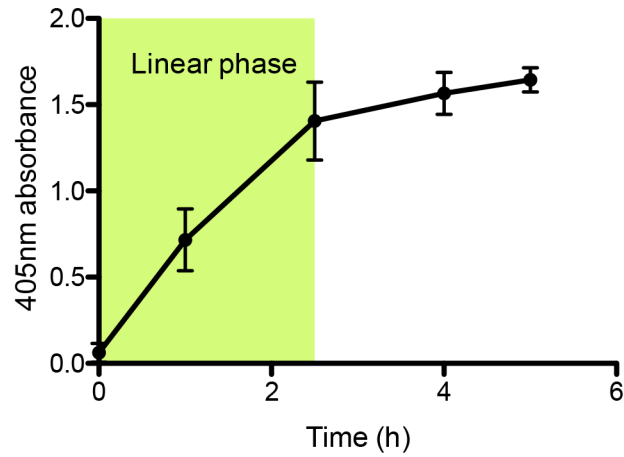
2.15 Neutrophil elastase activity assay

Bone marrow cells were isolated as described previously. Cells were pelleted and lysed in 100µl Radioimmunoprecipitation buffer (RIPA; Sigma-Aldrich) per 10⁶ cells. Lysates were stored at -80° until use. Neutrophil elastase (NE) activity was measured by a colourimetric assay monitoring the degradation of a specific substrate. The substrate is the synthetic peptide Methoxysuccinyl-Alanine-Alanine-Proline-Valin-p-nitroaniline (Elastase Substrate I, Colorimetric, Calbiochem, La Jolla, CA, USA). 20µl of the lysates were mixed with 200µl of reaction buffer containing 0.1 M Tris-HCl and 0.5M NaCl (pH 7.9) and 1mM substrate in a 96-well plate and place at 37°C. The reaction was monitored by mean of the absorbance at 405nm. The values were corrected against the background by subtracting the absorbance from wells with RIPA only. One unit of NE activity was defined as the quantity of enzyme that liberated 1µmol of p-nitroaniline per hour. The following formula was used:

$$\begin{aligned} & \text{Units per } 10^6 \text{ cells} \\ = & \frac{\Delta Abs_{405}}{\text{Extinction coefficient}_{p\text{-nitroaniline}} \times L \times \text{cell concentration}_{\text{lysate}} \times \text{sample volume}} \end{aligned}$$

Where ΔAbs_{405} is the slope of the linear regression curve calculated from the linear phase of the kinetics, as described in **Figure 2-3**. The millimolar extinction coefficient of the p-nitroaniline at 405nm is estimated at 9.62M⁻¹cm⁻¹ in these conditions. The value L corresponds to the light path length, estimated at 0.5cm for a volume of 200µl 96-well plate. The cell concentration in lysate is expressed in million per ml of lysis buffer. The sample volume, expressed in ml, corresponds to the volume of lysate used in the reaction.

A



B

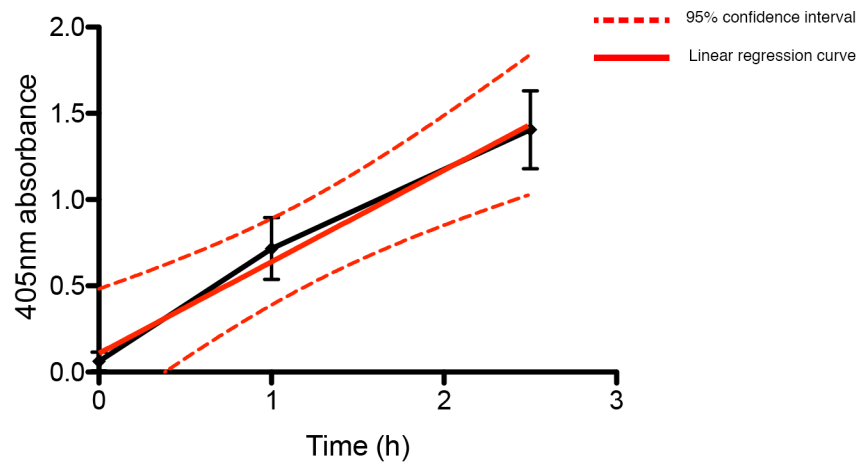


Figure 2-3. Calculate of neutrophil elastase activity. (A) The reaction rate was determined using data points from the linear phase of the reaction. (B) Linear regression computed from the linear phase of the reaction. The slope of the linear curve was used to calculate the neutrophil elastase activity.

2.16 Measurement of mRNA accumulation by RT-qPCR

2.16.1 RNA extraction

Bone marrow cells were isolated as previously described. At least 10^6 cells were pelleted by centrifugation and the supernatant was removed. Cell pellets were stored at -80°C until ribonucleic acid (RNA) extraction. Fragments of spleens were cut and put in RNAlater™ (QIAGEN, Hilden, Germany) then kept at -80°C until RNA extraction. Total RNA was extracted using QIAGEN's mini RNeasy kit, according to the manufacturer's protocol. This kit enables the enrichment of RNA molecules that are longer than 200base-pair (bp). Molecules, such as ribosomal RNA (rRNA), transfer RNA (tRNA) and micro RNA (miRNA), are smaller than 200bp. Therefore, the kit allows the enrichment of messenger RNA (mRNA), which is typically longer than 200bp. To ensure high enough concentration of mRNA for the synthesis of complementary deoxyribonucleic acid (cDNA), which matters more than higher yields for this application, the membranes were washed twice with $50\mu\text{l}$ the same elution solution. The concentration and purity of RNA was assessed with a Nanodrop™ spectrophotometer (Thermo Fisher Scientific). The ratios 260/280 and 260/280 were considered indicators of purity and considered acceptable when close to 2.0 and 2.2, respectively.

2.16.2 cDNA synthesis

Non-specific cDNA synthesis was performed with a High Capacity cDNA Reverse Transcription kit (Applied Biosystems™, Waltham, MA, USA). The mRNA was diluted to $1\mu\text{g}$ in $10\mu\text{l}$ and mixed with $10\mu\text{l}$ of reverse transcription master mix. The master mix was made per sample of $2\mu\text{l}$ 10X reverse transcription buffer, $0.8\mu\text{l}$ 100mM deoxynucleotides tri-phosphate (dNTP) mix, $2.0\mu\text{l}$ 10X random primers, $1.0\mu\text{l}$ of MultiScribe™ reverse transcriptase and $4.2\mu\text{l}$ H_2O . mRNA samples were mixed with the master mix and retro-transcribed in a thermal cycler. The conditions were set as 25°C for 10min (annealing), 37°C for 120min (reverse transcription), 85°C for 5min (enzyme inactivation). The products were cooled down to 4°C until they were removed from the thermal cycler, after what they were transferred to -20°C . Concentrations of cDNA were not measured. Instead, it was assumed that the reverse transcription efficacy was of 100%, therefore yielding $1\mu\text{g}$ of cDNA.

2.16.3 Quantitative polymerase-chain reaction

Quantitative polymerase-chain reaction (qPCR) was performed using Fast SYBR Green Master Mix (Applied Biosystems). The cDNA sample synthesised previously were diluted

to 10ng/ μ l and 4 μ l was used per reaction. A master mix was prepared for each primer pair and made of 10 μ l 2X Fast SYBR Green Master Mix, 1 μ l of 10 μ M forward and reverse primer mix and 5 μ l H₂O per reaction. First the cDNA samples were added inside a 96-well plate then 19 μ l of the master mix were added. The plates were transferred to the real-time PCR detection instrument (StepOne Plus, Applied Biosystems) within 30min after all reagents were added. The PCR reaction was started with the activation of the AmpliTaq Fast DNA polymerase at 95°C for 20sec, then 40 cycles consisting of 95°C for 3sec (denaturation) and 60°C for 30 sec (annealing and extension). Specific primers are described in **Table 2-2**.

2.16.4 Primer design and melt curve

Primers were checked for specificity against a mRNA database. Both forward and reverse sequences were compared to the *Mus musculus* RefSeq RNA database using the Basic Local Alignment Search Tool (BLAST, US National Library of Medicine) algorithm. To avoid amplification of genomic DNA, the primers were chosen in order to cover exon-exon junction of the mRNA sequence. Primers were ordered as lyophilised oligo DNA and suspended in DNase-free water to a stock concentration of 100 μ M. After the amplification steps, a melt curve was done to assess the specificity of primer pairs. The reaction mix was exposed to rising temperature and the fluorescence was recorded. Since SYBR Green is only fluorescent when incorporated into double-stranded DNA, fluorescence decreases as the temperature rises and DNA starts to denature. The derivative of fluorescence shows peaks which result from sudden drops in fluorescence, each peak is specific to a PCR product. Therefore, the presence of a single peak indicates that only one product has formed (i.e. the amplicon) while multiple peaks suggest other double-stranded DNA was produced and detected such as primer dimers or contaminating DNA. Examples of melt curves for validated and invalidated primers are shown in **Figure 2-4**.

2.16.5 Analysis of RT-qPCR data

Data were analysed with the StepOne™ software (Applied Biosystems). A threshold was placed automatically and adjusted if needed, intercepting all amplification plots in the linear phase of amplification. The number of cycles at which the fluorescence reaches the threshold was computed for each sample and termed Ct. Expression of the gene of interest was normalised to a housekeeping gene. For each gene and sample analysed, the average Ct values of the sample for the housekeeping gene, in this case *Hprt*, were subtracted from the gene of interest's Ct value. The resulting value was called Δ Ct. The average Δ Ct from a

control group was then subtracted from the other groups, giving the value $\Delta\Delta Ct$. Fold-change for the relative expression of each gene of interest was calculated as $2^{(-\Delta\Delta Ct)}$.

2.17 Statistical analyses

2.17.1 Comparison between groups

Data were analysed using GraphPad Prism 5.0 (Prism Software, Irvine, CA, USA). The Kolmogorov-Smirnoff test was used to determine if the distributions of values within individual groups were normal. When comparing two groups, Student's t-test or Mann-Whitney test was used according to the data distribution. Welch's correction was applied for the Student's t-test in cases of unequal variances between the two groups. In multiple comparison, One-way ANOVA or Kruskal-Wallis tests were used according to the data distribution followed by Turkey's or Dunn's multiple comparison tests, respectively. Student's t-test or one-way ANOVA were used to compare groups distributed normally. If one or more group did not follow a normal distribution, a non-parametric test was used. When the number of samples in a group was too low, it was assumed the distribution was normal and a parametric test was used.

2.17.2 Determination of reference interval

Reference intervals, or normal ranges, were calculated as follow using GraphPad Prism 5.0 (Prism Software). The Kolmogorov-Smirnoff test was used to determine if the distribution of values for a given parameter was normal. The skewness of the data was also calculated. The skewness refers to the symmetry of the distribution for a set of values. Non-skewed data are symmetrically distributed around the mean and have a skewness of 0, while a positive skewness means the distribution is skewed towards the right and a for negative skewness towards left. Skewed data can lead to unreliable reference intervals, such as negative lower limit²²⁴. Arbitrarily the limits to consider a set of values non-skewed was -1 to 1. Skewness was corrected by transforming the data into a logarithmic (log) scale. If the values were normally distributed, the reference interval was calculated using the standard deviation (δ) of the mean. The lower limit of the range was calculated as the mean - 2δ and the upper limit as the mean + 2δ ²²⁴. For log-transformed data, the limits were converted back to a linear scale to give the normal range. The reference intervals for data whose distribution were not normal was calculate with percentiles. The lower limit was calculated as 2.5 centile and the upper limit as the 97.5 centile, so as to determine the interval in which 95% of values are expected to fall²²⁴.

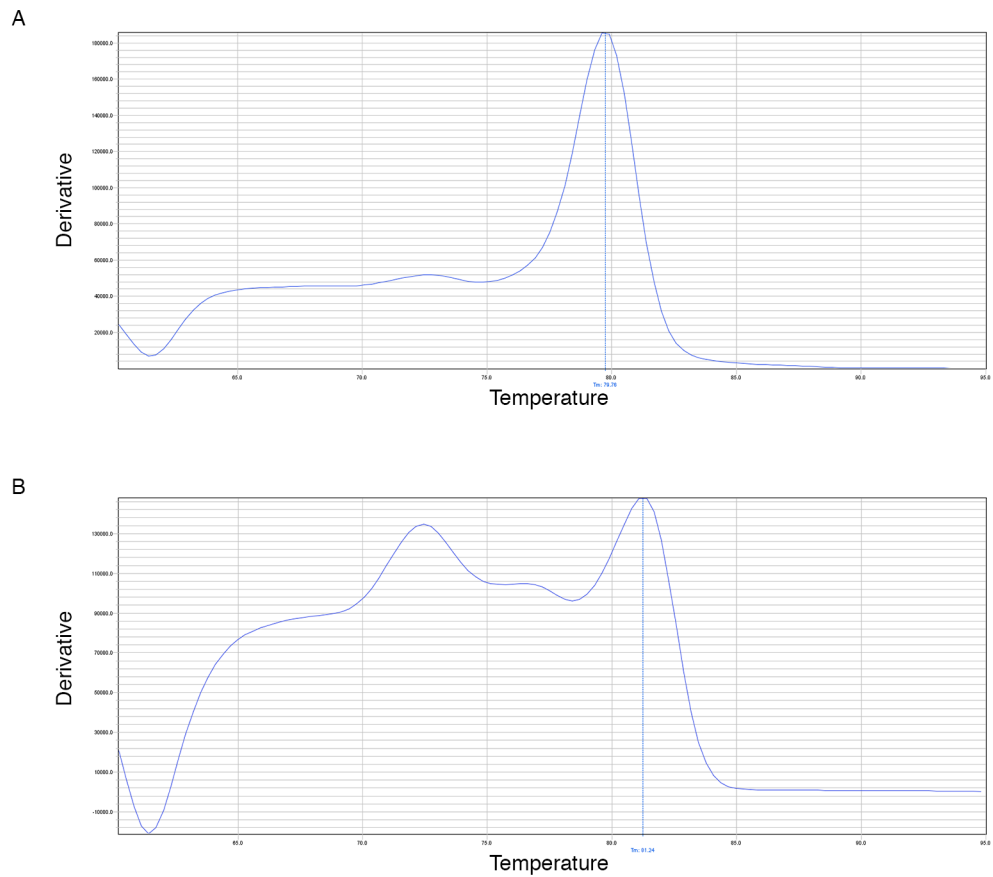


Figure 2-4. Assessment of qPCR-specificity by melt curves. Derivative of the fluorescence curve in function of the temperature produces two types of melt curves. (A) Melt curve with a single peak, indicating only one amplicon. (B) Melt curve with multiple peaks, two in this example, suggesting the presence of non-specific amplicons.

Table 2-1. List of antibodies (FC = flow cytometry, IHC = immunochemistry, Neut = cytokine neutralisation)

Primary antibodies							
Target	Fluorophore / conjugation	Manufacturer	Application	Clone	Host	Istopye	Dilution
BMP4	Purified	abcam	IHC	polyclonal	Rabbit	IgG	1/100
CD115	PE	eBioscience	FC	AFS98	Rat	IgG2a	1/200
CD11b	biotin	eBioscience	IHC	M1/70	Rat	IgG2b	1/200
CD16/32 (Fc Block)	purified	eBioscience	FC	93	Rat	IgG2a	1/5000
CD169	eFluor 660	eBioscience	FC	SER-4	Rat	IgG2a	1/100
	Biotin	AbD Serotec	IHC	MOMA-1	Rat	IgG2a	1/100
CD3	BV421	BioLegend	FC	17A2	Rat	IgG2b	1/200
CD4	APC	BioLegend	FC	GK1.5	Rat	IgG2b	1/200
CD45	APC-Cy7	BioLegend	FC	30-F11	Rat	IgG2b	1/200
CD45.1	PE-CY5	eBioscience	FC	A20	Mouse	IgG2a	1/200 or 1/400
CD68	AlexaFluor 647	AbD Serotec	IHC	FA-11	Rat	IgG2a	1/200
CD71	PE	BioLegend	FC	R17217	Rat	IgG2a	1/200 or 1/400
	FITC	eBioscience	IHC / FC				1/100 (IHC); 1/200 (FC)

Target	Fluorophore / conjugation	Manufacturer	Application	Clone	Host	Istopye	Dilution
CD8a	PerCP-Cy5.5	BioLegend	FC	53-6.7	Rat	IgG2a	1/200
F4/80	AlexaFluor 488	eBioscience	FC	BM8	Rat	IgG2a	1/200
	AlexaFluor 647	BioLegend	IHC				1/100
G-CSF	purified	R and D	Neu	# 67604	Rat	IgG1	see Methods
Gr-1	PE-Cy7	eBioscience	FC	RB6-8C5	Rat	IgG2a	1/200
Laminin	FITC	Sigma	IHC	polyclonal	Rabbit	IgG	1/100
TER119	PE-Cy7	eBioscience	FC	TER119	Rat	IgG2b	1/200
	biotin		IHC				1/100

Secondary antibodies/streptavidin

Anti-rabbit IgG	Alexa Fluor 488	Thermo Fisher Scientific	IHC	polyclonal	Goat	IgG	1/100
Streptavidin	Alexa Fluor 488	Thermo Fisher Scientific	IHC	na	na	na	1/100
	Alexa Fluor 647	Thermo Fisher Scientific	IHC				1/100

Table 2-2 List of primers for real-time quantitative polymerase chain reaction

Target	Primer sequence 5' - 3'	
Csf3 (G-CSF)	Forward	ATCCCGAAGGCTTCCCTGAGTG
	Reverse	AGGAGACCTTGGTAGAGGCAGA
Cxcl12	Forward	GGAGGATAGATGTGCTCTGGAAC
	Reverse	AGTGAGGATGGAGACCGTGGTG
Angpt1	Forward	AACCGAGCCTACTCACAGTACG
	Reverse	GCATCCTTCGTGCTGAAATCGG
Kit1	Forward	ATCTGCGGGAATCCTGTGACTG
	Reverse	CCATATCTCGTAGCCAACAATGAC
Vcam1	Forward	GCTATGAGGATGGAAGACTCTGG
	Reverse	ACTTGTGCAGCCACCTGAGATC
HPRT	Forward	AGGAGTCCTGTTGATGTTGCCAGT
	Reverse	GGGACGCAGCAACTGACATTTCTA

Chapter 3 Visceral leishmaniasis and erythropoiesis

3.1 Introduction

Visceral leishmaniasis is a systemic infectious disease responsible for an estimated 20 000 to 40 000 deaths per year. In contrast to the cutaneous form of the disease, which is self-healing, the visceral form is a chronic disease, lethal in close to 100% of patients if left untreated²²⁵. Clinical manifestations of the disease typically include splenomegaly, hepatomegaly, cachexia, bleeding disorders and jaundice. Yet patients might only present some symptoms and in endemic areas these often overlap with other diseases sharing similar clinical signs. Symptoms usually appear months to years after infection when they do and vary depending on age or geographical location, especially between the Old World (eastern hemisphere) and the New World (America). The variations in species or strains, with the emergence of antibiotics-resistant strains make it more challenging to treat accordingly²²⁶. For these reasons, understanding the immunological and haematological bases for blood disorders in the broad context of parasitic infections and specifically in VL is essential as it could lead to potential new therapies to relieve the symptoms of the disease.

Anaemia is the decrease of red blood cells in the blood circulation, it has been reported in most species naturally infected with *L. donovani* or *L. infantum*^{67,69,72,81}. Anaemia has systemic consequences. Because red blood cells are responsible for supplying oxygen to all and tissues in the body, anaemia can cause a reduction of function in many organs. As a consequence, the main overt symptom of anaemia is a general fatigue, known as cachexia. Anaemia has never been associated with the lethality of the disease, but its contribution to pathogenesis should not be excluded.

Data from the human disease suggest anaemia is due to the utilisation of heme, an essential component of haemoglobin by the parasites⁹⁵, haemophagocytosis^{84,227–229} or splenic capture⁶². Iron deficiency has been suggested as a major cause for anaemia of VL^{4,95}. However, evidence suggest that the production of red blood cells in the bone marrow is also involved. The bone marrow is the tissue inside long bones such as the femur, the humerus or the hip bone and is the main site of haematopoiesis in adult mammals. It is a complex organ in which HSCs and their daughter cells interact with various non-haematopoietic cells called stromal cells. With the spleen and the liver, the bone marrow is a major site of amastigote replication. A wealth of knowledge regarding the biology of parasites in the spleen and liver as well as the tissue-specific immune responses is available. But very little is known about the biology of VL in the context of the bone

marrow. Ethical challenges render its study difficult in humans because the required techniques are invasive. The murine model has been extensively studied for the immune response to *L. donovani* in the spleen and liver, but very few immunological or haematological studies in the bone marrow have been reported. In the murine model, it has been shown that haematopoietic activity is increased in the bone marrow and the spleen of chronically infected BALB/c mice. Infection of stromal macrophages has been suggested as a cause for changes in haematopoietic activity^{19,86}. In the human disease, the bone marrow shows evidence of myelodysplasia, i.e. ineffective production of blood cells^{3,4}. More specifically to erythropoiesis, an experimental model of hamster has been used to show that ineffective erythropoiesis caused by VL is linked to a higher rate of apoptosis in erythroid precursors through the up-regulation of IFN δ and TNF-related apoptosis inducing ligand (TRAIL)⁶⁷.

Anaemia is a serious complication of VL and appears to be multifactorial. The murine model has been hardly studied for haematological changes associated with VL. As a consequence, the mechanisms for the reduction of blood cells are still poorly understood.

3.1.1 Aims

Because murine EVL has a very different outcome from natural human, canine and feline infections, as well as EVL in hamsters, it has been poorly studied from a haematological perspective. As a consequence, very little is known about the haematological status of infected mice. Yet the profusion of biological and technical tools for murine studies allows more refined mechanistic studies than it is currently possible in other *in vivo* models or clinical settings. Using mice as an experimental model for the the study of haematological alterations would benefit the research into the pathogenesis of VL, provided the model proves similar enough to the human disease in this respect.

The aims of the work presented in this chapter therefore were:

1. To establish the haematological profile of mice chronically infected with *L. donovani*, especially in regards to red blood cells.
2. To collect and compare clinical data with the murine haematological profile in order to find the similitudes and discrepancies between the human disease and the experimental murine model.
3. To quantify erythropoiesis in the bone marrow, the main haematopoietic organ in adult mammals.
4. To determine alterations in the bone marrow potentially underlying the reduction of medullar erythropoiesis.
5. To study the role of the spleen in the anaemia of EVL.
6. To find out the mechanisms responsible for alteration of erythropoiesis in mice infected with *L. donovani*.

3.3 Results

3.3.1 Haematological profile of mice chronically infected with *L. donovani*

C57BL/6 mice were infected with *L. donovani* LV9 amastigotes by the intravenous route and blood parameters were measured 4 weeks later (**Table 3.1**). This time point was chosen as it has been shown as the beginning of the chronic phase of infection in EVL. The first 4 weeks of infection correspond to acute infection in the liver. Hepatic parasite burden peaks at 4 weeks post-infection then decreases and parasites are cleared by the 8th week. By opposition, parasites number slowly grow over time in the spleen and the bone marrow and the infection is chronic²³⁰. The 28-day time is therefore commonly used in study of EVL as the beginning of chronic infection. Blood was collected by cardiac puncture and analysed by an automated blood analyser. Data from 14 naïve mice were used to calculate the reference interval, or normal range, for each parameter. No significant change in circulating lymphocyte, granulocyte or monocyte was measured between naïve and infected mice. A single infected mouse presented both lymphopenia and an eosinophilia according to the reference interval. The red blood cell (RBC) count per μl of blood was $8.11 \pm 0.14 \times 10^6$ in naïve mice. In chronically infected mice, the RBC count per volume was 19% lower at $56.57 \pm 0.022 \times 10^6$ RBC/ μl . 70% of infected mice had RBC counts under the normal range. Similarly, the haemoglobin (Hb) content in the blood of infected mice was reduced by 15%, down to 8.17 ± 0.22 g/dl while the baseline was measured at 9.60 ± 0.21 g/dl in naïve mice. 30% of infected mice had Hb levels below the reference interval. The average volume of erythrocytes was unchanged, with a mean corpuscular volume (MCV) of 51 femtoliter (fl) in both groups but 3 out of 13 infected mice (23%) had developed a macrocytic anaemia, with MCV above the normal range. Contrary to the global haemoglobin concentration, the mean corpuscular haemoglobin (MCH), which indicates the average content of haemoglobin in individual erythrocytes, was significantly increased in infected mice by about 6%. However, all individual mice had MCH within the normal range. The mean corpuscular haemoglobin concentration (MCHC), which is computed from the MCH and the MCV was unaltered as well. These results all point towards development of a normochromic anemia, i.e. a reduction of circulating RBC with normal Hb content, in mice infected with *L. donovani*. Although the comparison group-wise suggests the anaemia is normocytic, some of the infected mice developed a macrocytic anaemia with MCV higher than the normal range. Data regarding platelets are discussed in Chapter 4.

Table 3-1 Haematological parameters of mice infected with *L. donovani*. Mice were killed 28 days after infection. Blood was collected by cardiac puncture under terminal anaesthesia and analysed by an automated blood analyser.

	Naïve (n=14) Mean ± SEM	Infected (n=13) Mean ± SEM	p	Test
WBC ($\times 10^3 / \mu\text{l}$)	6.803 ± 0.864	5.758 ± 0.659	ns	Mann Whitney
NE ($\times 10^3 / \mu\text{l}$)	1.671 ± 0.309	1.108 ± 0.128	ns	t-test
LY ($\times 10^3 / \mu\text{l}$)	4.486 ± 0.455	4.072 ± 0.626	ns	Mann Whitney
MO ($\times 10^3 / \mu\text{l}$)	0.296 ± 0.072	0.230 ± 0.017	ns	Mann Whitney
EO ($\times 10^3 / \mu\text{l}$)	0.259 ± 0.077	0.108 ± 0.058	ns	Mann Whitney
BA ($\times 10^3 / \mu\text{l}$)	0.077 ± 0.026	0.013 ± 0.003	ns	Mann Whitney
RBC ($\times 10^6 / \mu\text{l}$)	8.110 ± 0.143	6.572 ± 0.241	< 0.0001	t-test
HB (g/dl)	9.593 ± 0.213	8.169 ± 0.219	< 0.0001	t-test
HCT (%)	41.860 ± 0.900	34.020 ± 1.091	< 0.0001	t-test
MCV (fl)	51.610 ± 0.577	51.990 ± 1.035	ns	Mann Whitney
MCH (pg)	11.860 ± 0.227	12.520 ± 0.199	< 0.05	Mann Whitney
MCHC (g/dl)	23.040 ± 0.663	24.130 ± 0.509	ns	Mann Whitney
PLT ($\times 10^3 / \mu\text{l}$)	583.000 ± 45.680	281.500 ± 26.390	< 0.0001	t-test
MPV (fl)	4.293 ± 0.143	5.354 ± 0.084	< 0.0001	Mann Whitney

Table 3-2. Reference interval of haematological parameters and distribution of infected mice in relative to the intervals. Reference interval (or normal range) were calculated from the values of naïve mice (n=14). Calculations for the reference intervals are detailed in Chapter 2.

	Reference interval			Distribution of haematological parameters from infected mice relative to the reference interval		
				Under	Within	Above
WBC ($\times 10^3 / \mu\text{l}$)	2.40	-	15.73	0.00%	100.00%	0.00%
NE ($\times 10^3 / \mu\text{l}$)	0.37	-	5.03	0.00%	100.00%	0.00%
LY ($\times 10^3 / \mu\text{l}$)	1.96	-	9.01	7.69%	92.31%	0.00%
MO ($\times 10^3 / \mu\text{l}$)	0.05	-	0.92	0.00%	100.00%	0.00%
EO ($\times 10^3 / \mu\text{l}$)	0.01	-	0.71	0.00%	92.31%	7.69%
BA ($\times 10^3 / \mu\text{l}$)	0.00	-	0.26	0.00%	100.00%	0.00%
RBC ($\times 10^6 / \mu\text{l}$)	7.04	-	9.18	69.23%	30.77%	0.00%
Hb (g/dl)	8.00	-	11.19	30.77%	69.23%	0.00%
HCT (%)	35.12	-	48.60	61.54%	38.46%	0.00%
MCV (fl)	47.30	-	55.92	0.00%	76.92%	23.08%
MCH (pg)	10.16	-	13.56	0.00%	100.00%	0.00%
MCHC (g/dl)	18.08	-	28.00	0.00%	100.00%	0.00%
PLT ($\times 10^3 / \mu\text{l}$)	241.20	-	924.80	38.46%	61.54%	0.00%
MPV (fl)	3.60	-	5.00	0.00%	23.08%	76.92%

3.3.2 Medullary erythropoiesis is repressed during EVL

Decrease in haematocrit can be caused by reduced number of circulating erythrocytes or increase in plasma volume. The latter was not investigated here. Reduction of circulating erythrocytes can be caused by impairment of erythropoiesis or by peripheral destruction of RBC. To determine if erythropoiesis was altered in EVL, the bone marrow of infected mice was analysed. Femurs, the more marrow-rich bone and main site of hematopoiesis in adult mammals, appeared pale in comparison with naïve mice, in which the femurs have a purple-red coloration (**Figure 3.1A**). Because this phenomenon has been preciously associated with impairment of erythropoiesis^{169,231,232}, femurs were sectioned and stained with TER119, a marker of erythroid cells in the mouse²³³ and with DAPI. Nucleated TER119⁺ cells were visibly reduced in the bone marrow of infected mice (**Figure 3.1B and C**). These results indicate that erythropoiesis is reduced in the bone marrow during chronic infection with *L. donovani*.

3.3.3 Identification of erythroid precursors

Erythropoiesis was quantified in the bone marrow by single cell analysis. The bone marrow was flushed out of the bone cavity with PBS and the resulting cell suspension reflected the colours of complete bones (data not shown). The first observation after preparing single cell suspensions is that fewer cells could be recovered from infected bones (**Figure 3.1D**). Erythroid progenitors were identified based on the surface expression of CD71 and TER119²³³. After exclusion of doublets and dead cells, only CD45⁻ cells were included in the analysis. It was assumed that the efficacy of RBC lysis was of one hundred percent, thus no mature cells were present in the final cell suspensions. Indeed, TER119 is also expressed on immature erythroblasts as well as mature reticulocytes and erythrocytes. Reticulocytes and erythrocytes can be excluded by a nucleic staining since they are enucleated cells but no DNA dye was included in the staining mixes. Control experiments have shown that most DNA-negative cells were removed following RBC lysis with the ACK buffer (**Figure 3-2**). Up to four populations of erythroblasts can be identified by flow cytometry based on their size and the surface expression of the erythroid marker TER119 and the transferrin receptor CD71 (**Figure 3-3A**). The TER119^{med} CD71^{high} population corresponds to the pro-erythroblasts. They are the most immature precursors in the erythroid-specific lineage identifiable by flow cytometry and differentiate from the BFU-E and CFU-E. The TER119^{high} population can be divided into three more populations based on CD71 and size. Respectively, pro-erythroblasts differentiate into CD71^{high} FSC^{high} basophilic erythroblasts then CD71^{high} FSC^{low} polychromatic erythroblasts and finally

CD71^{low} FSC^{low} orthochromatic erythroblasts and reticulocytes²³³. Reticulocytes are finally released in the blood and mature into erythrocytes. Because all populations of erythroblasts could not be consistently resolved, it was decided to group all TER119^{high} cells as a single population called erythroblasts (**Figure 3-3A**). Pro-erythroblasts were defined as CD71⁺TER119^{low} cells and erythroblasts as CD71^{-/+}TER119^{high} (**Figure 3-3A**).

Erythroid precursors were measured in the bone marrow of naïve and infected mice (**Figure 3-4 A and B**). The frequency of pro-erythroblasts in the bone marrow was $1.00 \pm 0.22\%$ in naïve mice and was not significantly different in infected mice ($1.03\% \pm 0.16\%$; **Figure 3-4C**). On the other hand, the frequency of erythroblasts in infected mice was on average reduced by 5-fold compared to the naïve group (**Figure 3-3D**). The decrease in erythroblasts was also reflected in the absolute number of cells (**Figure 3-3E and F**). A single leg (femur + tibia) contains 0.32×10^6 and 2.66×10^6 pro-erythroblasts and erythroblasts in naïve mice respectively, against 0.27×10^5 and 0.55×10^6 in infected mice. These results all confirm that erythropoiesis, at least in its final stages, is impaired in the bone marrow of infected mice

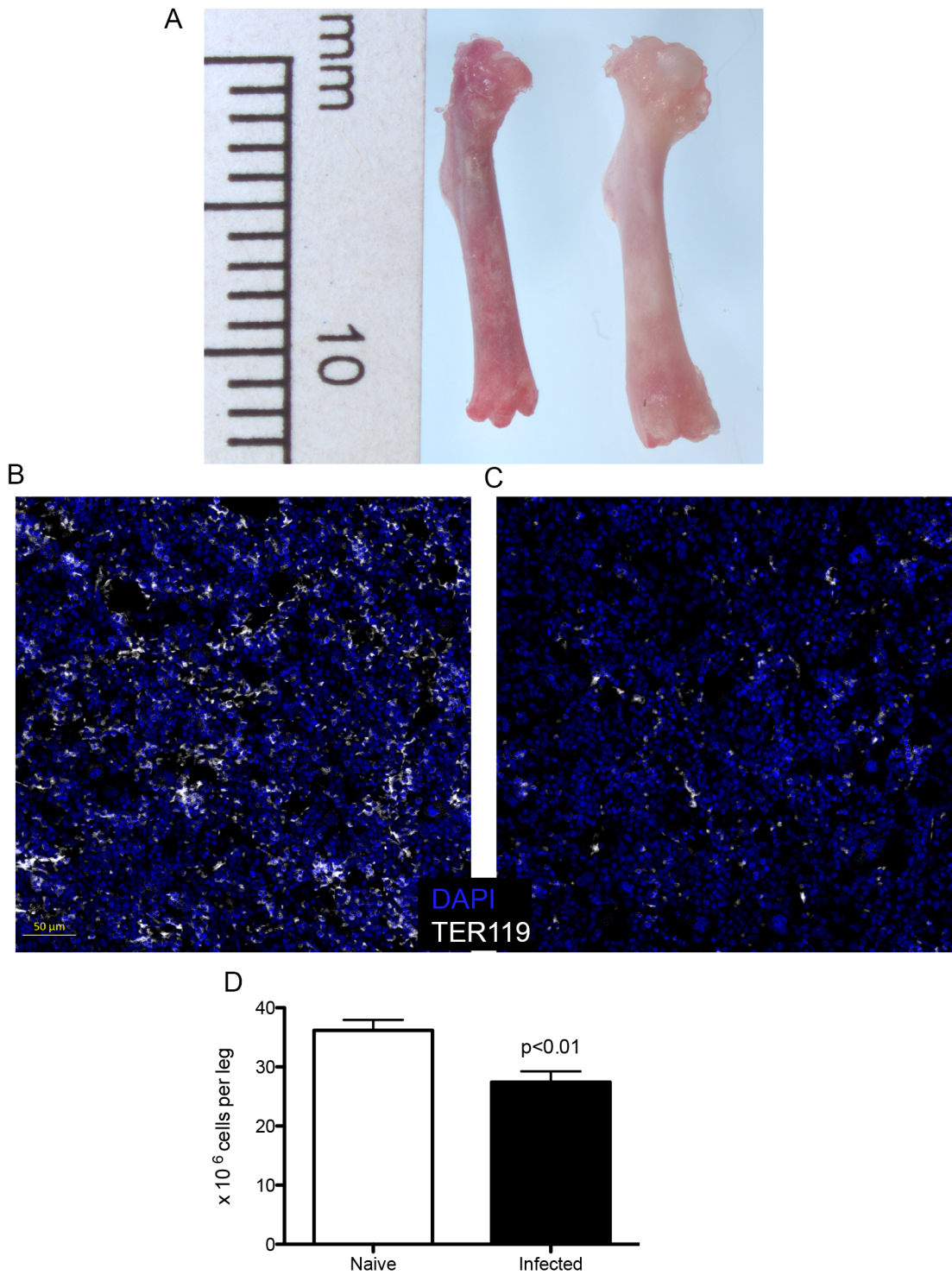


Figure 3-1. Signs associated with reduction in medullary erythropoiesis in *L. donovani* infected mice. (A) External view of femurs isolated from naïve (left) and infected (right) mice (representative of more than 30 individual mice per group in more than 10 experiments). (B-C) Confocal imaging of 5µm femoral sections from naïve (B) and 28d-infected (C) mice stained with DAPI (blue) and the erythroid lineage marker TER119 (white; representative of 6 mice per group from 2 independent experiments). (D) Quantification of total viable bone marrow cell numbers flushed from 1 femur + 1 tibia. Data represent mean + SEM (Mann Whitney test; n=23 mice per group from 7 independent experiments).

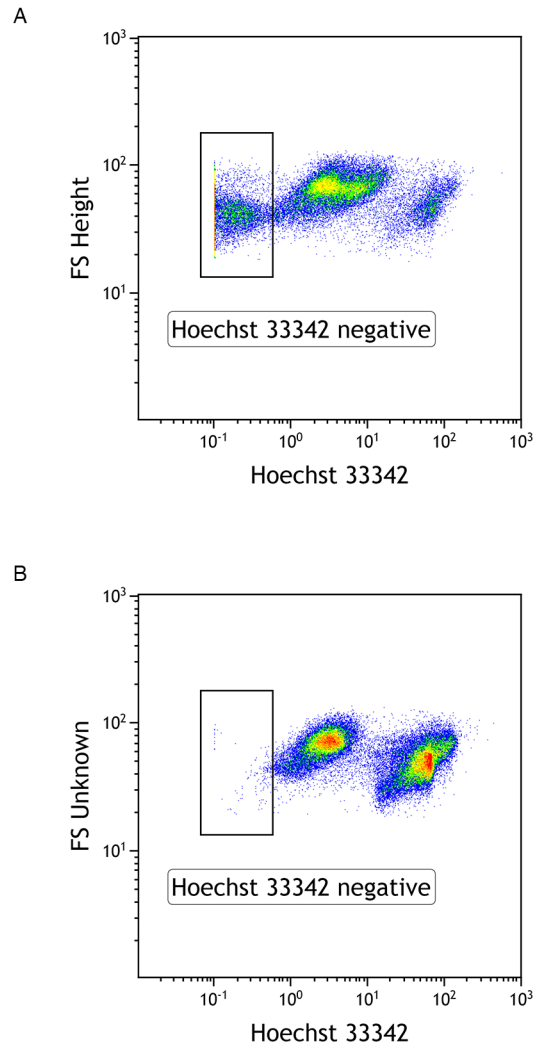


Figure 3-2 Optimal red blood cell lysis takes away the need to use a DNA label to exclude mature erythrocytes. (A) Staining of non-lysed bone marrow samples with Hoechst 33342 shows DNA⁻ cells, which comprise enucleated reticulocytes and erythrocytes, and DNA⁺ cells. (B) After RBC lysis, the number of anucleate cells is negligible. Therefore, it was judged unnecessary to use a DNA stain in conjunction with lysis of the samples.

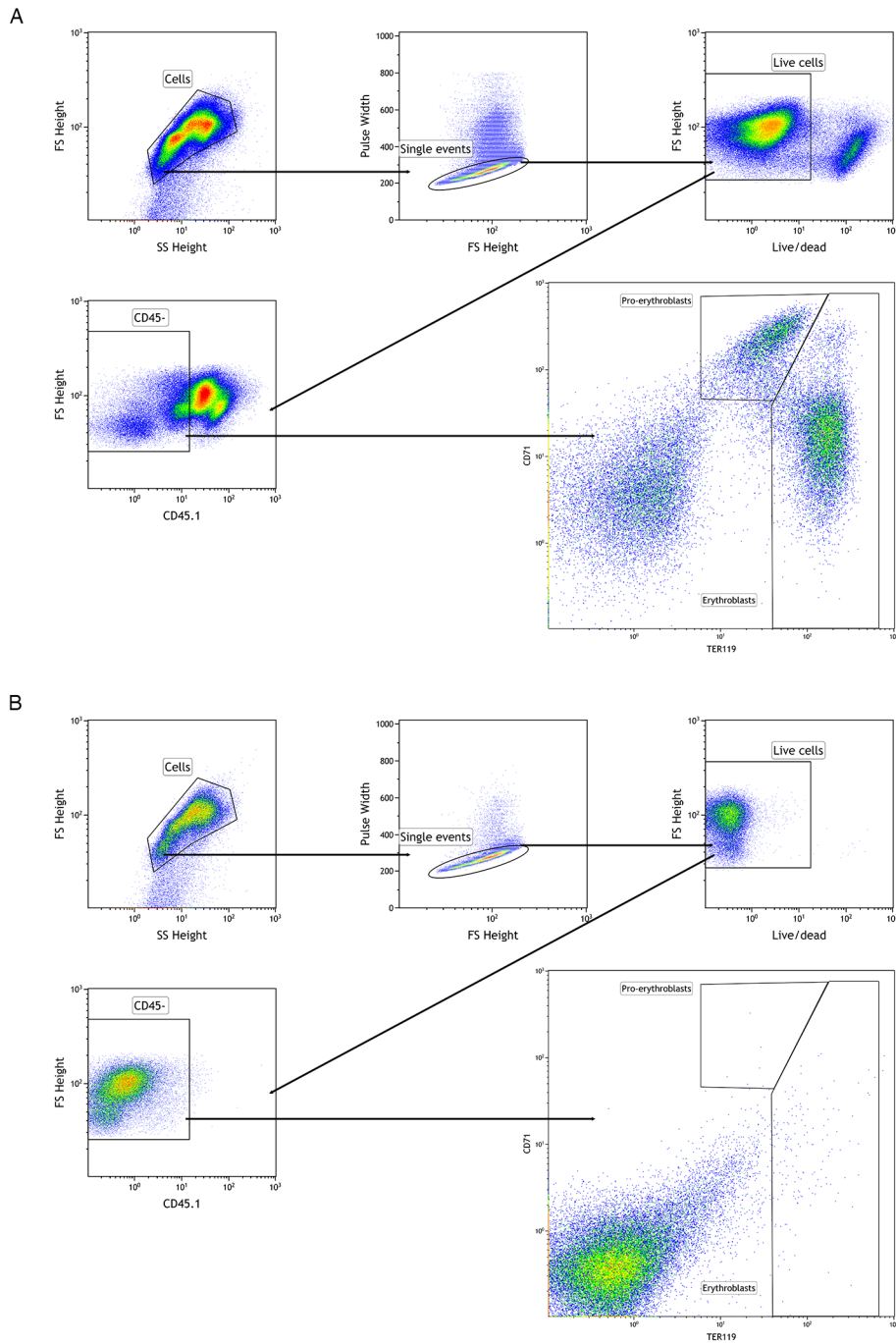


Figure 3-3 Gating strategy to identify subsets of erythroid progenitors. (A) Gating strategy used to quantify erythroid progenitors from the bone marrow and the spleen, representative naïve mice. Debris were excluded based on their smaller size. Only single cells were included by discriminating events with a high pulse width. Analysis was based on live cells which are negative for a fixable live/dead staining. Erythroid progenitors are defined as CD45⁻ cells. Pro-erythroblasts correspond to the CD71⁺ TER119^{low} population whereas erythroblasts are defined as CD71⁻ /⁺TER119^{high} cells. (B) Isotype control representative for naïve and infected mice.

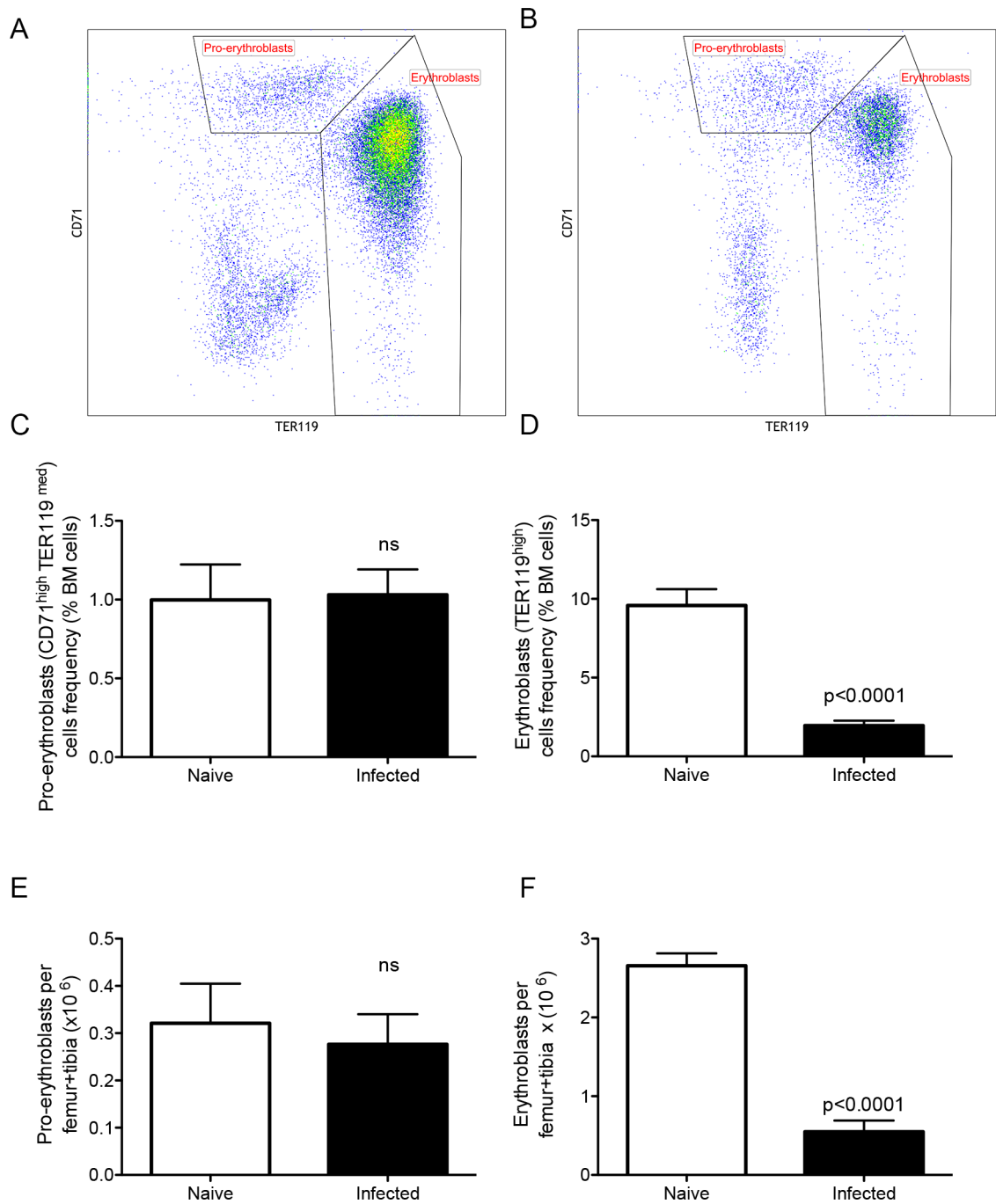


Figure 3-4. Medullary erythropoiesis is repressed in chronically infected C57BL/6 mice. (A and B) Flow cytometry analysis of CD45⁻ bone marrow cells using the erythroid surface markers CD71 (transferrin receptor) and TER-119. Pro-erythroblasts are CD45⁻ CD71⁺ TER119^{low} and erythroblasts are CD45⁻ CD71^{+/+} TER119^{high}. (C) Frequency of pro-erythroblasts in the bone marrow. (D) Frequency of erythroblasts in the bone marrow. (E) Absolute number of pro-erythroblasts and (F) erythroblasts per femur + tibia. (Mann Whitney test; n=14 mice per group from 4 independent experiments). Data represent mean + SEM All results were obtained 28 days after infection with *L. donovani*.

3.3.4 *L. donovani* parasites reside in bone marrow macrophages

Because erythropoiesis was impaired upon infection with *L. donovani*, the bone marrow was studied in the context of EVL to determine whether the microenvironment was altered. Bone marrow sections from naïve and infected mice were stained with haematoxylin and eosin to investigate if distinctive features appeared at the tissue level following *L. donovani* infection. Optimisation of the decalcification and sectioning protocol enabled the preservation of anatomical details such as the vasculature, cortical and trabecular bones (**Figure 3-5**). Microscopic investigation revealed accumulation of cells resembling macrophages (**Figure 3-5B, arrow**), a feature exclusive to infected mice. These cells were characterised by a large cytoplasm and cellular projections similar to the filopodia of macrophages²³⁴. However, this method did not allow for the identification of intracellular amastigotes. The bone marrow, together with the spleen and the liver, is a major site for parasite replication. Amastigotes typically reside in mononuclear phagocytes¹. In BALB/c mice, *L. donovani* amastigotes reside inside stromal macrophages of the bone marrow characterised by the cell surface marker CD169¹⁹. To confirm these results, immunohistochemistry of bone marrow was performed at day-28 post-infection (**Figure 3-6**). For this purpose, mice were infected with a *L. donovani* LV9 strain expressing a membrane-tdTomato fluorescent protein. Unfortunately, chronic infection of C57BL/6 mice proved harder to achieve with this strain of parasite than the wild-type strain. Instead immunocompromised B6 RAG2^{-/-} mice were used. These mice were chosen because of the higher parasite burden when compared to wild-type strains infected with the LV9-tdTomato strain, allowing easier detection of infected cells. CD68, a lysosome-associated glycoprotein expressed by macrophages and monocytes was used to identify tissue macrophages. Confocal analysis shows a co-localisation of parasites with the CD68 staining, a marker of macrophages²³⁵. The fluorescent parasites and the CD68 staining also co-localised CD169 (**Figure 3-6A**). However, single cells could not be identified from these images. The integrin α M (CD11b), a common marker of macrophages but with a low expression in bone marrow stromal macrophages¹⁴⁷, was undetectable on infected cells (**Figure 3-6B**). Taken together, these results confirm that parasites reside in bone marrow macrophages including stromal macrophages described previously as host cells in BALB/c mice by Cotterell et al.¹⁹. In order to get a better insight into the anatomical localisation of parasites within the bone marrow, an approximately 1mm-thick femoral section was imaged by multi-photon confocal microscopy and a deep z-stack projection was reconstituted. The vasculature was highlighted by staining with an anti-laminin antibody, which binds to a family of glycoproteins part of the extracellular matrix surrounding the

bone marrow vasculature^{126,236}. It was chosen to study the localisation of parasites in relation to the vasculature since the distance to the bone marrow vasculature informs on the niche which the cells are part of. The HSC niche in particular has been shown to be closely associated with the vasculature^{126,237}. Imaging of parasites in relation to the vasculature suggests parasites are localised close to the vasculature but the distance between parasites and blood vessels was not quantified (**Figure 3-6C and D**). This indicates that infected cells are in close proximity to the perivascular niches where most HSPCs and stromal cells typically reside^{126,221} (typically <10µm from blood vessels). Because of the difficulty associated with histological studies of long bones, there is no report of precise localisation of infected cells in relation to the bone marrow environment..

3.3.5 EVL induces alterations of bone marrow macrophages populations

Haematopoiesis is a complex process which requires a specific microenvironment and a variety of secreted factors¹²⁷. While HSPCs can be directly affected by multiple conditions, perturbations to the microenvironment have also been shown to alter haematopoiesis. We focused on two major components of the haematopoietic niche, stromal macrophages and CAR cells. CD169⁺ bone marrow stromal macrophages are essential component of the niche for erythropoiesis¹⁶⁹ as well as important regulators of the stromal cells in the HSC niche^{147,148}. It has been shown here and in a previous study that these cells can be infected by *L. donovani*. To identify these cells by flow cytometry, the gating strategy originally used by Chow et al.¹⁴⁷ was applied. Bone marrow macrophages were identified as Gr-1⁻ CD115⁻ F4/80⁺ low side scatter (SSC^{low}) cells (**Figure 3-7A**). The surface expression of CD169 was then quantified. In naïve mice, two populations of macrophages were resolved based on the intensity of CD169 staining; CD169^{low} and CD169^{high} (**Figure 3-7B**). The gating of these two populations was made arbitrarily based on the clear separation in naïve mice (green histogram). In naïve mice, CD169^{low} macrophages accounted for 2.77±0.59% of bone marrow cells or 5.35x10⁵ cells per leg. The CD169^{high} stromal macrophages accounted for 1.70±0.29%/3.36x10⁵ (**Figure 3-7C**). In infected mice, macrophages populations were differentially affected. There was no significant change in the absolute numbers of CD169^{low} (6.92x10⁵ cells per leg, ns) but the CD169^{high} population was significantly reduced by 36% (2.14x10⁵, p<0,01). In spite of the reduction of CD169^{high} macrophages, the numbers of total macrophages were similar between the two groups (**Figure 3-7D**), suggesting that a loss of CD169-expression by bone marrow macrophages is more likely than an absolute loss of macrophages. The ratio CD169^{low}/CD169^{high} was approximately 62/38 in naïve mice. Infected mice showed a distribution of bone marrow macrophages skewed towards the left (red histogram), with a ratio of 76/24.

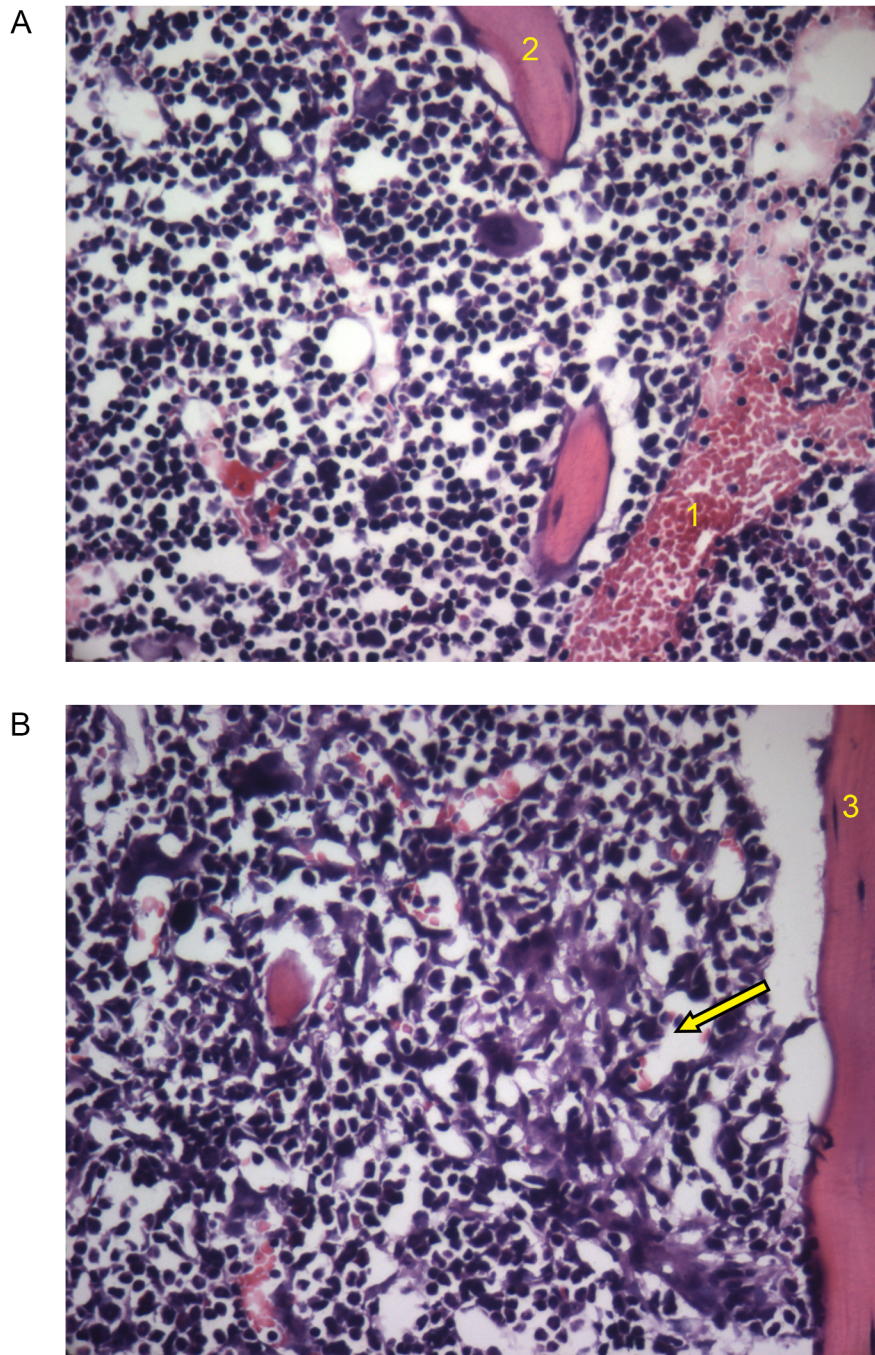


Figure 3-5. EVL results in focal accumulation of macrophage-like cells in the bone marrow. Haematoxylin-eosin staining of naïve (A) and infected (B) 5 μ m femoral sections. Unusual accumulation of macrophage-like cells is shown in B (arrow). Other notable features include the vasculature (1), trabecular bones (2) and cortical bone (3). Representative of 6 mice per group from 2 independent experiments.

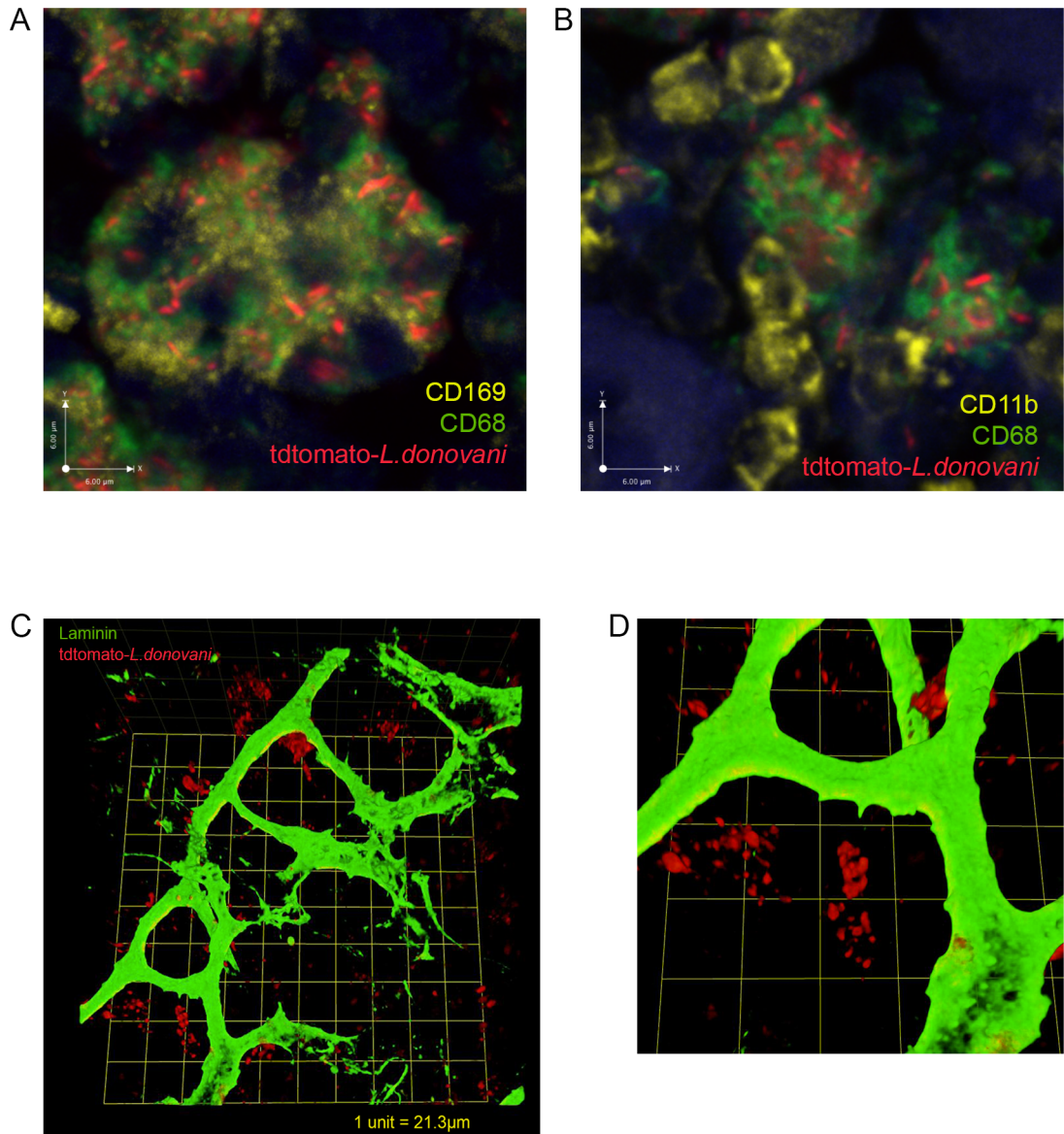


Figure 3-6. Markers of bone marrow stromal macrophages co-localise with *L. donovani* amastigotes in B6 RAG2^{-/-} mice. (A and B) Confocal imaging of a 5µm femoral section from a B6 RAG2^{-/-} mice infected with a membrane tdTomato-expressing strain *L. donovani* amastigotes (tdTomato-LV9, red) and stained with DAPI (blue), CD169 (yellow) and CD68 (green) in (A) and with DAPI (blue), CD11b (yellow) and CD68 (green) in (B). (C) Confocal imaging of thick bone marrow sections in B6 RAG2^{-/-} mice infected with tdTomato-LV9 (red) and stained with an anti-Laminin antibody (green). Images represent maximum intensity projection of success confocal slices in the z-axis. (D) Enlargement of a portion of image C.

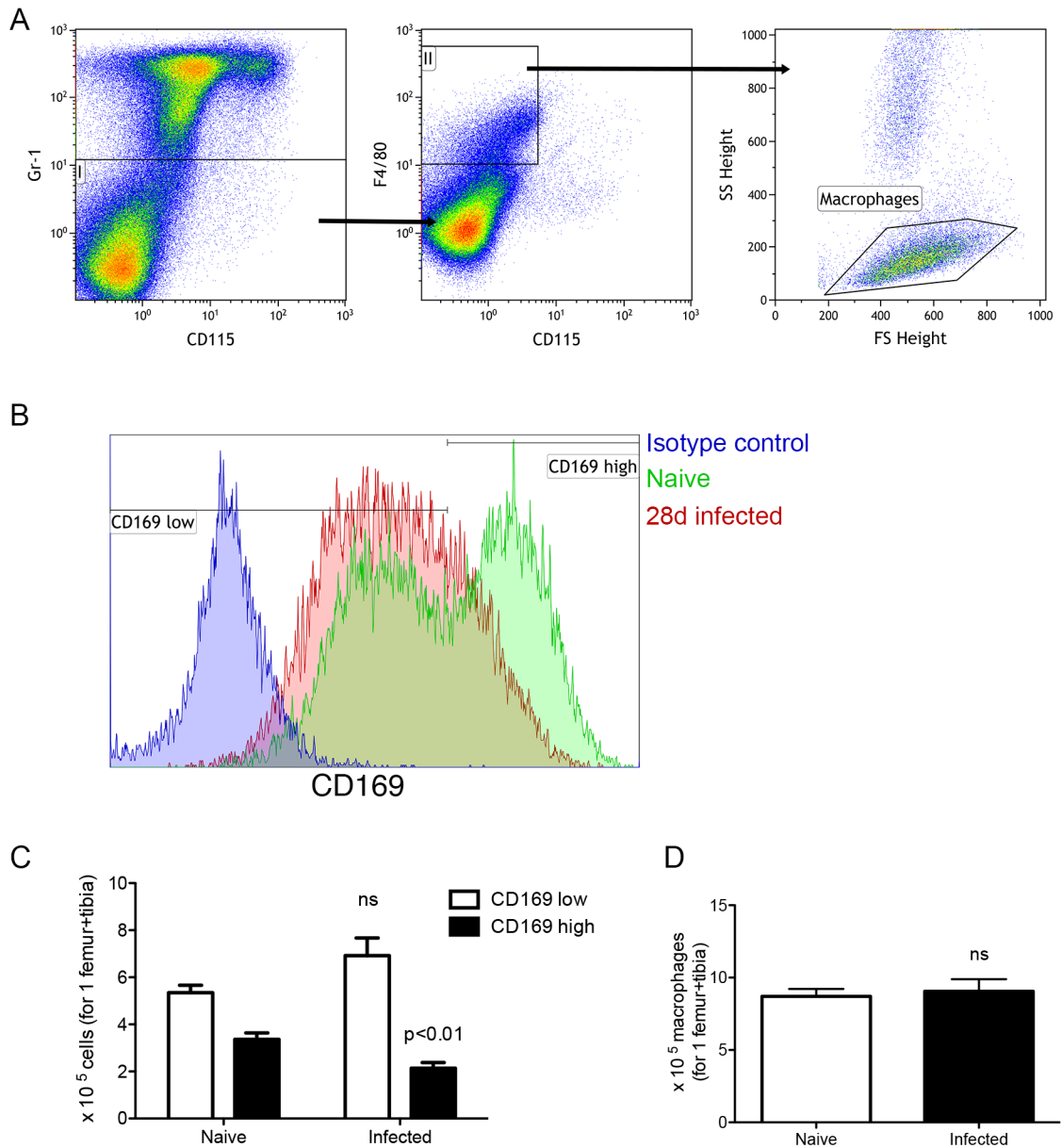


Figure 3-7. Bone marrow macrophage populations are altered following *L. donovani* infection. (A) Bone marrow macrophages are identified as Gr-1⁻ CD115⁻ F4/80⁺ SSC^{low} cells¹⁴⁷. (B) CD169 expression on bone marrow macrophages of naïve (green) and infected (red) mice. Isotype control (blue) is representative of both naïve and infected mice. (C) Absolute numbers of macrophages per leg (1 femur + 1 tibia) according to the gating described in A and B. Absolute numbers were calculated from the frequencies multiplied by the total bone marrow cells isolated from each mouse. Data represent mean + SEM. All experiments were performed 28 days after infection. (unpaired t-test; n=10 mice per group from 2 independent experiments)

3.3.6 EVL correlates with repression of the bone marrow stromal support

The data described here indicate an impairment of erythropoiesis as well as an alteration of stromal macrophages. While CD169⁺ bone marrow macrophages are important for erythropoiesis¹⁶⁹, their depletion also causes a more general disruption of haematopoiesis, characterised by an alteration of the stromal niche retaining HSPCs in the bone marrow¹⁴⁷. The expression of Kit-ligand (Kitl or Scf), Angiopoietin 1 (Angpt1), vascular cell adhesion molecule 1 (Vcam1) and Cxcl12, genes expressed by stromal cells and involved in the quiescence and retention of HSCs, was measured^{140,144,238,239}. RT-qPCR analysis of total bone marrow cells from chronically infected mice shows no change in expression of Kitl, Angpt1 or Vcam1 but a 50% decrease in Cxcl12 expression (**Figure 3-8A-D**). This can be either a result of gene down-regulation or a difference in relative stromal cell frequencies. In Cxcl12^{DsRed} mice, fluorescent DsRed protein was inserted inside the Cxcl12 coding sequence, so that the expression of DsRed is regulated by the promoter of Cxcl12. This model, as described previously²²¹, highlights CXCL12-abundant reticular (CAR) cells, a population of mostly perivascular stromal cells, where the HSC-niche is typically located (**Figure 3-9A**). CAR cells were also observed in the bone marrow of day 28-infected Cxcl12^{DsRed} mice (**Figure 3-9B**). An attempt to quantify cells from images of tissue sections resulted in a frequency of DsRed-positive cells of approximately 5% (**Figure 3-9C**), with no difference between the two groups. This frequency was much higher than the reported frequency of CAR cells in the bone marrow, which is estimated at 0.26%¹⁴⁵. This is most likely due to the morphology of CAR cells. They are fibroblastic cells with cytoplasmic projections²⁴⁰ in the 3 dimensions, so a 2-dimensional analysis is likely to over-estimate cells by counting the projections as a single cell. The bone marrow was therefore flushed and analysed by flow cytometry, a method judged more reliable for quantification of CAR cells (**Figure 3-10A**). The frequency of CAR cells in control mice was then measured at 0.32±0.02% of total bone marrow cells, corresponding to 4.84±0.49x10⁴ cells per femur. The frequency and absolute number of Ds-Red⁺ cells were reduced in infected mice, down to 0.11±0.01% and 1.36±0.20x10⁴ cells per femur, confirming that fewer cells express detectable levels of CXCL12 in the reporter mouse model (**Figure 3-10B and C**). To determine whether this reduction in Cxcl12 in the bone marrow at the tissue level was a reflection of lower number of stromal cells or down regulation of Cxcl12 expression at the single cell level, I sought to quantify the absolute numbers of stromal cells in the bone marrow. It has been shown that CAR cells are mainly composed of mesenchymal stem and progenitor cells MSPCs, characterised by their ability to produce adherent fibroblastic colonies (CFU-F) *in vitro*¹⁴⁵. A CFU-F assay is accepted

as a reflection of the number of MSCs in the bone marrow. As shown in **Figure 3-10D**, there was also a reduction in the absolute number of CFU-F in the bone marrow of infected mice, an average 32.6 ± 3.4 CFU-F could be recovered from 1 million bone marrow cells in naïve mice, while only 11.8 ± 4.5 could be recovered from infected mice. Taken altogether, these results suggest that chronic EVL leads to a reduction of stromal support in the bone marrow. This is characterised by a loss of CXCL12-expressing stromal cells. Molecular factors for the reduction of CD169^{high} macrophages and CAR cells was then investigated.

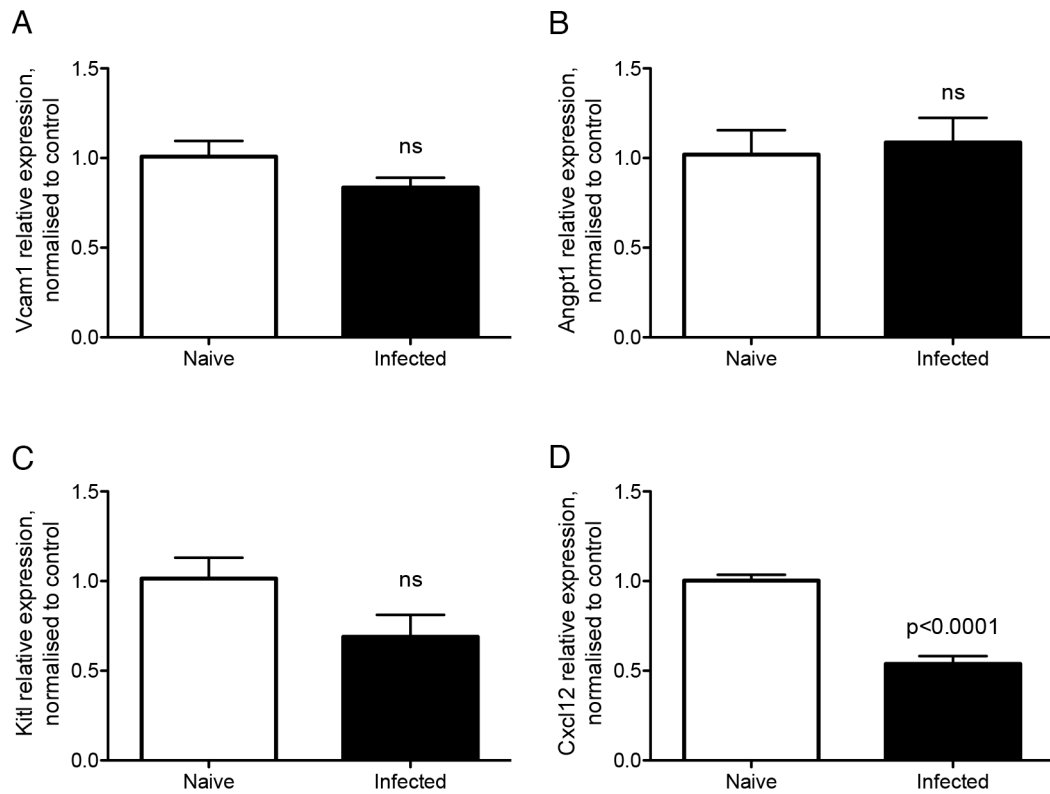


Figure 3-8. Effect of *L. donovani* infection on the expression of HSC niche-essential genes in total bone marrow. RNA was extracted from total bone marrow cells and analysed by RT-qPCR for the expression of vascular cell adhesion molecule 1 (Vcam1) (A), Angiopoietin 1 (Angpt1, B), Kit-ligand (Kitl, C) and Cxcl12 (D). Intra-sample standardisation was done by normalisation to the house-keeping gene HPRT and inter-sample standardisation was done by normalisation to the average expression of the naïve group. (unpaired t-test; n=3 mice per group from one experiment for Vcam1, Angpt1 and Kitl; n=8 mice per group from two experiments for Cxcl12). Data represent mean + SEM. All experiments were performed 4 weeks after infection.

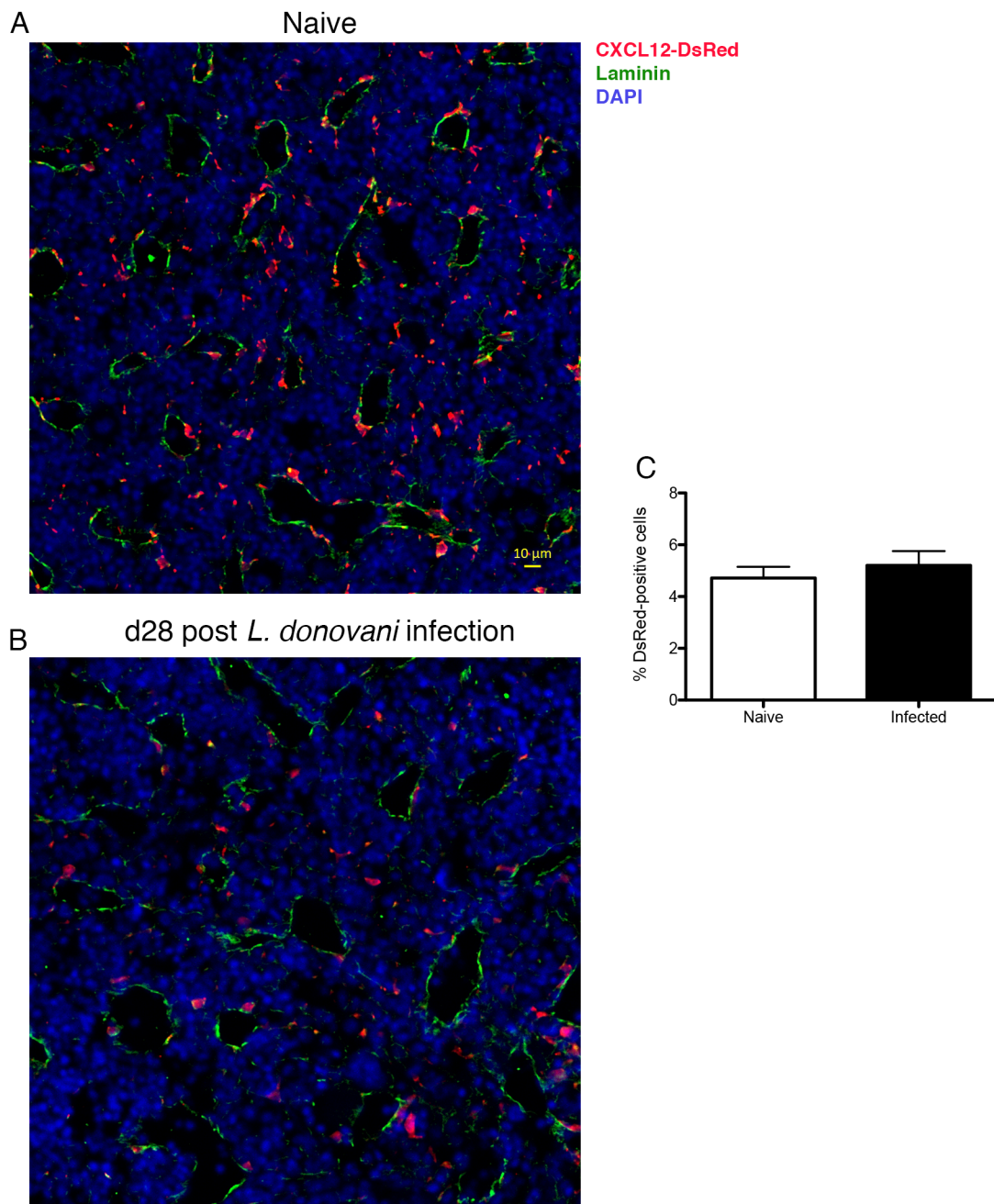


Figure 3-9. Visualisation of CXCL12-expressing cells using *Cxcl12*-DsRed reporter mice strain. 5µm-thick bone marrow sections from naïve (A) and d28-infected (B) CXCL12-DsRed mice were stained with an anti-laminin antibody (green) and DAPI (blue) before confocal analysis. Images are representative of 3 mice per group from one experiment. (C) Quantification of DsRed+ cells from image-analysis. Data represent mean + SEM (unpaired t-test; n=3 mice per group; 1 image per mouse).

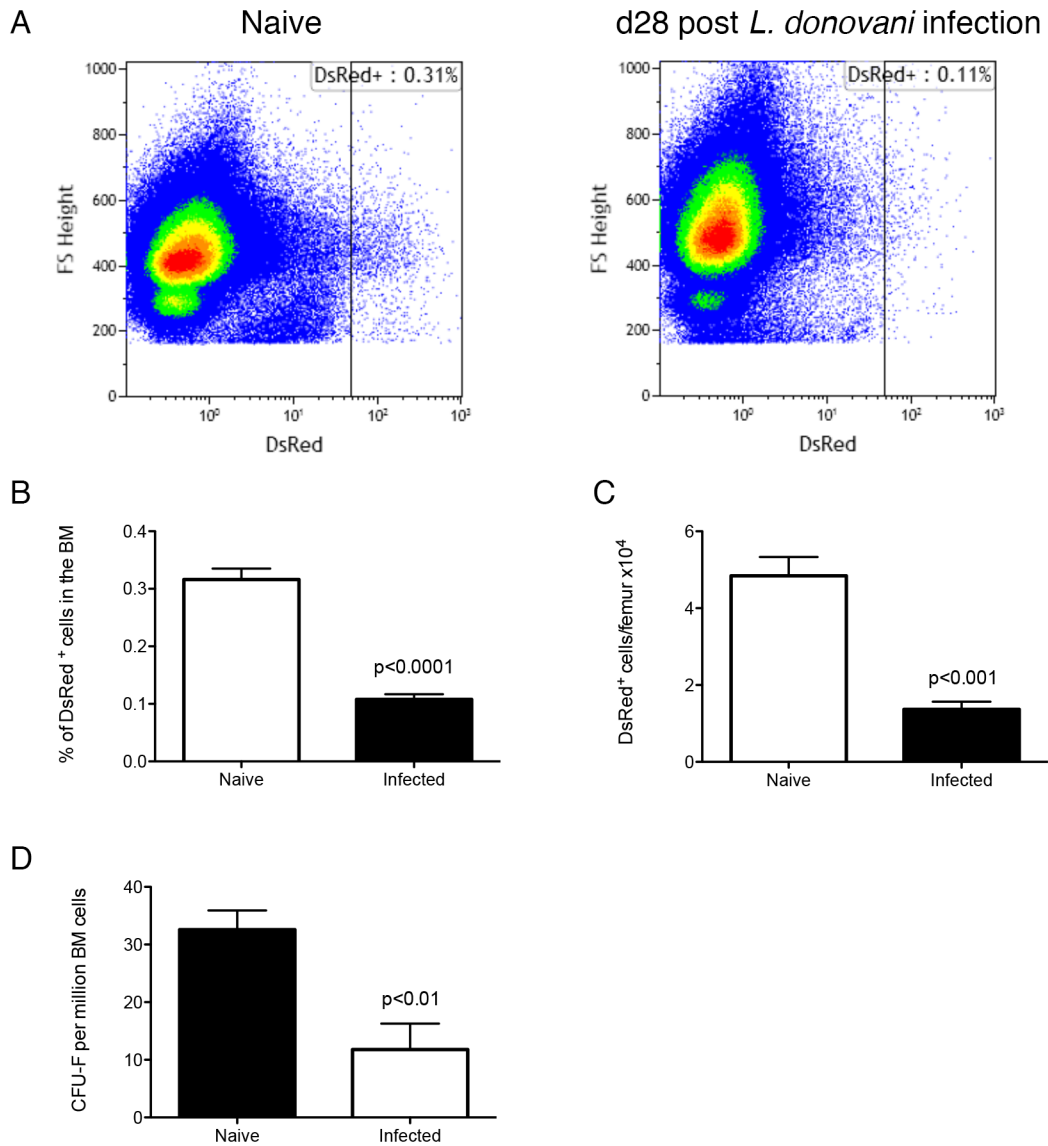


Figure 3-10. The bone marrow stromal compartment is impaired during chronic EVL. (A) Flow cytometry analysis of DsRed-positive cells in naïve and infected CXCL12-DsRed reporter mice. Dot plots show identical number of cells, gated on live single cells (unpaired t-test). (B) Frequency of DsRed⁺ cells. (C) Absolute number of DsRed⁺ cells per femur, calculated from the frequency of DsRed⁺ cells in A multiplied by the total bone marrow cell count (Mann Whitney test; A and B= Data from 5 naïve mice and 9 infected mice from 2 independent experiments). (D) Number of CFU-F per million bone marrow cells. (Unpaired t-test; n=7 mice per group from 2 independent experiments). Data represent mean + SEM. All experiments were performed 28 days post-infection with *L. donovani*.

3.3.7 G-CSF is up-regulated during EVL

The regulation of the granulocyte-colony stimulating factor (G-CSF) was investigated. In a recent study, G-CSF has been shown to block medullar erythropoiesis by depleting a subset of stromal macrophages expressing CD169 in the mouse²³². In addition, Petit et al. have demonstrated that G-CSF inhibits bone marrow Cxcl12 expression²⁴¹. Because the effects of G-CSF share similarities with events in EVL, the levels of G-CSF were measured in the plasma of naïve and *L. donovani*-infected mice. A 4-fold increase of G-CSF was detected at the protein level in infected compared to naïve mice (**Figure 3-11A**). Average normal concentration were of 110 ± 6 pg/ml with a reference interval calculated from 13 naïve mice from 3 experiments of 51 pg/ml to 134 pg/ml. In 28-day infected mice, the average was 599 ± 94 pg/ml and 92% (12 out of 13 infected mice) of the mice had values above the reference interval. RT-qPCR analysis of *Csf3*, the gene encoding G-CSF, in total bone marrow and spleen cells was performed to identify the source of circulating G-CSF. No significant up or down-regulation of *Csf3* was detected in the bone marrow (**Figure 3-11B**) or the spleen (**Figure 3-11C**) of infected mice. Hence, increased G-CSF detected in plasma may be derived from cellular source residing outside the bone marrow or spleen. All organs are virtually capable of producing G-CSF, and the cellular source is thought to be endothelial cells, fibroblasts and macrophages²⁴². Microarray data from the Immunological Genome Project consortium shows no cell type with a notably high level of *Csf3* (**Figure 3-11E and F**). No dataset from the Immgen database showed a cell type with a normalised expression value above the 120 threshold. The Immgen consortium recommends this value as the threshold for gene expression. Under the 120 value, genes have a less than 95% probability of being expressed. The only cell type with a higher signal than other types is the blood endothelial cells from subcutaneous lymph nodes (**Figure 3-11F**, BEC SLN, in red), in accordance with other studies showing that endothelial cells express G-CSF²⁴³. To test whether G-CSF up-regulation participates in alterations of medullar erythropoiesis, 25 µg of a G-CSF neutralising antibody was injected daily into mice with EVL. The mice had been infected for 6 weeks prior to treatment, which lasted 1 week. Treatment with the antibody had no measurable effect on the erythropoiesis when compared to the isotype control group. Reduction of erythroblasts was not rescued by administration of the anti-G-CSF antibody (**Figure 3-12B**). Pro-erythroblasts levels were unaffected by the infection or the treatment (**Figure 3-12A**). Interestingly, levels of circulating G-CSF were higher in the treated group than in the isotype control, suggesting that the treatment may have induced a feedback loop resulting in increased production of G-CSF (**Figure 3-12C**).

G-CSF is known to inhibit the CXCL12/CXCR4 signalling axis through the repression of CXCL12 expression by stromal cells and by inducing the degradation of extracellular CXCL12 by neutrophil elastase²⁴¹. Therefore, the neutrophil elastase activity in the bone marrow of naïve and infected mice was assessed by a biochemical assay monitoring the degradation of a specific peptide (**Figure 3-11D**). Lysates were prepared from bone marrow cell pellets and incubated with N-methoxysuccinyl-Alanine-Alanine-Proline-Valine-p-nitroanilide (Calbiochem). This peptide is specifically cleaved by neutrophil elastase and the liberation of 4-nitroaniline can be measured by its specific absorbance. The rate of 4-nitroaniline production is considered a reflection of neutrophil elastase activity. The peptide was degraded at the same rate in naïve and infected mice, meaning there is no difference in neutrophil elastase activity from bone marrow cells (**Figure 3-11D**). Systemic neutrophil elastase activity was not measured, so it cannot be excluded that neutrophil elastase secreted at a distant site is present in the bone marrow. Indeed, cell lysates were used here instead of bone marrow supernatant as done in the original study²⁴¹.

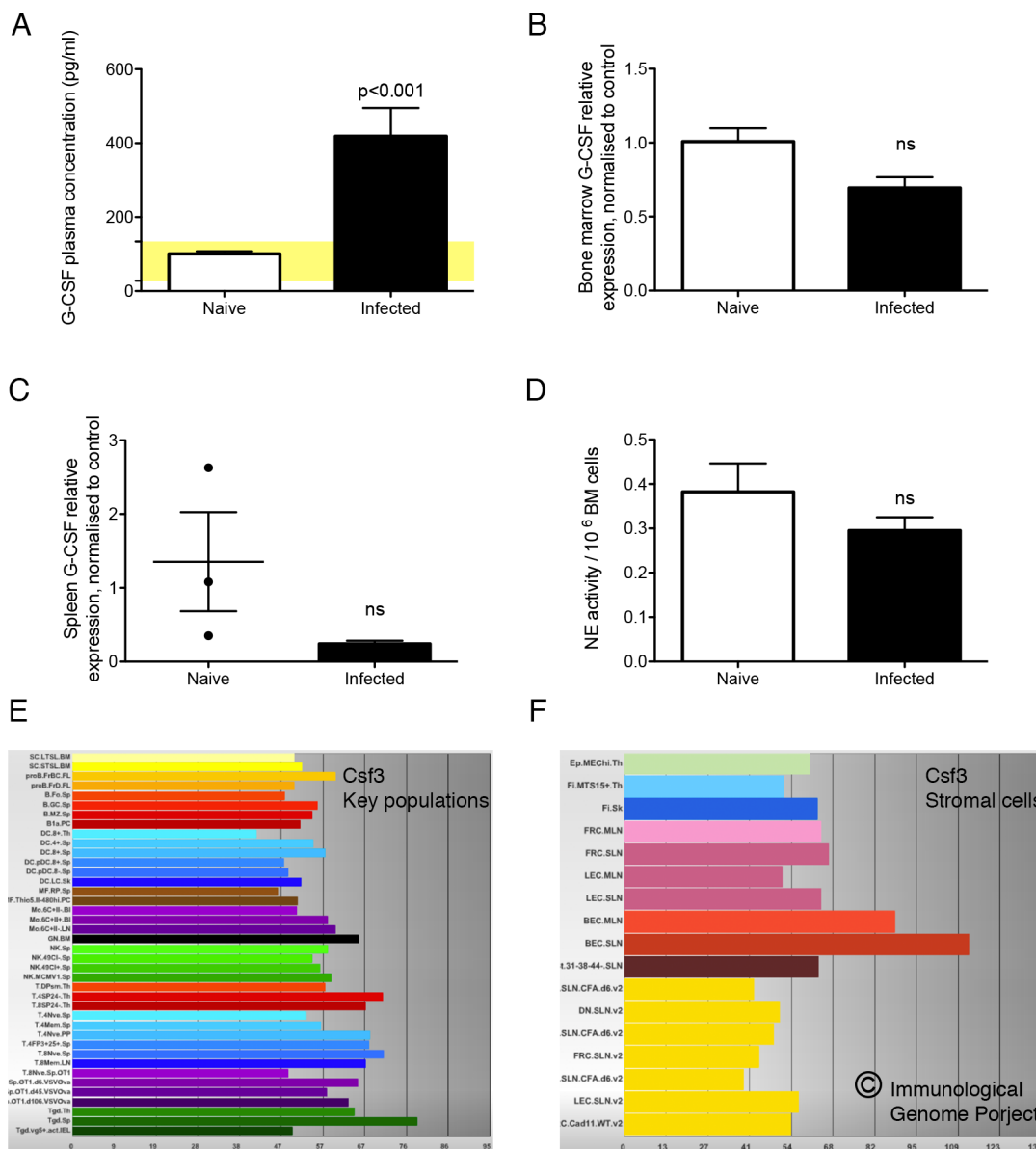


Figure 3-11. EVL induces down-regulation of CXCL12 expression in the bone marrow in correlation with up-regulation of systemic G-CSF. (A) Concentration of G-CSF in the blood of mice. (Mann Whitney test; n=13 mice per group from 3 independent experiments). (B-C) Quantification of G-CSF expression in total bone marrow (B) and spleen (C) cells. G-CSF mRNA expression was normalised by RT-qPCR against a housekeeping-gene in each sample and expressed relatively to the average expression of the naïve group (Unpaired t-test; n=3 mice per group from 1 experiment). (D) Neutrophil-elastase (NE) activity from bone marrow cell lysates. Identical numbers of cells were used. NE activity was monitored by a colorimetric assay using a specific substrate. One unit of neutrophil elastase activity is defined as the quantity of enzyme that liberated 1µmol of substrate per hour. (Unpaired t-test; n=5 mice per group from 1 experiment). All data represent mean ± SEM of experiments at day 28 p.i. (E and F) Expression atlas of the Csf3 gene in the “Key population” and “Stromal cells” panels from the Immunological Genome project.

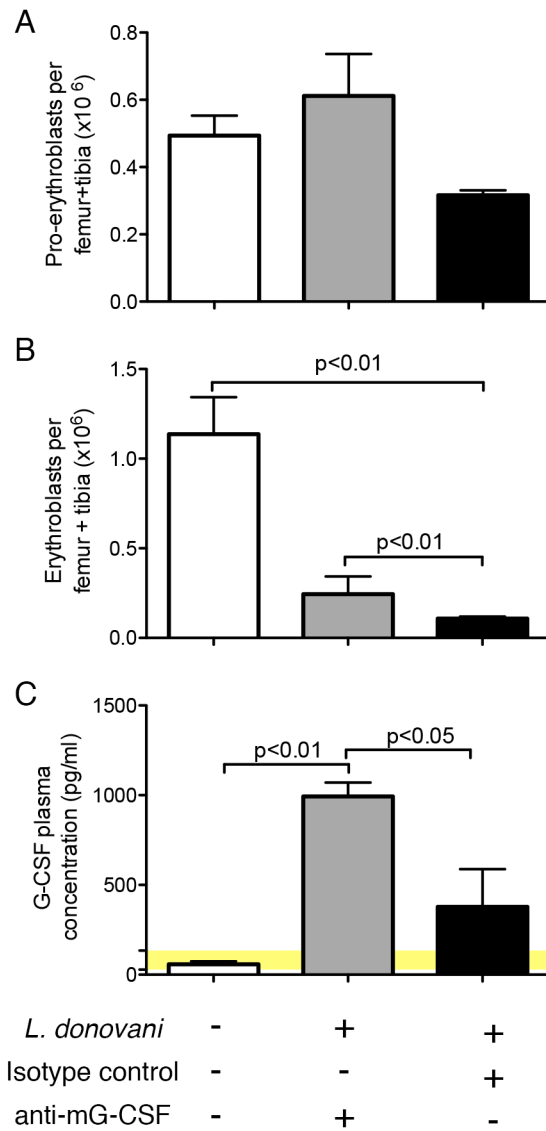


Figure 3-12. Effect of treatment with a neutralising anti-G-CSF antibody (mG-CSF) on erythropoiesis and circulating G-CSF in mice infected with *L. donovani*. Mice were infected with *L. donovani* for 5 weeks. They were then administered 25 μ g of monoclonal mouse IgG1 antibody or IgG isotype control i.p. daily for one week before being killed. (A and B) Pro-erythroblasts and erythroblasts were quantified as described in Fig. 3-2. (C) Quantification of circulating G-CSF in the plasma measured by ELISA assay. (One-way ANOVA with Turkey's multiple comparison test; n=3 mice per group from a single experiment). Data represent mean + SEM.

3.3.8 Splenic erythropoiesis is increased during EVL

One of the hallmarks of VL, both in humans and experimental models, is a dramatic increase in spleen size. The spleen weight of C57BL/6 mice 4 weeks after infection averaged $637\pm 36\text{mg}$ whereas the baseline in naïve mice was measured at $73\pm 3\text{mg}$, corresponding to a 9-fold increase (**Fig. 3-13A**). This increase in weight correlated with a 5-fold increase in cellularity (**Fig. 3-13B**). Splensens were dissociated into single cells suspensions and analysed for erythropoiesis in the same way as the bone marrow. Total erythroid precursors (pro-erythroblasts + erythroblasts) frequency was quantified in infected mice over time. Interestingly, the curves of spleen weight and frequency of erythroid precursors followed very similar trends (**Fig. 3-13C**). The spleen is capable of erythropoiesis and it produces erythrocytes in a steady state (**Fig. 3-14A**). Indeed, pro-erythroblasts and erythroblasts represented $0.85\pm 0.20\%$ and $0.16\pm 0.06\%$ of total splenocytes respectively in naïve mice (**Figure 3-14**). In infected mice the frequencies of both were dramatically increased, by 16 and 45-fold respectively ($9.00\pm 1.50\%$ and $7.19\pm 1.00\%$) (**Figure 3-14**). Because splenomegaly was associated with an increase in the spleen cellularity (**Figure 3-13B**), the discrepancies in absolute numbers were even higher (**Figure 3-14E and F**). These results indicate that splenomegaly correlates with splenic erythropoiesis, a process in which a specific population of erythropoietic precursors, called stress erythroblasts, proliferate in response to anaemia or hypoxia^{244,245}. From day 3 after infection with *L. donovani* to day 21, the frequencies of cumulated pro-erythroblasts and erythroblasts in the bone marrow were similar between the naïve and the infected groups. A significant 70% reduction of medullar erythroblasts in the infected mice was measured by day 28 (**Figure 3-21A**). The frequencies of splenic erythroblasts during the course of infection mirrored the trend seen in the bone marrow. Indeed, splenic erythropoiesis was similar between the two groups from day 3 to day 21 then a sharp rise of splenic erythropoiesis was measured at day 28. This suggests that splenic erythropoiesis occurs in response to impairment of medullar erythropoiesis.

3.3.9 Splenomegaly correlates with changes of the splenic architecture

In order to understand the contribution of extramedullary erythropoiesis to splenomegaly, spleen tissues were analysed by immunohistochemistry. Spleen weight increases massively between day 21 and day 28 post-infection (**Figure 3-15A**). This corresponds to a remodelling of the tissue, characterised by an area-wise increase in F4/80 staining (**Figure 3-15B**). Based on the F4/80 staining which highlights red pulp macrophages and the DAPI nuclear staining which allows distinction between red pulp and the more cell-dense white

pulp, the gross architecture of the spleen was quantified at day 28 post-infection. The white pulp area per tissue section did not increase significantly (**Figure 3-16A**). The red pulp was more dramatically dilated with a 5-fold increase in area per tissue section (**Figure 3-16B**). This resulted in a ratio red pulp/white pulp of 1.9 in naïve mice vs. 6.4 in infected mice (**Figure 3-16C**). Taken together, these results show that the spleen remodelling is characterised by a dilatation of the red pulp more than the white pulp.

3.3.10 Extramedullary erythropoiesis occurs in the splenic red pulp

The spleen sections were then stained with antibodies specific for CD71 and TER119 to highlight erythroid precursors. At day 28 post-infection, the spleens from infected mice contained visibly more erythroid precursors (**Figure 3-17A**). Interestingly, the staining with CD71 and TER119 revealed that erythroid precursors co-localised exclusively with red pulp F4/80⁺ macrophages, both in naïve and infected mice (**Figure 3-17B**). These results indicate that proliferation of erythroid precursors in the spleen is linked to the expansion of the red pulp. Molecular pathways for the induction of extramedullary erythropoiesis are known. Indeed, the bone morphogenetic protein 4 (BMP4) is necessary to trigger splenic erythropoiesis and mice with a mutation altering the BMP-signalling pathway do not develop extramedullary erythropoiesis in response to anaemia²⁴⁴. To understand if infection with *L. donovani* triggers BMP4 signalling in the spleen, the expression of BMP4 in the spleen of infected mice was investigated by immunohistochemistry. In naïve mice, BMP4 expressing cells were more prominent in the red pulp, although BMP4 was also detected in the white pulp (**Figure 3-18A**). Despite the extramedullary erythropoiesis, fewer BMP4-expressing cells could be seen in infected mice (**Figure 3-18A and B**).

3.3.11 Reduction of medullar erythropoiesis is independent of splenomegaly

In our model of EVL, any causality between the alterations of the bone marrow and changes in the spleen still needs to be established. It is unclear whether extramedullary erythropoiesis is triggered by reduction of erythropoiesis in the bone marrow or the opposite. Hypersplenism-induced pancytopenia has been suggested previously since haematological parameters return to normal value following splenectomy in VL patients⁶². However direct evidence linking the two have never been reported so far. To understand the contribution of the spleen to the anaemia caused by *L. donovani*, splenectomised C57BL/6 mice were infected and analysed for haematological changes. Mice were splenectomised or sham-operated prior to delivery. They were allowed to recover for 3 weeks before being infected with *L. donovani* and were killed 4 weeks after infection.

Infected splenectomised mice had a mild anaemia, similarly to their sham-operated counterparts (**Figure 3-19A**). The nature of anemia was as described in paragraph 1.2.1, i.e. normochromic (**Figure 3-19B**) with a macrocytic tendency in sham-operated infected mice (**Figure 3-19C**). When comparing averages, no difference in MCV was measured. However, on an individual level, 7 mice out of 15 sham-operated infected mice showed macrocytosis, according to the values in Table 3.1. Only one splenectomised infected mice had a MCV above the reference interval. Interestingly, thrombocytopenia was less pronounced in splenectomised mice than sham-operated. These data are discussed in **Chapter 4**. The bone marrow was analysed for erythropoiesis to determine if the pathogenesis was similar in splenectomised and sham-operated mice. Decolouration of the femurs was observed both in the absence and presence of a spleen, indicating that erythropoiesis is altered independently of the spleen (**Figure 3-20A**). The bones from splenectomised infected mice were slightly more red in colour than the sham-operated infected mice, suggesting erythropoiesis was not as repressed in the former. This was confirmed by flow cytometry analysis of total bone marrow stained for erythroid precursors. Matching what has been described here before, there was no decrease in CD71^{high}TER119^{low} pro-erythroblasts numbers in infected mice (**Figure 3-20B**). On the other hand, a significant decrease in erythroblasts numbers was measured (**Figure 3-20C**). No significant difference was measured between splenectomised infected mice and sham-operated infected mice but the numbers of erythroblasts dropped less dramatically in splenectomised (-59%) than in sham-operated mice (-79%) when compared to their naïve counterparts. These results indicate that *L. donovani* infection can decrease medullar erythropoiesis in the absence of a spleen. However, they also suggest that loss of erythropoiesis is milder in splenectomised mice, so a partial contribution of the spleen can not be excluded.

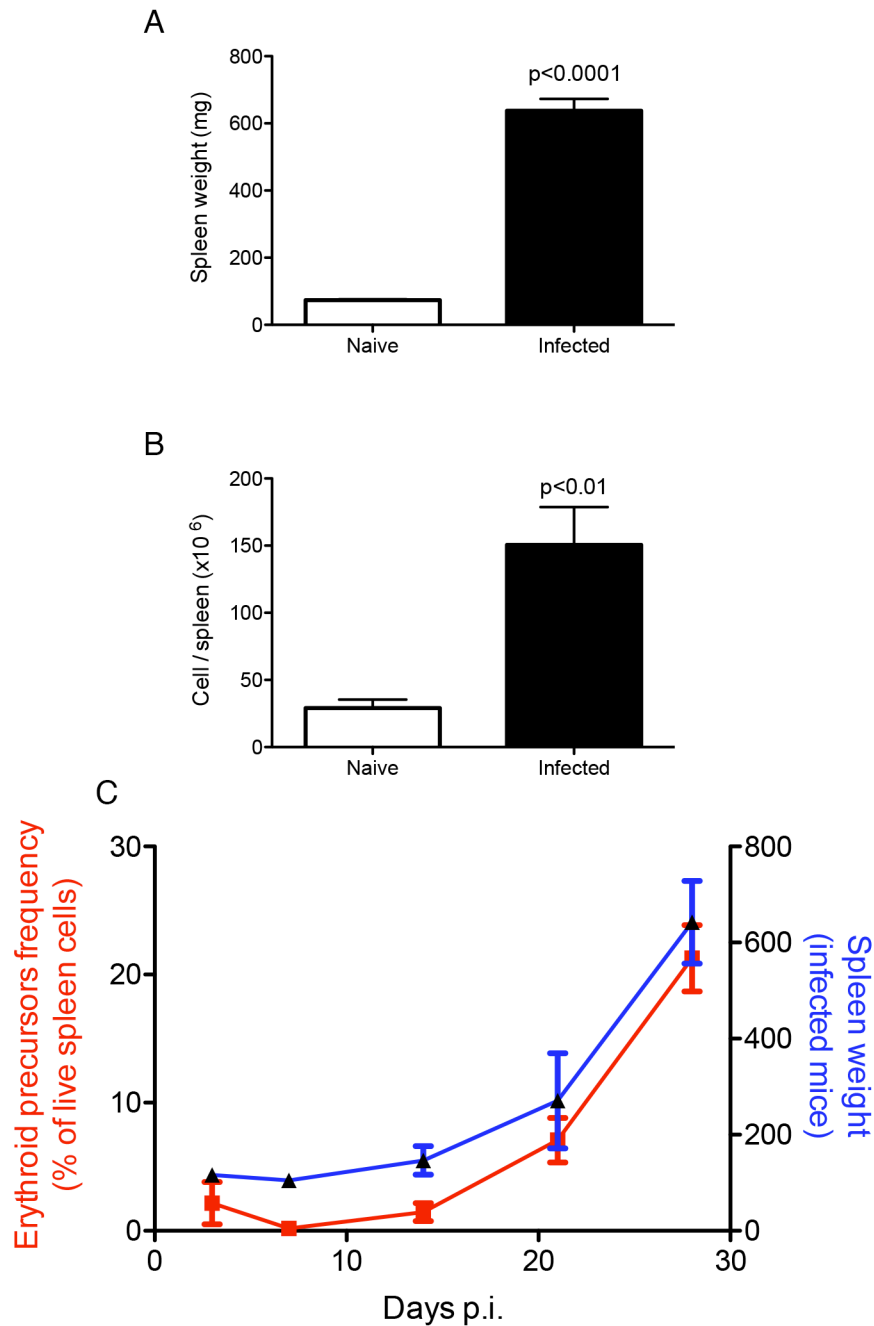


Figure 3-13. Chronic EVL induces splenomegaly. (A) Spleen weight from naïve and infected mice (n=20 from 6 independent experiments) (B) Absolute numbers of cells per spleen. Splens were dissociated into single cells suspension and cells were counted with an automatic cells counter. Dead cells were excluded from the counts based on Trypan blue inclusion. All mice were infected for 28 days (unpaired t-test with Welch’s correction; n=8 mice per group from two independent experiments). (C) Total erythroid precursors frequency (pro-erythroblasts and erythroblasts) and spleen weight during *L donovani* infection. (n=3 or 4 mice per time point, from a single experiment). Data represent mean \pm SEM.

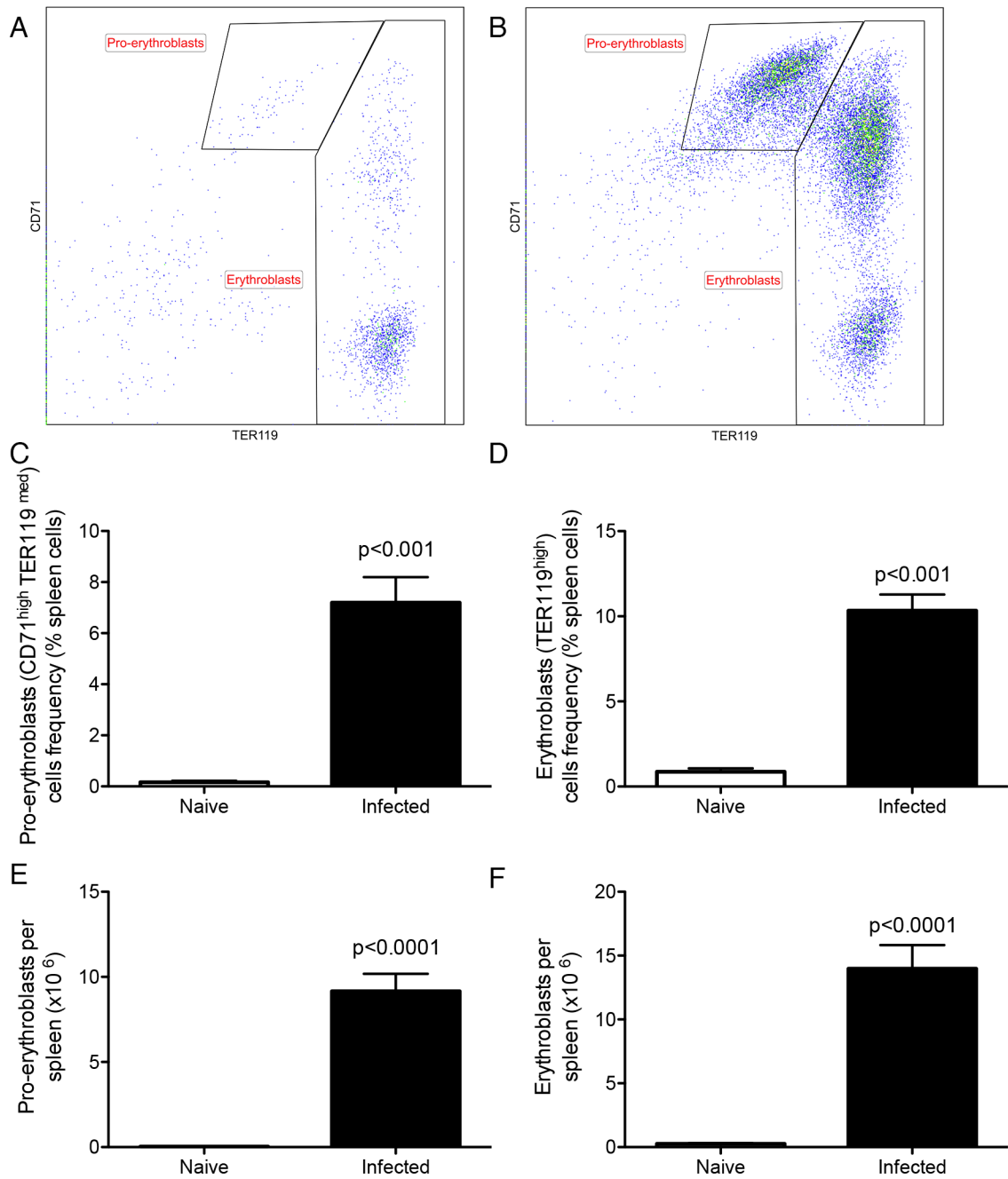


Figure 3-14. Chronic EVL induces extramedullary erythropoiesis in the spleen. (A and B) Gating strategy for identification of pro-erythroblasts (CD45⁻CD71^{high}TER119^{low}) and erythroblasts (CD45⁻CD71^{high/low}TER119^{high}) in the spleens of naïve (A) and infected (B) mice. Plots are gated on CD45⁻ live cells and equal number of live cells. (C) Frequency of pro-erythroblasts in the spleen. (D) Frequency of pro-erythroblasts in the spleen. (E) Absolute number of erythroblasts per spleen. (F) Absolute number of erythroblasts per spleen. Absolute numbers were calculated by multiplying the cell frequencies by the total numbers of cells per spleen. All mice were infected for 28 days. Data represent mean + SEM (unpaired t-test with Welch's correction; n=8 mice per group from two independent experiments).

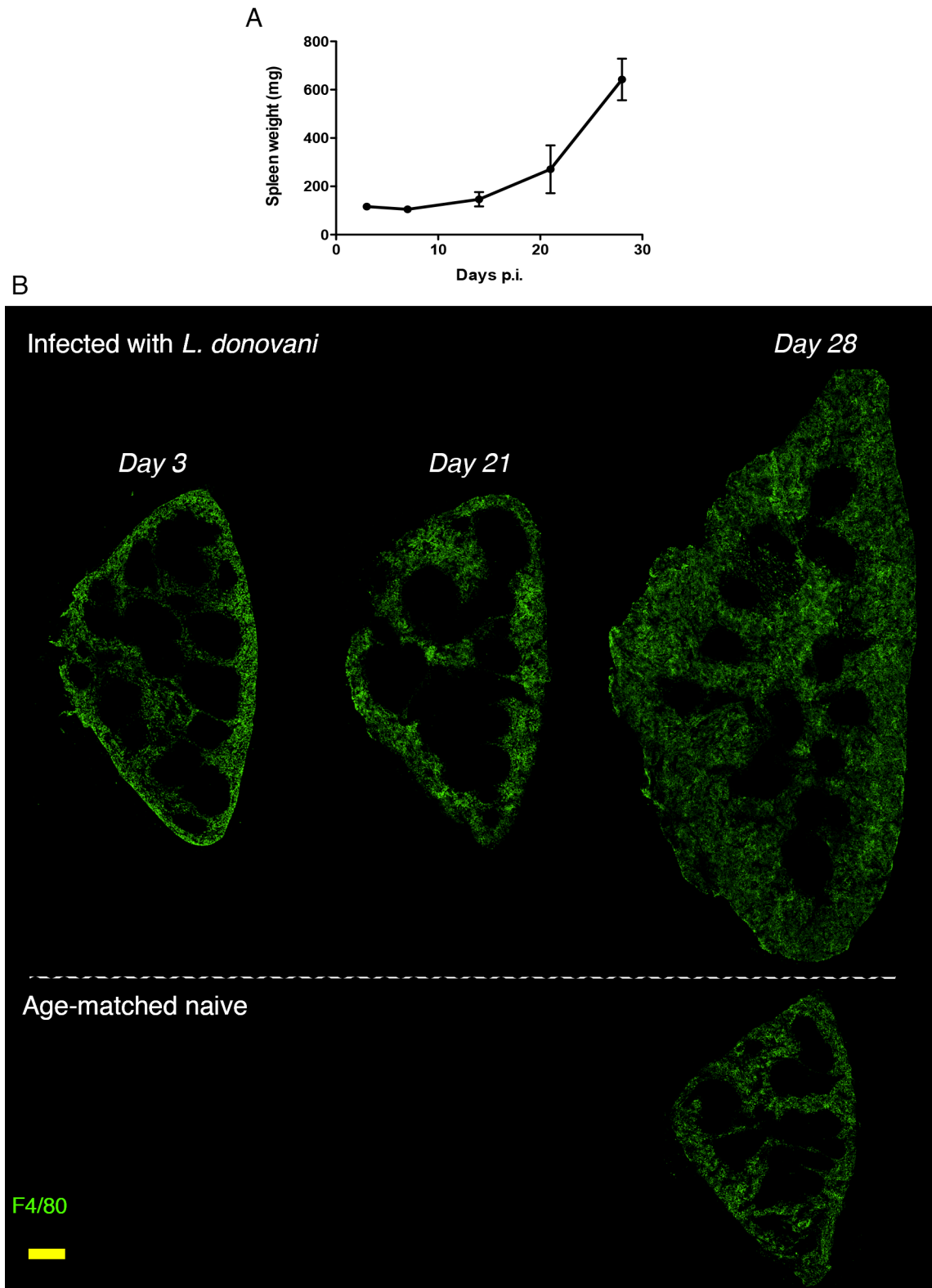


Figure 3-15. Histological changes in the spleen associated with chronic EVL. (A) Evolution of spleen weight in infected mice other time (n=3 mice per time point from one experiment). Data represent mean \pm SEM. (B) Fluorescent scans of 5 μ m-thick spleen sections stained with anti-F4/80 antibody in infected mice at different time points. The naïve control is age-matched with the day-28 mice (data representative of 3 mice per time point from one experiment). Scale bar = 1mm.

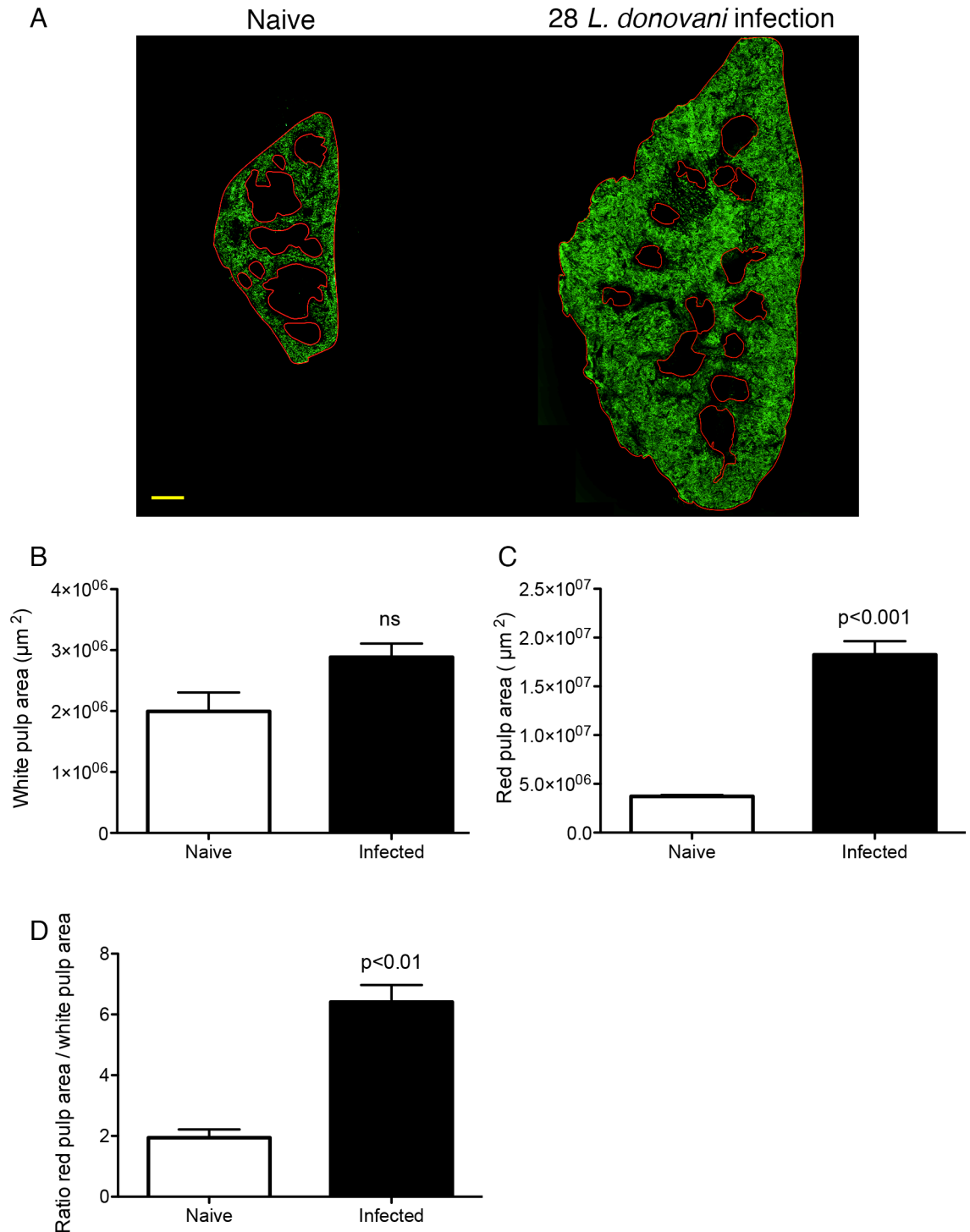


Figure 3-16. Chronic EVL induces induces remodelling of the splenic red pulp. (A) Manual identification of white pulp and red pulp area based on F4/80 staining (green). The red pulp is defined as F4/80⁺ and the white pulp is F4/80⁻. Scale bar = 1mm. (B) White pulp area per spleen section. (C) Red pulp area per spleen section. (D) Ratio of red pulp/white pulp. Areas were measured from a single section per spleen. Data represent mean + SEM (unpaired t-test; n=3 mice per group from one experiment).

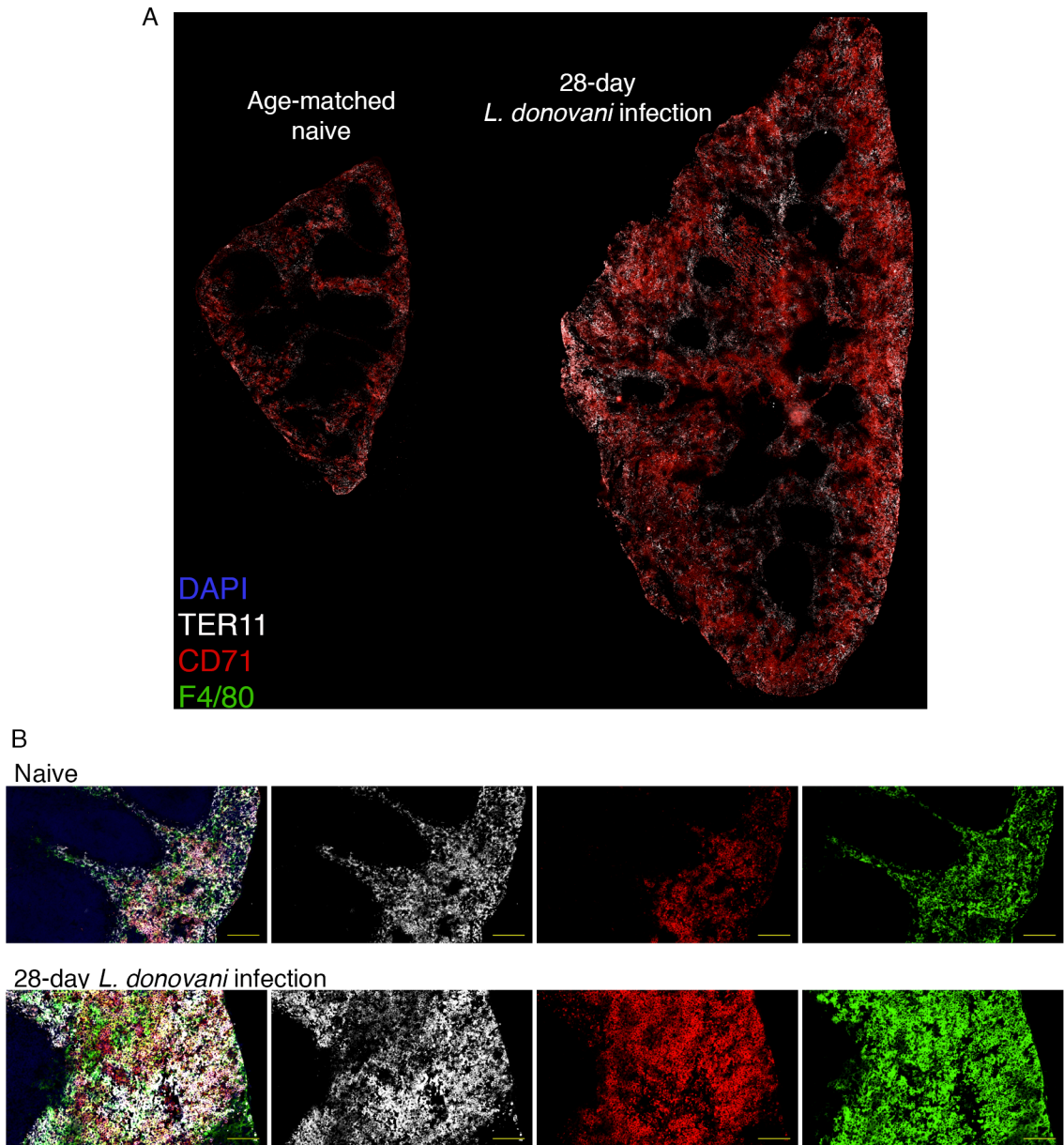


Figure 3-17. EVL-induced extramedullary erythropoiesis is characterised by increase of erythroid progenitors in the splenic red pulp. (A) Spleen sections stained with CD71 (red) and TER119 (white). (B) Detail of spleen section highlighting the interface between the splenic red pulp, F4/80+ (green) and the white pulp F4/80-, together with CD71 and TER119 (scale bar = 100 μ m). Representative from 3 mice per group from one experiment.

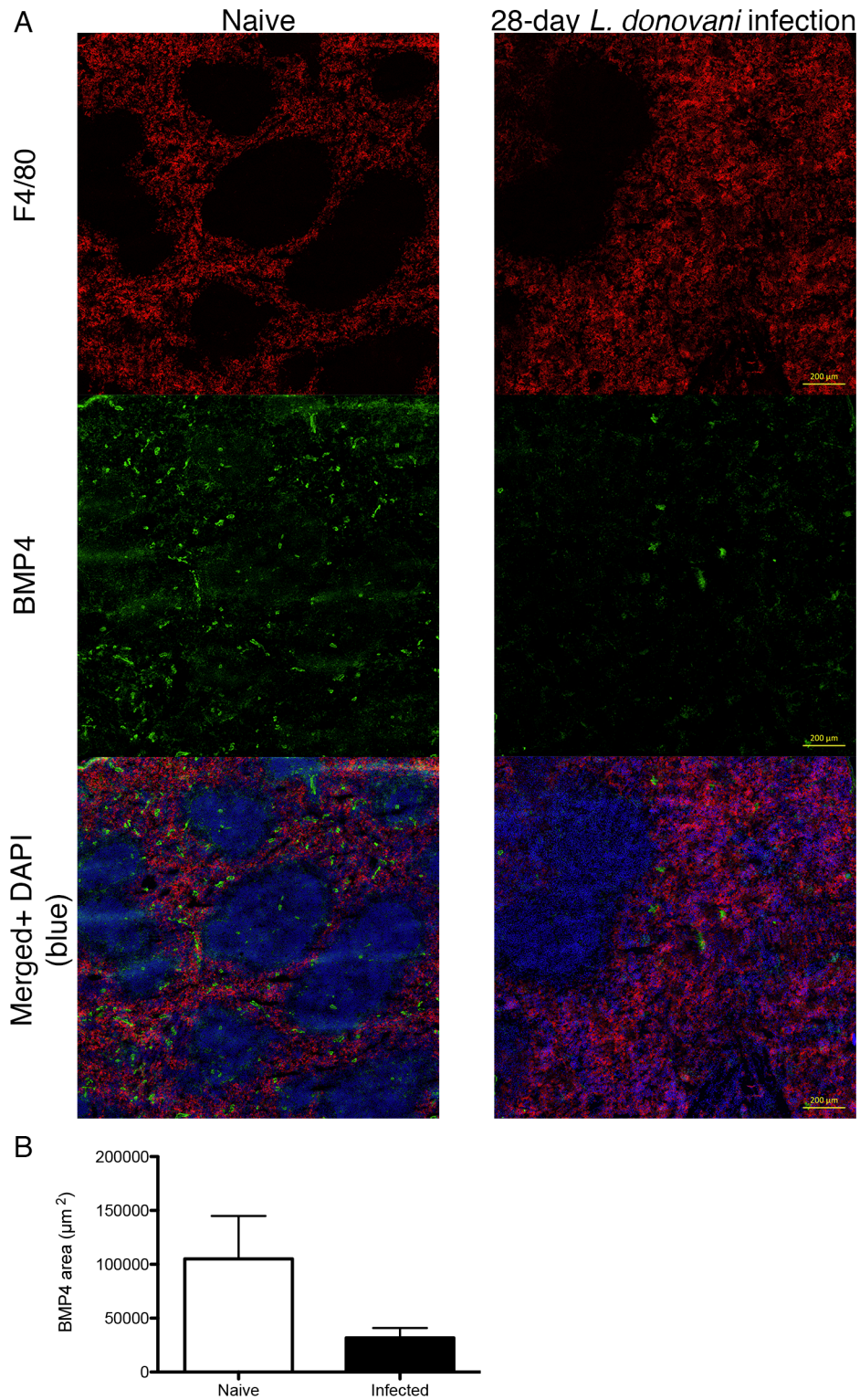


Figure 3-18. Splenic erythropoiesis is not associated with increased BMP4 staining after 28 day-infection with *L. donovani*. (A) Confocal imaging of spleen sections staining with anti-F4/80 (red) and BMP4 (green) antibodies. (B) Automated quantification of BMP4 staining area by the Volocity software package (Perkin Elmer). Data from one section per mouse (n=3 mice per group from one experiment).

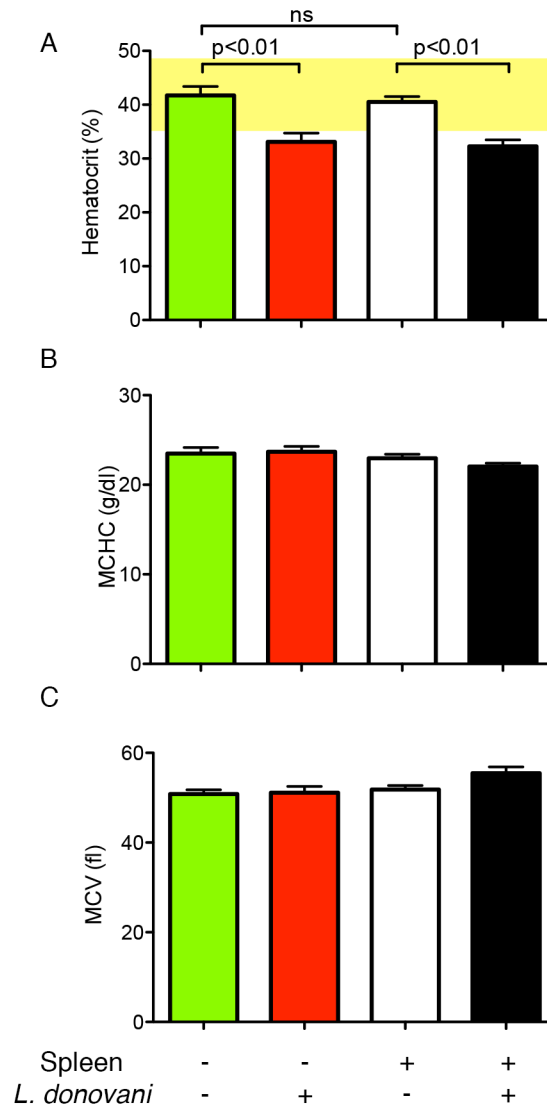


Figure 3-19. EVL-induced anaemia is independent of the spleen. Mice were splenectomised and allowed to recover before infection with *L. donovani*. Blood analysis was performed 4 weeks after infection. (A) Haematocrit. (B) Mean corpuscular haemoglobin concentration. (C) Mean corpuscular volume. Data represent mean + SEM. Absence of statistics means there is no significant difference between the four groups (Kruskal-Wallis test with Dunn's multiple comparison test; n=15 mice per group from 3 independent experiments).

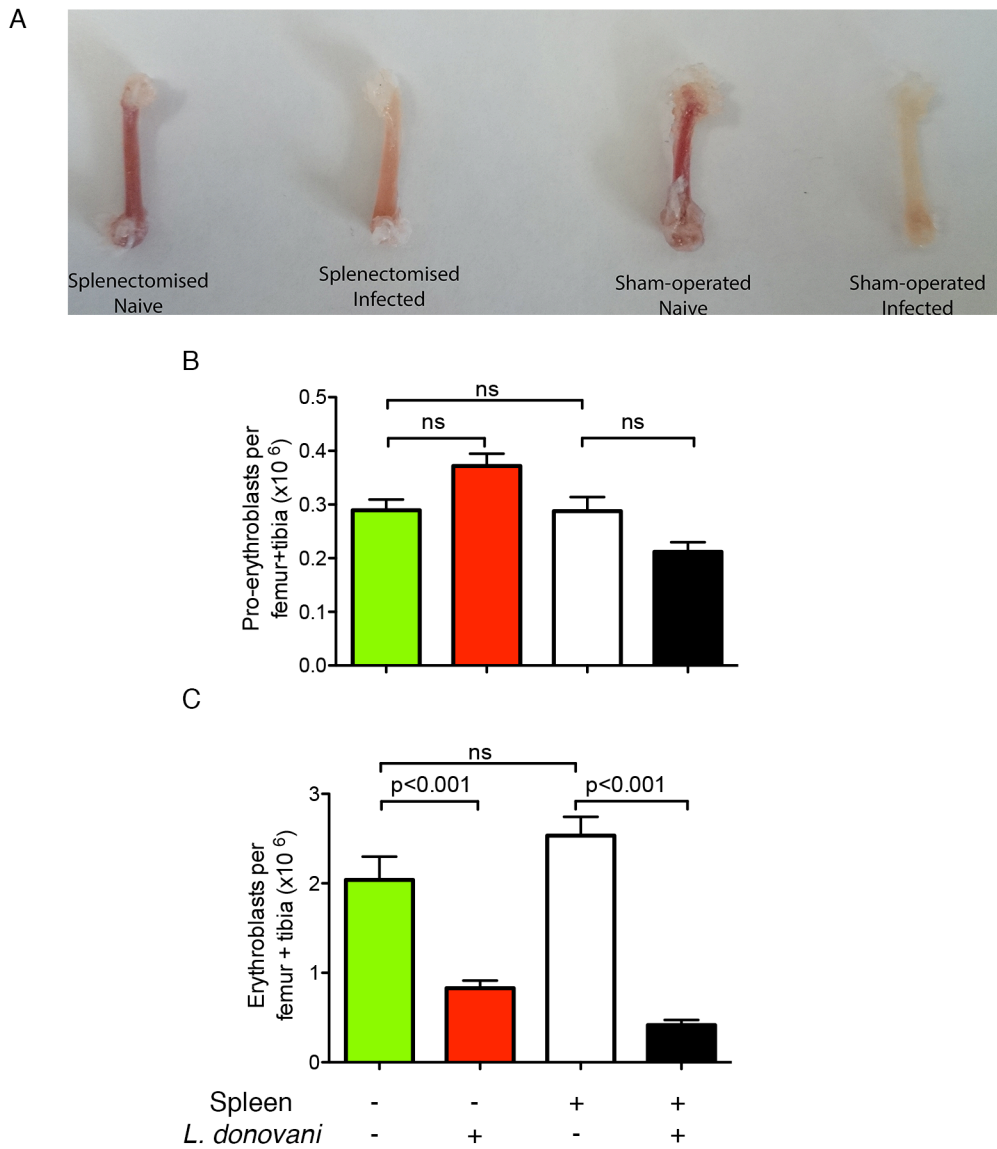


Figure 3-20. Repression of medullary erythropoiesis is independent of the spleen during *L. donovani* infection. Mice were splenectomised and allowed to recover before infection with *L. donovani*. Experiments were performed 4 weeks after infection. (A) Femurs representative of 15 mice per group from 3 independent experiments. (B) Quantification of pro-erythroblasts in the bone marrow. (C) Quantification of erythroblasts in the bone marrow. The gating strategy in Fig. 3-2 was used. Absolute numbers were calculated by multiplying frequencies by the total bone marrow cell counts. (One-way ANOVA with Turkey's multiple comparison test; n=10 mice per group from 2 independent experiments). Data represent mean + SEM

3.3.12 The onset of medullar erythropoiesis reduction correlates with local accumulation of T cells in the bone marrow

To better understand the pathogenesis EVL, a time-course study was performed. The frequencies of T cells, based on the expression of CD3, were measured in parallel with erythropoiesis. CD3 is the co-receptor of the T cell receptor and is highly specific to T cells²⁴⁶. Erythroid precursors (pro-erythroblasts and erythroblasts) decreased steadily over time in infected mice (**Figure 3-21A**). However, these frequencies have been shown to fluctuate, as shown by the control group. Therefore, erythropoiesis in the bone marrow was only significantly repressed by day 28. The onset of medullar erythropoiesis repression was between day 21 and day 28. No increase in the frequency of CD3⁺ cells was detected in the spleens of infected mice over time (**Figure 3-21B**). This frequency fluctuated around 35% of live splenocytes and was never significantly different between the infected and the naïve group. On the other hand, the frequency of T cells in the bone marrow increased by 3-fold between day 21 and day 28 post-infection (**Figure 3-21B**). The frequency is similar to naïve mice during the acute phase of infection, up to day 21, then rises at day 28. The frequency of bone marrow T cells was then 3.7 times higher in the infected mice than in the control group. The frequency of T cells was also measured in the peripheral blood and no difference between infected and control mice was detected during the course of infection (**Figure 3-21B**). Contrary to T cells, data from Ana Pinto show that a decrease in B cell frequency, identified on the basis of B220 expression, occurs in the bone marrow of chronically infected mice (**Figure 3-21C**).

3.3.13 Visualisation of T cells in the bone marrow

Single cell analysis revealed an augmentation of CD3⁺ T cell frequency in the bone marrow of infected mice which correlated with the reduction of bone marrow erythropoiesis. In order to gain better insights into the role of lymphocytes, hCD2.DsRed reporter mice were infected with *L. donovani*. In these mice, expression of DsRed is restricted to T cells^{222,247}, allowing the visualisation of these cells *ex vivo*. They were killed 28 days later and the bone marrow was processed to visualise T cells within the medullar compartment. Confocal images show sparse DsRed⁺ cells in the bone marrow of naïve mice (**Figure 3-22A**). This concurs with studies showing the bone marrow harbours T cells in a physiological state²⁴⁸⁻²⁵⁰. DsRed⁺ cells appeared more numerous in the bone marrow of infection mice, with a less diffuse distribution (**Figure 3-22B**). Image analysis confirmed an increase of T cells in the sections scanned (**Figure 3-22E**). The morphology of lymphocytes was also different between the two groups (**Figure 3-22C and D**). T cells from naïve mice were rounder in shape whereas T cells in infected bone marrow had more

convoluted shapes. This was confirmed by image analysis and measure of the cell shape factor. This value indicates how close to a circle individual cells are, 1 being the maximum value (perfect circle). CD2⁺ bone marrow cells from infected mice had an average shape factor of 0.390 ± 0.085 whereas the average shape factor of CD2⁺ cells from naïve mice was 0.543 ± 0.121 (**Figure 3-22F**). The difference was however non-significant. Therefore, bone marrow T cells, had irregular shapes, possibly related to the process of cell spreading seen during T cell activation²⁵¹. To investigate if the uneven distribution of T cells was a consequence of the migration towards intracellular amastigotes, hCD2-GFP mice were infected with tdTomato-LV9 parasites. The bone marrow was then fixed and analysed by confocal microscopy. The images suggest some T cells are close to parasites (**Figure 3-23A and B**).

3.3.14 Both CD4⁺ and CD8⁺ T cells accumulate in the bone marrow of infected mice

The role of T cells in the pathogenesis of EVL was further investigated by measuring the distribution of the two main subsets of T cells, the CD4 and CD8 subsets (**Figure 3-24A and B**). In a physiological state in naïve mice, the frequencies of CD4 and CD8-T cells were measured at $0.625 \pm 0.85\%$ and $1.143 \pm 0.113\%$ of total bone marrow cells, respectively (**Figure 3-24B**). Augmentations of both frequencies were detected on day 28 p.i. in infected mice. Of both subtypes, CD4 T cells were the most dramatically increased at $8.275 \pm 0.578\%$, representing a 13-fold increase. A more moderate 2.6-fold increase was measured for the frequency of CD8 T cells at $3.036 \pm 0.244\%$ (**Figure 3-24B**). These results show a correlation between the loss of erythropoiesis in the bone marrow and the accumulation of T cells in the bone marrow, so the role of adaptive immunity in the alteration of erythropoiesis was investigated.

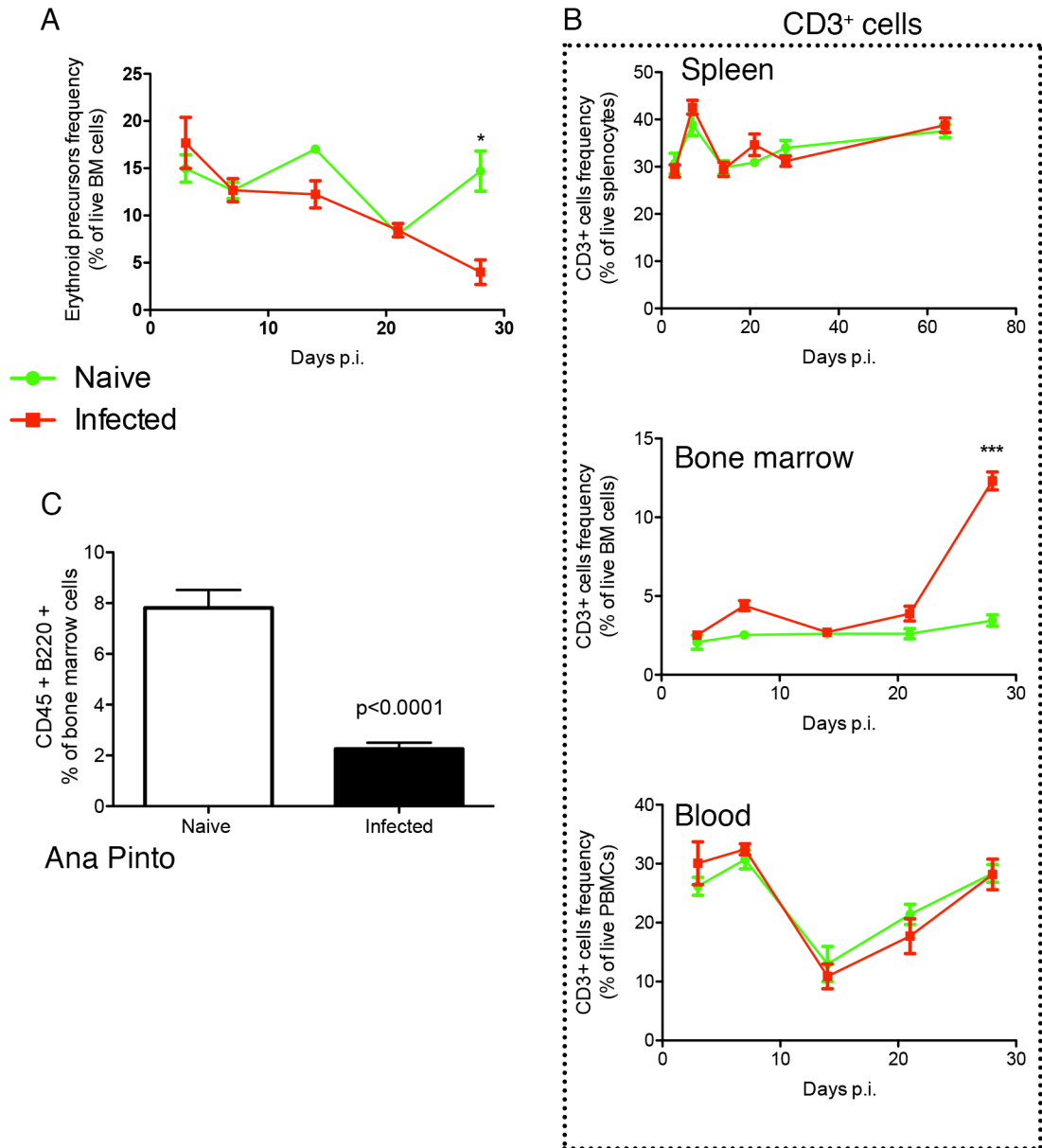


Figure 3-21. The onset of medullary erythropoiesis repression corresponds to local accumulation of T cells in the bone marrow. (A) Frequency of erythroid precursors (proerythroblasts and erythroblasts) in the bone marrow over time. Precursors were identified on the basis of TER119 and CD71 staining. (B) Frequency of CD3⁺ cells in the bone marrow, spleen and blood over time. (unpaired t-test; n=3 mice per group per time point, except naïve spleen analysis at day 21 where n=1) (C) Frequency of CD45⁺B220⁺ cells in the bone marrow, data from Ana Pinto (unpaired t-test with Welch's correction, n=14 mice per group from 3 independent experiments). Data represent mean ± SEM.

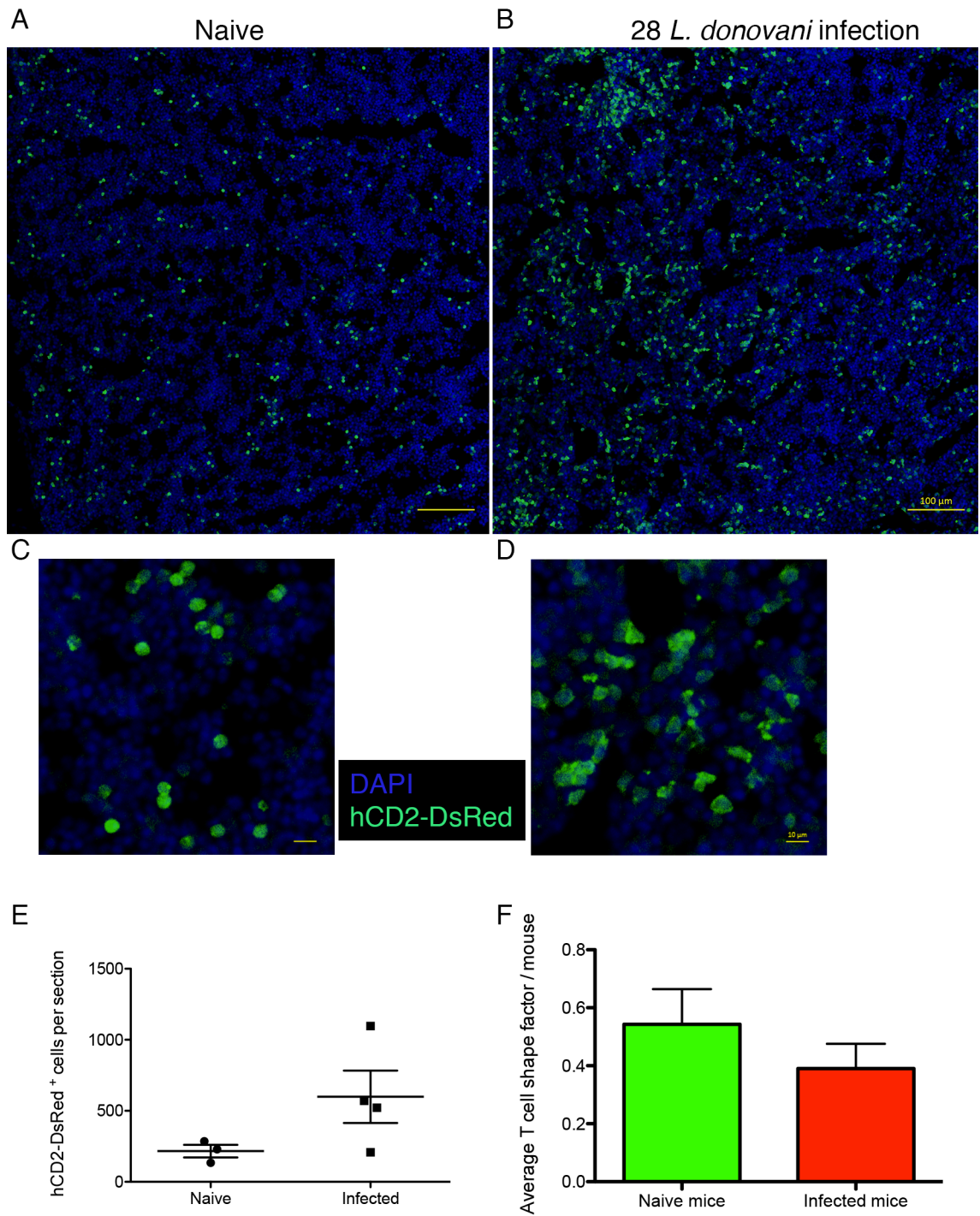


Figure 3-22. Visualisation of T cells in the bone marrow during EVL. (A) Confocal imaging of a bone marrow section from a naive hCD2-DsRed mouse. (B) Magnification of a detail from A. (C) Confocal imaging of a bone marrow section from a 28 day-infected hCD2-DsRed mouse. (D) Magnification of a detail from C. (E) Shape factor of DsRed+ cells, determined with the Velocity analysis software (Perkin Elmer). 1 corresponds to a cell with a perfect circle shape in a 2D plan. (n=3 naive mice and 4 infected mice; cells were analysed from 1 section per mouse from a single experiment). Data represent mean \pm SEM.

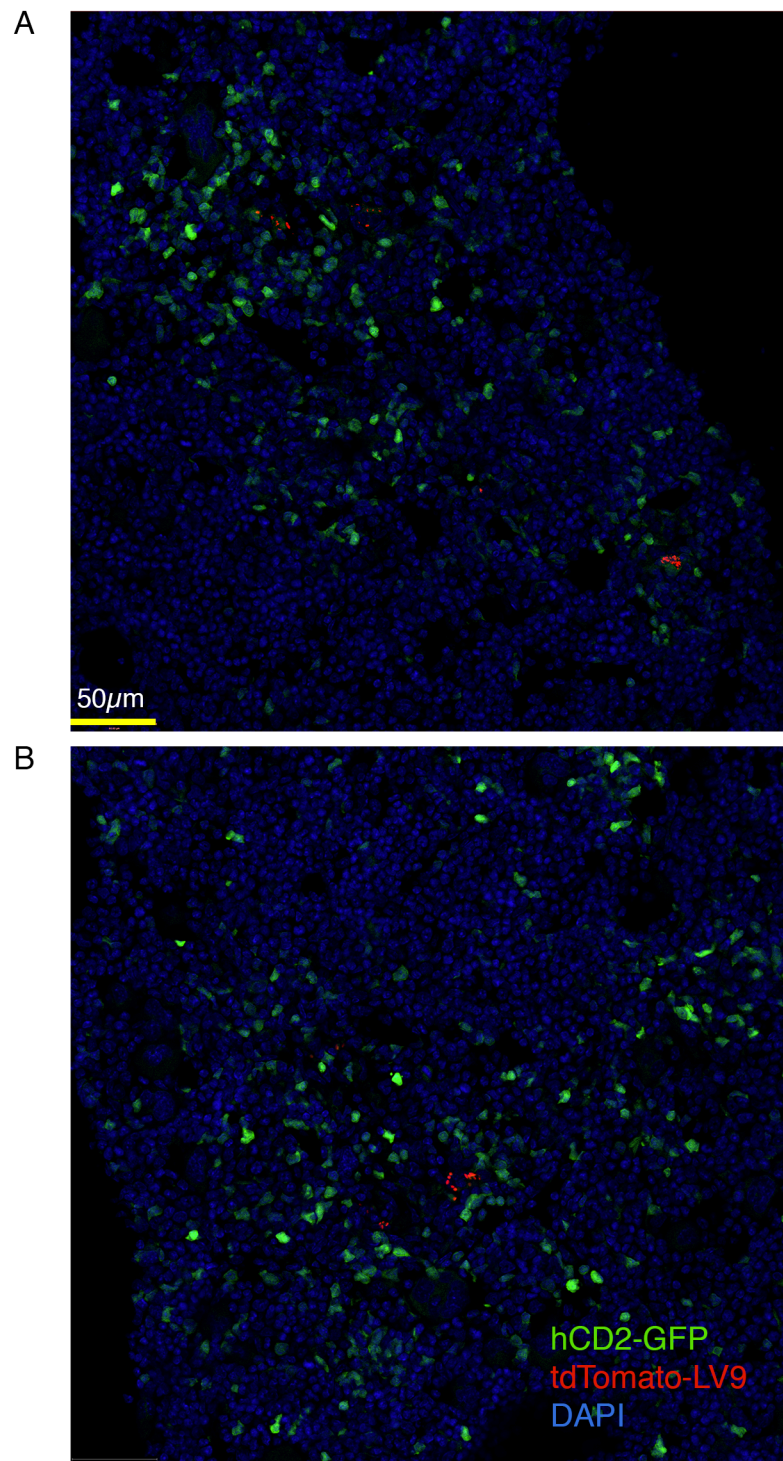


Figure 3-23. Imaging of T cells in relation to *L. donovani* parasites in the bone marrow of infected mice. (A and B) Confocal images from a single mouse with T-cell restricted expression of GFP (hCD2-GFP, green) and infected for 28d with tdTomato-expressing *L. donovani* amastigotes (red) and stained with DAPI (blue). Images are representative of 2 mice from a single experiment.

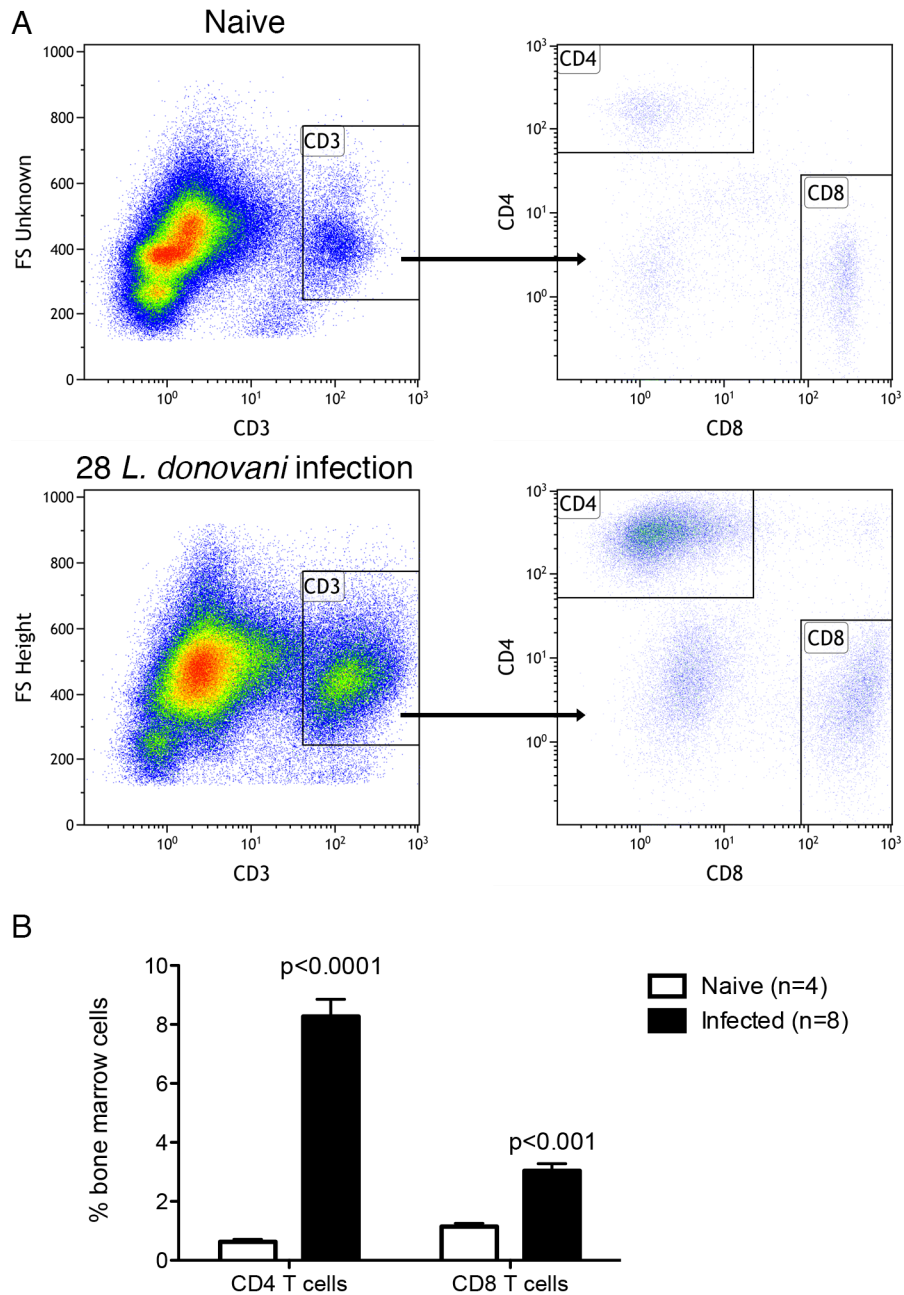


Figure 3-24. CD4⁺ and CD8⁺ frequencies increase in the bone marrow of mice chronically infected with *L. donovani*. (A) Flow cytometry analysis of CD3⁺CD4⁺ and CD3⁺CD8⁺ cells in the bone marrow. Left plots are gated on identical numbers of live single cells. (B) Frequencies of T cell subsets in the bone marrow according to the gating strategy described in A. All experiments were performed 4 weeks after infection. Data represent mean + SEM (n=4 naïve and 8 infected from 2 independent experiments).

3.3.15 Absence of overt pathogenesis in chronically infected immunocompromised B6 RAG2^{-/-} mice

Because the data reported in the previous paragraphs show a correlation between the onset of medullar erythropoiesis repression and accumulation of T cells in the bone marrow, the hypothesis that T cells participate in pathogenesis was tested. B6 RAG2^{-/-} mice are characterised by a loss-of-function mutation in the Recombination-activating gene 2 which is necessary for the V(D)J recombination required to build the antibody repertory. Without recombination, the development of lymphocytes is halted and no mature T or B lymphocytes are produced²⁵². Therefore, the B6 RAG2^{-/-} strain is devoid of adaptive immune response and is a good model to study the effect of *L. donovani* infection in an immune-deficient context. B6 RAG2^{-/-} mice were infected in parallel to WT mice to compare the course of infection between the two. Both strains developed a chronic infection as determined by the parasite load in the spleen. While the parasite count was really high in the spleen of infected B6 RAG2^{-/-} (**Figure 3-25A**), the LDUs were lower when compared to the WT group (**Figure 3-25B**). However, caution has to be taken in comparing LDUs between the two strains since the spleen weight (which is taken into account in the calculations of LDUs) differs in the steady state due to different cellular composition. Indeed, spleens from B6 RAG2^{-/-} do not contain lymphocytes. No splenomegaly was observed in infected B6 RAG2^{-/-} since spleen weight were identical between naïve and infected mice (**Figure 3-26A**). The haematological profile of B6 RAG2^{-/-} mice showed no alterations in haematocrit (**Figure 3-25C**). This indicates that visceral leishmaniasis in immune-compromised mice does not lead to anaemia. To confirm that no pathogenesis was detectable in EVL in B6 RAG2^{-/-} mice, the bone marrow was analysed for the erythropoiesis.

3.3.16 Erythropoiesis is not altered in B6 RAG2^{-/-} mice

Erythropoiesis was quantified in the bone marrow of B6 RAG2^{-/-} mice by flow cytometry. Infection with *L. donovani* does not result in a reduction of pro-erythroblasts after 28 days in either wild-type or RAG2^{-/-} mice (**Figure 3-25D**). By contrast to wild-type where *L. donovani* reduces erythroblast in the bone marrow, there was no significant reduction in the absolute number of erythroblast either (**Figure 3-25E**). These results further confirm the link between reduction of haematocrit and deficit of RBC production in the bone marrow. The data discussed in paragraph 3.2.9 show that extramedullary erythropoiesis occurs in the spleen during the chronic phase of infection. Contrary to their wild-type counterparts, the RAG2^{-/-} mice had no splenomegaly (**Figure 3-26A**) and no increase in absolute numbers of erythroid precursors in the spleen (**Figure 3-26B and C**). This further

confirms that splenomegaly is induced by the alteration of erythropoiesis in the bone marrow. To know whether infection with *L. donovani* also changes the bone marrow microenvironment, the expression levels of Cxcl12 were measured and the stromal macrophages analysed in RAG2^{-/-} mice. No reduction of Cxcl12 was detected after 4 weeks of infection, by opposition to the 50% decrease in wild-type mice (**Figure 3-27A**). Interestingly, this correlated with no up-regulation in circulating G-CSF (**Figure 3-27B**), thus re-affirming the potential role of G-CSF in the alterations seen in wild-type mice. Direct evidence is still needed to show that G-CSF is actually causing alterations of the bone marrow. In addition, the bone marrow macrophages were unaffected by the infection in regards with the expression of CD169 (**Figure 3-27C**). The numbers of the CD169^{low} and CD169^{high} subsets of macrophages were similar between the infected and the control groups (**Figure 3-27D**).

3.3.17 Lymphocytes are required for the alteration of the medullar erythropoiesis in infected B6 RAG2^{-/-} mice

The results presented so far suggest a link between the adoptive immune response to *L. donovani* amastigotes and the deficit of RBC production in the bone marrow since immune-compromised mice do not have the same defects as the wild-type in regards to erythropoiesis. To confirm this, RAG2^{-/-} mice were infected for 4 weeks before transferring 10⁷ splenocytes from a naïve mouse. The mice were then killed 1 week later. The aim was to determine whether an immune reconstitution would induce the alterations described previously in regards to erythropoiesis. A group of naïve RAG2^{-/-} was also injected with splenocytes in order to exclude side effects of the immune reconstitution that would be independent of the infection. The first observation that was made was that the transfer of splenocytes lead to a splenomegaly exclusively in infected mice (**Figure 3-28A**). The spleen weight for the infected group with splenocytes reached an average of 147±7mg whereas in naïve mice with splenocytes and infected mice without splenocytes the spleens weighed averages of 41±2mg and 43±8mg, respectively. Erythropoiesis was quantified in the bone marrow by flow cytometry (**Figure 3-28C**). Infection only or splenocytes only did not cause a significant drop in pro-erythroblasts or erythroblasts numbers in the bone marrow. However, infection together with adoptive transfer of splenocytes depleted both pro-erythroblasts and erythroblasts from the bone marrow (**Figure 3-28D and E**). Interestingly, the reduction of medullar erythropoiesis correlated with an up-regulation of G-CSF in the plasma, which is another indication that G-CSF may be involved in alterations of erythropoiesis in the context of EVL.

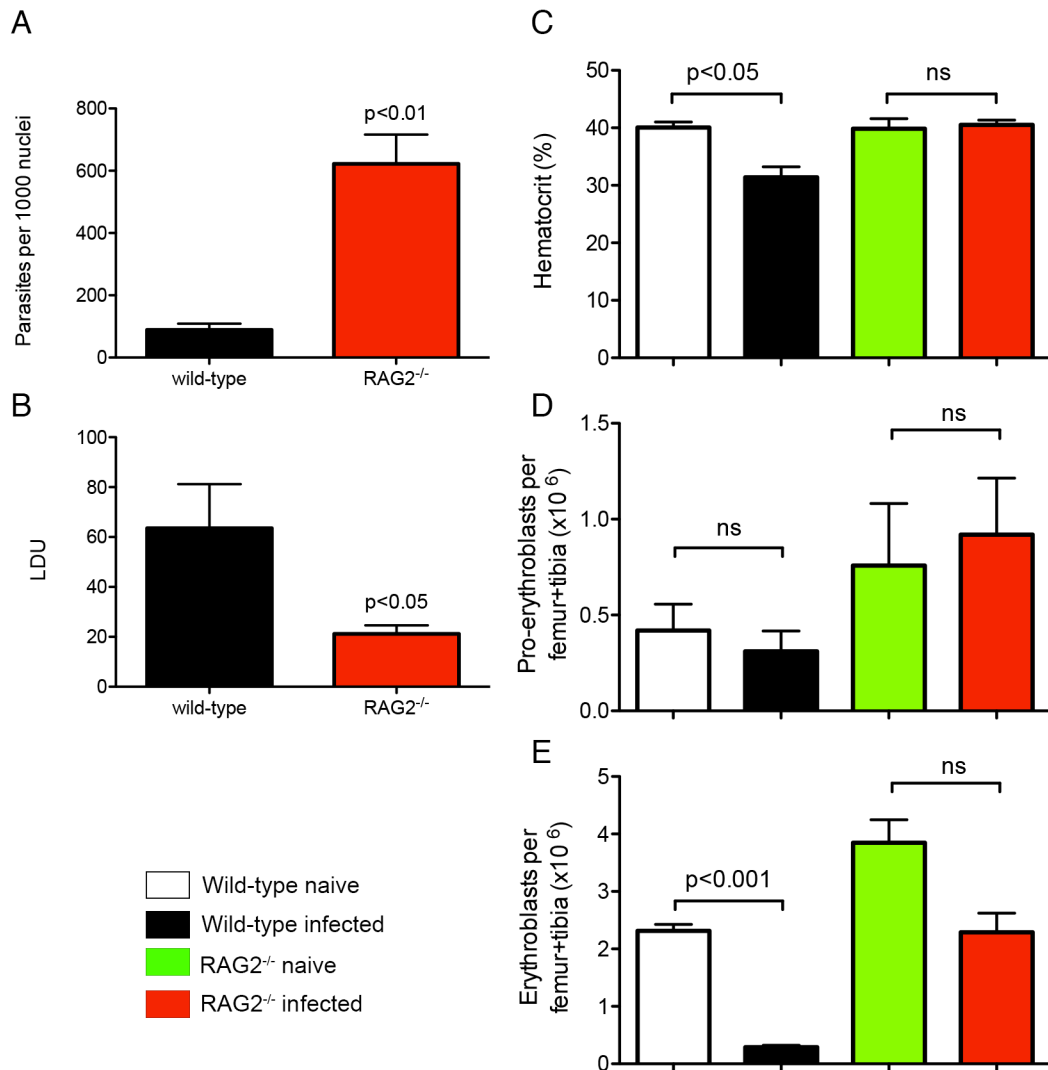


Figure 3-25. Infection of RAG2^{-/-} mice with *L. donovani* does not alter medullar erythropoiesis. (A) Parasites per 1000 nuclei in the spleen. Splens impressions were made on glass slides and stained with Giemsa. Parasites and nuclei were counted microscopically. (B) Leishman-Donovan units calculated from parasite counts in A multiplied by the spleen weight in grams (unpaired t-test with Welch's correction (A) and Mann Whitney test (B); n=8 wild-type and B6 RAG2^{-/-} mice from 2 independent experiments). (C) Haematocrit of mice at day 28 post-infection (Kruskal-Wallis test with Dunn's multiple comparison test; n=5 wild-type mice per group, 3 B6 RAG2^{-/-} naïve and 4 B6 RAG2^{-/-} infected). (D) Pro-erythroblasts per 1 leg (femur + tibia). (E) Erythroblasts per leg. Erythroid precursors were identified by flow cytometry as described in Fig. 3-2. (Kruskal-Wallis test with Dunn's multiple comparison test; n=8 wild-type mice per group, 5 B6 RAG2^{-/-} naïve and 7 B6 RAG2^{-/-} infected). Data represent mean + SEM. All experiments were performed 4 weeks after infection.

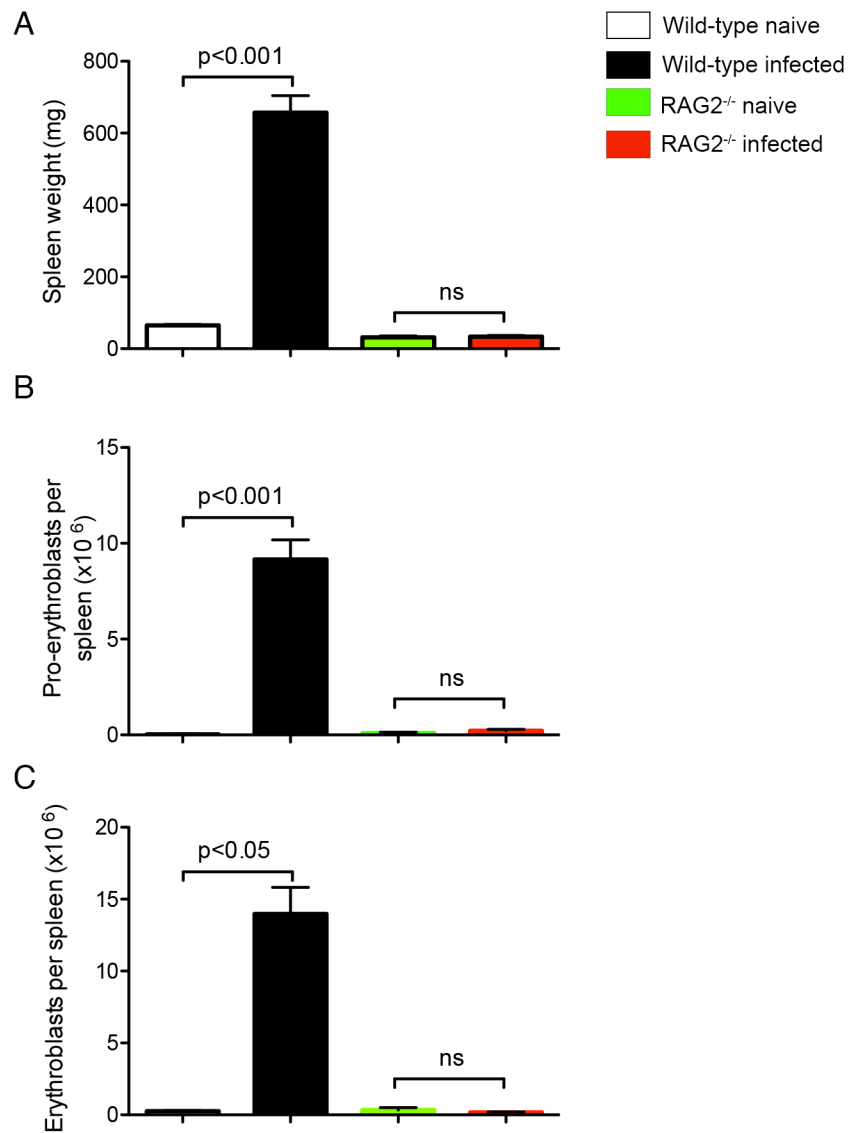


Figure 3-26. Absence of splenomegaly in RAG2^{-/-} mice infected with *L. donovani*. (A) Spleen weight of wild-type and RAG2^{-/-} mice. (B) Absolute numbers of pro-erythroblasts in the spleen. (C) Absolute numbers of erythroblasts in the spleen. Erythroid precursors were identified by flow cytometry as described in Fig. 3-12. (one-way ANOVA (A) followed by Turkey's multiple comparison test or Kruskal-Wallis test followed by Dunn's multiple comparison test (B and C); n=8 wild-type mice per group, 5 RAG2^{-/-} naïve and 7 RAG2^{-/-} infected). All experiments were performed 4 weeks after infection.

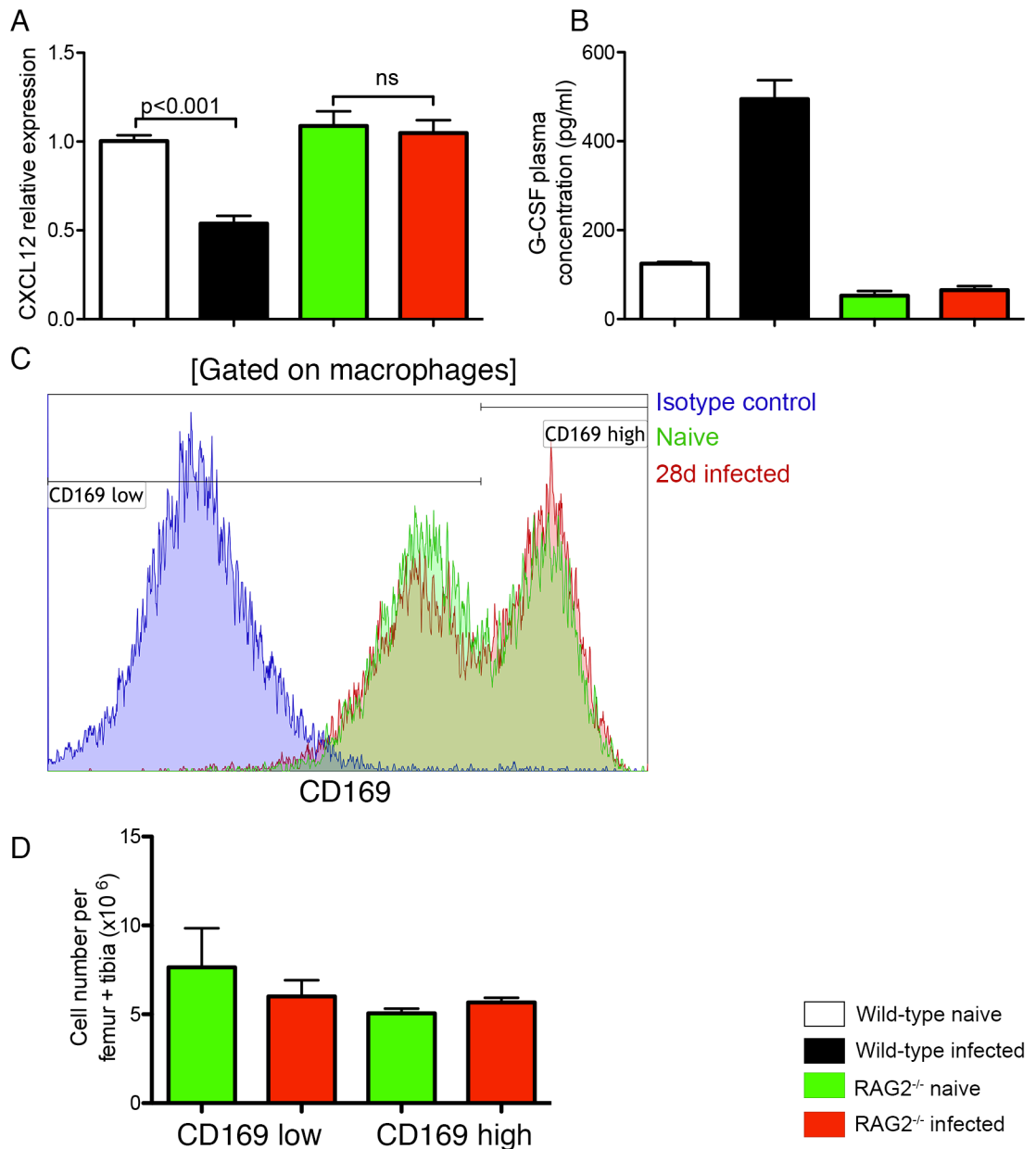


Figure 3-27. Absence of G-CSF up-regulation and alteration of the bone marrow microenvironment in infected RAG2^{-/-} mice. (A) Cxcl12 expression in total bone marrow cells. Intra-sample standardisation was done by normalisation to the house-keeping gene HPRT and inter-sample standardisation was done by normalisation to the average expression of the naïve group. (n=8 wild-type mice per group, 5 RAG2^{-/-} naïve and 7 RAG2^{-/-} infected from one experiment) (B) Concentration of G-CSF in the plasma. (n=5 wild-type mice per group, 3 RAG2^{-/-} naïve and 4 RAG2^{-/-} infected from one experiment) (C) CD169 expression on bone marrow macrophages of naïve (green) and infected (red) RAG2^{-/-} mice. Isotype control (blue) is representative of both naïve and infected mice. (D) Absolute numbers of macrophages per leg (1 femur + 1 tibia) according to the gating described in C. Absolute numbers were calculated from the frequencies multiplied by the total bone marrow cells isolated from each mouse (n=3 naïve and 4 infected mice from one experiment). All experiments were performed 28 days after infection.

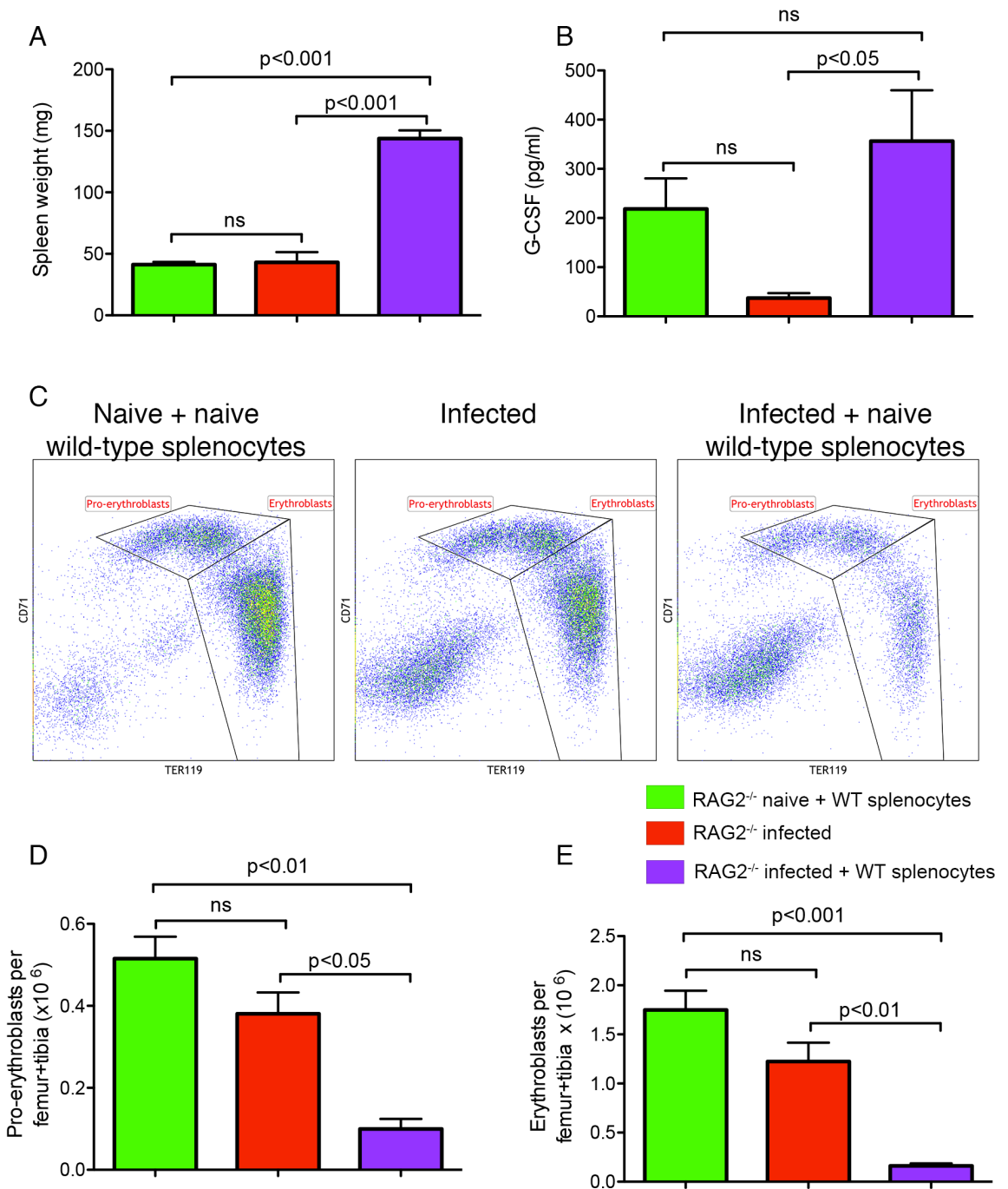


Figure 3-28. Adoptive transfer of wild-type splenocytes into chronically infected RAG2^{-/-} mice induces repression of medullar erythropoiesis. Mice were infected for 4 weeks before being injected with splenocytes from a single wild-type naïve donor. The mice were killed 1 week after adoptive transfer. (A) Spleen weight of mice at the experiment's endpoint. (B) G-CSF plasma level determined by ELISA assay. (C) Identification of pro-erythroblasts and erythroblasts by flow cytometry. Pro-erythroblasts are CD45⁻ CD71⁺ TER119^{low} and erythroblasts are CD45⁻ CD71⁺ TER119^{high}. (D and E) Quantification of pro-erythroblasts and erythroblasts. Absolute numbers were calculated by multiplying frequencies of erythroid precursors (% of live cells) by the total bone marrow cell counts. (one-way ANOVA followed by Turkey's multiple comparison test; n=3 per group from a single experiment) Data represent mean + SEM.

3.4 Discussion

In the human disease, patients rarely show signs of acute infection and clinical symptoms will appear months to year after the initial infection. Therefore, patients diagnosed with VL are most often diagnosed when already in the chronic phase of infection, which is why we chose to study the chronic phase of EVL. Analysis of the blood from chronically infected C57BL/6 mice shows that murine EVL does indeed result in haematological changes. In terms of absolute numbers, two lineages were affected, namely RBCs and the platelets. Alterations in platelet count are discussed in Chapter 4. Haematocrit as well as haemoglobin levels were reduced by 28 days post-infection. Haematocrit reduction can arise from fewer circulating RBC or an increase in plasma volume. The latter is called dilutional anaemia and has not been investigated here but can not be excluded, especially in the context of VL. Indeed, splenomegaly is commonly associated with higher plasma volume due to a physiological mechanism involving hypertension of the liver portal vein subsequent to the increased splenic blood flow²⁵³. Reduction of circulating RBC can also participate in reduction of haematocrit. This can be linked to an impairment of erythropoiesis in the bone marrow or a peripheral lysis of erythrocytes. Reduction of erythropoiesis is discussed further in this chapter. Peripheral haemolysis is a potential mechanism for anaemia. In human VL, auto-antibodies against erythrocytes can be found in patients and their detection is often associated with anaemia^{82,254,255}.

The biosynthesis of haemoglobin is a complex process and requires iron. Heme is a cofactor essential for many metabolic pathways made of organic ferrous iron Fe^{2+} , by opposition to inorganic ferric iron Fe^{3+} , and an organic compound called porphyrin. Iron and heme are essential for the growth of *Leishmania spp.* at the amastigotes and promastigotes stages⁹⁴. However most trypanosomatids have lost the ability to synthesise their own heme²⁵⁶. As a result, *in vitro* growth of parasites requires heme-containing media. An exception was found in a trypanosomatid, *Strigomonas oncopelti*, which does not require heme²⁵⁷. Further studies have demonstrated that trypanosomatids that do not require exogenous heme rely on betaproteobacterial endosymbiont for the synthesis of heme^{256,258}. Others, including *Leishmania spp.*, rely on heme from their hosts. *L. donovani* promastigotes are capable of haemolysis²⁵⁹, a process shared with other species of trypanosomes such as *T. cruzi*²⁰⁷ and *T. brucei*²⁶⁰. However, free *Leishmania* promastigotes do not enter the circulatory systems of mammalian hosts, contrary to *Trypanosoma brucei spp.* or *Trypanosoma cruzi*. Anaemia in trypanosomiasis is explained by a complex and multifactorial haemolysis, notably by haemolysins from the parasites and by erythrophagocytosis by the innate immune system in cattle²⁰⁶ or mouse model²⁶¹.

Haemolysis by *Leishmania spp.* is more likely to be beneficial for parasite replication within the gut of sand flies where promastigotes are in contact with blood from blood meals. This mechanism would release heme, from lysed erythrocytes. While haemolysis is a potential way for promastigotes to find iron in the sand fly, it is more challenging to find iron in parasitophorous vacuoles of macrophages. A membrane iron-transporter, LIT1²⁶², a ferric iron reductase, LFR1²⁶³, and a plasma membrane heme-transporter, LHR1²⁶⁴, have been identified in *L. amazonensis*. All three proteins are essential for intracellular growth of parasites. In addition, *L. amazonensis* amastigotes induce iron retention in infected macrophages to promote their growth²⁶⁵. *Leishmania*-induced iron retention involves up-regulation of hepcidin in macrophages which promotes degradation of ferroportin, a transmembrane iron-export protein. Subversion of the host's iron metabolism has been suggested as a cause for anaemia in VL patients⁹⁵. While *Leishmania*-specific mechanism for iron retention exist, chronic inflammation is also known to trigger iron deficiency anaemia. The pro-inflammatory cytokine IL-6 is elevated in VL patients as well as in dogs²⁶⁶⁻²⁶⁸. IL-6 is known to up-regulate hepcidin production in the liver, causing iron retention inside macrophages and reduced absorption of nutritional iron²¹³. Therefore, chronic VL can potentially cause iron-deficiency anaemia. However, iron deficiency anaemia is characterised by a microcytic hypochromic anaemia^{88,187}, i.e. smaller RBC with less haemoglobin. Iron metabolism was not investigated in this study. Mild hypochromia has been reported in VL patients but associated to a macrocytosis⁷³. Here in the murine VL model reduction of haemoglobin was observed in parallel to reduction of RBC so the average haemoglobin content per RBC was similar between naïve and infected mice. The higher MCV values show that erythrocytes tend to be bigger in infected mice, so the anaemia can be qualified of macrocytic normochromic anaemia. Reports of the MCV in patients are rare. Cartwright et al. gathered studies on VL anaemia in humans that point towards an anisocytosis⁶², i.e. RBC of unequal size, with a tendency of size distribution curves (Price-Jones curve) to be skewed towards the right. Two studies report macrocytosis^{66,73} in children who have developed VL from *L. donovani* and *L. infantum* infections, respectively. A variety of conditions can cause macrocytic anaemia such as vitamin B12 deficiency or primary bone marrow disorders⁸⁷. Vitamin B12 was not measured here but a study of two children with VL presenting myelodysplastic features shows none of them had a B12 deficiency⁴. Because young RBC, the reticulocytes, are bigger than mature erythrocytes, an increase in reticulocyte frequency in the blood (reticulocytosis), is also known to cause macrocytosis. No record of reticulocytosis, sign of

a rapid turnover of RBC, in VL could be found. It was therefore decided to focus on erythropoiesis in the bone marrow.

The infected mice had paler femurs than their naïve counterparts 4 weeks after infection. Deletion of CD169⁺ bone marrow macrophages¹⁶⁹ or administration of G-CSF²³² have been shown to cause pale femurs as well and have been linked to a reduction of erythropoiesis in the bone marrow. A similar phenomenon also happens following a local irradiation of femur which damages the bone marrow microenvironment²³¹. Here, we have shown that infection with *L. donovani* impaired erythropoiesis in the bone marrow, based on the flow cytometry-quantification of pro-erythroblasts and erythroblasts. Previous work by Cotterell et al. suggests that *L. donovani* increases haematopoietic activity in BALB/c mice⁸⁶. This study showed, using a colony-formation assay, that haematopoiesis is increased in the bone marrow of infected mice, including erythroid precursors. Similar results were shown in hamster infected with *L. donovani*⁶⁸. The erythroid colony-forming units measured in this study are the BFU-E, representing progenitors upstream of the pro-erythroblast stage. Since the data reported here indicate an impairment of erythropoiesis at the erythroblast stage, these data are not inconsistent with that reported in mice or hamsters. In the hamster model of VL, it has been suggested that apoptosis bone marrow erythroblasts is increased. However, the analysis of erythroblasts is based on the expression of E-cadherin, a marker of erythroid precursors in human that has not yet been described in hamster^{269,270}. Many conditions reduce erythropoiesis in the bone marrow, such as myelodysplastic syndromes. Additional data from Ana Pinto, show that the number of MEP is unchanged at a similar stage of the disease. These progenitors represent the last stage of differentiation before an exclusive commitment to the erythroid lineage. This last observation indicates that the repression in medullary erythropoiesis only affects the last stages of erythropoiesis after the BFU-E stage.

Because bone marrow resident stromal macrophages are part of the erythroid niche¹⁶⁷, changes in bone marrow macrophage populations were investigated. Microscopic observation of the bone marrow with a non-specific staining reveals cellular alterations characterised by an accumulation of cells resembling macrophages. It is possible that these macrophages participate in a local inflammation similar to the granulomas formed in the liver following infection with visceralising *Leishmania* species²⁷¹. However the spatial correlation between these features and amastigotes has not been investigated and they do not match the histological description of granulomatous lesions in the bone marrow²⁷². In immunocompromised mice, macrophages expressing CD68 and CD169 were shown to be infected. Unfortunately, this was not possible to repeat in wild-type C57BL/6 mice because

of the low bone marrow parasitemia associated with the tdTomato-LV9 strain. One possible explanation for this is that the expression of a tdTomato protein at the surface of the parasite is highly immunogenic, resulting in the destruction of many parasites. Flow cytometry analysis revealed that the bone marrow of mice infected with *L. donovani* harboured fewer CD169^{high} macrophages. These macrophages are known to be indispensable for the retention of HSCs¹⁴⁷ and erythroblasts¹⁶⁹ in the bone marrow. In regards to erythropoiesis, depletion of CD169⁺ cells has been shown to reduce the number of CFU-E, pro-erythroblasts and erythroblasts but not BFU-E¹⁶⁹. Stromal macrophages regulate the retention of HSCs indirectly through the production of CXCL12 by bone marrow stromal cells¹⁴⁷. Stromal macrophages interaction with other stromal cells requires signalling through the liver X receptor (LXR) and follows a circadian rhythm in the steady state¹⁴⁸. This rhythm is imposed by the clearance of senescent neutrophils which migrate back to the bone marrow. Experimental disruptions of this process, such as depletion of CD169-expressing cells, pharmacological inhibition of LXR or depletion of neutrophil, have been reported to alter the HSC niche in the bone marrow^{147,148}. Inter-experiment variability due to the circadian rhythm was avoided by sampling in between 7am and 9am, assuming the infection with *L. donovani* did not alter the rhythm.

The cytokine G-CSF is known to be a potent regulator of the bone marrow stromal compartment. It is important to note that cytokine concentration values may differ in plasma and in serum²⁷³. The primary function of G-CSF is to induce granulopoiesis and the maturation of neutrophils. Here, despite the increase in levels of circulating G-CSF, infected mice did not display neutrophilia at this timepoint (i.e. high number of neutrophils in the blood, **Table 3-1**). G-CSF was investigated here because it has been recently shown that administration of G-CSF in mice causes depletion of erythroblastic island macrophages expressing CD169 in the bone marrow of mice²³². G-CSF is also capable of mobilising HSCs from the bone marrow by interfering with the CXCL12-CXCR4 axis. The first mechanism to be reported is through the cleavage of secreted CXCL12 in parallel with the up-regulation of CXCR4. G-CSF induces neutrophil elastase and other proteases in the bone marrow that are in turn responsible for the proteolytic cleavage of CXCL12²⁴¹. The mechanisms of action of G-CSF were subsequently investigated by others who demonstrated that down-regulation of CXCL12 still occurred in absence of proteolytic activity²⁷⁴. Indeed, G-CSF inhibits the expression of CXCL12 at the mRNA level in the bone marrow, indicating that different pathways, protease-dependent and protease-independent, contribute to the regulation of the HSC niche. Several studies have demonstrated that G-CSF was up-regulated in different situations, including

infection^{275,276}. Disruption of cholesterol efflux pathways in transgenic mice mobilises HSCs correlating with up-regulation of G-CSF and down-regulation of CXCL12²⁷⁷. Interestingly, bone marrow stromal cells are able to sense the infection of mice with *Escherichia Coli* (*E. coli*) through cooperative signalling of the NOD and TLR receptors, causing an up-regulation of G-CSF and mobilising HSCs²⁷⁵. Punctual mobilisation of HSCs from the bone marrow is thought to be a defence mechanism enabling an increase in myelopoiesis in distant site such as the spleen to respond to the infection. In a murine breast tumour model, development of anaemia in tumour-bearing mice was correlated with up-regulation of G-CSF²⁷⁶. While punctual disruption of the niche has no overt adverse effect in the *E. coli* infection model, EVL is a chronic infection and chronic disruption of the HSC niche has potentially more negative effects such as the depletion of the pool of HSCs. In addition to higher levels of circulating G-CSF, a 50% reduction of CXCL12 expression in the bone marrow at day 28p.i. as well as a decrease in the number of CXCL12-expressing cells is a notable change associated with EVL. The hypothesis in this study was therefore that G-CSF contributes to bone marrow alterations in the context of EVL, making it a candidate as a potential target for treatment. Few conditions have been linked to elevated G-CSF so reports of G-CSF neutralisation are rare. G-CSF has been linked to the severity of inflammatory arthritis in a mouse model²⁷⁸. However, the large quantities of antibodies used in this study to neutralise G-CSF, show how difficult pharmacological inhibition of G-CSF is. The attempt at neutralising G-CSF in mice infected with *L. donovani* did not alter the pathogenesis. It is unclear whether it is the result of a failure to effectively reduce the cytokine or of a feedback loop which would explain the higher levels of G-CSF measured in antibody-treated mice compared to the isotype-treated group.

The spleen is an essential organ in regards to the homeostasis of RBC. It filtrates the blood and captures aging or damaged RBC²⁷⁹. Red pulp macrophages capture phagocytose RBC or part of them²⁸⁰. Splenomegaly is associated with an increased blood flow through the spleen²⁵³. While this causes physiological changes leading to dilutional anaemia, it is also possible then that splenomegaly causes anaemia by depleting the blood of more RBC. In mice infected with *L. donovani* the splenic red pulp is larger and the red pulp/white pulp ratio is above 6, while control values approximated 2. Thus, the structure responsible for the filtration of RBC is larger. In order to test if splenomegaly is the main cause of anaemia in EVL, mice were splenectomised prior to infection. The infection resulted in anaemia in both splenectomised and sham-operated mice, indicating that EVL-induced anaemia is independent of the spleen. The RBC were slightly different in regards to the

presence of the spleen. More mice had MCV above the reference interval in the sham-operated group than in the splenectomised. This suggests that splenomegaly, although not responsible for anaemia, potentially has an effect (most likely physiological) on RBC. Here the data suggests that splenomegaly is a response to the loss of erythropoiesis in the bone marrow. Progressive splenomegaly correlates with the increase of splenic erythroid precursors in the red pulp. The onset of extramedullary erythropoiesis also correlated with the reduction of medullary erythropoiesis time-wise. Both events happened between day 21 and day 28 post infection. Extramedullary erythropoiesis has been reported recently in a mouse model of *Salmonella enterica* infection²⁸¹. This study confirms that splenic erythropoiesis is associated with an increase of F4/80⁺ cells in the spleen and the proliferation of erythroid precursors in the red pulp. However, the authors have not addressed the question of what happens to erythropoiesis in the bone marrow in this model, it is therefore unclear if splenic erythropoiesis develops independently of the bone marrow. The classical molecular mechanism inducing extramedullary erythropoiesis involves the production of BMP4 in the spleen^{244,245,276,282}. Spleens did not show an increase of BMP4 4 weeks after induction of EVL. One possible explanation is that the mice were actually recovering at this point. Long-term experiments (post-day28) have sometimes resulted in mice clearing the infection and in spleens recovering a normal weight. It is possible in this experiment that BMP4 signalling had stopped by day 28. A better time point to consider would have been between day 21 and day 28, as it is in this time frame that extramedullary erythropoiesis starts according to our data. The other possible explanation is that extramedullary erythropoiesis is independent of BMP4. BMP4-independent splenic erythropoiesis can be achieved by overexpressing MyrAkt1 in endothelial cells of mice²⁸³. This erythropoiesis is also independent of anaemia and EPO. One argument in favour of a BMP4-induced is a recent study about the remodelling of the spleen in the context of EVL. In this study, a population of splenic F4/80^{high}CD11b^{low} macrophages are linked to neo-vascularisation of the spleen following infection with *L. donovani*²⁸⁴. The top differentially expressed gene when compared to other populations of macrophages is Bmp4 and the third is Cxcl12, both involved in extramedullary erythropoiesis^{244,285,286}.

Haematological data are generally considered clinically relevant when they are associated with life-threatening conditions, which is not the case in EVL. Despite a mild anaemia and a pronounced thrombocytopenia, no cachexia or excessive bleeding have been observed. However previous studies in mice have shown how resilient they can be to alteration of erythropoiesis. Systemic suppression of CD169-expressing cell or G-CSF administration induce a more than 70% reduction of erythroblasts number but no peripheral

anaemia^{169,232}. Compensatory splenic erythropoiesis has been suggested as a rescue mechanism in the two studies, but splenectomy following suppression of bone marrow macrophages did not induce anaemia¹⁶⁹. Splenectomised mice infected with *L. donovani* had the same degree of anaemia as the sham-operated ones. The splenectomy experiments done here and the studies mentioned before suggest that more mechanisms, in addition to splenic erythropoiesis, cancel the deficit of RBC production in the bone marrow. The liver is often overlooked in haematological studies, and it has not been studied here, but evidence suggest that Kupffer cells are capable of supporting extramedullary erythropoiesis in splenectomised mice with bone marrow failure²⁸⁷. In the CD169-positive cell depletion model, mice did not become spontaneously anaemic but recovery from chemically-induced anaemia was impaired¹⁶⁹. Recovery from anaemia was not investigated in this study.

The data were consistent between individual mice and between independent experiments. Clinical data shows that haematological disorders in human VL do not show such consistency and patients present with reduced numbers of only some or all of the lineages^{62,64}. The basis for these variations is unknown but it is expected that controlled experimental conditions as in our study might yield similar haematological profiles. It has been demonstrated that genetics play an important part in the response to *Leishmania* infections in mice and only congenic mice were used in this study. Patients infected with visceral strains typically develop symptoms months to years after initial infection, thus clinical studies include patients who have been infected for different periods of time, contrary to the strict 28-day infection used here. In addition, the parasite strain and the quantity of parasites in the *inoculum* were constant. All these factors are very likely to explain that the majority of mice developed anaemia and thrombocytopenia only.

Because experimental data on the haematological alterations induced by VL are rare, the mechanisms responsible for alterations of erythropoiesis are unclear. It has been shown that haematopoietic activity is increased in BALB/C mice infected with *L. donovani* but not Severe Combined Immune Deficient (*scid*) mice⁸⁶. *Scid* mice like B6 RAG2^{-/-} also lack mature B or T lymphocytes. Here the evidence suggest that RAG2^{-/-} mice have no repression of medullar erythropoiesis and no splenomegaly despite the high parasite burden. Altogether, the data suggest that alteration of haematopoiesis is not a direct consequence of the infection but is linked to the adaptive immune response to the parasites. Confocal analysis of the bone marrow show that T cells tend to accumulate around parasites in the bone marrow. This is probably the bone marrow equivalent of granulomas found in the liver. It is likely that T cells infiltrate the bone marrow in order to fight the

infection. However, this response seems to have negative collateral effects (i.e. alteration of haematopoiesis). Contrary to the liver, the immune response is not protective in the bone marrow since intracellular parasites subsist chronically. The role of T cells in bone marrow disorders in infectious disease has been studied very little. Contrary to what is reported here in EVL, a role for T cells has been excluded in anaemia of trypanosomiasis since depletion of both CD4 and CD8 T cells did not change the levels of haemoglobin^{206,261,288}. In this regard, anaemia of VL could be closer to aplastic anaemia (AA), which is characterised by hypocellular bone marrow and pancytopenia. It has been linked experimentally with infiltration of T cells²⁸⁹ in the bone marrow and increase in IFN δ production^{290,291}.

In conclusion, this work demonstrates that infection with *L. donovani* induces alteration of RBC homeostasis in mice. The red blood cells numbers were reduced, but haemoglobin contents were stable. Infected mice also had a tendency of developing a macrocytic anaemia. These alterations reflect closely what has been reported in the human disease. Therefore, the mouse model can help provide useful insights into the human disease. The anaemia is associated with deep changes in the bone marrow microenvironment, namely the reduction of CXCL12-expressing cells and the loss of CD169^{high} macrophages. The cytokine G-CSF was up-regulated upon infection and is thought to be in part responsible for the bone marrow changes, as it has been shown to affect macrophages of stromal cells in other studies. We have strong evidence that splenomegaly is due to extramedullary erythropoiesis and is a consequence of the deficit of RBC production in the bone marrow, not the cause of it. This initiation of these alterations is dependent on the adaptive immune response since erythropoiesis was not affected by infection in immune deficient mice. These data all show a novel mechanistic model in which the adaptive immune response to *L. donovani* triggers a cascade of events starting by reduction of stromal support in the bone marrow in correlation with reduction of erythropoiesis and anaemia which in turns induces extramedullary erythropoiesis and splenomegaly. As the following chapter demonstrates, the events originating in the bone marrow causing a splenic reaction have further physiological impacts, notably on platelets.

Chapter 4 Regulation of platelets during EVL

4.1 Introduction

The majority of studies on the pathology of VL focus on the immune response to the infection, thus very little is known about the associated haematological alterations in general, and about the coagulopathies in particular. Yet excessive bleeding is a common feature of VL⁶² and has been linked to the lethality of disease. Indeed, a recent study retrospectively collected data from cases in Brazil from 2007 to 2011 and scored risk factors for death from VL⁷⁷. Apart for the age, the risk factor with the highest score was bleeding with an odd ratio of 3.8. This confirmed previous studies linking death from VL with bleeding in Brazil^{75,76} and Sudan⁷⁹. Coagulopathies can arise from a reduction of platelets, the “scaffolds” of blood clots, or anomalies affecting coagulation factors. Clinical data suggest haemorrhagic tendencies are primarily linked to a reduction in the number of circulating platelets⁶² that is usually restored to physiological levels after treatment⁷³. Auto-immune platelet destruction has been reported in dogs⁹⁶ but not in humans. It is therefore thought that the spleen is responsible for thrombocytopenia. Splenomegaly is associated with a multitude of conditions and is known to cause sequestration of circulating cells⁹⁷. Epistaxis (nose bleeding) has been reported in VL clinical studies²⁹² and studies of naturally infected dogs^{293–296}. In the human disease, thrombocytopenia correlated with epistaxis²⁹². However, no study of haemostasis in humans is available as of today. In dogs, epistaxis does not always correlate with thrombocytopenia but dogs infected with *L. infantum* had consistent alterations of haemostasis (longer coagulation time and reduced platelet aggregation). It is unclear how VL results in impairment of haemostasis in dogs, and if a similar phenomenon occurs in humans, which highlights the need for more studies. It is unlikely that treating patients in order to correct haemostasis in the context of VL will cure the disease. However, with the emergence of resistant strains of parasites, managing symptoms becomes a necessity when antibiotics fail. Because bleeding is associated with the lethality of VL in humans, treating haemostatic disorders would help to reduce the mortality associated with VL worldwide.

4.2 Aims

Coagulopathies have a negative impact on the prognosis of VL in humans. The statistics show haemorrhagic tendencies participates in the lethality of the disease. Correcting or preventing the coagulopathies in patients is likely to help reduce the mortality associated with VL. To this end, it is essential to understand the mechanisms underlying this symptom. Very little is known about the causes for haemorrhages in the context of VL.

In this study the aims were to:

1. Determine the nature of thrombocytopenia in infected C57BL/6 mice
2. Find possible causes for thrombocytopenia. Because the bone marrow and the spleen are both involved in the regulation of circulating platelets, the roles of these organs were investigated.
 - a. Determine if megakaryopoiesis is altered in infected mice.
 - b. Determine the role of the spleen in thrombocytopenia by comparing platelets in splenectomised vs. sham-operated infected mice.
3. Determine if *L. donovani*-induced thrombocytopenia responds to the growth factor thrombopoietin (TPO)

4.3 Results

4.3.1 Chronic *L. donovani* infection induces thrombocytopenia

Mice were infected for 28 days with *L. donovani* before blood was collected and analysed. This chapter focuses on platelets. Other haematological parameters, especially RBC, are discussed in Chapter 3. The platelet counts (**Fig. 4-1A**) in naïve mice was of $583 \pm 45 \times 10^3$ platelets per mm^3 of blood. Because of quite large standard deviation (170), the normal range was quite broad, from 241 to 924 (the normal range is calculated for a normal distribution as mean \pm 2 standard deviations). The infected group had a much lower average platelet count, down to $281 \pm 26 \times 10^3$ platelets per mm^3 of blood (-52%). Thrombocytopenia was defined by values below the reference interval. According to this definition, close to 40% of mice were thrombocytopenic. The platelets were also significantly bigger in chronically infected mice (**Fig. 4-1B**), with a mean platelet volume of 5.4 ± 0.1 femtoliter (fl). By comparison, naïve mice had an average MPV of 4.3 ± 0.1 fl and resulting normal range of 3.6 to 5 fl. Thus 76% of mice were considered to have abnormally large platelets. Therefore, chronic EVL induces thrombocytopenia characterised by an increase in platelet volume. Although infection caused thrombocytopenia, no excessive bleeding or epistaxis was ever reported. The thrombocytopenia of EVL was not associated with a pathology.

4.3.2 Megakaryopoiesis is unaltered during experimental visceral leishmaniasis

We reported in the previous chapter that anaemia was the result of a deficit of production of RBC cells in the bone marrow. Following the same logic, megakaryopoiesis was measured in the bone marrow of mice infected with *L. donovani* in order to determine if thrombocytopenia was the consequence of a reduced megakaryopoiesis. To this end, femurs were processed, sectioned and stained with haematoxylin and eosin. Megakaryocytes, the precursors of platelets, were counted manually, as they are easily recognisable. The average numbers of megakaryocytes per field of view were compared (**Fig. 4-1C**). No significant difference was detected between naïve and infected mice, despite the drop in platelet counts. Interestingly, no change in plasma TPO levels were detected either (**Fig. 4-1D**).

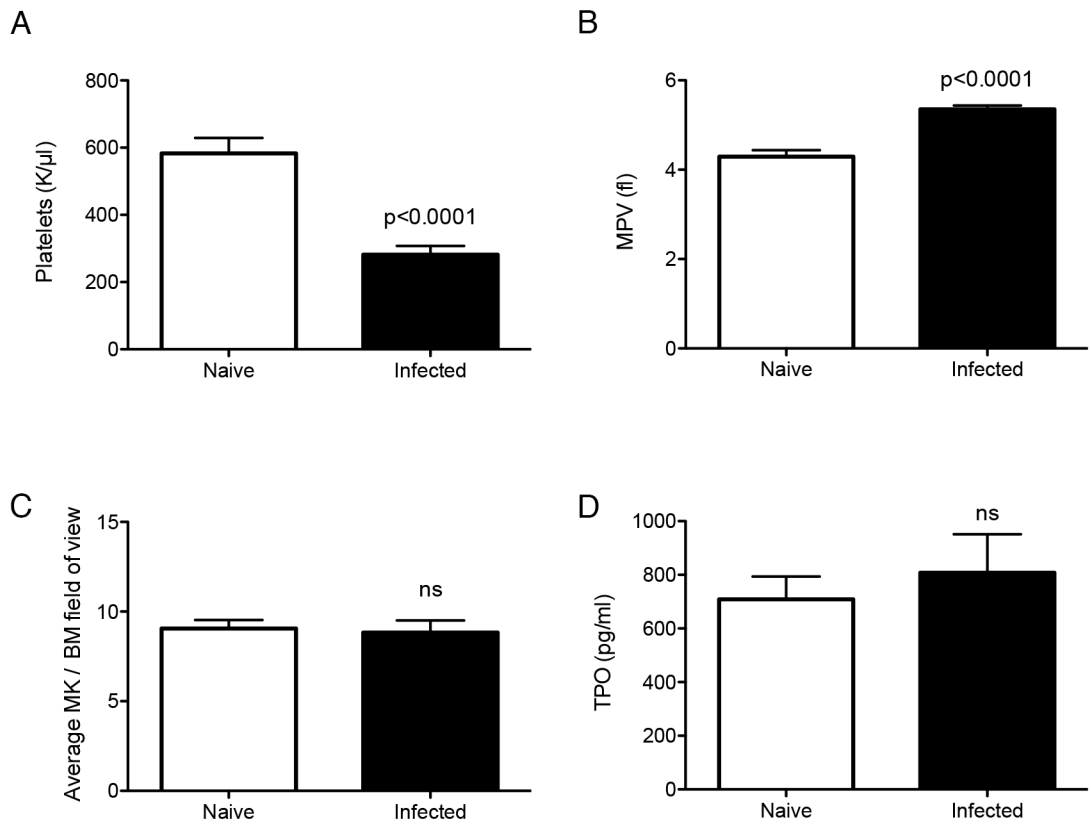


Figure 4-1. *L. donovani* infection induces thrombocytopenia. (A) Platelet counts (unpaired t-test, n=14 naïve and 13 infected mice from 3 independent experiments). (B) Mean platelet volume (Mann-Whitney test, n=14 naïve and 13 infected mice from 3 independent experiments). (C) Average megakaryocytes (MK) counts per field of view from bone marrow sections stained with haematoxylin and eosin. MK were manually counted on the basis of their morphology on 5 random fields of view per section, 3 sections per animal were analysed. (unpaired t-test, n=4 mice per group from one experiment). (D) Circulating TPO levels measured by ELISA from the plasma (unpaired t-test, n=3 naïve and 4 infected mice from one experiment). All experiments were performed 4 weeks after infection with *L. donovani*.

4.3.3 Platelet production is stimulated by TPO in infected mice

Previous data indicate that the thrombocytopenia induced by *L donovani* infection is not the consequence of a reduction of platelet production. The hypothesis is then that thrombocytopenia is not aplastic, i.e. megakaryopoiesis is normal and can be stimulated by growth factors. To test this hypothesis, mice were treated with recombinant TPO (rhTPO) when they were already in the chronic phase of infection and the platelets were counted. In a pilot experiment, naïve mice only were infected with *L. donovani*. 4 weeks later, mice were injected with rhTPO ranging from 500ng to 1µg daily i.p. for 5 days. Experiments were performed after a resting phase of 5 days. The first five days of treatment aim to stimulate the growth of megakaryocytes. It has been shown that platelets continue to being release 3 to 5 days after withdrawal of TPO²⁹⁷. The platelet counts in the treated with rhTPO mice were between 1.6 and 1.9 times higher than in the PBS-treated control (**Fig. 4-2A**). No difference was measured between the doses. The maximum response was reached at the dose of 500ng already. Because rhTPO is not known to have any side effect in mice, a dose of 1µg per day for 5 days was chosen for the treatment of infected mice to maximise the chances of mice responding to the treatment. Chronic infection resulted in a low platelet count in PBS-treated mice ($353\pm 32 \times 10^6$ per µl of blood) but rhTPO-treated mice had a 2.6-fold increase in circulating platelets (**Fig. 4-2B**; $725\pm 125 \times 10^6/\mu\text{l}$). However, the platelet volume was still expanded in both infected groups (**Fig. 4-2C**).

4.3.4 Thrombocytopenia is associated with splenomegaly

An interesting observation was made from the treatment of infected mice with rhTPO. Although the average platelet counts raised to normal levels compared to PBS-treated mice, the efficacy of rhTPO was very uneven. The standard deviation of the platelet count was high, resulting in a coefficient of variation (standard deviation/average) of 65%. This variability could be partly due to natural variations in sensitivity to rhTPO or technical inconsistencies, but possible factors for the variations were also looked for. Individual spleen weights of mice treated with rhTPO were therefore plotted against the corresponding platelet counts (**Fig. 4-2D**). A linear model was fit from the data. The goodness-of-fit was determined from the R-squared value which was in in this case of 0.65. This means that the fit explains 65% of the variability of the data. It was considered as a good fit for biological data. The resulting line had a negative slope. This indicates that the bigger the spleens are, the lower the platelet counts are following rhTPO treatment.

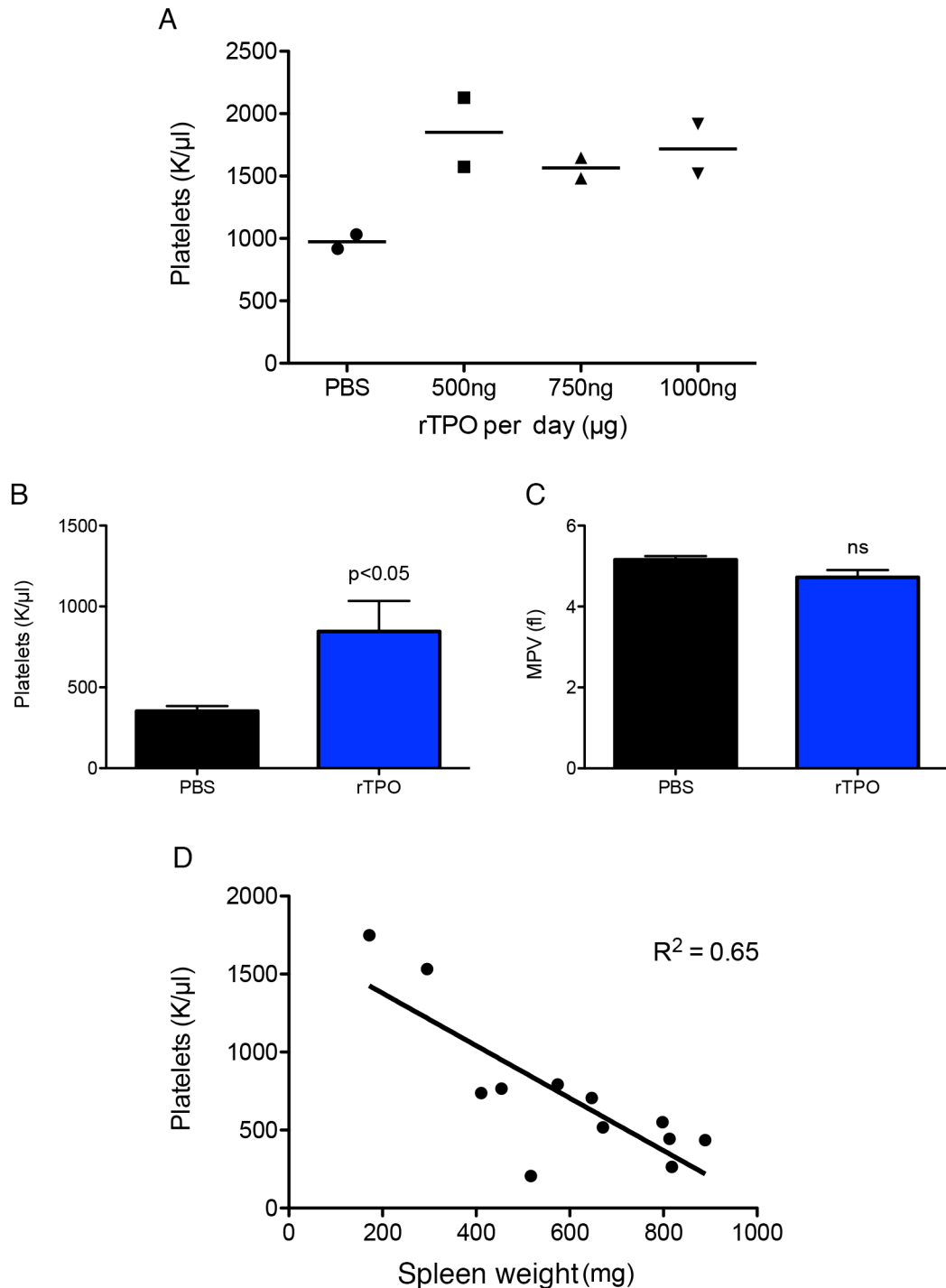


Figure 4-2. Treatment of infected mice with recombinant TPO increases circulating platelets.

(A) Study of dose-response in naïve mice. Mice were injected i.p. daily for five consecutive days with rhTPO. Blood was collected 5 days after the last injection and analysed (n=2 mice per dose). (B) Platelet counts from infected mice treated with 1 μg rhTPO daily rhTPO or PBS, following the regime described in A, starting 4 weeks after infection. (Mann-Whitney test, n=7 PBS-treated mice and 8 rhTPO-treated mice) (C) Mean volume of platelets from infected mice treated with rhTPO or PBS (unpaired t-test, n=7 PBS-treated mice and 8 rhTPO-treated mice). (D) Platelet counts from infected mice treated with rhTPO plotted against the spleen weight. The black line corresponds to the best-fit linear regression. (n=12, including 4 sham-operated mice)

4.3.5 Splenectomy reduces thrombocytopenia

The negative correlation between the spleen weight and the efficacy of rhTPO injections to correct thrombocytopenia suggests a role for the spleen in the reduction of circulating platelets. To investigate this, splenectomised mice were infected with *L. donovani* (after having recovered from the surgery) and the platelets were counted (**Fig. 4-3A**). In sham-operated mice, the infection resulted in a 57% reduction of platelets in the blood compared to their naïve counterparts ($297 \pm 16 \times 10^6$ platelets/ μl in infected mice vs $685 \pm 32 \times 10^6/\mu\text{l}$ in naïve). Splenectomy did not affect the number of circulating platelets in the naïve mice compared to sham-operated naïve mice. However, upon chronic infection, the average platelet count was only reduced by 33% compared to the naïve splenectomised mice ($509 \pm 42 \times 10^6$ platelets/ μl in infected mice vs $756 \pm 38 \times 10^6/\mu\text{l}$ in naïve). When comparing the effect of infection between sham-operated and splenectomised mice, the platelet counts were in average 70% higher in splenectomised mice than in sham-operated. Altogether, these results confirm that the spleen factors into the EVL-induced thrombocytopenia. However, there was still a reduction of circulating platelets in splenectomised mice, indicating that other mechanisms participate to thrombocytopenia. Again, in infected mice, the decrease in platelets was associated with an increase in platelet volume (**Fig. 4-3B**). Sham-operated and splenectomised naïve mice had averages MPVs of 3.7fl and 3.9fl, respectively. Their infected counterparts had MPVs of 5fl and 5.4fl respectively. Unexpectedly, hepatomegaly was present in infected splenectomised mice but was consistently lower than sham-operated mice (**Fig. 4-4**). Splenectomised mice were injected with rhTPO along with sham-operated mice. The mice were submitted to the same regime described previously. rhTPO was moderately efficient in sham-operated mice with an average of $483 \pm 91 \times 10^3$ platelets/ μl , while the average was measured at $297 \times 10^3/\mu\text{l}$ in untreated sham-operated mice in previous experiments. By opposition, the treatment boosted the platelet counts up to $1953 \pm 55 \times 10^3$ platelets/ μl in splenectomised mice (**Fig. 4-5A**). In addition, the MPV (**Fig. 4-5B**) returned to values close to what was measured in naïve mice ($4.12 \pm 0.10\text{fl}$) while it remained high in sham-operated mice with treatment ($5.35 \pm 0.02\text{fl}$). This result confirms that the spleen counters the efficacy of rhTPO in regards to increasing the number circulating platelets and returning the platelet volume to normal levels.

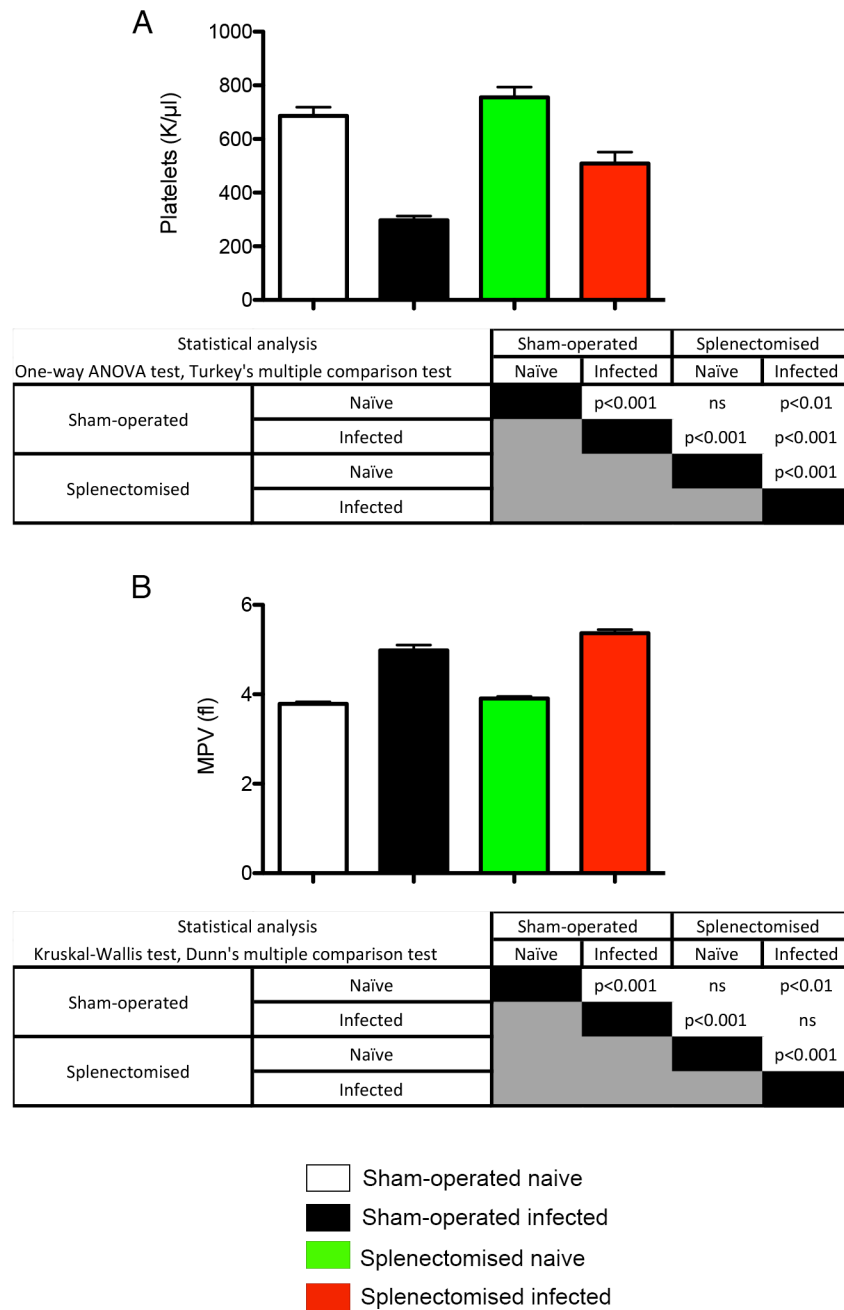


Figure 4-3. Infection results in higher platelet counts in splenectomised mice. (A) Platelet counts. (B) Mean platelet volume. All experiments were performed 4 weeks after infection (n=15 mice per group from 3 independent experiments).

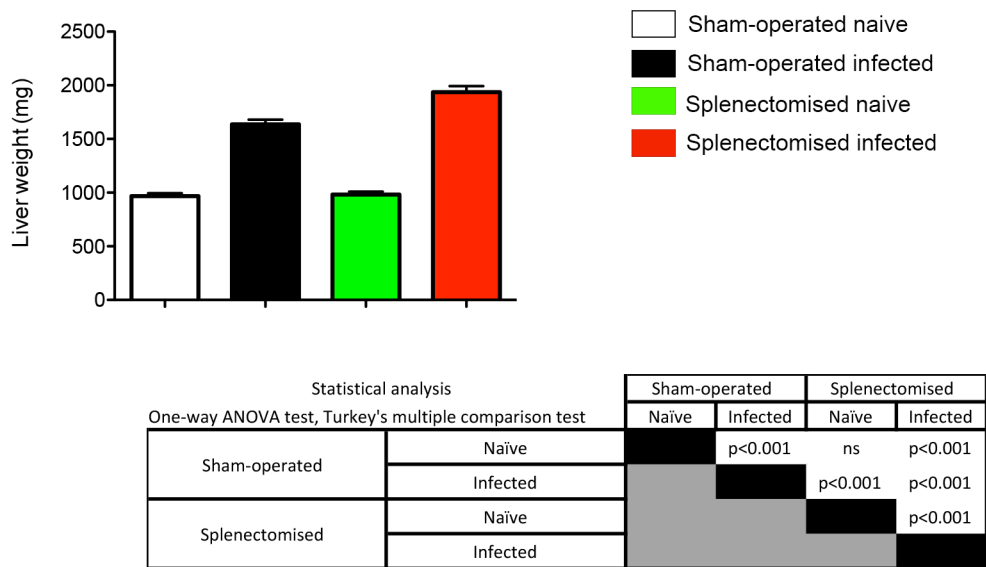


Figure 4-4 Splenectomy results in a reduced hepatomegaly in infected mice. All experiments were performed 4 weeks after infection with *L. donovani* (n=15 from 3 independent experiments).

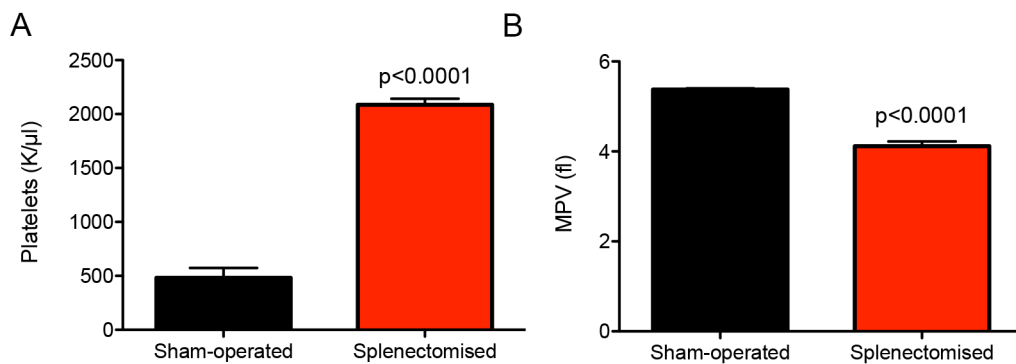


Figure 4-5. Better response of rhTPO in infected splenectomised mice. (A) Platelet counts. (B) Mean platelet volume. Already splenectomised mice or sham-operated mice were infected for 4 weeks then treated with 1 μ g rhTPO i.p. daily for 5 days. The blood was analysed 5 days after last injection (unpaired t-tests, n=4 sham-operated and 5 splenectomised mice).

4.4 Discussion

In the experimental murine model of VL, chronic infection causes thrombocytopenia and an increase in platelet volume. The bone marrow of infected mice had similar numbers of megakaryocytes as the naïve mice, indicating that megakaryopoiesis was unaltered. However, it is possible that thrombopoiesis (the production of platelets from megakaryocytes) is altered at the megakaryocyte stage, i.e. mature megakaryocytes do not release platelets. It is still unclear how megakaryocytes release platelets. Two models co-exist as of today, one involving proplatelets (pseudopodial formations that megakaryocytes project into the bone marrow vasculature and are released as platelets) and another in which megakaryocytes enter the the circulation and reach the lung vasculature where they are fragmented²⁹⁸. Without discussing which of the two models is the most accurate, this shows how complex the final stages of thrombopoiesis can be. For this reason, we can not definitely exclude that thrombocytopenia is not caused by a deficit of production. Interestingly, despite the low platelet counts, circulating levels of TPO were not altered.

Here we also report that EVL-induced thrombocytopenia is associated with an increase in platelet volume. Studies of platelet regulation have shown that thrombocytopenia, independently of the cause, generally results in platelets being bigger. Generally speaking, the body preserves the total mass of platelets before restabilising the platelet number¹⁹⁴. In human patients with splenomegaly, the platelet mass was similar to healthy individuals, despite the thrombocytopenia⁹⁷. The same observation was made in experimental rat models²⁹⁹. It has been shown that thrombocytopenia causes ultrastructural changes in megakaryocytes resulting in an increased volume of platelets^{300,301}. It is very likely that the increase of MPV in our model of VL is a compensation mechanism. A non-linear correlation between MPV and platelet counts has been reported³⁰², therefore platelet mass cannot be calculated by the product of MPV by the total platelets. Therefore, with the present data we are unable to determine if the platelet mass is preserved during *L. donovani* infection in mice.

Thrombocytopenia was not associated with increase in TPO plasma levels. Generally, levels of TPO correlate inversely with the number of platelets. Platelets express a high-affinity receptor for TPO. Platelets regulate TPO by capturing circulating TPO³⁰³. As a consequence, a decrease of platelets is expected to result in an increase of TPO in the blood. However, in contexts of platelet destruction such as immune thrombocytopenic purpura, the levels of TPO do not correlate with platelet counts^{198,304}. The two studies therefore corroborate our data which show that the cause of thrombocytopenia is a peripheral destruction, not a central deficit of production. By contrast, TPO production is

up-regulated in patients with aplastic anaemia^{198,304}. The bone marrow produces little TPO in physiological conditions, but TPO mRNA has been shown to increase in bone marrow stromal cells of patients with thrombocytopenia, including in immune thrombocytopenia¹⁹⁷. In the eventuality that TPO produced by bone marrow stromal cells only has a paracrine action, by opposition to endocrine signalling, then it would not be detected in the systemic circulation. Here we only report unchanged systemic levels of TPO, but the local regulation of TPO in VL has not been investigated. It cannot be excluded that up-regulation of TPO occurs at the tissue level.

In our mouse model of EVL, thrombocytopenia was not considered aplastic as it responded to recombinant human TPO therapy. Eltrombopag is an NHS and FDA-approved drug used for the treatment of immune-thrombocytopenia. It is an agonist of Mpl, the main receptor of TPO, and has very little side effect. The reconditioning of Eltrombopag for treatment of thrombocytopenia in VL patients is an option that we would recommend investigating. However, as the data show here, stimulation of platelet production yields best results when the splenomegaly is not too severe and reaches a maximum efficacy in splenectomised mice. Assuming splenic capture is the main cause for thrombocytopenia in VL, it is likely that platelet production has to overcome the rate of splenic capture in order to raise platelet counts. In addition, our experimental design for the study of rhTPO in EVL did not include time points after treatment. It is possible that experiments were performed after the peak of platelet release. In this case, it cannot be excluded that rhTPO worked but that platelet counts had dropped faster in mice with the bigger spleens.

Our data indicate that the decrease in platelets following infection with *L. donovani* is not as severe in splenectomised mice than normal mice. This confirms the involvement of splenomegaly in EVL-induced thrombocytopenia. In the steady state, about one-third of the platelet mass is sequestered in the spleen and is exchangeable with the circulating fraction. The splenic pool of platelets is increased in relation to the splenomegaly. The volume of total circulating platelets in human approximate 5 to 10ml, which is quite small compared to the total volume of RBC, approximately 25-30ml/kg of body weight³⁰⁵. It is estimated that the spleen can pool up to 20% of the RBC in the worst cases of splenomegaly. Because the total volume of platelets is so small, the spleen can potentially capture a bigger fraction than for the RBC. Liver dysfunction is also a common cause of thrombocytopenia²¹⁸. Viral infection with HCV causes fibrosis of the tissue and liver damage in HCV patients is associated with the severity of thrombocytopenia^{219,220}. Visceralising species of *Leishmania spp.* infect Kupffer cells of the liver and induce the formation of granulomas^{223,271}. Liver damage has been reported in VL patients^{306,307}. For

this reason, the liver may participate in the pathogenesis of thrombocytopenia during VL. This would explain why the platelets counts, although higher than in their sham-operated counterparts, were still reduced in infected splenectomised mice compared to naïve mice.

The *Salmonella* Typhimurium infection model in the mouse has shown that innate inflammation can cause local thrombosis and exhaust the pool of circulating platelets via the up-regulation of podoplanin on monocytes and Kupffer cells. Platelets express CLEC-2, which binds to podoplanin and causes their activation²¹⁵⁻²¹⁷. Disseminated intravascular coagulation of platelets has only been reported once in a dog naturally infected with *Leishmania infantum* but is a unusual finding in VL³⁰⁸. In this work, mice infected with *L. donovani* have never shown signs of intravascular coagulations.

Another model providing insights into the thrombocytopenia of parasitic infection is trypanosomiasis³⁰⁹⁻³¹¹. Infection with *Trypanosoma brucei* or *Trypanosoma cruzi* leads to thrombocytopenia among other symptoms. *Trypanosoma cruzi* is known to obtain sialic acids, complex carbohydrates found on the outer cell membrane, from cells of the host³¹². The trans-sialidase expressed by *Trypanosoma cruzi* has been shown to induce thrombocytopenia³¹³. Indeed, a platelet's half-life is defined by its content in sialic acids, which diminishes over time. Platelets with low sialic acids are phagocytised by Kupffer cells in the liver³¹³, which stimulates TPO production via the Ashwell-Morell receptor²⁰⁰. This mechanism do not seem to be involved in leishmaniasis since *Leishmania* species do not express a trans-sialidase³¹⁴. *Leishmania* and *Trypanosoma* parasites have been shown to express platelet activating factors^{315,316}. This is unlikely to cause thrombocytopenia since *Leishmania* parasites are intracellular and not found in the circulation in chronic infection. This mechanism appears to help initial infection, since platelet activation has been shown to attract monocytes to the sites of *Leishmania major* infection³¹⁷, thus attracting more potential host cells.

Epistaxis (nose bleeding) is a clinical symptom often reported as sign of haemorrhagic tendencies. Many studies focus on epistaxis because it is a spontaneous phenomenon, whereas bleeding tests would require invasive techniques. Contrary to the mouse model, epistaxis or mucosal bleeding are common findings in naturally infected dogs. Thrombocytopenia is a frequent occurrence in infected dogs, naturally⁶⁹ or experimentally³¹⁸. However, in some cases, thrombocytopenia has been ruled out as a factor for epistaxis. No difference in the frequencies of thrombocytopenia was noted between symptomatic dogs with epistaxis and symptomatic dogs without epistaxis²⁹⁵. It is also mentioned in this study that thrombocytopenia is not severe enough to explain epistaxis. Other studies reports epistaxis in dogs with no thrombocytopenia²⁹³. The main

factor for epistaxis is not thrombocytopenia but thrombocytopathy, i.e. defect in platelet function. Platelet aggregation can be triggered by adenosine di-phosphate (ADP) and collagen. Platelet aggregation tests on dogs have shown a reduced aggregation response of platelets from the blood of infected dogs^{294,295,318}. The mechanism underlying thrombocytopathy in infected dogs is unclear. Here we focused on the thrombocytopenia of EVL, which is not always linked to epistaxis. In addition, mice chronically infected with *L. donovani* did not show any spontaneous sign of haemostasis impairment. If epistaxis is taken as a reflection of haemorrhagic tendencies, then treating thrombocytopenia might not be clinically relevant. Further studies are required to establish the link between thrombocytopenia and clinical symptoms.

Chapter 5 General discussion

5.1 Principal findings and relevance

5.1.1 Murine visceral leishmaniasis as a model for haematological studies

Many experimental studies of VL have used the mouse model and have provided very useful insights into the immunobiology of the disease¹. The human disease is also characterised by profound alterations of the bone marrow and changes in circulating cells but very little is known about this aspect of the disease^{3,62}. Much of what is known comes from clinical studies and to a certain extent other experimental models such as hamsters. The mouse model has often been disregarded because EVL is not associated with lethality of overt symptoms. To our knowledge, this is the first report of an extensive haematological profile comparing chronically infected and naïve mice. Two types of blood cells were reduced during chronic infection, the red blood cells and the platelets. The anaemia was mild, normochromic and some mice also showed macrocytic anaemia. Reports about VL in humans consistently report a normochromic anaemia with a macrocytic tendency. Anaemia did not appear to have a physiological impact on the mice, certainly not to the extent of being lethal. Other studies about regulation of erythropoiesis in mice show that dramatic decrease in erythropoiesis do not necessarily lead to anaemia. Data about thrombocytopenia are rare and there is no experimental study on the thrombocytopenia of VL. In the human disease, thrombocytopenia is a common occurrence⁶². The results presented here show that experimentally infected mice and human patients have similar haematological alterations. We suggest that the mouse model can be used as a model for haematological disorders in VL, hopefully paving the way for more studies.

5.2 Erythropoiesis is impaired as a consequence of alterations of the bone marrow microenvironment

A decrease in the late stages of erythropoiesis was observed in the bone marrow of infected mice chronically infected with *L. donovani*. The CD71^{high}TER119^{low} pro-erythroblasts numbers were unchanged but the CD71^{high/low}TER119^{high} erythroblasts, which include all final stages of erythropoiesis, were reduced. This is the first time erythropoiesis has been quantified in detail in the mouse. Previous work by Cotterell et al. has suggested that earlier stages of erythropoiesis, the BFU-E, were increased in the bone marrow of infected BALB/c mice. Taken together, this suggests that the last stages of erythropoiesis are specifically impaired. The microenvironment supporting erythropoiesis was investigated. Macrophages are important regulators of erythroid precursors. Here we show that

macrophages number are similar upon infection but a relative loss of macrophages expressing high levels of CD169 was measured. We and other have demonstrated that these macrophages harbour amastigotes, but infection of immunocompromised mice did not cause alterations of macrophages. Therefore, the reduction of CD169⁺ macrophages is not a direct consequence of intracellular parasitism. Not only these macrophages are known to be essential for erythropoiesis, they have also been linked in previous studies to the regulation of the bone marrow microenvironment supporting HSCs. Here, levels of CXCL12 were decreased at the mRNA level, corresponding with a decrease in CAR cells. These cells have been shown to contain most MSPCs in the bone marrow. The number of MSPCs, reflected by the number of CFU-F in the bone marrow was also decreased by *L. donovani* infection, suggesting an actual loss of cells. Previous work has suggested a role for stromal macrophages in the pathology of EVL, but here is the first detailed investigation into the role of the bone marrow microenvironment *in vivo*.

5.2.1 Cells of the adaptive immune system are required for the onset of erythropoiesis repression and alterations of the microenvironment in the bone marrow

One of the major findings in this work is the connection between haematological alterations associated with EVL and the immune system. T cells were shown to migrate towards parasites in the bone marrow and accumulation of CD3 cells correlated time-wise with the decrease of erythropoiesis in the bone marrow. From these observations we hypothesised that T cells were responsible for the pathogenesis of VL. The role of adaptive immunity in general was confirmed by the lack of alteration in immunocompromised RAG2^{-/-} mice. The population of CD169^{high} macrophages, the levels of CXCL12 and G-CSF as well as erythropoiesis were unchanged. This reinforced the potential link between all these alterations. Immune reconstitution resumed the reduction of erythropoiesis in the bone marrow together with splenomegaly and higher levels of G-CSF, confirming that the adaptive immune response is in part responsible for the defects in erythropoiesis. All these findings fit in a model supported by our data and the literature described in **Figure 5-1**.

5.2.2 Alterations of the bone marrow underlie extramedullary erythropoiesis and remodelling the spleen

In other models, the connection between decrease of medullar erythropoiesis and splenomegaly has been established. The causes for splenomegaly in VL are unclear. Often, splenomegaly and increase in splenic capture of circulating cells is cited as the source for haematological alterations. By contrast, we show that changes in the bone marrow described above have an impact in the spleen. The alterations in the bone marrow

described above were still induced by *L. donovani* in splenectomised mice. While erythropoiesis was decreased in the bone marrow, we measured a dramatic up-regulation of splenic erythropoiesis. Histological investigations have shown that erythropoiesis occurs exclusively in the red pulp. As a consequence, the red pulp of the spleens from infected mice was dilated, especially in comparison to the white pulp. This led to an increase in the red pulp/white ratio in 2D image analysis. No up-regulation of BMP4, an essential factor inducing extramedullary erythropoiesis, was detected. A recent work by Dalton et al. have shown that a population of splenic macrophages is responsible for the splenic remodelling during EVL. These macrophages express high levels of Bmp4 compared to other populations. Therefore, a role for bone BMP4 signalling cannot be excluded. This is the very first report linking alterations of erythropoiesis in the bone marrow and splenic remodelling in the context of VL.

5.2.3 **Thrombocytopenia is caused by splenomegaly and can be rescued by recombinant TPO injections**

In addition to anemia, infection with *L. donovani* resulted in thrombocytopenia. Thrombocytopenia was reduced when mice were splenectomised before the infection. No deficit of megakaryocyte production was measured as both infected and naïve mice had identical number of megakaryocytes in their bone marrow. The production of platelets could be stimulated by injections of rhTPO. This treatment was however only efficient in rescuing the thrombocytopenia when the splenomegaly was only mild, again indicating that the spleen was involved in the reduction of circulating platelets. This was further confirmed by injecting rhTPO into splenectomised infected mice, where the platelet counts were much higher than what was measured even in naïve mice treated with rhTPO. Therefore, the efficacy of rhTPO in driving the platelet count up appears to depend on its capacity to stimulate the production of enough platelets to overcome the splenic capture. Eltrombopag is a drug used to treat thrombocytopenia. It is an agonist of the c-Mpl receptor, the receptor of TPO. This drug is already FDA-approved and associated with very little side effect. The demonstration that thrombocytopenia of EVL can be rescued by rhTPO suggest that Eltrombopag could be useful in treatment of thrombocytopenia in human VL. This work supports the idea that such a drug should be tested in clinical settings for the treatment of thrombocytopenia in human VL.

As a conclusion, we have shown that the adaptive immune response to *L. donovani* drives alterations in the bone marrow, resulting in a loss of erythropoiesis and a mild anaemia. These changes are linked to extramedullary erythropoiesis and splenomegaly, which in turns involved in generation of thrombocytopenia, as shown in **Figure 5-2**. The novelty of

this work lies in the demonstration of the complex immunopathogenesis of haematological disorders in the context of VL. The individual mechanisms reported in this study have been reported previously, but for the first time haematological disorders have been studied not in isolation but as part of a whole system, linking anaemia and thrombocytopenia.

5.3 Outstanding questions and future work

5.3.1 Confirm the link between G-CSF up-regulation and repression of erythropoiesis

The concluding model from this work involves G-CSF as a mediator between inflammation and repression of erythropoiesis. Absence of G-CSF up-regulation in immunocompromised mice correlated with stable expression of CXCL12 and no change in CD169-expressing macrophages but it cannot be excluded that these events happen independently. The connection between G-CSF and alterations of the bone marrow is supported by the literature but experimental data in the context of EVL are still needed. Here neutralisation of G-CSF was attempted but was unsuccessful at lowering the levels of circulating G-CSF. Further work is therefore needed to confirm the role of G-CSF in the pathogenesis of EVL. If a central role for G-CSF in alterations of the bone marrow is confirmed, neutralisation of G-CSF could be the base of a novel therapy to relieve symptoms of VL. Unfortunately, except for transgenic mouse models, neutralisation of G-CSF is hard to achieve. Very few conditions have been linked to G-CSF. It has been linked to the severity of inflammatory arthritis, but the long treatment and amount of antibody used in the study show how difficult G-CSF neutralisation is *in vivo*²⁷⁸.

5.3.2 Functional study of infected macrophages in regards to support of erythropoiesis

We show that infection with *L. donovani* causes a decrease of CD169^{high} macrophages. But the ability of macrophages in mice infected with *L. donovani* to support erythropoiesis is not known. The hypothesis that reduction of CD169^{high} macrophages impairs erythropoiesis is supported by the study which shows that depletion of CD169-expressing macrophages causes a diminution of erythropoiesis in the bone marrow. Testing the ability of macrophages from infected mice to support erythropoiesis would confirm that repression of erythropoiesis in EVL is due in part to the loss of stromal macrophages that support erythropoiesis.

5.3.3 Cells of the adaptive immune system responsible for haematological alterations

This work demonstrates a role of the adaptive immune system for the onset of bone marrow alterations. Analysis of the bone marrow show that T cells are more numerous in infected mice, and images show that T cells come towards infected cells. It is unclear if these cells are specifically reacting to parasite antigens, and if they are responsible for the defects in haematopoiesis. Immune reconstitution experiments confirm the role for adaptive immunity in the pathogenesis of haematological alterations. However, work is still needed to demonstrate a) if a specific subset of T or B cell is responsible for the alterations of the bone marrow b) if haematological alterations are the result of the local inflammation in the bone marrow alone or if immune cells at distant sites also participate.

5.3.4 Study the role of the liver in thrombocytopenia

Thrombocytopenia is a common complication of chronic liver diseases²¹⁸. VL is associated with fibrosis of the liver^{306,307}. The liver has not been studied in this work. The data presented here show a contribution of the spleen to thrombocytopenia since the infected splenectomised mice have higher platelet counts than there sham-operated counterparts. However, a decrease in circulating platelets was still measured in infected splenectomised mice, so another mechanism may contribute to thrombocytopenia. Further study is required to investigate the role between the liver and thrombocytopenia in the context of VL.

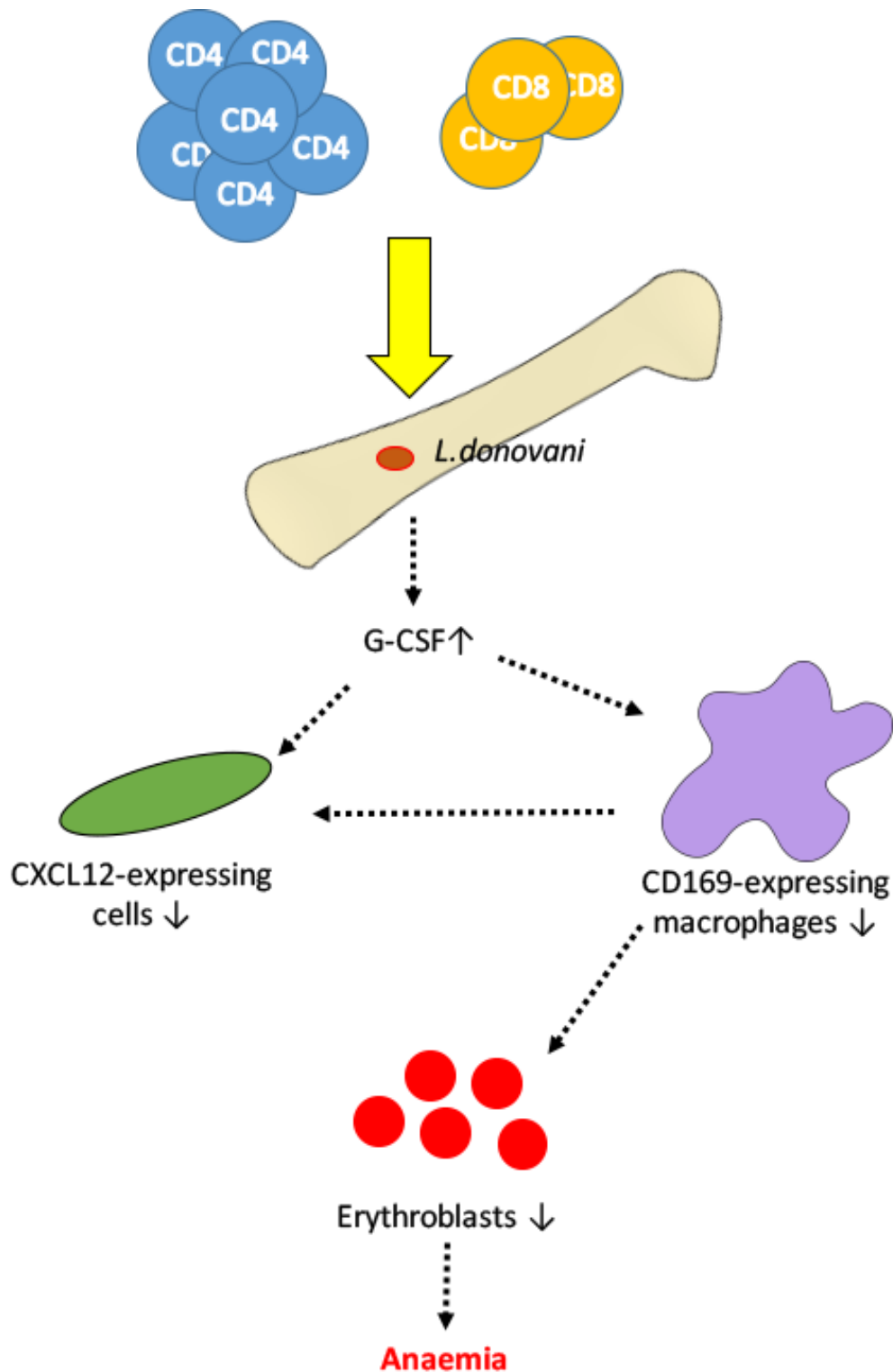


Figure 5-1. Hypothetical model for the mechanisms of anaemia in experimental visceral leishmaniasis. Infection of the bone marrow (bone marrow) with *L. donovani* causes CD4 T cells mostly, but also CD8 T cells, to infiltrate the tissue. Adaptive immune response drives the up-regulation of G-CSF in an unidentified source. G-CSF causes alterations of the bone marrow microenvironment which consists of CXCL12-secreting fibroblasts and CD169-expressing macrophages, the latter also being essential for stimulating CXCL12 production by stromal cells. Loss of stromal support for erythropoiesis, especially from stromal macrophages, contributes to the decrease of erythropoiesis in the bone marrow and the subsequent anaemia. Dotted arrows represent hypothetical connections supported by the literature.

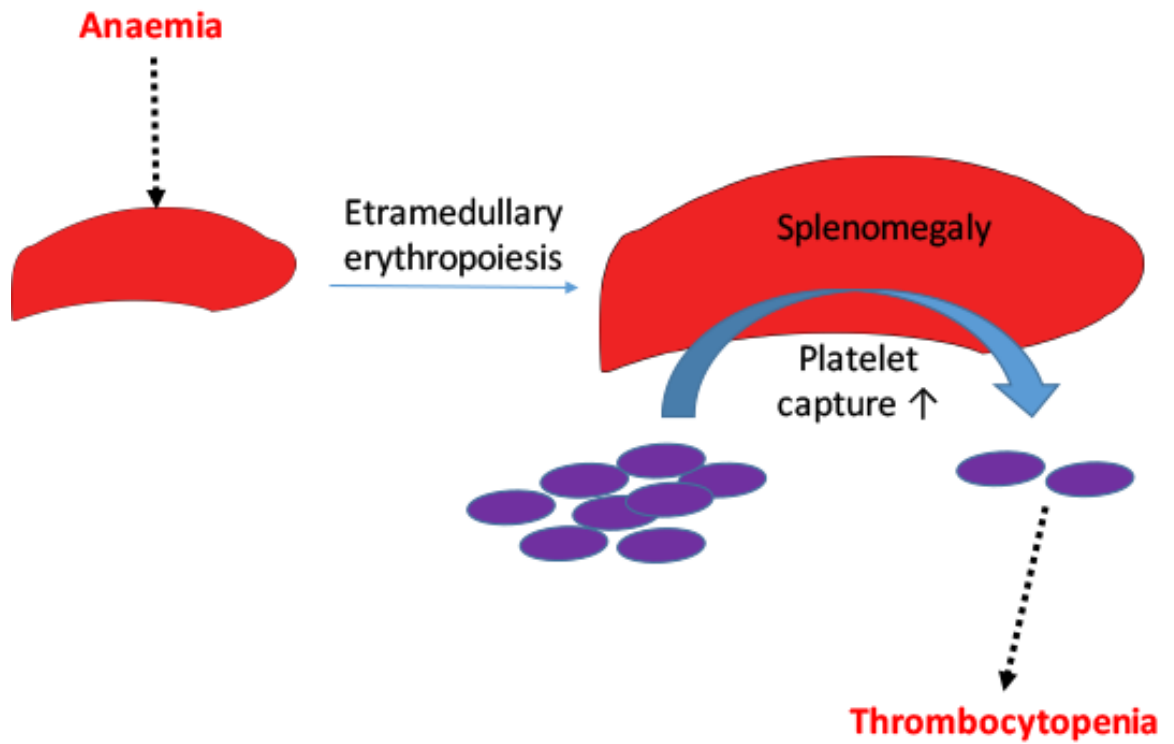


Figure 5-2. Hypothetical model for the mechanisms of thrombocytopenia in experimental visceral leishmaniasis. In response to anaemia, erythropoiesis is induced in the spleen. The proliferation of stress erythroid progenitors in the red pulp of the spleen causes a remodelling of the tissue resulting in splenomegaly. The enlarged spleens capture more circulating platelets, which eventually leads to thrombocytopenia.

List of abbreviations

°C	degree Celsius
Angpt1	angiopoietin 1
BFU-E	erythroid-burst forming unit
BSA	bovine serum albumin
CAR	CXCL12-abundant reticular
CD"x"	cluster of differentiation "x"
cDNA	complementary deoxyribonucleic acid
CFU-E	erythroid-colony forming unit
CFU-F	fibroblast-colony forming unit
CL	cutaneous leishmaniasis
CLEC-2	C-type lectin-like receptor
CLP	common lymphoid progenitor
CMP	common myeloid progenitor
DAPI	4',6-diamidino-2-phenylindole
DC	dendritic cell
DCL	diffuse cutaneous leishmaniasis
DNA	deoxyribonucleic acid
<i>E. coli</i>	<i>Escherichia coli</i>
ELISA	enzyme-linked immunosorbent assay
Emp	erythroblast macrophage protein
EVL	experimental visceral leishmaniasis
FSC	forward scatter
G-CSF	granulocyte-colony stimulating factor
G-CSF	granulocyte-colony stimulating factor
GPVI	glycoprotein VI

GM-CSF	granulocyte monocyte-colony stimulating factor
Hb	haemoglobin
HSC	haematopoietic stem cell
IL	interleukin
LT-HSC	long-term haematopoietic stem cell
LXR	liver X receptor
M	mole/litre (mM: millimole/litre)
MCH	mean corpuscular haemoglobin
MCV	mean corpuscular volume
MEP	megakaryocyte-erythrocyte progenitor
MK	megakaryocyte
Mpl	myeloproliferative leukaemia protein
MPV	mean platelet volume
MSC	mesenchymal stem cell
MSPC	mesenchymal stem and progenitor cell
NK	natural killer
nm	nanometre
NO	nitric oxide
OD	optical density
PBS	phosphate-buffered saline
pg	picograms
PKDL	post kala-azar dermal leishmaniasis
RAG2	recombination-activating gene 2
RBC	red blood cells
rhTPO	recombinant human thrombopoietin
RIPA	radioimmunoprecipitation buffer
RNA	ribonucleic acid
RT	room temperature

Scf	stem cell factor
SLAM	signalling lymphocytic activation molecules
SNARE	soluble N-ethylmaleimide attachment protein receptor
SSC	side scatter
SSG	stibogluconate
ST-HSC	short-term haematopoietic stem cell
STAT	signal transducers and activators of transcription
TGF β	transforming growth factor beta
T _H 1	type 1 helper T cell
TNF	tumour necrosis factor
TPO	thrombopoietin
TRAIL	TNF-related apoptosis inducing factor
Vcam1	vascular cell adhesion molecule 1
VL	visceral leishmaniasis
μ l	microliter

Bibliography

1. Kaye, P. & Scott, P. Leishmaniasis: complexity at the host-pathogen interface. *Nat. Rev. Microbiol.* **9**, 604–15 (2011).
2. Varma, N. & Naseem, S. Hematologic Changes in Visceral Leishmaniasis/Kala Azar. *Indian J. Hematol. Blood Transfus.* **26**, 78–82 (2010).
3. Kopterides, P., Halikias, S. & Tsavaris, N. Visceral leishmaniasis masquerading as myelodysplasia. *Am. J. Hematol.* **74**, 198–9 (2003).
4. Yarali, N., Fişgin, T., Duru, F. & Kara, A. Myelodysplastic features in visceral leishmaniasis. *Am. J. Hematol.* **71**, 191–5 (2002).
5. Singh, S., Sharma, U. & Mishra, J. Post-kala-azar dermal leishmaniasis: recent developments. *Int.J.Dermatol.* **50**, 1099–1108 (2011).
6. Bern, C., Maguire, J. H. & Alvar, J. Complexities of assessing the disease burden attributable to leishmaniasis. *PLoS Negl. Trop. Dis.* **2**, e313 (2008).
7. Claborn, D. M. The biology and control of leishmaniasis vectors. *J. Glob. Infect. Dis.* **2**, 127–34 (2010).
8. Medlock, J. M., Hansford, K. M., Van Bortel, W., Zeller, H. & Alten, B. A summary of the evidence for the change in European distribution of phlebotomine sand flies (Diptera: Psychodidae) of public health importance. *J. Vector Ecol.* **39**, 72–7 (2014).
9. Rose, K. *et al.* Cutaneous leishmaniasis in red kangaroos: isolation and characterisation of the causative organisms. *Int. J. Parasitol.* **34**, 655–64 (2004).
10. Dougall, A. M. *et al.* Evidence incriminating midges (Diptera: Ceratopogonidae) as potential vectors of *Leishmania* in Australia. *Int. J. Parasitol.* **41**, 571–9 (2011).
11. Seblova, V. *et al.* The Biting Midge *Culicoides sonorensis* (Diptera: Ceratopogonidae) Is Capable of Developing Late Stage Infections of *Leishmania enriettii*. *PLoS Negl. Trop. Dis.* **9**, e0004060 (2015).
12. Killick-Kendrick, R. Phlebotomine vectors of the leishmaniasis: a review. *Med. Vet. Entomol.* **4**, 1–24 (1990).
13. Seblova, V., Sadlova, J., Carpenter, S. & Volf, P. Speculations on biting midges and other bloodsucking arthropods as alternative vectors of *Leishmania*. *Parasit. Vectors* **7**, 222 (2014).

14. Antoine, J. C., Prina, E., Lang, T. & Courret, N. The biogenesis and properties of the parasitophorous vacuoles that harbour *Leishmania* in murine macrophages. *Trends Microbiol.* **6**, 392–401 (1998).
15. Leifso, K., Cohen-Freue, G., Dogra, N., Murray, A. & McMaster, W. R. Genomic and proteomic expression analysis of *Leishmania* promastigote and amastigote life stages: the *Leishmania* genome is constitutively expressed. *Mol Biochem Parasitol* **152**, 35–46 (2007).
16. Leprohon, P. *et al.* Gene expression modulation is associated with gene amplification, supernumerary chromosomes and chromosome loss in antimony-resistant *Leishmania infantum*. *Nucleic Acids Res* **37**, 1387–1399 (2009).
17. Rogers, M. B. *et al.* Chromosome and gene copy number variation allow major structural change between species and strains of *Leishmania*. *Genome Res* **21**, 2129–2142 (2011).
18. Engwerda, C. R., Ato, M. & Kaye, P. M. Macrophages, pathology and parasite persistence in experimental visceral leishmaniasis. *Trends Parasitol.* **20**, 524–30 (2004).
19. Cotterell, S. E., Engwerda, C. R. & Kaye, P. M. *Leishmania donovani* infection of bone marrow stromal macrophages selectively enhances myelopoiesis, by a mechanism involving GM-CSF and TNF- α . *Blood* **95**, 1642–1651 (2000).
20. Ng, L. G. *et al.* Migratory dermal dendritic cells act as rapid sensors of protozoan parasites. *PLoS Pathog* **4**, e1000222 (2008).
21. León, B., López-Bravo, M. & Ardavín, C. Monocyte-derived dendritic cells formed at the infection site control the induction of protective T helper 1 responses against *Leishmania*. *Immunity* **26**, 519–31 (2007).
22. Hurrell, B. P. *et al.* Rapid Sequestration of *Leishmania mexicana* by Neutrophils Contributes to the Development of Chronic Lesion. *PLoS Pathog.* **11**, e1004929 (2015).
23. Thalhofer, C. J., Chen, Y., Sudan, B., Love-Homan, L. & Wilson, M. E. Leukocytes infiltrate the skin and draining lymph nodes in response to the protozoan *Leishmania infantum chagasi*. *Infect. Immun.* **79**, 108–17 (2011).
24. Peters, N. C. *et al.* In vivo imaging reveals an essential role for neutrophils in leishmaniasis transmitted by sand flies. *Science* **321**, 970–4 (2008).

25. Laskay, T., van, Z. G. & Solbach, W. Neutrophil granulocytes--Trojan horses for *Leishmania major* and other intracellular microbes? *Trends Microbiol.* **11**, 210–214 (2003).
26. Ravichandran, K. S. & Lorenz, U. Engulfment of apoptotic cells: signals for a good meal. *Nat. Rev. Immunol.* **7**, 964–74 (2007).
27. Fadok, V. A. *et al.* Macrophages that have ingested apoptotic cells in vitro inhibit proinflammatory cytokine production through autocrine/paracrine mechanisms involving TGF-beta, PGE2, and PAF. *J. Clin. Invest.* **101**, 890–8 (1998).
28. Voll, R. E. *et al.* Immunosuppressive effects of apoptotic cells. *Nature* **390**, 350–1 (1997).
29. Ribeiro-Gomes, F. L., Peters, N. C., Debrabant, A. & Sacks, D. L. Efficient capture of infected neutrophils by dendritic cells in the skin inhibits the early anti-leishmania response. *PLoS Pathog.* **8**, e1002536 (2012).
30. Bogdan, C. *et al.* Fibroblasts as host cells in latent leishmaniasis. *J. Exp. Med.* **191**, 2121–2130 (2000).
31. Svensson, M., Maroof, A., Ato, M. & Kaye, P. M. Stromal cells direct local differentiation of regulatory dendritic cells. *Immunity.* **21**, 805–816 (2004).
32. Kaye, P. M. *et al.* The immunopathology of experimental visceral leishmaniasis. *Immunol. Rev.* **201**, 239–253 (2004).
33. Nguyen Hoang, A. T. *et al.* Stromal cell-derived CXCL12 and CCL8 cooperate to support increased development of regulatory dendritic cells following *Leishmania* infection. *J. Immunol.* **185**, 2360–2371 (2010).
34. Flannagan, R. S., Cosío, G. & Grinstein, S. Antimicrobial mechanisms of phagocytes and bacterial evasion strategies. *Nat. Rev. Microbiol.* **7**, 355–66 (2009).
35. Chang, K. P. & Dwyer, D. M. Multiplication of a human parasite (*Leishmania donovani*) in phagolysosomes of hamster macrophages in vitro. *Science (80-.).* **193**, 678–680 (1976).
36. Chang, K. P. & Dwyer, D. M. *Leishmania donovani*. Hamster macrophage interactions in vitro: cell entry, intracellular survival, and multiplication of amastigotes. *J. Exp. Med.* **147**, 515–30 (1978).
37. Moradin, N. & Descoteaux, A. *Leishmania* promastigotes: building a safe niche within macrophages. *Front. Cell. Infect. Microbiol.* **2**, 121 (2012).

38. Matheoud, D. *et al.* Leishmania evades host immunity by inhibiting antigen cross-presentation through direct cleavage of the SNARE VAMP8. *Cell Host Microbe* **14**, 15–25 (2013).
39. Arango Duque, G. & Descoteaux, A. Leishmania survival in the macrophage: where the ends justify the means. *Curr. Opin. Microbiol.* **26**, 32–40 (2015).
40. Mukkada, A. J., Meade, J. C., Glaser, T. A. & Bonventre, P. F. Enhanced metabolism of Leishmania donovani amastigotes at acid pH: an adaptation for intracellular growth. *Science* **229**, 1099–101 (1985).
41. Pham, N.-K., Mouriz, J. & Kima, P. E. Leishmania pifanoi amastigotes avoid macrophage production of superoxide by inducing heme degradation. *Infect. Immun.* **73**, 8322–33 (2005).
42. Lodge, R. & Descoteaux, A. Phagocytosis of Leishmania donovani amastigotes is Rac1 dependent and occurs in the absence of NADPH oxidase activation. *Eur. J. Immunol.* **36**, 2735–44 (2006).
43. Stern, J. J., Oca, M. J., Rubin, B. Y., Anderson, S. L. & Murray, H. W. Role of L3T4+ and LyT-2+ cells in experimental visceral leishmaniasis. *J. Immunol.* **140**, 3971–7 (1988).
44. Ghalib, H. W. *et al.* IL-12 enhances Th1-type responses in human Leishmania donovani infections. *J. Immunol.* **154**, 4623–9 (1995).
45. Kushawaha, P. K., Gupta, R., Sundar, S., Sahasrabudhe, A. A. & Dube, A. Elongation factor-2, a Th1 stimulatory protein of Leishmania donovani, generates strong IFN- γ and IL-12 response in cured Leishmania-infected patients/hamsters and protects hamsters against Leishmania challenge. *J. Immunol.* **187**, 6417–27 (2011).
46. Sundar, S., Reed, S. G., Sharma, S., Mehrotra, A. & Murray, H. W. Circulating T helper 1 (Th1) cell- and Th2 cell-associated cytokines in Indian patients with visceral leishmaniasis. *Am. J. Trop. Med. Hyg.* **56**, 522–5 (1997).
47. Karp, C. L. *et al.* In vivo cytokine profiles in patients with kala-azar. Marked elevation of both interleukin-10 and interferon-gamma. *J. Clin. Invest.* **91**, 1644–8 (1993).
48. Melby, P. C., Chandrasekar, B., Zhao, W. & Coe, J. E. The Hamster as a Model of Human Visceral Leishmaniasis: Progressive Disease and Impaired Generation of Nitric Oxide in the Face of a Prominent Th1-Like Cytokine Response. *J. Immunol.*

- 166**, 1912–1920 (2001).
49. Nylén, S. & Sacks, D. Interleukin-10 and the pathogenesis of human visceral leishmaniasis. *Trends Immunol.* **28**, 378–84 (2007).
 50. Kumar, R. & Nylen, S. Immunobiology of visceral leishmaniasis. *Front Immunol.* **3**, 251 (2012).
 51. Sacks, D. L., Lal, S. L., Shrivastava, S. N., Blackwell, J. & Neva, F. A. An analysis of T cell responsiveness in Indian kala-azar. *J. Immunol.* **138**, 908–13 (1987).
 52. White, A. C., Castes, M., Garcia, L., Trujillo, D. & Zambrano, L. Leishmania chagasi antigens recognized in cured visceral leishmaniasis and asymptomatic infection. *Am. J. Trop. Med. Hyg.* **46**, 123–31 (1992).
 53. Gautam, S. *et al.* CD8 T cell exhaustion in human visceral leishmaniasis. *J. Infect. Dis.* **209**, 290–9 (2014).
 54. Murphy, M. L., Cotterell, S. E., Gorak, P. M., Engwerda, C. R. & Kaye, P. M. Blockade of CTLA-4 enhances host resistance to the intracellular pathogen, *Leishmania donovani*. *J. Immunol.* **161**, 4153–60 (1998).
 55. Zubairi, S., Sanos, S. L., Hill, S. & Kaye, P. M. Immunotherapy with OX40L-Fc or anti-CTLA-4 enhances local tissue responses and killing of *Leishmania donovani*. *Eur. J. Immunol.* **34**, 1433–40 (2004).
 56. Gurung, P. *et al.* An NLRP3 inflammasome-triggered Th2-biased adaptive immune response promotes leishmaniasis. *J. Clin. Invest.* **125**, 1329–38 (2015).
 57. Smelt, S. C., Cotterell, S. E. J., Engwerda, C. R. & Kaye, P. M. B Cell-Deficient Mice Are Highly Resistant to *Leishmania donovani* Infection, but Develop Neutrophil-Mediated Tissue Pathology. *J. Immunol.* **164**, 3681–3688 (2000).
 58. Moore, E. M. & Lockwood, D. N. Treatment of visceral leishmaniasis. *J. Glob. Infect. Dis.* **2**, 151–8 (2010).
 59. Sundar, S. & Chakravarty, J. Liposomal amphotericin B and leishmaniasis: dose and response. *J. Glob. Infect. Dis.* **2**, 159–66 (2010).
 60. Croft, S. L., Neal, R. A., Pendergast, W. & Chan, J. H. The activity of alkyl phosphorylcholines and related derivatives against *Leishmania donovani*. *Biochem. Pharmacol.* **36**, 2633–6 (1987).
 61. Dorlo, T. P. C., Balasegaram, M., Beijnen, J. H. & de Vries, P. J. Miltefosine: a review of its pharmacology and therapeutic efficacy in the treatment of

- leishmaniasis. *J. Antimicrob. Chemother.* **67**, 2576–97 (2012).
62. Cartwright, G. E., Chung, H. L. & Chang, A. Studies on the pancytopenia of kala-azar. *Blood* **3**, 249–75 (1948).
 63. Alexandropoulou, O., Tsolia, M., Kossiva, L., Giannaki, M. & Karavanaki, K. Visceral leishmaniasis: a common cause of post-infectious febrile pancytopenia in children in an endemic area: experience of a children's tertiary hospital. *Pediatr. Emerg. Care* **28**, 533–7 (2012).
 64. Chouchene, S. *et al.* [Hematologic abnormalities in infantile visceral leishmaniasis]. *Arch. pédiatrie organe Off. la Société Fr. pédiatrie* **22**, 1107–11 (2015).
 65. Besada, E., Njålla, R. J. & Nossent, J. C. Imported case of visceral leishmaniasis presenting as pancytopenia in a Norwegian patient treated with methotrexate and etanercept for psoriasis arthritis. *Rheumatol. Int.* **33**, 2687–9 (2013).
 66. Bafghi, A. F., Shahcheraghi, S. H. & Nematollahi, S. Comparison of hematological aspects: Visceral leishmaniasis and healthy children. *Trop. Parasitol.* **5**, 133–5 (2015).
 67. Biswas, T., Chakraborty, M., Naskar, K., Ghosh, D. K. & Ghosal, J. Anemia in experimental visceral leishmaniasis in hamsters. *J. Parasitol.* **78**, 140–2 (1992).
 68. Lafuse, W. P. *et al.* *Leishmania donovani* infection induces anemia in hamsters by differentially altering erythropoiesis in bone marrow and spleen. *PLoS One* **8**, e59509 (2013).
 69. Foglia Manzillo, V., Restucci, B., Pagano, A., Gradoni, L. & Oliva, G. Pathological changes in the bone marrow of dogs with leishmaniosis. *Vet. Rec.* **158**, 690–4 (2006).
 70. Momo, C. *et al.* Morphological changes in the bone marrow of the dogs with visceral leishmaniasis. *Vet. Med. Int.* **2014**, 150582 (2014).
 71. De Tommasi, A. S. *et al.* Evaluation of blood and bone marrow in selected canine vector-borne diseases. *Parasit. Vectors* **7**, 534 (2014).
 72. Marcos, R. *et al.* Pancytopenia in a cat with visceral leishmaniasis. *Vet. Clin. Pathol.* **38**, 201–5 (2009).
 73. al-Jurayyan, N. A. *et al.* The haematological manifestations of visceral leishmaniasis in infancy and childhood. *J. Trop. Pediatr.* **41**, 143–8 (1995).
 74. Marwaha, N., Sarode, R., Gupta, R. K., Garewal, G. & Dash, S. Clinico-

- hematological characteristics in patients with kala azar. A study from north-west India. *Trop. Geogr. Med.* **43**, 357–62 (1991).
75. de Araújo, V. E. M., Morais, M. H. F., Reis, I. A., Rabello, A. & Carneiro, M. Early clinical manifestations associated with death from visceral leishmaniasis. *PLoS Negl. Trop. Dis.* **6**, e1511 (2012).
 76. Madalosso, G. *et al.* American Visceral Leishmaniasis: Factors Associated with Lethality in the State of São Paulo, Brazil. *J. Trop. Med.* **2012**, 1–7 (2012).
 77. Coura-Vital, W. *et al.* Prognostic Factors and Scoring System for Death from Visceral Leishmaniasis: An Historical Cohort Study in Brazil. *PLoS Negl. Trop. Dis.* **8**, e3374 (2014).
 78. Belo, V. S. *et al.* Risk Factors for Adverse Prognosis and Death in American Visceral Leishmaniasis: A Meta-analysis. *PLoS Negl. Trop. Dis.* **8**, e2982 (2014).
 79. Collin, S. *et al.* Conflict and kala-azar: determinants of adverse outcomes of kala-azar among patients in southern Sudan. *Clin. Infect. Dis.* **38**, 612–9 (2004).
 80. Seaman, J., Mercer, A. J., Sondorp, H. E. & Herwaldt, B. L. Epidemic visceral leishmaniasis in southern Sudan: treatment of severely debilitated patients under wartime conditions and with limited resources. *Ann. Intern. Med.* **124**, 664–72 (1996).
 81. Woodruff, A. W., Topley, E., Knight, R. & Downie, C. G. The anaemia of kala-azar. *Br. J. Haematol.* **22**, 319–29 (1972).
 82. Dotis, J. *et al.* Immune haemolytic anaemia due to visceral leishmaniasis in a young child. *Eur. J. Pediatr.* **162**, 49–50 (2003).
 83. Kokkini, G., Vrionis, G., Liosis, G. & Papaefstathiou, J. Cold agglutinin syndrome and hemophagocytosis in systemic leishmaniasis. *Scand. J. Haematol.* **32**, 441–445 (1984).
 84. Gagnaire, M. H., Galambrun, C. & Stéphan, J. L. Hemophagocytic syndrome: A misleading complication of visceral leishmaniasis in children--a series of 12 cases. *Pediatrics* **106**, E58 (2000).
 85. Bain, B. J. Dyserythropoiesis in visceral leishmaniasis. *Am. J. Hematol.* **85**, 781 (2010).
 86. Cotterell, S. E., Engwerda, C. R. & Kaye, P. M. Enhanced hematopoietic activity accompanies parasite expansion in the spleen and bone marrow of mice infected

- with *Leishmania donovani*. *Infect. Immun.* **68**, 1840–8 (2000).
87. Aslinia, F., Mazza, J. J. & Yale, S. H. Megaloblastic anemia and other causes of macrocytosis. *Clin. Med. Res.* **4**, 236–41 (2006).
 88. Lopez, A., Cacoub, P., Macdougall, I. C. & Peyrin-Biroulet, L. Iron deficiency anaemia. *Lancet (London, England)* (2015). doi:10.1016/S0140-6736(15)60865-0
 89. Weiss, G. & Goodnough, L. T. Anemia of chronic disease. *N. Engl. J. Med.* **352**, 1011–23 (2005).
 90. Gomes, A. C. & Gomes, M. S. Hematopoietic niches, erythropoiesis and anemia of chronic infection. *Exp. Hematol.* **44**, 85–91 (2016).
 91. Hom, J., Dulmovits, B. M., Mohandas, N. & Blanc, L. The erythroblastic island as an emerging paradigm in the anemia of inflammation. *Immunol. Res.* **63**, 75–89 (2015).
 92. Ghosh, K. & Ghosh, K. Pathogenesis of anemia in malaria: a concise review. *Parasitol. Res.* **101**, 1463–9 (2007).
 93. Sinha, A. K., Rijal, S., Karki, P. & Majhi, S. Incidence of megaloblastic anaemia and its correction in leishmaniasis--a prospective study at BPKIHS hospital, Nepal. *Indian J. Pathol. Microbiol.* **49**, 528–31 (2006).
 94. Flannery, A. R., Renberg, R. L. & Andrews, N. W. Pathways of iron acquisition and utilization in *Leishmania*. *Curr. Opin. Microbiol.* **16**, 716–21 (2013).
 95. Thakur, A. K. *et al.* Degree of anemia correlates with increased utilization of heme by *Leishmania donovani* parasites in visceral leishmaniasis. *Exp. Parasitol.* 8–11 (2013). doi:10.1016/j.exppara.2013.09.008
 96. Cortese, L. *et al.* Secondary immune-mediated thrombocytopenia in dogs naturally infected by *Leishmania infantum*. *Vet. Rec.* **164**, 778–782 (2009).
 97. Aster, R. H. Pooling of platelets in the spleen: role in the pathogenesis of ‘hypersplenic’ thrombocytopenia. *J. Clin. Invest.* **45**, 645–57 (1966).
 98. Boelaert, M. *et al.* Evaluation of rapid diagnostic tests: visceral leishmaniasis. *Nat. Rev. Microbiol.* **5**, S30–S39 (2007).
 99. Tajbakhsh, S. Stem cell: what’s in a name? *Nat. Reports Stem Cells* (2009). doi:10.1038/stemcells.2009.90
 100. Kondo, M., Weissman, I. L. & Akashi, K. Identification of clonogenic common

- lymphoid progenitors in mouse bone marrow. *Cell* **91**, 661–72 (1997).
101. Akashi, K., Traver, D., Miyamoto, T. & Weissman, I. L. A clonogenic common myeloid progenitor that gives rise to all myeloid lineages. *Nature* **404**, 193–7 (2000).
 102. Arinobu, Y. *et al.* Reciprocal activation of GATA-1 and PU.1 marks initial specification of hematopoietic stem cells into myeloerythroid and myelolymphoid lineages. *Cell Stem Cell* **1**, 416–27 (2007).
 103. Ardavin, C., Wu, L., Li, C. L. & Shortman, K. Thymic dendritic cells and T cells develop simultaneously in the thymus from a common precursor population. *Nature* **362**, 761–3 (1993).
 104. Wada, H. *et al.* Adult T-cell progenitors retain myeloid potential. *Nature* **452**, 768–772 (2008).
 105. Bell, J. J. & Bhandoola, A. The earliest thymic progenitors for T cells possess myeloid lineage potential. *Nature* **452**, 764–7 (2008).
 106. Adolfsson, J. *et al.* Identification of Flt3+ lympho-myeloid stem cells lacking erythro-megakaryocytic potential a revised road map for adult blood lineage commitment. *Cell* **121**, 295–306 (2005).
 107. Ceredig, R., Rolink, A. G. & Brown, G. Models of haematopoiesis: seeing the wood for the trees. *Nat. Rev. Immunol.* **9**, 293–300 (2009).
 108. Robb, L. Cytokine receptors and hematopoietic differentiation. *Oncogene* **26**, 6715–23 (2007).
 109. Till, J. E. & McCulloch, E. A. A direct measurement of the radiation sensitivity of normal mouse bone marrow cells. *Radiat. Res.* **14**, 213–22 (1961).
 110. Wu, A. M., Till, J. E., Siminovitch, L. & McCulloch, E. A. Cytological evidence for a relationship between normal hemotopoietic colony-forming cells and cells of the lymphoid system. *J. Exp. Med.* **127**, 455–64 (1968).
 111. Dick, J. E., Magli, M. C., Huszar, D., Phillips, R. A. & Bernstein, A. Introduction of a selectable gene into primitive stem cells capable of long-term reconstitution of the hemopoietic system of W/W^v mice. *Cell* **42**, 71–9 (1985).
 112. Lemischka, I. R., Raulet, D. H. & Mulligan, R. C. Developmental potential and dynamic behavior of hematopoietic stem cells. *Cell* **45**, 917–27 (1986).
 113. Smith, L. G., Weissman, I. L. & Heimfeld, S. Clonal analysis of hematopoietic

- stem-cell differentiation in vivo. *Proc. Natl. Acad. Sci. U. S. A.* **88**, 2788–92 (1991).
114. Morita, Y., Ema, H. & Nakauchi, H. Heterogeneity and hierarchy within the most primitive hematopoietic stem cell compartment. *J. Exp. Med.* **207**, 1173–82 (2010).
 115. Morrison, S. J. & Weissman, I. L. The long-term repopulating subset of hematopoietic stem cells is deterministic and isolatable by phenotype. *Immunity* **1**, 661–73 (1994).
 116. Spangrude, G., Heimfeld, S. & Weissman, I. Purification and characterization of mouse hematopoietic stem cells. *Science (80-.)*. **241**, 58–62 (1988).
 117. Kiel, M. J. *et al.* SLAM family receptors distinguish hematopoietic stem and progenitor cells and reveal endothelial niches for stem cells. *Cell* **121**, 1109–21 (2005).
 118. Sieburg, H. B. *et al.* The hematopoietic stem compartment consists of a limited number of discrete stem cell subsets. *Blood* **107**, 2311–6 (2006).
 119. Dykstra, B. *et al.* Long-term propagation of distinct hematopoietic differentiation programs in vivo. *Cell Stem Cell* **1**, 218–29 (2007).
 120. Challen, G. A., Boles, N. C., Chambers, S. M. & Goodell, M. A. Distinct hematopoietic stem cell subtypes are differentially regulated by TGF-beta1. *Cell Stem Cell* **6**, 265–78 (2010).
 121. Cheshier, S. H., Morrison, S. J., Liao, X. & Weissman, I. L. In vivo proliferation and cell cycle kinetics of long-term self-renewing hematopoietic stem cells. *Proc. Natl. Acad. Sci.* **96**, 3120–3125 (1999).
 122. Cheng, T. *et al.* Hematopoietic stem cell quiescence maintained by p21cip1/waf1. *Science* **287**, 1804–8 (2000).
 123. Orford, K. W. & Scadden, D. T. Deconstructing stem cell self-renewal: genetic insights into cell-cycle regulation. *Nat. Rev. Genet.* **9**, 115–28 (2008).
 124. Wilson, A. *et al.* Hematopoietic stem cells reversibly switch from dormancy to self-renewal during homeostasis and repair. *Cell* **135**, 1118–29 (2008).
 125. Sims, N. A. & Martin, T. J. Coupling the activities of bone formation and resorption: a multitude of signals within the basic multicellular unit. *Bonekey Rep.* **3**, 481 (2014).
 126. Nombela-Arrieta, C. *et al.* Quantitative imaging of haematopoietic stem and progenitor cell localization and hypoxic status in the bone marrow

- microenvironment. *Nat Cell Biol* **15**, 533–543 (2013).
127. Morrison, S. J. & Scadden, D. T. The bone marrow niche for haematopoietic stem cells. *Nature* **505**, 327–34 (2014).
 128. Ding, L., Saunders, T. L., Enikolopov, G. & Morrison, S. J. Endothelial and perivascular cells maintain haematopoietic stem cells. *Nature* **481**, 457–62 (2012).
 129. Méndez-Ferrer, S. *et al.* Mesenchymal and haematopoietic stem cells form a unique bone marrow niche. *Nature* **466**, 829–34 (2010).
 130. Omatsu, Y. *et al.* The Essential Functions of Adipo-osteogenic Progenitors as the Hematopoietic Stem and Progenitor Cell Niche. *Immunity* **33**, 387–399 (2010).
 131. Siminovitch, L., Till, J. E. & McCulloch, E. A. Decline in colony-forming ability of marrow cells subjected to serial transplantation into irradiated mice. *J. Cell. Comp. Physiol.* **64**, 23–31 (1964).
 132. Schofield, R. The relationship between the spleen colony-forming cell and the haemopoietic stem cell. *Blood Cells* **4**, 7–25 (1978).
 133. Dexter, T. M., Allen, T. D. & Lajtha, L. G. Conditions controlling the proliferation of haemopoietic stem cells in vitro. *J. Cell. Physiol.* **91**, 335–44 (1977).
 134. Katayama, Y. *et al.* Signals from the sympathetic nervous system regulate hematopoietic stem cell egress from bone marrow. *Cell* **124**, 407–21 (2006).
 135. Huang, E. *et al.* The hematopoietic growth factor KL is encoded by the Sl locus and is the ligand of the c-kit receptor, the gene product of the W locus. *Cell* **63**, 225–33 (1990).
 136. Zsebo, K. M. *et al.* Stem cell factor is encoded at the Sl locus of the mouse and is the ligand for the c-kit tyrosine kinase receptor. *Cell* **63**, 213–224 (1990).
 137. Geissler, E. N., Ryan, M. A. & Housman, D. E. The dominant-white spotting (W) locus of the mouse encodes the c-kit proto-oncogene. *Cell* **55**, 185–92 (1988).
 138. McCulloch, E. A., Siminovitch, L. & Till, J. E. Spleen-Colony Formation in Anemic Mice of Genotype WW. *Science (80-.)*. **144**, 844–846 (1964).
 139. McCulloch, E. A., Siminovitch, L., Till, J. E., Russell, E. S. & Bernstein, S. E. The cellular basis of the genetically determined hemopoietic defect in anemic mice of genotype Sl-Sld. *Blood* **26**, 399–410 (1965).
 140. Kent, D. *et al.* Regulation of hematopoietic stem cells by the steel factor/KIT

- signaling pathway. *Clin. Cancer Res.* **14**, 1926–30 (2008).
141. Weiler, S. R. *et al.* JAK2 is associated with the c-kit proto-oncogene product and is phosphorylated in response to stem cell factor. *Blood* **87**, 3688–93 (1996).
 142. Levine, R. L., Pardanani, A., Tefferi, A. & Gilliland, D. G. Role of JAK2 in the pathogenesis and therapy of myeloproliferative disorders. *Nat. Rev. Cancer* **7**, 673–83 (2007).
 143. Aiuti, A. The Chemokine SDF-1 Is a Chemoattractant for Human CD34+ Hematopoietic Progenitor Cells and Provides a New Mechanism to Explain the Mobilization of CD34+ Progenitors to Peripheral Blood. *J. Exp. Med.* **185**, 111–120 (1997).
 144. Sugiyama, T., Kohara, H., Noda, M. & Nagasawa, T. Maintenance of the hematopoietic stem cell pool by CXCL12-CXCR4 chemokine signaling in bone marrow stromal cell niches. *Immunity.* **25**, 977–988 (2006).
 145. Frenette, P. S., Pinho, S., Lucas, D. & Scheiermann, C. Mesenchymal stem cell: keystone of the hematopoietic stem cell niche and a stepping-stone for regenerative medicine. *Annu Rev Immunol* **31**, 285–316 (2013).
 146. Greenbaum, A. *et al.* CXCL12 in early mesenchymal progenitors is required for haematopoietic stem-cell maintenance. *Nature* **495**, 227–30 (2013).
 147. Chow, A. *et al.* Bone marrow CD169+ macrophages promote the retention of hematopoietic stem and progenitor cells in the mesenchymal stem cell niche. *J Exp Med* **208**, 261–271 (2011).
 148. Casanova-Acebes, M. *et al.* Rhythmic modulation of the hematopoietic niche through neutrophil clearance. *Cell* **153**, 1025–35 (2013).
 149. Debili, N. *et al.* Characterization of a bipotent erythro-megakaryocytic progenitor in human bone marrow. *Blood* **88**, 1284–96 (1996).
 150. Sanjuan-Pla, A. *et al.* Platelet-biased stem cells reside at the apex of the haematopoietic stem-cell hierarchy. *Nature* **502**, 232–6 (2013).
 151. Yamamoto, R. *et al.* Clonal analysis unveils self-renewing lineage-restricted progenitors generated directly from hematopoietic stem cells. *Cell* **154**, 1112–26 (2013).
 152. Heath, D. S., Axelrad, A. A., McLeod, D. L. & Shreeve, M. M. Separation of the erythropoietin-responsive progenitors BFU-E and CFU-E in mouse bone marrow by

- unit gravity sedimentation. *Blood* **47**, 777–92 (1976).
153. Clarke, B. J. & Housman, D. Characterization of an erythroid precursor cell of high proliferative capacity in normal human peripheral blood. *Proc. Natl. Acad. Sci. U. S. A.* **74**, 1105–9 (1977).
 154. Stumpf, M. *et al.* The mediator complex functions as a coactivator for GATA-1 in erythropoiesis via subunit Med1/TRAP220. *Proc. Natl. Acad. Sci. U. S. A.* **103**, 18504–9 (2006).
 155. Terszowski, G. *et al.* Prospective isolation and global gene expression analysis of the erythrocyte colony-forming unit (CFU-E). *Blood* **105**, 1937–45 (2005).
 156. Flygare, J., Rayon Estrada, V., Shin, C., Gupta, S. & Lodish, H. F. HIF1alpha synergizes with glucocorticoids to promote BFU-E progenitor self-renewal. *Blood* **117**, 3435–44 (2011).
 157. Chen, K. *et al.* Resolving the distinct stages in erythroid differentiation based on dynamic changes in membrane protein expression during erythropoiesis. *Proc. Natl. Acad. Sci. U. S. A.* **106**, 17413–8 (2009).
 158. Jelkmann, W. & Wiedemann, G. Serum erythropoietin level: relationships to blood hemoglobin concentration and erythrocytic activity of the bone marrow. *Klin. Wochenschr.* **68**, 403–7 (1990).
 159. Grover, A. *et al.* Erythropoietin guides multipotent hematopoietic progenitor cells toward an erythroid fate. *J. Exp. Med.* **211**, 181–8 (2014).
 160. Wu, H., Liu, X., Jaenisch, R. & Lodish, H. F. Generation of committed erythroid BFU-E and CFU-E progenitors does not require erythropoietin or the erythropoietin receptor. *Cell* **83**, 59–67 (1995).
 161. Koury, M. J. & Bondurant, M. C. Erythropoietin retards DNA breakdown and prevents programmed death in erythroid progenitor cells. *Science* **248**, 378–81 (1990).
 162. Zhao, W., Kitidis, C., Fleming, M. D., Lodish, H. F. & Ghaffari, S. Erythropoietin stimulates phosphorylation and activation of GATA-1 via the PI3-kinase/AKT signaling pathway. *Blood* **107**, 907–15 (2006).
 163. Nocka, K. *et al.* Expression of c-kit gene products in known cellular targets of W mutations in normal and W mutant mice--evidence for an impaired c-kit kinase in mutant mice. *Genes Dev.* **3**, 816–26 (1989).

164. von Lindern, M., Schmidt, U. & Beug, H. Control of erythropoiesis by erythropoietin and stem cell factor: a novel role for Bruton's tyrosine kinase. *Cell Cycle* **3**, 876–9 (2004).
165. Munugalavada, V. & Kapur, R. Role of c-Kit and erythropoietin receptor in erythropoiesis. *Crit. Rev. Oncol. Hematol.* **54**, 63–75 (2005).
166. Uoshima, N. *et al.* Changes in c-Kit expression and effects of SCF during differentiation of human erythroid progenitor cells. *Br. J. Haematol.* **91**, 30–6 (1995).
167. BESSIS, M. [Erythroblastic island, functional unity of bone marrow]. *Rev. d'hématologie* **13**, 8–11 (1958).
168. Chasis, J. A. & Mohandas, N. Erythroblastic islands: niches for erythropoiesis. *Blood* **112**, 470–8 (2008).
169. Chow, A. *et al.* CD169(+) macrophages provide a niche promoting erythropoiesis under homeostasis and stress. *Nat Med* **19**, 429–436 (2013).
170. Dzierzak, E. & Philipsen, S. Erythropoiesis: development and differentiation. *Cold Spring Harb. Perspect. Med.* **3**, a011601 (2013).
171. Hanspal, M., Smockova, Y. & Uong, Q. Molecular identification and functional characterization of a novel protein that mediates the attachment of erythroblasts to macrophages. *Blood* **92**, 2940–50 (1998).
172. Sadahira, Y., Yoshino, T. & Monobe, Y. Very late activation antigen 4-vascular cell adhesion molecule 1 interaction is involved in the formation of erythroblastic islands. *J. Exp. Med.* **181**, 411–5 (1995).
173. Lee, G. *et al.* Targeted gene deletion demonstrates that the cell adhesion molecule ICAM-4 is critical for erythroblastic island formation. *Blood* **108**, 2064–71 (2006).
174. Skutelsky, E. & Danon, D. On the expulsion of the erythroid nucleus and its phagocytosis. *Anat. Rec.* **173**, 123–6 (1972).
175. Soni, S. *et al.* Absence of erythroblast macrophage protein (Emp) leads to failure of erythroblast nuclear extrusion. *J. Biol. Chem.* **281**, 20181–9 (2006).
176. Lee, S. H. *et al.* Isolation and immunocytochemical characterization of human bone marrow stromal macrophages in hemopoietic clusters. *J. Exp. Med.* **168**, 1193–8 (1988).
177. Crocker, P. R. & Gordon, S. Mouse macrophage hemagglutinin (sheep erythrocyte

- receptor) with specificity for sialylated glycoconjugates characterized by a monoclonal antibody. *J Exp Med* **169**, 1333–1346 (1989).
178. Rhodes, M. M., Kopsombut, P., Bondurant, M. C., Price, J. O. & Koury, M. J. Adherence to macrophages in erythroblastic islands enhances erythroblast proliferation and increases erythrocyte production by a different mechanism than erythropoietin. *Blood* **111**, 1700–1708 (2008).
 179. Laurell, C. & Ingelman, B. The iron-binding protein of swine serum. *Acta Chem. Scand.* **1**, 770–776 (1947).
 180. Aisen, P. Transferrin receptor 1. *Int. J. Biochem. Cell Biol.* **36**, 2137–43 (2004).
 181. Jandl, J. H., Inman, J. K., Simmons, R. L. & Allen, D. W. Transfer of iron from serum iron-binding protein to human reticulocytes. *J. Clin. Invest.* **38**, 161–85 (1959).
 182. Conner, S. D. & Schmid, S. L. Differential requirements for AP-2 in clathrin-mediated endocytosis. *J. Cell Biol.* **162**, 773–9 (2003).
 183. Fleming, M. D. *et al.* Nramp2 is mutated in the anemic Belgrade (b) rat: evidence of a role for Nramp2 in endosomal iron transport. *Proc. Natl. Acad. Sci. U. S. A.* **95**, 1148–53 (1998).
 184. Pigeon, C. *et al.* A new mouse liver-specific gene, encoding a protein homologous to human antimicrobial peptide hepcidin, is overexpressed during iron overload. *J. Biol. Chem.* **276**, 7811–9 (2001).
 185. Nemeth, E. *et al.* Hepcidin regulates cellular iron efflux by binding to ferroportin and inducing its internalization. *Science* **306**, 2090–3 (2004).
 186. Donovan, A. *et al.* The iron exporter ferroportin/Slc40a1 is essential for iron homeostasis. *Cell Metab.* **1**, 191–200 (2005).
 187. Nicolas, G. *et al.* Severe iron deficiency anemia in transgenic mice expressing liver hepcidin. *Proc. Natl. Acad. Sci. U. S. A.* **99**, 4596–601 (2002).
 188. Nicolas, G. *et al.* The gene encoding the iron regulatory peptide hepcidin is regulated by anemia, hypoxia, and inflammation. *J. Clin. Invest.* **110**, 1037–44 (2002).
 189. Junt, T. *et al.* Dynamic visualization of thrombopoiesis within bone marrow. *Science* **317**, 1767–70 (2007).
 190. Thon, J. N. & Italiano, J. E. Platelet formation. *Semin. Hematol.* **47**, 220–6 (2010).

191. Nieswandt, B. & Watson, S. P. Platelet-collagen interaction: is GPVI the central receptor? *Blood* **102**, 449–61 (2003).
192. Adams, R. L. C. & Bird, R. J. Review article: Coagulation cascade and therapeutics update: relevance to nephrology. Part 1: Overview of coagulation, thrombophilias and history of anticoagulants. *Nephrology (Carlton)*. **14**, 462–70 (2009).
193. Versteeg, H. H., Heemskerk, J. W. M., Levi, M. & Reitsma, P. H. New fundamentals in hemostasis. *Physiol. Rev.* **93**, 327–58 (2013).
194. Kuter, D. J. The Physiology of Platelet Production. *Stem Cells* **14**, 88–101 (1996).
195. Kaushansky, K. Thrombopoietin: the primary regulator of platelet production. *Blood* **86**, 419–31 (1995).
196. Kaushansky, K. *et al.* Promotion of megakaryocyte progenitor expansion and differentiation by the c-Mpl ligand thrombopoietin. *Nature* **369**, 568–71 (1994).
197. Sungaran, R., Markovic, B. & Chong, B. H. Localization and regulation of thrombopoietin mRNA expression in human kidney, liver, bone marrow, and spleen using in situ hybridization. *Blood* **89**, 101–7 (1997).
198. Kosugi, S. *et al.* Circulating thrombopoietin level in chronic immune thrombocytopenic purpura. *Br. J. Haematol.* **93**, 704–6 (1996).
199. Sørensen, A. L. *et al.* Role of sialic acid for platelet life span: exposure of beta-galactose results in the rapid clearance of platelets from the circulation by asialoglycoprotein receptor-expressing liver macrophages and hepatocytes. *Blood* **114**, 1645–54 (2009).
200. Grozovsky, R. *et al.* The Ashwell-Morell receptor regulates hepatic thrombopoietin production via JAK2-STAT3 signaling. *Nat. Med.* **21**, 47–54 (2015).
201. Maier, A. G., Cooke, B. M., Cowman, A. F. & Tilley, L. Malaria parasite proteins that remodel the host erythrocyte. *Nat. Rev. Microbiol.* **7**, 341–354 (2009).
202. Deitsch, K. W. & Wellem, T. E. Membrane modifications in erythrocytes parasitized by *Plasmodium falciparum*. *Mol. Biochem. Parasitol.* **76**, 1–10 (1996).
203. Casals-Pascual, C. *et al.* Suppression of erythropoiesis in malarial anemia is associated with hemozoin in vitro and in vivo. *Blood* **108**, 2569–77 (2006).
204. Thawani, N. *et al.* Plasmodium products contribute to severe malarial anemia by inhibiting erythropoietin-induced proliferation of erythroid precursors. *J. Infect. Dis.* **209**, 140–9 (2014).

205. Lamikanra, A. A., Theron, M., Kooij, T. W. A. & Roberts, D. J. Hemozoin (malarial pigment) directly promotes apoptosis of erythroid precursors. *PLoS One* **4**, e8446 (2009).
206. Naessens, J. Bovine trypanotolerance: A natural ability to prevent severe anaemia and haemophagocytic syndrome? *Int. J. Parasitol.* **36**, 521–8 (2006).
207. Andrews, N. W. & Whitlow, M. B. Secretion by *Trypanosoma cruzi* of a hemolysin active at low pH. *Mol. Biochem. Parasitol.* **33**, 249–256 (1989).
208. Facer, C. A., Crosskey, J. M., Clarkson, M. J. & Jenkins, G. C. Immune haemolytic anaemia in bovine trypanosomiasis. *J. Comp. Pathol.* **92**, 393–401 (1982).
209. Assoku, R. K. & Gardiner, P. R. Detection of antibodies to platelets and erythrocytes during infection with haemorrhage-causing *Trypanosoma vivax* in Ayrshire cattle. *Vet. Parasitol.* **31**, 199–216 (1989).
210. Rifkin, M. R. & Landsberger, F. R. Trypanosome variant surface glycoprotein transfer to target membranes: a model for the pathogenesis of trypanosomiasis. *Proc. Natl. Acad. Sci. U. S. A.* **87**, 801–5 (1990).
211. Mabbott, N. & Sternberg, J. Bone marrow nitric oxide production and development of anemia in *Trypanosoma brucei*-infected mice. *Infect. Immun.* **63**, 1563–6 (1995).
212. Musaya, J., Matovu, E., Nyirenda, M. & Chisi, J. Role of cytokines in *Trypanosoma brucei*-induced anaemia: A review of the literature. *Malawi Med. J.* **27**, 45–50 (2015).
213. Wrighting, D. M. & Andrews, N. C. Interleukin-6 induces hepcidin expression through STAT3. *Blood* **108**, 3204–9 (2006).
214. Ludwiczek, S., Aigner, E., Theurl, I. & Weiss, G. Cytokine-mediated regulation of iron transport in human monocytic cells. *Blood* **101**, 4148–54 (2003).
215. Hitchcock, J. R. *et al.* Inflammation drives thrombosis after *Salmonella* infection via CLEC-2 on platelets. *J. Clin. Invest.* **125**, 4429–46 (2015).
216. Christou, C. M. *et al.* Renal cells activate the platelet receptor CLEC-2 through podoplanin. *Biochem. J.* **411**, 133–40 (2008).
217. Suzuki-Inoue, K. *et al.* Involvement of the snake toxin receptor CLEC-2, in podoplanin-mediated platelet activation, by cancer cells. *J. Biol. Chem.* **282**, 25993–6001 (2007).
218. Afdhal, N. *et al.* Thrombocytopenia associated with chronic liver disease. *J.*

- Hepatology*. **48**, 1000–7 (2008).
219. Wang, C.-S., Yao, W.-J., Wang, S.-T., Chang, T.-T. & Chou, P. Strong association of hepatitis C virus (HCV) infection and thrombocytopenia: implications from a survey of a community with hyperendemic HCV infection. *Clin. Infect. Dis.* **39**, 790–6 (2004).
 220. Weksler, B. B. Review article: the pathophysiology of thrombocytopenia in hepatitis C virus infection and chronic liver disease. *Aliment. Pharmacol. Ther.* **26 Suppl 1**, 13–9 (2007).
 221. Ding, L. & Morrison, S. J. Haematopoietic stem cells and early lymphoid progenitors occupy distinct bone marrow niches. *Nature* **495**, 231–5 (2013).
 222. de Boer, J. *et al.* Transgenic mice with hematopoietic and lymphoid specific expression of Cre. *Eur. J. Immunol.* **33**, 314–25 (2003).
 223. Beattie, L. *et al.* Dynamic imaging of experimental *Leishmania donovani*-induced hepatic granulomas detects Kupffer cell-restricted antigen presentation to antigen-specific CD8 T cells. *PLoS Pathog.* **6**, e1000805 (2010).
 224. Bland, M. *An Introduction to Medical Statistics, Third Edition.* (2000).
 225. WHO | Leishmaniasis. at <<http://www.who.int/mediacentre/factsheets/fs375/en/>>
 226. Kedzierski, L. *et al.* Leishmaniasis: current treatment and prospects for new drugs and vaccines. *Curr Med Chem* **16**, 599–614 (2009).
 227. Kokkini, G., Vrionis, G., Liosis, G. & Papaefstathiou, J. Cold agglutinin syndrome and hemophagocytosis in systemic leishmaniasis. *Scand. J. Haematol.* **32**, 441–5 (1984).
 228. Tapisiz, A., Belet, N., Ciftçi, E., Ince, E. & Dogru, U. Hemophagocytic lymphohistiocytosis associated with visceral leishmaniasis. *J. Trop. Pediatr.* **53**, 359–61 (2007).
 229. Cançado, G. G. L., Freitas, G. G., Faria, F. H. F., de Macedo, A. V. & Nobre, V. Hemophagocytic lymphohistiocytosis associated with visceral leishmaniasis in late adulthood. *Am. J. Trop. Med. Hyg.* **88**, 575–7 (2013).
 230. Faleiro, R. J. *et al.* Immune Regulation during Chronic Visceral Leishmaniasis. *PLoS Negl. Trop. Dis.* **8**, e2914 (2014).
 231. Cao, X. *et al.* Irradiation induces bone injury by damaging bone marrow microenvironment for stem cells. *Proc. Natl. Acad. Sci. U. S. A.* **108**, 1609–14

- (2011).
232. Jacobsen, R. N. *et al.* Mobilization with granulocyte colony-stimulating factor blocks medullar erythropoiesis by depleting F4/80(+)VCAM1(+)CD169(+)ER-HR3(+)Ly6G(+) erythroid island macrophages in the mouse. *Exp. Hematol.* **42**, 547–61.e4 (2014).
 233. Koulunis, M. *et al.* Identification and analysis of mouse erythroid progenitors using the CD71/TER119 flow-cytometric assay. *J. Vis. Exp.* (2011). doi:10.3791/2809
 234. Mattila, P. K. & Lappalainen, P. Filopodia: molecular architecture and cellular functions. *Nat. Rev. Mol. Cell Biol.* **9**, 446–54 (2008).
 235. Holness, C. L. & Simmons, D. L. Molecular cloning of CD68, a human macrophage marker related to lysosomal glycoproteins. *Blood* **81**, 1607–13 (1993).
 236. Hallmann, R. *et al.* Expression and function of laminins in the embryonic and mature vasculature. *Physiol. Rev.* **85**, 979–1000 (2005).
 237. Winkler, I. G. *et al.* Positioning of bone marrow hematopoietic and stromal cells relative to blood flow in vivo: serially reconstituting hematopoietic stem cells reside in distinct nonperfused niches. *Blood* **116**, 375–385 (2010).
 238. Simmons, P. J. *et al.* Vascular cell adhesion molecule-1 expressed by bone marrow stromal cells mediates the binding of hematopoietic progenitor cells. *Blood* **80**, 388–395 (1992).
 239. Arai, F. *et al.* Tie2/angiopoietin-1 signaling regulates hematopoietic stem cell quiescence in the bone marrow niche. *Cell* **118**, 149–161 (2004).
 240. Tokoyoda, K., Egawa, T., Sugiyama, T., Choi, B.-I. & Nagasawa, T. Cellular Niches Controlling B Lymphocyte Behavior within Bone Marrow during Development. *Immunity* **20**, 707–718 (2004).
 241. Petit, I. *et al.* G-CSF induces stem cell mobilization by decreasing bone marrow SDF-1 and up-regulating CXCR4. *Nat. Immunol.* **3**, 687–94 (2002).
 242. Bendall, L. J. & Bradstock, K. F. G-CSF: From granulopoietic stimulant to bone marrow stem cell mobilizing agent. *Cytokine Growth Factor Rev.* **25**, 355–67 (2014).
 243. Boettcher, S. *et al.* Endothelial cells translate pathogen signals into G-CSF-driven emergency granulopoiesis. *Blood* **124**, 1393–403 (2014).
 244. Lenox, L. E., Perry, J. M. & Paulson, R. F. BMP4 and Madh5 regulate the erythroid

- response to acute anemia. *Blood* **105**, 2741–8 (2005).
245. Perry, J. M., Harandi, O. F. & Paulson, R. F. BMP4, SCF, and hypoxia cooperatively regulate the expansion of murine stress erythroid progenitors. *Blood* **109**, 4494–502 (2007).
 246. Guy, C. S. & Vignali, D. A. A. Organization of proximal signal initiation at the TCR:CD3 complex. *Immunol. Rev.* **232**, 7–21 (2009).
 247. Kirby, A. C., Coles, M. C. & Kaye, P. M. Alveolar macrophages transport pathogens to lung draining lymph nodes. *J. Immunol.* **183**, 1983–9 (2009).
 248. Feuerer, M. *et al.* Bone marrow as a priming site for T-cell responses to blood-borne antigen. *Nat. Med.* **9**, 1151–7 (2003).
 249. Feuerer, M. *et al.* Bone marrow microenvironment facilitating dendritic cell: CD4 T cell interactions and maintenance of CD4 memory. *Int. J. Oncol.* **25**, 867–76 (2004).
 250. Tripp, R. A., Topham, D. J., Watson, S. R. & Doherty, P. C. Bone marrow can function as a lymphoid organ during a primary immune response under conditions of disrupted lymphocyte trafficking. *J. Immunol.* **158**, 3716–20 (1997).
 251. Reinhold, M. I., Green, J. M., Lindberg, F. P., Ticchioni, M. & Brown, E. J. Cell spreading distinguishes the mechanism of augmentation of T cell activation by integrin-associated protein/CD47 and CD28. *Int. Immunol.* **11**, 707–18 (1999).
 252. Shinkai, Y. RAG-2-deficient mice lack mature lymphocytes owing to inability to initiate V(D)J rearrangement. *Cell* **68**, 855–867 (1992).
 253. Hess, C. E. *et al.* Mechanism of dilutional anemia in massive splenomegaly. *Blood* **47**, 629–44 (1976).
 254. Mahajan, V. & Marwaha, R. K. Immune mediated hemolysis in visceral leishmaniasis. *J. Trop. Pediatr.* **53**, 284–6 (2007).
 255. Dilber, E., Erduran, E. & Işık, Y. Visceral leishmaniasis and Coombs' positive hemolytic anemia: a rare association in an infant treated with liposomal amphotericin B. *Turk. J. Pediatr.* **44**, 354–6 (2002).
 256. Alves, J. M. P. *et al.* Identification and phylogenetic analysis of heme synthesis genes in trypanosomatids and their bacterial endosymbionts. *PLoS One* **6**, e23518 (2011).
 257. Newton, B. A. A synthetic growth medium for the trypanosomid flagellate *Strigomonas* (*Herpetomonas*) *oncopelti*. *Nature* **177**, 279–80 (1956).

258. Du, Y., Maslov, D. A. & Chang, K. P. Monophyletic origin of beta-division proteobacterial endosymbionts and their coevolution with insect trypanosomatid protozoa *Blastocrithidia culicis* and *Crithidia* spp. *Proc. Natl. Acad. Sci. U. S. A.* **91**, 8437–41 (1994).
259. Chakravarty, R., Sharma, M. C., Gupta, A. K., Prakash, N. & Saran, R. *Leishmania donovani*: hemolytic activity of promastigotes. *Exp. Parasitol.* **78**, 253–8 (1994).
260. Tizard, I. R., Sheppard, J. & Neilsen, K. The characterization of a second class of haemolysins from *Trypanosoma brucei*. *Trans. R. Soc. Trop. Med. Hyg.* **72**, 198–200 (1978).
261. Noyes, H. A. *et al.* Mechanisms controlling anaemia in *Trypanosoma congolense* infected mice. *PLoS One* **4**, e5170 (2009).
262. Huynh, C., Sacks, D. L. & Andrews, N. W. A *Leishmania amazonensis* ZIP family iron transporter is essential for parasite replication within macrophage phagolysosomes. *J. Exp. Med.* **203**, 2363–75 (2006).
263. Flannery, A. R., Huynh, C., Mittra, B., Mortara, R. A. & Andrews, N. W. LFR1 ferric iron reductase of *Leishmania amazonensis* is essential for the generation of infective parasite forms. *J. Biol. Chem.* **286**, 23266–79 (2011).
264. Huynh, C. *et al.* Heme uptake by *Leishmania amazonensis* is mediated by the transmembrane protein LHR1. *PLoS Pathog.* **8**, e1002795 (2012).
265. Ben-Othman, R. *et al.* *Leishmania*-mediated inhibition of iron export promotes parasite replication in macrophages. *PLoS Pathog.* **10**, e1003901 (2014).
266. van der Poll, T., Zijlstra, E. E. & Mevissen, M. Interleukin 6 during active visceral leishmaniasis and after treatment. *Clin. Immunol. Immunopathol.* **77**, 111–4 (1995).
267. Ansari, N. A., Saluja, S. & Salotra, P. Elevated levels of interferon-gamma, interleukin-10, and interleukin-6 during active disease in Indian kala azar. *Clin. Immunol.* **119**, 339–45 (2006).
268. de Lima, V. M. F., Peiro, J. R. & de Oliveira Vasconcelos, R. IL-6 and TNF-alpha production during active canine visceral leishmaniasis. *Vet. Immunol. Immunopathol.* **115**, 189–93 (2007).
269. Armeanu, S., Bühring, H. J., Reuss-Borst, M., Müller, C. A. & Klein, G. E-cadherin is functionally involved in the maturation of the erythroid lineage. *J. Cell Biol.* **131**, 243–9 (1995).

270. Lammers, R. *et al.* Monoclonal antibody 9C4 recognizes epithelial cellular adhesion molecule, a cell surface antigen expressed in early steps of erythropoiesis. *Exp. Hematol.* **30**, 537–545 (2002).
271. Murray, H. W. Tissue granuloma structure-function in experimental visceral leishmaniasis. *Int. J. Exp. Pathol.* **82**, 249–267 (2008).
272. Pease, G. L. Granulomatous lesions in bone marrow. *Blood* **11**, 720–34 (1956).
273. Alsaif, M. *et al.* Analysis of serum and plasma identifies differences in molecular coverage, measurement variability, and candidate biomarker selection. *Proteomics. Clin. Appl.* **6**, 297–303 (2012).
274. Levesque, J.-P. *et al.* Characterization of hematopoietic progenitor mobilization in protease-deficient mice. *Blood* **104**, 65–72 (2004).
275. Burberry, A. *et al.* Infection mobilizes hematopoietic stem cells through cooperative NOD-like receptor and Toll-like receptor signaling. *Cell Host Microbe* **15**, 779–91 (2014).
276. Liu, M. *et al.* Macrophages support splenic erythropoiesis in 4T1 tumor-bearing mice. *PLoS One* **10**, e0121921 (2015).
277. Westerterp, M. *et al.* Regulation of hematopoietic stem and progenitor cell mobilization by cholesterol efflux pathways. *Cell Stem Cell* **11**, 195–206 (2012).
278. Lawlor, K. E. *et al.* Critical role for granulocyte colony-stimulating factor in inflammatory arthritis. *Proc. Natl. Acad. Sci. U. S. A.* **101**, 11398–403 (2004).
279. Mebius, R. E. & Kraal, G. Structure and function of the spleen. *Nat. Rev. Immunol.* **5**, 606–16 (2005).
280. Schnitzer, B., Sodeman, T., Mead, M. L. & Contacos, P. G. Pitting function of the spleen in malaria: ultrastructural observations. *Science* **177**, 175–7 (1972).
281. Rosche, K. L., Aljasham, A. T., Kipfer, J. N., Piatkowski, B. T. & Konjufca, V. Infection with *Salmonella enterica* Serovar Typhimurium Leads to Increased Proportions of F4/80+ Red Pulp Macrophages and Decreased Proportions of B and T Lymphocytes in the Spleen. *PLoS One* **10**, e0130092 (2015).
282. Millot, S. *et al.* Erythropoietin stimulates spleen BMP4-dependent stress erythropoiesis and partially corrects anemia in a mouse model of generalized inflammation. *Blood* **116**, 6072–81 (2010).
283. O'Donnell, R. K., Goldstein, W. E., Perruzzi, C., Benjamin, L. E. & Aird, W.

- Overexpression of MyrAkt1 in endothelial cells leads to erythropoietin- and BMP4-independent splenic erythropoiesis in mice. *PLoS One* **8**, e55095 (2013).
284. Dalton, J. E. *et al.* The neurotrophic receptor Ntrk2 directs lymphoid tissue neovascularization during *Leishmania donovani* infection. *PLoS Pathog.* **11**, e1004681 (2015).
285. Miwa, Y. *et al.* Up-regulated expression of CXCL12 in human spleens with extramedullary haematopoiesis. *Pathology* **45**, 408–416 (2013).
286. Inra, C. N. *et al.* A perisinusoidal niche for extramedullary haematopoiesis in the spleen. *Nature advance on*, (2015).
287. Otsuka, H., Yagi, H., Endo, Y., Nonaka, N. & Nakamura, M. Kupffer cells support extramedullary erythropoiesis induced by nitrogen-containing bisphosphonate in splenectomized mice. *Cell Immunol* **271**, 197–204 (2011).
288. Sileghem, M. & Naessens, J. Are CD8 T cells involved in control of African trypanosomiasis in a natural host environment? *Eur. J. Immunol.* **25**, 1965–71 (1995).
289. Arieta Kuksin, C., Gonzalez-Perez, G. & Minter, L. M. CXCR4 expression on pathogenic T cells facilitates their bone marrow infiltration in a mouse model of aplastic anemia. *Blood* **125**, 2087–94 (2015).
290. Lin, F. C. *et al.* IFN-gamma causes aplastic anemia by altering hematopoietic stem/progenitor cell composition and disrupting lineage differentiation. *Blood* **124**, 3699–3708 (2014).
291. Chen, J., Feng, X., Desierto, M. J., Keyvanfar, K. & Young, N. S. IFN- γ -mediated hematopoietic cell destruction in murine models of immune-mediated bone marrow failure. *Blood* **126**, 2621–31 (2015).
292. Sigdel, B., Bhandary, S. & Rijal, S. Epistaxis in visceral leishmaniasis with hematological correlation. *Int. J. Otolaryngol.* **2012**, 809056 (2012).
293. Jüttner, C., Rodríguez Sánchez, M., Rollán Landeras, E., Slappendel, R. J. & Fragío Arnold, C. Evaluation of the potential causes of epistaxis in dogs with natural visceral leishmaniasis. *Vet. Rec.* **149**, 176–9 (2001).
294. Ciaramella, P. *et al.* Altered platelet aggregation and coagulation disorders related to clinical findings in 30 dogs naturally infected by *Leishmania infantum*. *Vet. J.* **169**, 465–7 (2005).

295. Petanides, T. A. *et al.* Factors associated with the occurrence of epistaxis in natural canine leishmaniasis (*Leishmania infantum*). *J. Vet. Intern. Med.* **22**, 866–72 (2008).
296. Koutinas, A. F. & Koutinas, C. K. Pathologic mechanisms underlying the clinical findings in canine leishmaniasis due to *Leishmania infantum/chagasi*. *Vet. Pathol.* **51**, 527–38 (2014).
297. Thomas, G. R. *et al.* In vivo biological effects of various forms of thrombopoietin in a murine model of transient pancytopenia. *Stem Cells* **14 Suppl 1**, 246–55 (1996).
298. Geddis, A. E. The regulation of proplatelet production. *Haematologica* **94**, 756–9 (2009).
299. Gabriele, G. de & Penington, D. G. Regulation of Platelet Production: ‘Hypersplenism’ in the Experimental Animal. *Br. J. Haematol.* **13**, 384–393 (1967).
300. Corash, L. *et al.* Regulation of thrombopoiesis: effects of the degree of thrombocytopenia on megakaryocyte ploidy and platelet volume. *Blood* **70**, 177–85 (1987).
301. Stenberg, P. E. & Levin, J. Ultrastructural analysis of acute immune thrombocytopenia in mice: dissociation between alterations in megakaryocytes and platelets. *J. Cell. Physiol.* **141**, 160–9 (1989).
302. Graham, S. S., Traub, B. & Mink, I. B. Automated platelet-sizing parameters on a normal population. *Am. J. Clin. Pathol.* **87**, 365–9 (1987).
303. Kuter, D. J. & Rosenberg, R. D. The reciprocal relationship of thrombopoietin (c-Mpl ligand) to changes in the platelet mass during busulfan-induced thrombocytopenia in the rabbit. *Blood* **85**, 2720–30 (1995).
304. Ichikawa, N. *et al.* Regulation of serum thrombopoietin levels by platelets and megakaryocytes in patients with aplastic anaemia and idiopathic thrombocytopenic purpura. *Thromb. Haemost.* **76**, 156–60 (1996).
305. Recommended methods for measurement of red-cell and plasma volume: International Committee for Standardization in Haematology. *J. Nucl. Med.* **21**, 793–800 (1980).
306. el Hag, I. A. *et al.* Liver morphology and function in visceral leishmaniasis (Kala-azar). *J. Clin. Pathol.* **47**, 547–51 (1994).
307. Prakash, A. *et al.* Visceral leishmaniasis masquerading as chronic liver disease. *J. Assoc. Physicians India* **54**, 893–4 (2006).

308. Honse, C. O. *et al.* Disseminated intravascular coagulation in a dog naturally infected by Leishmania (Leishmania) chagasi from Rio de Janeiro - Brazil. *BMC Vet. Res.* **9**, 43 (2013).
309. Davis, C. E., Robbins, R. S., Weller, R. D. & Braude, A. I. Thrombocytopenia in experimental trypanosomiasis. *J. Clin. Invest.* **53**, 1359–67 (1974).
310. Marcondes, M. C., Borelli, P., Yoshida, N. & Russo, M. Acute Trypanosoma cruzi infection is associated with anemia, thrombocytopenia, leukopenia, and bone marrow hypoplasia: reversal by nifurtimox treatment. *Microbes Infect.* **2**, 347–52 (2000).
311. Ngotho, M. *et al.* Influence of trypanocidal therapy on the haematology of vervet monkeys experimentally infected with Trypanosoma brucei rhodesiense. *Acta Trop.* **119**, 14–8 (2011).
312. Freire-de-Lima, L. *et al.* Sialic acid: a sweet swing between mammalian host and Trypanosoma cruzi. *Front. Immunol.* **3**, 356 (2012).
313. Tribulatti, M. V., Mucci, J., Van Rooijen, N., Leguizamón, M. S. & Campetella, O. The trans-sialidase from Trypanosoma cruzi induces thrombocytopenia during acute Chagas' disease by reducing the platelet sialic acid contents. *Infect. Immun.* **73**, 201–7 (2005).
314. Medina-Acosta, E. *et al.* Trans-sialidase and Sialidase Activities Discriminate between Morphologically Indistinguishable Trypanosomatids. *Eur. J. Biochem.* **225**, 333–339 (1994).
315. Pawlowic, M. C. & Zhang, K. Leishmania parasites possess a platelet-activating factor acetylhydrolase important for virulence. *Mol. Biochem. Parasitol.* **186**, 11–20 (2012).
316. Gazos-Lopes, F. *et al.* Structural and functional analysis of a platelet-activating lysophosphatidylcholine of Trypanosoma cruzi. *PLoS Negl. Trop. Dis.* **8**, e3077 (2014).
317. Goncalves, R., Zhang, X., Cohen, H., Debrabant, A. & Mosser, D. M. Platelet activation attracts a subpopulation of effector monocytes to sites of Leishmania major infection. *J. Exp. Med.* **208**, 1253–65 (2011).
318. Valladares, J. E. *et al.* Study of haemostatic disorders in experimentally induced leishmaniasis in Beagle dogs. *Res. Vet. Sci.* **64**, 195–8 (1998).

